



LIBRARY
COPY

THE DYNAMIC BEHAVIOR OF AN
AMMONIA SYNTHESIS REACTOR

by
JEAN-PIERRE EYMERY

Diplome d'Ingenieur E.N.S.I.C. Nancy
(1959)

S.M., Ch.E., Massachusetts Institute of Technology
(1960)

SUBMITTED IN PARTIAL FULFILLMENT OF THE
REQUIREMENTS FOR THE DEGREE OF
DOCTOR OF SCIENCE

at the

MASSACHUSETTS INSTITUTE OF TECHNOLOGY
February, 1964

Signature of Author Signature redacted
Department of Chemical Engineering

Certified by Signature redacted
R.F. Baddour, Thesis Supervisor

Signature redacted
P.L. Th. Brian, Thesis Supervisor

Accepted by _____
G.C. Williams, Chairman
Departmental Committee on Graduate Thesis

↓

THE DYNAMIC BEHAVIOR OF AN AMMONIA SYNTHESIS REACTOR

by

Jean Pierre Eymery

Submitted to the Department of Chemical Engineering on December 11, 1963 in partial fulfillment of the requirements for the degree of Doctor of Science in Chemical Engineering.

ABSTRACT

This work is an investigation of the dynamic behavior of an ammonia reactor. The objective was to understand the dynamic behavior of this reactor in order to allow for stable and optimum conditions of operation.

A mathematical model retaining the major transport, generation and accumulation processes of enthalpy was derived and solved by finite difference approximation methods on a digital computer. The results of the simulation were interpreted physically by considering the changes occurring during a transient for each transport and generation process of enthalpy. The changes in temperature during the first instants of the transient resulting from a step change in the feed temperature were described in terms of the propagation of a thermal perturbation introduced at the entrance of the catalyst section, and of the results of changes in the wall temperature separating the catalyst from the feed gases.

It was shown that because of the poor reactivity of the catalyst investigated the rate of propagation of the thermal perturbation is almost unaffected by the extent of the chemical reaction. The instability resulting from the "blow out" of the reactor was described as a "snow ball" type of instability. The dynamics of the reactor were demonstrated linear for perturbations in the feed temperature smaller than 5°C around the conditions of maximum production. Under these conditions the dynamics of the ammonia reactor were described by frequency response curves, and by simplified transfer functions retaining the major features of the transient.

The results of the present investigation were used to design and test an ideal controller which was shown adequate to avoid the blow off of the reactor when changes in ammonia mole fraction in the feed, occurred, but which did not optimize the production of the reactor.

Thesis Supervisor: R.F. Baddour
Title: Professor Chemical Engineering

P.L. Brian
Assoc. Professor of Chem. Eng.

ACKNOWLEDGEMENT

The Author wishes to express all his appreciation to his thesis supervisors Professors R.F. Baddour and P.L.T. Brian of the Department of Chemical Engineering for their immeasurable support given during all phases of this thesis. He also wishes to acknowledge the valuable direction and suggestions of Professor L.A. Gould in the latter phase of the research.

The author wishes to thank the members of the Electronic Systems Laboratory Publication Department who typed the document - Mrs. Ionia Lewis, Miss Mary Berry, and Mrs. Laurel Retajczyk, and also those who did the drafting - Mr. Harold Tonsing, Miss Janet Mc Gonnigal, and Mr. Arthur Giordani.

Finally the author is greatly indebted to his wife, Marlene, whose enthusiasm, patience and faith have made this work possible.

The first part of this research has been supported by a N.A.T.O Scholarship. The last part by a National Science Foundation Grant GP376 M.I.T. DSR 9323. The computational work reported here was performed at the M.I.T. Computation Center.

CONTENTS

	page
CHAPTER I	SUMMARY
	1
CHAPTER II	INTRODUCTION
	4
CHAPTER III	LITERATURE SURVEY AND OBJECTIVE OF THE THESIS
	9
A.	Description and Conditions of Operation of a Haber-Bosch Reactor
	9
B.	Steady State Analysis of the T.V.A. Reactor
	13
C.	Literature Survey on Dynamics of Chemical Reactors
	22
D.	Objective of the Thesis
	25
CHAPTER IV	MATHEMATICAL MODEL OF THE T.V.A. REACTOR
	27
A.	Assumptions Used in the Derivation of the Mathematical Model
	27
B.	Derivation of the Mathematical Model Describing the T.V.A. Reactor
	32
1.	Material Balance in the Catalyst Section
	32
2.	Energy Balance
	37
C.	Discussions of the Assumptions Included in the Mathematical Model
	44
1.	Effect of Neglecting Radial Temperature Gradient
	44
2.	Temperature Difference between Catalyst and Gas
	46
3.	Relative Magnitude of Enthalpy Storage
	51
4.	Residence Times Compared to Thermal Time Constants
	51
5.	Comparison of Computed and Experimental Steady State Results
	52
CHAPTER V	COMPUTATION METHOD
	55
A.	Derivation of the Computer Algorithm
	56
1.	Variable Distance Grid
	56
2.	Solution of the Energy Equation for the Gas in the Empty Tube Section
	58
3.	Solution of the Energy Equation in the Catalyst Section
	60
4.	Solution of the Material Balance Equation
	70

CONTENTS (Continued)

B.	Accuracy Analysis of the Stone-Brian Computer Scheme	<u>page</u>	72
	1. Analysis of Stone-Brian's Results		74
	2. Extension of Stone-Brian's Results to the Case with a Sink or Source Term		77
C.	Convergence Study of the Proposed Scheme		87
D.	Comparison with the C.I.R. Scheme		196
CHAPTER VI	RESULTS AND DISCUSSION		100
A.	Steady State of the Reactor		100
B.	Dynamic Operation of the Reactor Under Stable Condition		108
	1. Description of the Results		108
	2. Discussion of the Results		118
C.	"Blow Out" of the Reactor		132
D.	Nonlinearity of the System		137
E.	Description of the Reactor in its Linear Range of Operation		145
F.	Effect of "Blow Out" Perturbation Imposed During a Finite Amount of Time		155
G.	Automatic Control of the T.V.A. Reactor		161
CHAPTER VII	CONCLUSION AND RECOMMENDATION		169
APPENDIX A	NUMERICAL VALUES OF THE MODEL PARAMETERS		173
APPENDIX B	SOLUTION OF THE STEADY STATE EQUATIONS		177
APPENDIX C	FORTRAN PROGRAM FOR THE COMPUTING ALGORITHM PRESENTED IN CHAPTER V AND NUMERICAL RESULTS		184
APPENDIX D	DERIVATION OF THE FREQUENCY RESPONSES		207
APPENDIX E	LITERATURE CITATIONS		215
APPENDIX F	NOMENCLATURE		218

LIST OF FIGURES

3.1	Simplified Diagram of a T.V.A. Reactor	<u>page</u>	10
3.2	Experimental Temperature Profile in the T.V.A. Reactor		12
3.3	Effect of Top Temperature on Production		15
3.4	Relationship Between Inlet and Top Temperatures		16
3.5	Ignition Temperature and Stability		18
3.6	Effect on Stability of Space Velocity		20
3.7	Effect on Stability of Ammonia Mole Fraction in the Feed		20
4.1	Lumped Model of the T.V.A. Reactor		28
4.2	Thermocouple Arrangement		47
4.3	Typical Temperature Profile		53
5.1	Dependence with Frequency of the Growth Factor ρ'		84
5.2	Dependence with Frequency of the Velocity Factor ϕ'		85
5.3	Effect of Distance Grid Size on Convergence of the Solution at $\alpha = 0$		89
5.4	Effect of Distance Grid Size on Convergence of the Solution at $\alpha = 0.052$		90
5.5	Effect of Distance Grid Size on Convergence of the Solution at $\alpha = 0.30$		91
5.6	Effect of Distance Grid Size on Convergence of the Solution at $\alpha = 0.80$		92
5.7	Effect of Time Increment on Convergence of the Solution at $\alpha = 0.052$		93
5.8	Effect of Time Increment on Convergence of the Solution at $\alpha = 0.30$		94
5.9	Effect of Distance Grid Size on the Convergence of the C.I.R. Solution at $\alpha = 0.028$		98
5.10	Effect of Distance Grid Size on the Convergence of the C.I.R. Solution at $\alpha = 0.052$		98
6.1	Steady State Relation Between Top and Feed Temperature		104
6.2	Steady State Relation Between Outlet Ammonia Mole Fraction and Feed Temperature		105
6.3	Changes in Temperature During a $+5^{\circ}\text{C}$ Step Transient		109

LIST OF FIGURES (Continued)

6.4	Changes in Temperature During the First Period of a 5°C Step Transient	110
6.5	Dynamic "Gains" of the Reactor	113
6.6	Location and Magnitude of the Hot Spot During a +5°C Step Transient	115
6.7	Changes in Ammonia Mole Fraction During a +5°C Step Transient	117
6.8	Dependence with Location of the Enthalpy Transport and Generation Processes	119
6.9	Effect of Temperature Change on the Heat Generation by Chemical Reaction	121
6.10	Effect of Ammonia Mole Fraction Change on the Heat Generation by Chemical Reaction	121
6.11	Correction for the Heat Capacity of the Gas Under Equilibrium Conditions	125
6.12	Changes in Temperature During a +5°C Step Transient for an Active Catalyst	128
6.13	Changes in Temperature During a "Blow Off"	133
6.14	Changes in Ammonia Mole Fraction During a "Blow Off"	134
6.15	Dynamic "Gain" of the Process During a "Blow Off"	136
6.16	Effect of the Magnitude of the Step Change on the Dynamic Gain at $\theta' = 0.964$	138
6.17	Effect of the Magnitude of the Step Change on the Dynamic Gain at $\theta' = 2.10$	140
6.18	Effect of the Magnitude of the Step Change on the Dynamic Gain for Location $\alpha = 0.374$	141
6.19	Effect of the Magnitude of the Step Change on the Dynamic "Gain" for Location $\alpha = 1.0$	142
6.20	Frequency Response Curves for Location $\alpha = 0$	148
6.21	Frequency Response Curves for Location $\alpha = 0.374$	149
6.22	Frequency Response Curves for Location $\alpha = 1.0$	151
6.23	Time Domain Comparison of Approximate Transfer Functions and Simulation Results	154
6.24	Temperature Variations During a Perturbation of Finite Duration	156
6.25	Temperature Variations During a Perturbation of Finite Duration	158
6.26	Outlet Ammonia Mole Fraction During a Perturbation of Finite Duration	161
6.27	Schematic Diagram of the Control Scheme	164

LIST OF FIGURES (Continued)

6.28	Block Diagram of the Close Control Loop	164
6.29	Changes in Temperature at $\alpha = 0$ Under Automatic Control of the Reactor	167
6.30	Changes in Temperature at $\alpha = 1.0$ Under Automatic Control of the Reactor	168

LIST OF TABLES

		page
3.1	Operating Conditions Corresponding to the Experimental Temperature Profile of Fig. 3.2	11
3.2	Effect of Operating Variables on the Stability of the T.V.A. Reactor	21
4.1	Experimental Temperature Profile	45
4.2	Relative Magnitude of the Enthalpy Storage	51
5.1	Effect of Various Choices of Weighting Coefficients α_1 on the Values of ρ' and ϕ' for the zero frequency	82
5.2	Parameter Investigated During the Accuracy Analysis	86
5.3	Conditions Investigated During the Convergence Study	88
6.1	Effect of Longitudinal Diffusion on the Reactor Steady State Profile	102
6.2	Conditions of Transients Performed in this Investigation	106
6.3	Steady State Gains	143
A.1	Numerical Value of the Group used in the Simulation	176
B.1	Runge Kutta Formulas	179
B.2	Steady State Relations	183
C.1	Fortram Nomenclature	184
C.2	Temperature Changes During a +5°C Step Transient	193
C.3	Ammonia Mole Fraction Changes During a +5°C Step Transient	194
C.4	Location and Magnitude of Peak Temperature	195
C.5	Transient Dynamic "Gain" of the Reactor During a +5°C Step Transient	196
C.6	Enthalpy Generation and Transport	197
C.7	Temperature Changes During a Blow Off Transient	198
C.8	Changes in Ammonia Mole Fraction During a Blow Off	199
C.9	Dynamic Gain During a "Blow Off"	200
C.10	Effects of the Magnitude of the Step Change on the Dynamic Gain at $\theta' = 0.964$	201
C.11	Effects of the Magnitude of the Step Change on the Dynamic Gain at $\theta' = 2.10$	201
C.12	Effect of the Magnitude of the Step Change on the "Gain" at $\alpha = 0.374$	202
C.13	Effect of the Magnitude of the Step Change on the Gain at $\alpha = 1.0$	203
C.14	Changes in Temperature During Restoration of the Reactor to its Original Conditions	204

LIST OF TABLES (continued)

		page
C.15	Ammonia Mole Fraction During Restoration of the Reactor to its Original Condition	205
C.16	Changes in Temperature for an Active Catalyst	206
D.1	Frequency Response for $\alpha = 0.0$	211
D.2	Frequency Response for $\alpha = 0.374$	212
D.3	Frequency Response for $\alpha = 1.0$	213
D.4	Comparison of Transient Data with Results of Approximate Transfer Functions	214

CHAPTER I

SUMMARY

The derivation and the solution of a mathematical model describing the dynamic behavior of a Haber-Bosh reactor is the objective of this research. All the previous investigations concerning this type of reactor have been limited to its steady state behavior. They have demonstrated the extreme sensitivity of the reactor to changes in the operating variables when it is operated under the conditions of maximum production. As a first step towards the design of an automatic controller providing safe and optimum operation of this reactor, a description of its dynamics was needed. Since experimental results on the dynamics of a Haber-Bosh reactor have not been published, a mathematical model has been derived. The proposed mathematical model lumps radially the reactor in three sections and takes into account the longitudinal variations in temperature and composition. Despite many simplifying assumptions, the proposed model is believed to retain the characteristic features of the behavior of the reactor.

The proposed model consists of four partial differential equations (one mass balance equation and three enthalpy balance equations). Because of the nonlinear terms representing the rate of reaction and the release of energy by chemical reaction, there is no analytical solution to the mathematical system to be solved. Finite difference analogs of these equations have been derived and solved on a digital computer (IBM-7090). The convergence of the numerical solutions obtained has been demonstrated. During the investigation of the computation method the use of the Stone-Brian method of approximating first order time and distance partial derivatives have appeared more effective

in terms of computer time than the Courant-Isaacson and Rees method recommended in the literature to solve the same type of equation.

The transient resulting from a step change in the feed temperature to the reactor has been described both during an approach to a new stable steady state and during the blow out of the reactor. During the first instants of the transient the changes in temperature observed in this reactor have been explained in terms

1. of the propagation of a thermal perturbation introduced at the entrance of the catalyst bed,
2. and the results of changes in the wall temperature of the tube separating the catalyst from the feed gases.

Near the entrance of the catalyst bed, the magnitude of the second effect has been found so small that it could be neglected. Near the outlet of the reactor it has been found predominant during the first instants of the transient. A second change in temperature has been observed after the passage of the initial thermal perturbation. The regenerative character of this process has been found responsible for the slow approach to steady state after the passage of the initial thermal perturbation through the reactor. The changes in temperature and composition have been interpreted through the effects of the transient on each transport and generation process of enthalpy. An analysis of the rate of propagation of the thermal perturbation shows that it is dependent on the ratio of heat capacity of the gases and catalyst charge but is almost unaffected by the extent of the reversible chemical reaction under consideration. The poor reactivity of the catalyst present in the reactor which never brings the reacting gases close to their equilibrium conditions has been used to explain this observation.

It has been shown that the instability, resulting from the decrease of the feed temperature below the "blow off" feed temperature, is of the "snowball"

type: never before have oscillations in temperature and composition been observed on the present model. To investigate the nonlinearity of the process, the effect of step changes of different magnitudes has been investigated. For the standard conditions under investigation, perturbations in the feed temperature have to be smaller than 5°C in order to consider the response as linear. Under these conditions the dynamics of the reactor have been described quantitatively by frequency response curves generated from the transient results of the simulation. Simplified transfer functions have been proposed to approximate the frequency response curves at these locations. The physical interpretation of the proposed transfer functions has confirmed the qualitative explanation offered for the transient. For perturbations outside the linear range of operation, resulting in the "blow off" of the reactor, the simulation has been recommended as the only way to describe and compute the dynamics of the reactor.

The results obtained from the linear behavior of the reactor have been used to design an ideal controller which has been demonstrated to avoid the "blow off" of the reactor caused by an increase in ammonia recycled in the feed. The proposed control scheme does not allow for optimization of the production and the simulation derived in this research has been proposed to test more elaborate control schemes which can both avoid the "blow off" of the reactor and optimize its production.

The recommendations for further work concern two areas

1. The description of the uncontrolled reactor during a transient in its linear range.
2. The description of the reactor under close loop control conditions and the derivation of an automatic controller optimizing the production of this reactor.

CHAPTER II

INTRODUCTION

Every time one considers a reversible exothermic catalytic reaction, the problem of optimum temperature arises. At low temperature when equilibrium is favorable the rate of reaction are too small for industrial purposes, at high temperature equilibrium is limiting and high degree of conversion cannot be obtained.

For a single reaction, once the dependence of the rate equation with temperature is known, it is possible to obtain the optimum temperature profile as a function of the degree of conversion by setting the partial derivative of the reaction rate with respect to temperature equal to zero. Annable² and Kjaer²¹ computed such profiles for the case of the ammonia synthesis, using kinetic equations derived from Temkin works;^{32, 33} Calderbank⁹ did a similar study for the sulfuric acid contact process.

In all cases the optimum temperature is infinite at the entrance of the reactor when no products are present in the feed stream. This is due to the fact that the reverse reaction has a rate equal to zero under these conditions. As one proceeds down the reactor the optimum temperature decreases as the conversion increases.

Because of the exothermicity of the reaction considered, the temperature inside the catalyst bed has the tendency to increase rather than to follow the optimum trend, and consequently, such optimum profiles can only be approximated in industrial reactors. One of the first attempts to approximate such a profile was to use a series of adiabatic beds provided with interstage coolers. The Chemico or Monsanto designed converter for the synthesis Sulfuric acid and the Montecantini converter for the synthesis of ammonia still use this principle.

But the most widely used type of equipment to carry out a reaction of this nature is the Haber-Bosh converter, first designed for the ammonia synthesis. In this reactor gas flow and heat exchange are arranged to reduce the increase in temperature associated with the reaction and in the case of stable operation to suppress the need for an external source of heat. A specific design of the Haber-Bosh converter is described in the first section of Chapter III.

The Haber-Bosh ammonia synthesis belongs to the category of "auto-thermic process"; this term was introduced by Van Heerden³⁴ to describe exothermic reaction in which the heat required to bring the reactants to the reaction temperature, is produced by the heat of reaction alone. Stable conditions of operation for these processes are obtained when the heat consumption is balanced by the heat produced by the reaction. Van Heerden³⁴ was the first to explain the properties of such processes as the need of an ignition by external heating, and the existence of a minimum reaction temperature below which the reaction will "blow out". For such reactors he reported that the most economical condition of operation, productionwise, corresponds to the limit of stability. Logeais work²² along this line showed, in fact, that the blow out temperature is different from the maximum production temperature but is still very close to it: less than 5°C in the cases he studied.

The actual problem in operating a Haber-Bosh reactor (Tennessee-Valley-Authority Design) was reported by Slack Allgood and Maune.²⁹ The existence of an optimum inlet temperature which is affected by the process variables and the catalyst activity was described. As the rate at which gases are fed to the reactor increases they reported that the stability of the reactor decreases and that the reactor tends to "blow out." In order to avoid this

problem Slack, Allgood and Maune reported that the reactor was operated away from its blow out limit and consequently away from the maximum production conditions of operation.

In order to investigate the stability of the Haber-Bosh converter from a steady state point of view, Van Heerden³⁴ Kjaer,²¹ Annable² and Logeais²² derived mathematical models describing the steady state behavior of the reactor and studied on such models, the effect of the various design and operating variables. The results of Logeais' investigations presented in Chapter III, Section B confirmed the general findings of Van Heerden, and demonstrated that the difference between the optimum temperature of operation and the "blow out" temperature is very small under most operating conditions.

Since the optimum feed temperature for a given feed rate is very close to the blow out temperature, the reactor must be closely controlled if it is to be operated at maximum capacity. The control philosophy proposed for the ammonia reactor is presented in Chapter VI, Section G. To design such a control scheme the dynamic behavior of the Haber-Bosh reactor needs to be investigated around its optimum conditions of operation. The objective of this thesis is to describe the dynamic behavior of an autothermic reactor, in a way to improve the understanding of this widely used class of reactor.

Dynamic studies of a packed bed reactor have been limited in most cases to mathematical analysis. Furthermore, the amount of results published to date is very small; due to the fact that any mathematical model describing the transient behavior of packed bed catalytic reactors includes nonlinear partial differential equations, without analytical solution, which have to be solved numerically. In Chapter III, Section C, the attempts made to simulate the transient behavior of chemical reactors are briefly reviewed.

For both control and design purposes the necessity to undertake a study of the dynamic behavior of the Harber-Bosh reactor arose. This study with objectives and goals presented in Chapter III Section D is made by deriving a mathematical model describing the changes in temperature and composition as a function of time and distance within the catalyst section of the reactor. The derivation of the mathematical model and the assumptions built into the model are presented in Chapter IV. Since a numerical method of solution had to be used, rather than arbitrary kinetics data and design characteristics, the present model uses the kinetics data and the design parameters retained by Logeais²² in his steady state analysis of a Tennessee Valley Authority (T.V.A.) reactor. The model as derived will, in fact, apply to any type of reaction (sulphuric acid synthesis, Methanol Synthesis) if provided with different kinetics or to other size of such a design of reactor. Chapter IV, Section C considers the major assumptions made in the derivation of the mathematical model, and estimates how close the results of the simulation represent the behavior of a real Tennessee Valley Authority ammonia reactor.

Chapter V presents the numerical method of computation used in solving the mathematical model. The extensive computation required to solve the mathematical model for any transient has been made feasible through the use of a digital computer (IBM 7090). Most of the numerical methods available to solve first order nonlinear partial differential equations are excessively time-consuming. In this research finite approximations to partial derivatives proposed by Stone and Brian³⁰ for the solution of convection problems are used.

The convergence of the finite difference approximations to the system of partial differential equations describing the dynamics of the reactor was tested and the results of this study are presented in Chapter V Section C.

To specify the steady state gain of this process, the equations representing the steady state behavior of the reactor are solved by the same method proposed by Logeais. The steady state conditions corresponding to the beginning and the ends of the transient under investigation are reported in the first section of Chapter VI.

The transient behavior of the reactor is investigated by making step changes in the feed temperature. Chapter VI, Section B describes the behavior of the reactor when the step change results in a stable condition of operation. Chapter VI, Section C presents the same results when the step brings the temperature beyond the "blow out" temperature.

The influence of the step size on the dynamic response of the reactor is investigated and the results reported in Chapter VI, Section D. From these results a region of dynamic linearity is defined. Within this region of linear behavior, the dynamics of the T.V.A. reactor are described by the classical methods of linear control theory: frequency response curves and approximated transfer functions. The results of this analysis presented in Chapter VI, Section E are used to design an ideal controller operating on the feed temperature of the reactor. The location of the thermocouple is chosen to allow for large values of the controller gain.

In Chapter VI, Section F the effect of "blow out" perturbations lasting for a finite amount of time are investigated. The scope of this section is to confirm that the return of the feed temperature to its initial value brings the reactor back to its optimum conditions of operation as long as the average bed temperature has not decreased below the ignition temperature associated with the optimum feed temperature.

In Chapter VI, Section G the results obtained with an ideal automatic controller are reported during perturbations which would have resulted in the "blow out" of the uncontrolled reactor.

CHAPTER III

LITERATURE SURVEY AND OBJECTIVES OF THE THESIS

A. DESCRIPTION AND CONDITIONS OF OPERATION OF A HABER-BOSCH REACTOR

The Tennessee Valley Authority reactor, (abbreviated T.V.A. reactor) is a particular design of the Haber-Bosh reactor. Van Heerden used it to characterize an autothermic process. The T.V.A. reactor was described in several papers by G.L. Bridger, G.R. Pole and A.W. Beinlich,⁷ L.B. Hein,¹⁷ A.V. Slack, H.Y. Allgood and H.E. Maune,²⁹ J. Kjaer,²¹, D. Annable² and B. Logeais.²²

A simplified diagram of the T.V.A. reactor is shown in Fig. 3.1. The converter consists of two sections:

1. A heat exchanger section presented at the lower part of the diagram
2. A catalyst bed section presented at the upper part of the diagram.

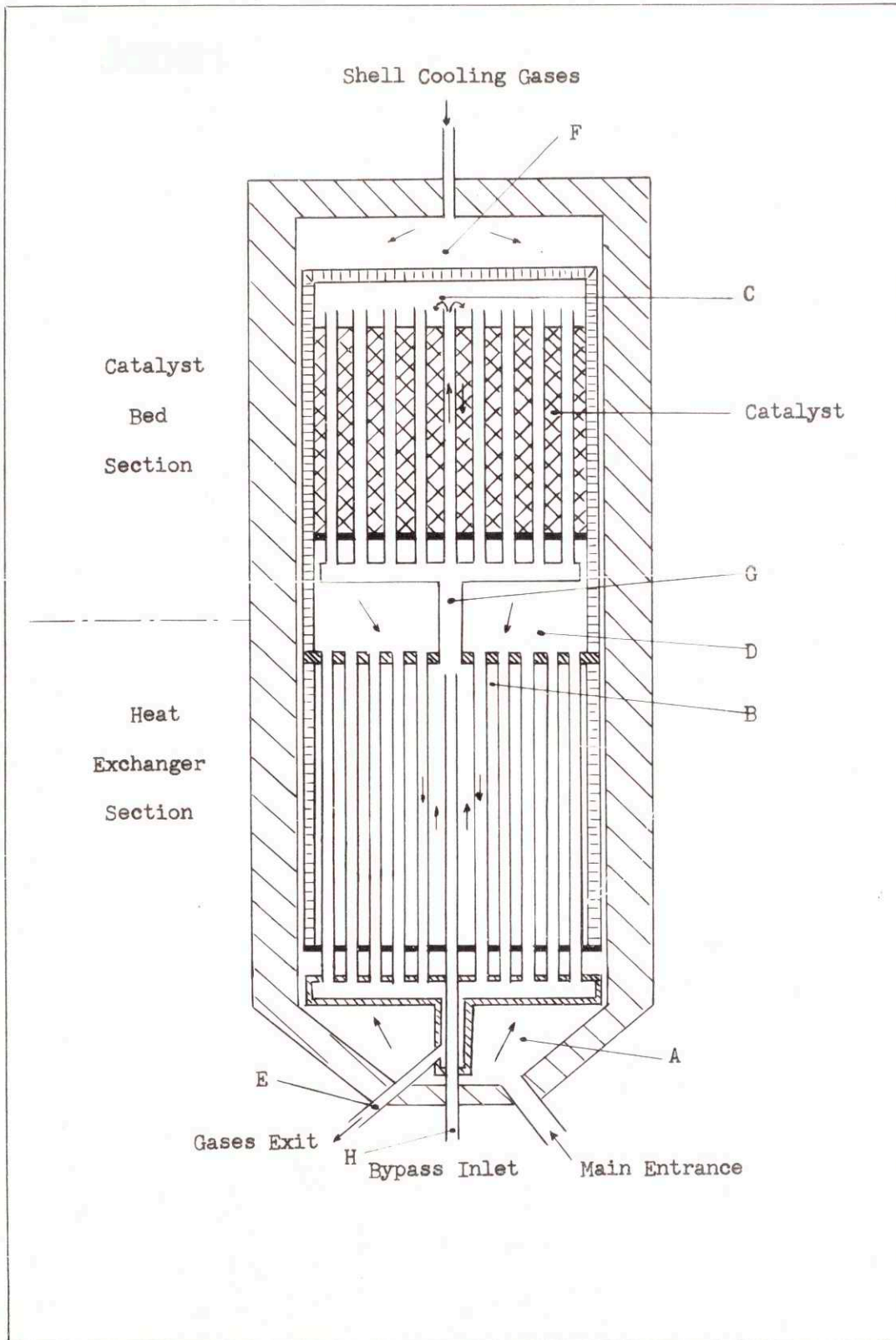
In the heat exchanger section, the feed gases A enter the shell side of a conventional heat exchanger and are heated by the hot gases leaving the catalyst bed section. The purpose of this heat exchanger section is to bring the feed gases to a temperature high enough to insure a stable condition of operation inside the catalyst bed section.

The feed gases leaving the heat exchanger section are mixed in G with fresh feed gas entered in H and which has bypassed the heating section.

The temperature of the gases entering the catalyst bed section can be consequently controlled within some limits by a proper setting of the bypass flow.

The catalyst bed section acts as a conventional heat exchanger and as a fixed bed catalytic reactor. The preheated feed flows inside a large number of small tubes imbedded in the catalyst. The heat produced by the exothermic reaction is transferred to the feed gases ascending through the tubes and raises their temperature until the gases reach the top of the reactor. There

Fig. 3-1
SIMPLIFIED DIAGRAM OF A TVA REACTOR



the feed gases reverse their direction and flow down the catalyst bed where the reaction takes place.

The outlet gases D from the catalyst bed section enters on the tube side of the heat exchanger section before leaving the reactor. In order to prevent the decomposition of steel by hydrogen at the high temperature (500°C) and under the high pressure (300 atm) where the T.V.A. reactor is operated, the reactor walls are insulated and cooled by a stream of fresh synthesis gas entering the reactor at the top F and which is mixed with the remaining of the feed gas in A.

Operating data taken from a T.V.A. reactor were reported by A.V. Slack, H.Y. Allgood and H.E. Maune,²⁹ and B. Logeais.²²

Figure 3.2 represents a steady-state temperature profile measured in the catalyst section of a T.V.A. reactor whose characteristics appear in Appendix A. The operating conditions corresponding to this run, as reported by Logeais, appear in Table 3.1.

TABLE 3.1
OPERATING CONDITIONS CORRESPONDING TO THE
EXPERIMENTAL TEMPERATURE PROFILE OF FIG. 3.2

Space Velocity*	13,800 1/hr
Pressure	287 atm
Feed Composition	mole fraction
H ₂	0.650
N ₂	0.212
NH ₃	0.052
INERT	0.072
Production	120 T/day

* The space velocity used to characterize the feed rate of synthesis gases is defined as the number of cubic feet of feed gases (under standard conditions of temperature and pressure), per cubic foot of catalyst, per hour.

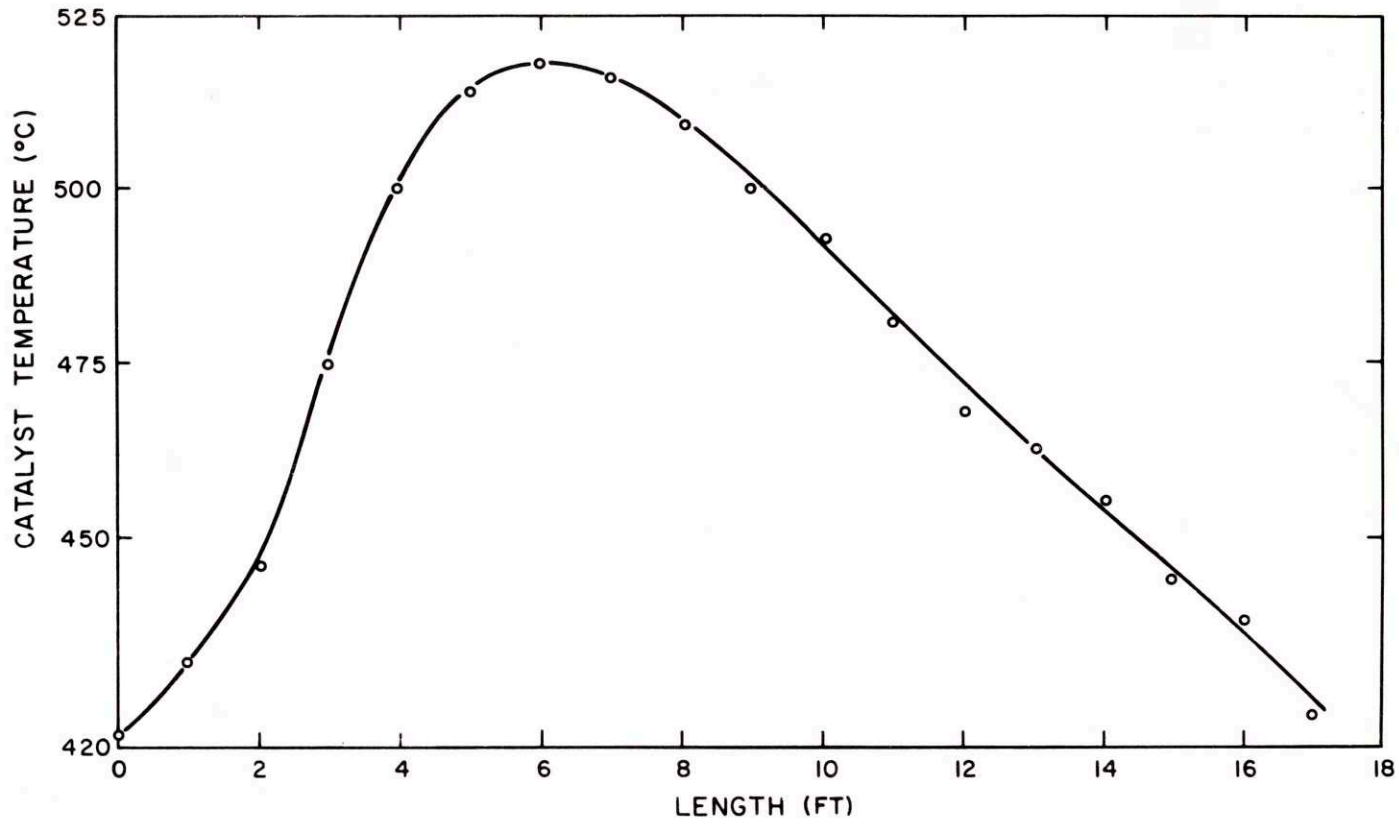


Fig. 3.2 Experimental Temperature Profile in the T.V.A. Reactor

The experimental temperature profile presents a maximum called the "hot spot". In this run the "hot spot" is located 6 feet down the reactor and corresponds to a temperature of 518°C . The location and the magnitude of the "hot spot" was reported to vary with operating conditions and catalyst activity.

Since the catalyst used in this reactor (reduced Iron promoted with Al_2O_3 and K_2O) is deteriorated when exposed to high temperatures, in operating the T.V.A. reactor efforts are made to keep this temperature at as low a level as is possible.

For a given space velocity and feed composition, changes in the hot spot temperature can be achieved by changes in the inlet temperature to the reacting section, that is to say, by different settings of the bypass stream to the heat exchanger section. In fact, it will appear in the next section that changes in feed temperature to the reactor affect not only the hot spot temperature but the production and the stability of the reactor giving rise to the general problems associated with the operating of an "autothermic process".

B. STEADY STATE ANALYSIS OF THE TVA REACTOR

Van Heerden³⁴ was the first to simulate the steady state behavior of a T.V.A. reactor in his study of autothermic processes. Kjaer²¹ later proposed a model which takes into account temperature and concentration variations in both longitudinal and radial directions. The system of three partial differential equations describing this reactor was then approximated by finite difference equations and solved by hand computations. Because of this time-consuming method of solution, the T.V.A. reactor was simulated for one set of parameters only.

Logeais²² returning to the one dimensional model of Van Heerden and with the use of a digital computer carried out an extensive investigation of the

effect of the design and operating variables on the steady state behavior of the T.V.A. reactor.

For a given reactor, and for a given choice of the operating parameters: space velocity, feed composition and operating pressure, Van Heerden and Logeais reported that there is a feed temperature which maximizes the production.

Figure 3.3, obtained from Logeais' results, describes the dependence of the production rate with the top temperature of the reactor. Figure 3.4 relates this top temperature to the feed temperature of the reacting section. The optimum feed temperature which corresponds to a top temperature of 426°C in the present case, is 229°C . Furthermore, the feed temperature of 224°C is found very critical as it is described below:

a. If the feed temperature is larger than 224°C : there are two top temperatures corresponding to one value of the feed temperature. This is to say that there are two different steady state conditions of operation feasible for the reactor. Logeais reported that there are, in fact, two different temperature profiles which would satisfy the steady state equations for the same value of the feed temperature.

Van Heerden and Logeais described the steady state corresponding to the higher conversion as a stable steady state; that is to say, a steady state at which the reactor can operate.

They described the equilibrium corresponding to the lower conversion as an unstable one. The reactor will not operate under these conditions unless provided with the proper control scheme.

In differentiating between stable and unstable conditions of operation, Van Heerden and Logeais used the following concept illustrated in Fig. 3.5 (which is a different method presenting the results described in Fig. 3.4).

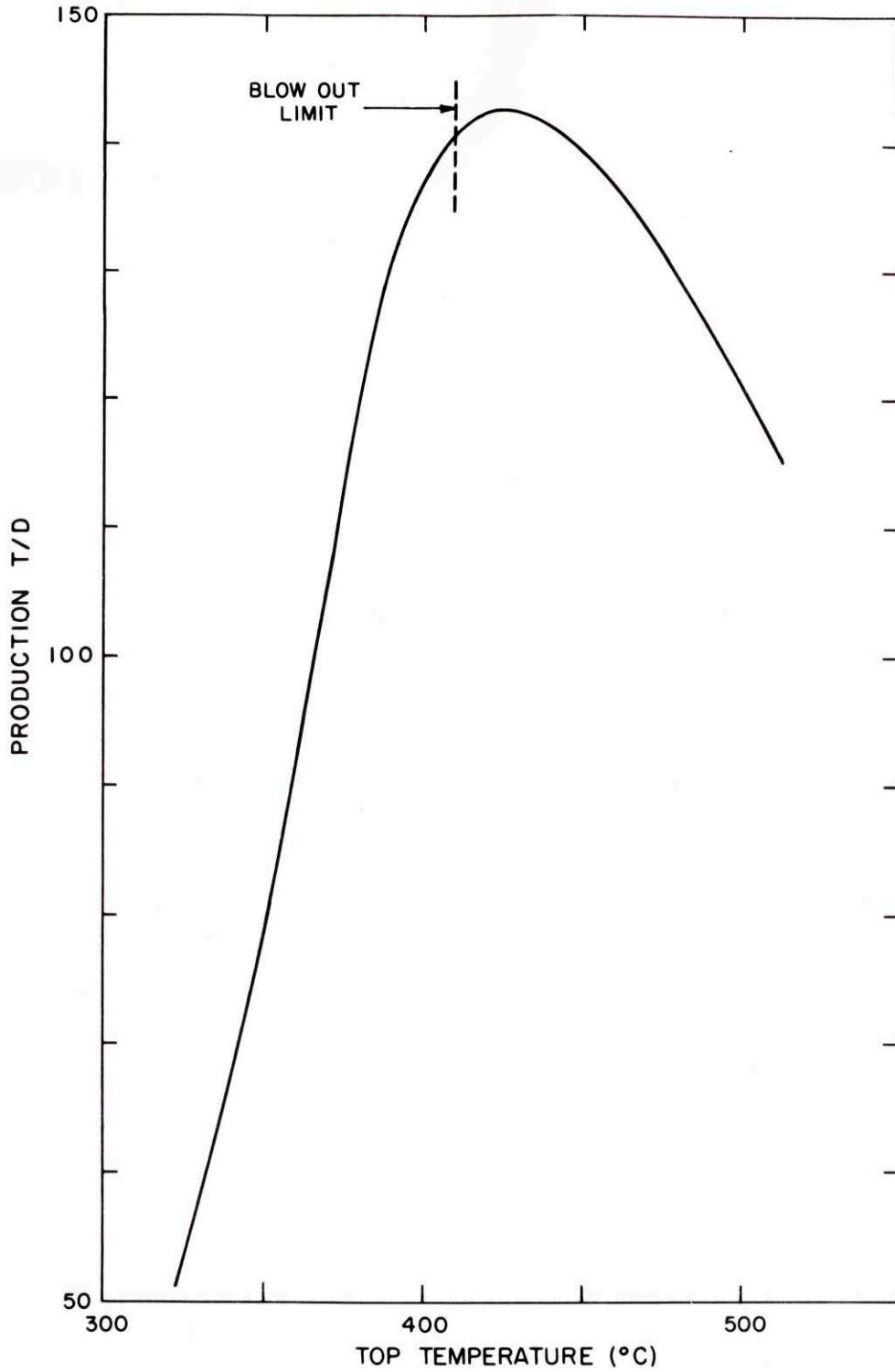


Fig. 3.3 Effect of Top Temperature on Production

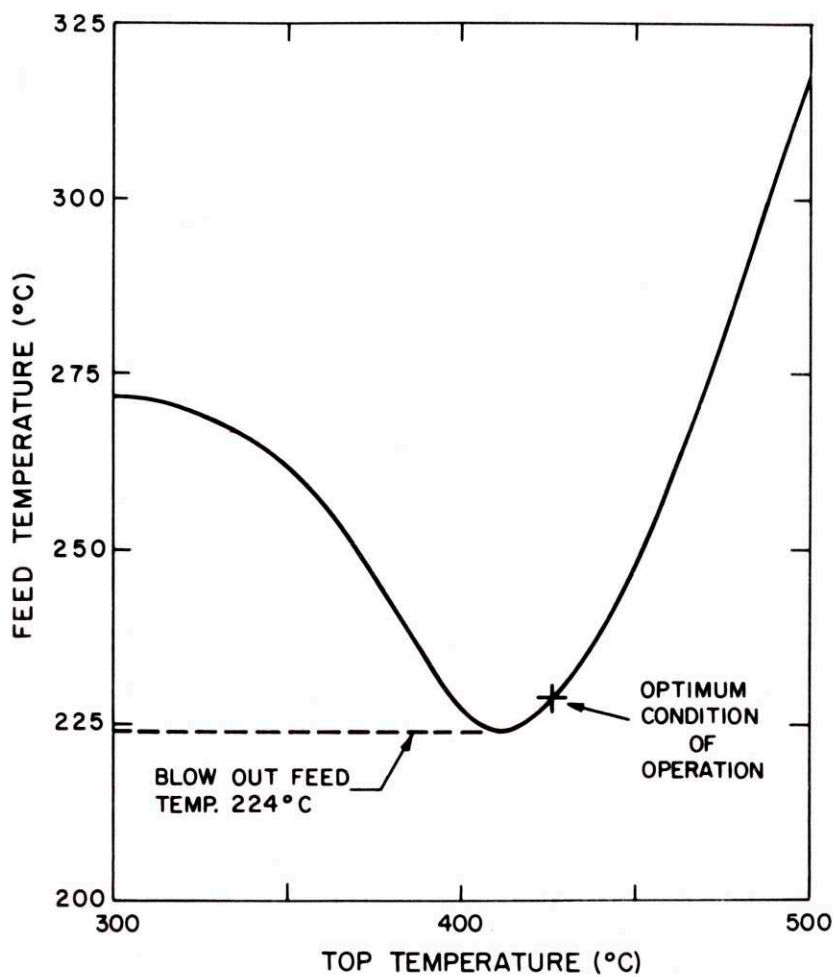


Fig. 3.4 Relationship between Inlet and Top Temperature

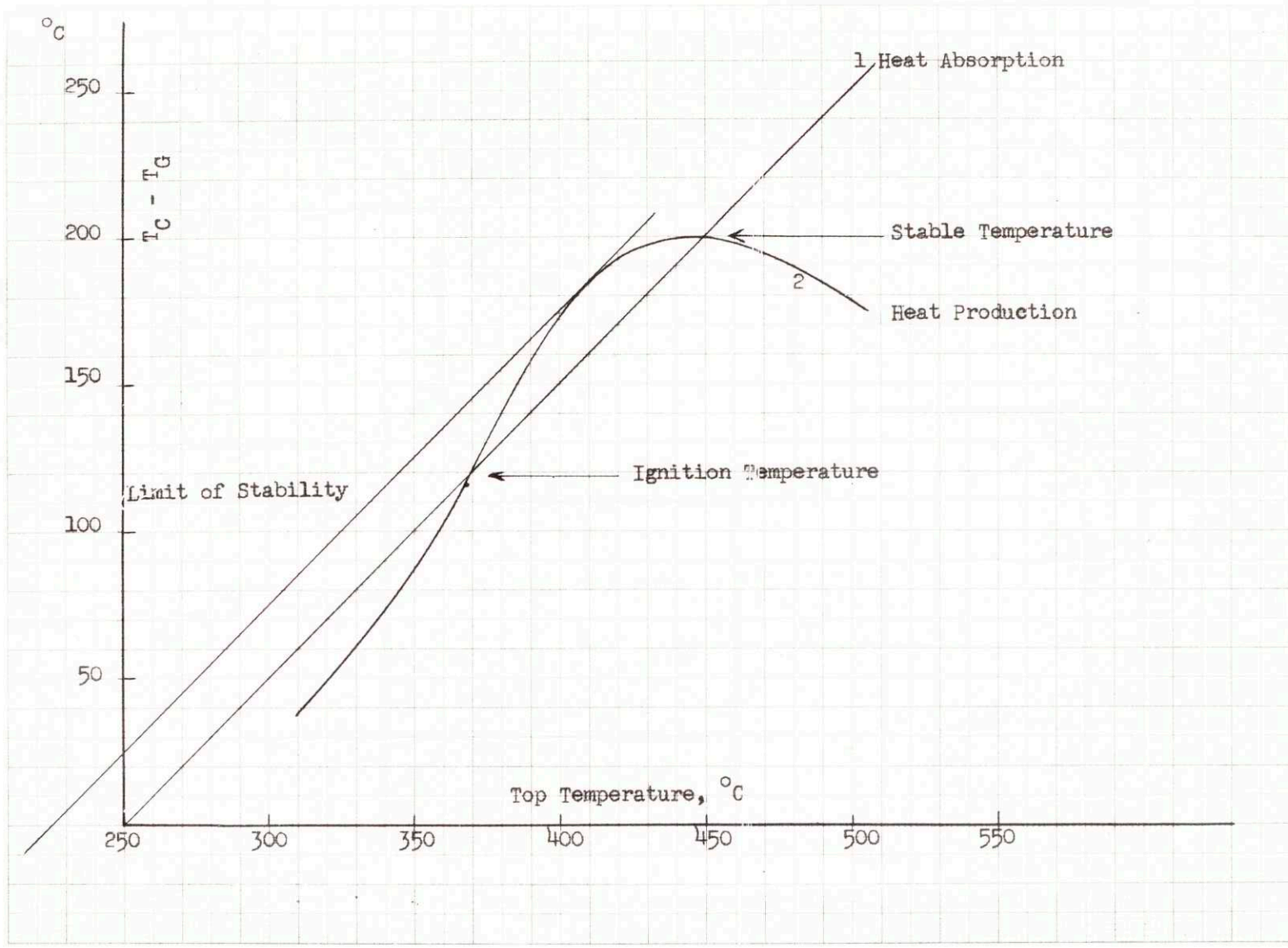
In Fig. 3.5 the difference between the top temperature and the feed temperature ($\Delta T = T_{\text{top}} - T_{\text{feed}}$) is plotted against the top temperature T_{top} for various steady state conditions computed by Logeais. For a given feed temperature T_{F}^* Fig. 3.5 allows one to determine the corresponding top temperature by intersecting the curve already presented with a straight line of equation

$$\Delta T = T_{\text{top}} - T_{\text{F}}^* \quad (3.1)$$

According to the values of T_{F}^* it is seen that the straight line representing Eq. 3.1 intersects the curve at one, two or three points corresponding to one, two or three possible equilibrium top temperatures.

If the ordinates of Fig. 3.5 are multiplied by the average heat capacity of the synthesis gas, it represents a quantity of heat. The straight line represents the amount of heat which is absorbed by the synthesis gases during their ascending travel in the tubes. The curve represents the amount of heat which is available for heat transfer when the top temperature of the reactor is allowed to vary. This amount of heat corresponds to the enthalpy generated by the chemical reaction minus the excess sensible heat convected by the gases at the outlet of the reactor over the sensible heat of the feed gases. The intersections of the straight line and the curve correspond to equilibrium conditions of operation for an autothermic process.

It can be demonstrated that the lower temperature (369°C) represents an unstable equilibrium by considering the effects of small perturbations in the top temperature around this equilibrium value: A slight drop in the top temperature results in the production of too little heat to maintain this temperature since the heat transferred to the feed gas is larger than the heat generated by chemical reaction; this will cause a further decrease in the top temperature. On the contrary, a slight increase in the top temperature results in production of too much heat to be absorbed by the synthesis gases and gives a further increase in the top temperature. For this last reason



IGNITION TEMPERATURE AND STABILITY
 Fig. 3-5

the lower equilibrium temperature is called the "ignition temperature". It is the lowest temperature at which the top temperature must be brought to, before high conversion steady state can exist.

On the other hand, the higher temperature is demonstrated to be a stable equilibrium since small perturbations around this condition will bring back the top temperature to its equilibrium value.

b. If the feed temperature is smaller than 224°C there are no steady state conditions of operation possible in the temperature range investigated. There is, in fact, a steady state condition achievable for feed temperature lower than 224°C but it corresponds to almost no reaction.

This minimum feed temperature of 224°C was called the "blow out feed temperature" by Logeais. In the case presented here the difference between the optimum feed temperature and the blow out feed temperature is of the order of 5°C . The fact that a small difference in feed temperature may create such a large difference in the production of the reactor, shows the sensitivity of the process under investigation to the temperature of the feed.

Logeais showed that the production of the T.V.A. reactor is similarly sensitive to changes in other operating conditions: space velocity, ammonia and inert mole fraction in the feed.

Figures 3.6 and 3.7 obtained from Logeais' work represent the relation between the top and the feed temperature for various values of the space velocity and ammonia concentration in the feed.

An increase in space velocity, that is to say, in feed rate to the reactor or an increase in ammonia recycled in the feed have the effect of increasing the "blow off" feed temperature since the minimum of the curves presented here has increased. Consequently, an increase in flow rate or ammonia mole fraction in the feed which are not compensated by an increase in feed temperature to the reactor will result in a "blow off" of the reactor. Similar

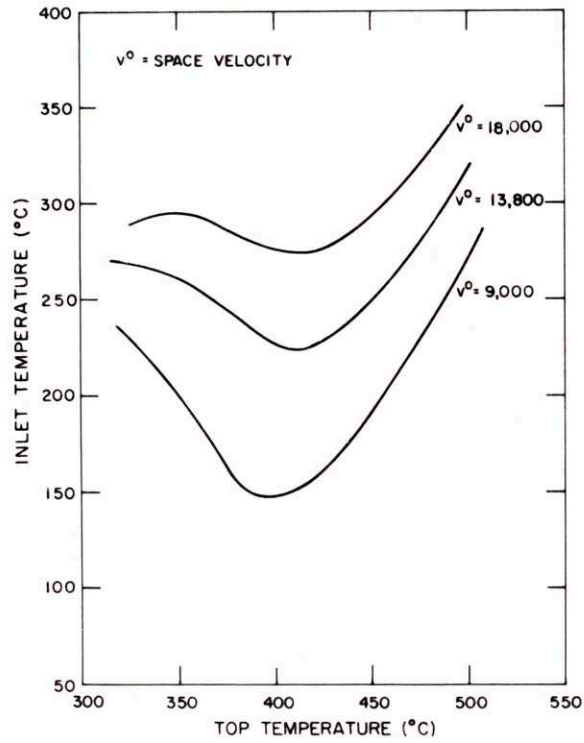


Fig. 3.6 Effect on Stability of Space Velocity

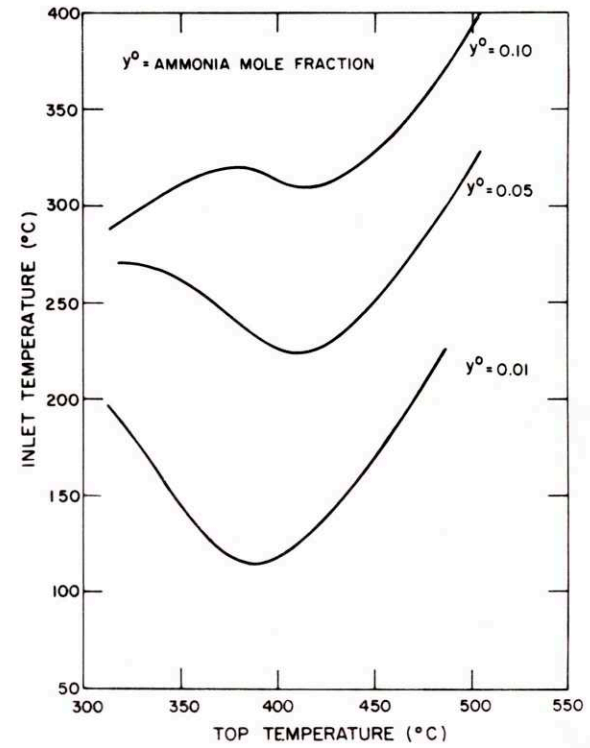


Fig. 3.7 Effect on Stability of Ammonia Mole Fraction in the Feed

"blow off" will result from an increase in the concentration of inert in the feed to the reactor or in a decrease in the catalyst activity. To characterize the stability of the T.V.A. reactor, Logeais determined the changes in operating variables which would result in an increase by 10°C of the "blow off feed temperature". These results appear in Table 3.2.

TABLE 3.2
EFFECT OF OPERATING VARIABLES ON THE
STABILITY OF THE T.V.A. REACTOR

<u>Operating variable</u>	<u>Reference condition</u>	<u>Changes which result in a $+10^{\circ}\text{C}$ change of the "blow out feed temperature"</u>
Space Velocity	13,800	+600
Ammonia Mole Fraction in the Feed	0.05	+0.008
Inert Mole Fraction in the Feed	0.08	+0.024
Catalyst Activity	1.0	-0.05

Assuming that the feed temperature to the reactor remains constant, the changes in operating conditions described in Table 3.2 will "blow out" the reactor if the margin of security existing between the operating feed temperature and the "blow off feed temperature" is smaller than 10°C .

Since it was seen previously that the difference between the optimum feed temperature and the "blow off temperature" is equal to 5°C , the perturbations described in Table 3.2 will, in fact, blow off the reactor operating at its optimum conditions of operation.

Slack, Allgood and Maune²⁹ reported that, in practice, the way to avoid the blow off of the reactor is to operate with a security margin of 15 to 25°C . With the present conditions of operation such a security margin results in a

daily production varying from 141 to 138.5 T/Day compared to the 143 T/Day reported under the optimum conditions of operation.

If the reactor is already designed and is to be operated at maximum production the extreme sensitivity of such a process to changes in the operating conditions suggests the use of automatic control on this equipment. If the reactor is to be designed for a given production, the engineer can avoid operating under the optimum conditions of production by overdesigning the catalyst quantity to be placed in the reactor. For example, a 5 percent increase in catalyst quantity will secure the required production with a 25°C operating margin. At that time economical considerations need to be brought into the picture. In this research the incentive to study the dynamic behavior of the reactor comes from the existence of an optimum feed temperature which is very sensitive to changes in operating variables. Since in this section gain in productivity varying from 1 to 2 percent of the total production on already designed equipment appeared feasible by the use of automatic control, it is the scope of this research to provide the control engineers with the transient data required to design and test various control schemes.

C. LITERATURE SURVEY ON DYNAMICS OF CHEMICAL REACTORS

The control of chemical reactors is playing an important role in maintaining smooth performance of today's chemical plants and in assuring the operation of a process under conditions as close as possible to the most economical operating conditions.

To be able to achieve such a goal, the need to understand the dynamic behavior of each class of chemical reactor emerges. Alan S. Foss¹⁴ defines the dynamics of a reactor as what "encompasses the interplay of the rates of heat generation, heat removal, chemical conversion, material transport and fluid mechanical aspects, and their effects on the transient excursions

of the major reactor variables such as temperature, concentration and pressure."

The first investigations in the field of reaction dynamics began in 1908 with the work of Hirniak¹⁸ on autocatalytic reactions. Both Hirniak and Lotka²³ discovered the effect of positive feedback on the reaction system. Later on the autocatalytic effect of the heat produced by exothermic reactions was studied by Frank Kamenetskii¹⁵ and Salinkov²⁵ in relation with their study of flame stability.

Denbigh¹³ for a reaction taking place in a continuously well stirred reactor and Van Heerden³⁴ for a tubular catalytic reactor, demonstrated the existence of inherently stable and unstable steady states for exothermic reactions whose rate dependence followed the Arrhenius law. Van Heerden classified such processes under the name "autothermic processes". He chose the Haber-Bosh reactor presented before as an example of reactor to characterize the stability problems associated with autothermic processes.

The phenomena describing the dynamics of well stirred reactors are represented by ordinary first order differential equations. For this reason the study of the dynamics of this type of reactor was the first to receive attention. Amundson and his co-workers^{1, 4, 31} carried an extensive study of the stability of reactions performed in stirred tank reactors.

They used the method of nonlinear mechanics as developed by Poincarre, Liapunoff and Minorsky to describe the dynamic behavior of the reactor around a steady state condition of operation. The perturbation method was used to derive transfer functions characterizing the process. Bilous, Block and Piret⁶ have reported transfer functions for several occurring kinetic systems and for the case of a series of well stirred reactors.

The dynamics of tubular reactors are usually described by nonlinear partial differential equations. For this reason the solution of the mathematical systems describing these dynamics is more complex.

Until today, two approaches have been used in this area.

1. Derivation of stability criteria from the steady state condition of operation
2. Description of the dynamic behavior of the reactor through simulation with the hope of defining transfer functions when the reactor operates in the linear range.

Van Heerden,³⁴ by steady state considerations, presented the stability problems associated with the Haber-Bosh reactor in the case of the ammonia synthesis. Logeais²² extended Van Heerden's results by studying the effect on stability of the design and operating variables. Derivation of empirical stability criteria from a large number of steady state results obtained in a tubular reactor were reported by Barkelew,³ but are, in fact, limited to the geometry and the form of kinetics studied. Bilous and Ammundson^{4, 5} using the perturbation theory presented a method to derive transfer functions for a tubular reactor. The method they proposed results in expressions too complicated to be used for control purposes and limited to small perturbations around a given steady state. As soon as the kinetics becomes complicated or the geometry of the reactor different from a simple tube with constant wall temperature the only source left is the simulation.

Grotch and Kipiniak¹⁶ have simulated on a digital computer the transient behavior of a fixed bed adiabatic reactor where butadiene synthesis is performed. They assume that the fluid flowing through the catalyst is at the same temperature as the catalyst particles and that overall rate constants are valid all along the reactor; the expressions describing this system are identical to the equations describing the dynamic of a tubular reactor. Their results were not generalized to other kinetics but used to control and optimize the production of this adiabatic catalytic reactor.

The most recent treatments in the field of reactor dynamics consider the difference between the catalyst temperature and the fluid temperature. Furthermore the effect of the resistance to mass and heat transfer between the catalyst and the fluid is taken into account.

Denbigh and Cannon¹² considered the stability of a catalyst particle from a steady state point of view. Liu Ammundson and Aris^{26, 27} extended Wicke and Vortmayer's^{35, 36, 37, 38} work simulating the transient behavior of a packed bed reactor in which the first order reaction $A \rightarrow B$, is occurring. Their investigation considered both the case of an adiabatic bed, and the case of a constant wall temperature reactor. Their model accounted for mass and heat transfer resistance at the surface of each particle. Under these conditions they reported that some particles along the bed can have one, two or three steady states, one of which is always unstable.

According to Liu, Ammundson and Aris, when in the final steady state each particle has a unique state, the reactor is absolutely stable and unique temperature and composition profiles are obtained from all initial particle temperatures. On the other hand, if any particle in the bed has multiple steady states, the system will be unstable for a certain value of the feed condition and the steady state profile obtained will depend on the initial particle temperature. Even though they computed transients from one steady state condition to another they did not attempt to describe these transients, concerning themselves only with some pathological case of this system.

This brief review of the different attempts to represent mathematically the dynamic behavior of fixed bed catalytic reactors shows that the problems associated with autothermic processes have never been treated from a dynamic point of view. Until today, the only data reported are dealing with the steady state behavior of such processes as it was is presented in Chapter III, Section B.

D. OBJECTIVE OF THE THESIS

In Section B of this chapter the necessity to investigate the dynamic behavior of the T.V.A. reactor appears from the extreme sensitivity of its production to changes in the operating variables. Since the T.V.A. reactor is

a packed bed flow reactor it falls into the class of distributed systems whose dynamics have not been investigated extensively, as it appeared in Section C of this chapter.

The objective of this research is to provide a mathematical model for a T.V.A. reactor which could be solved numerically and would describe the dynamic behavior of this widely used type of reactor. It is the scope of this research to confirm dynamically the unstable nature reported by Logeais and Van Heerden.

The dynamic behavior of the reactor will be described both during a transient resulting in a stable equilibrium, and during a "blow out" of the reactor, in order to characterize the internal feedback existing between the catalyst part and the heat exchanger part of the reacting section. Since the results of this investigation are to be used for the control of the reactor, the linearity of the dynamic results will be investigated. The method of linear control theory will be applied to describe the transient data corresponding to small perturbations. These results will be used in the derivation of a control scheme, which will be tested on the simulation to control for perturbations in the operating variables.

Besides the simulation of the dynamic behavior of the reactor, a major objective of this research lies in the computational method used to solve the mathematical model describing the reactor: It is the scope of this research to test the Stone-Brian method of approximating time and distance derivatives for convective problems in a nonlinear case.

CHAPTER IV

MATHEMATICAL MODEL OF THE T.V.A. REACTOR

A. ASSUMPTIONS USED IN THE DERIVATION OF THE MATHEMATICAL MODEL

In this research the mathematical model representing the dynamic behavior of the reacting section of a T.V.A. reactor is a one dimensional model. The temperature within the catalyst, the cooling tube, and the walls of these tubes varies only in the longitudinal direction. This assumption allows one to lump radially the reactor into four sections:

1. The empty tube section which includes all the feed gases during their ascending travel.
2. The tube wall section which includes all the metal of the wall separating the catalyst from the feed gases.
3. The catalyst section which includes all the catalyst granules.
4. The reacting gas section which consists of the gas flowing through the porous catalyst.

Furthermore, in this investigation the temperature of the reacting gases has been assumed constantly equal to the temperature of the catalyst materials through which they flow.

This additional assumption reduces the model into a three-lump model which is shown in Fig. 4.1.

1. The empty tube section, represented by the temperature T_T
2. The tube wall section, represented by the temperature T_W
3. The reacting section, represented by the catalyst temperature T_C

Throughout the model T_T , T_W and T_C are only functions of two variables time, and distance measured from the point in the reactor where the gases reverse their flow direction.

It has been seen in the description of the reactor that the gases leaving the empty tube section reverse their direction and flow into the catalyst section. In this model the "turn around section," where this change of direction takes place, is assumed to have a negligible hold-up. This is

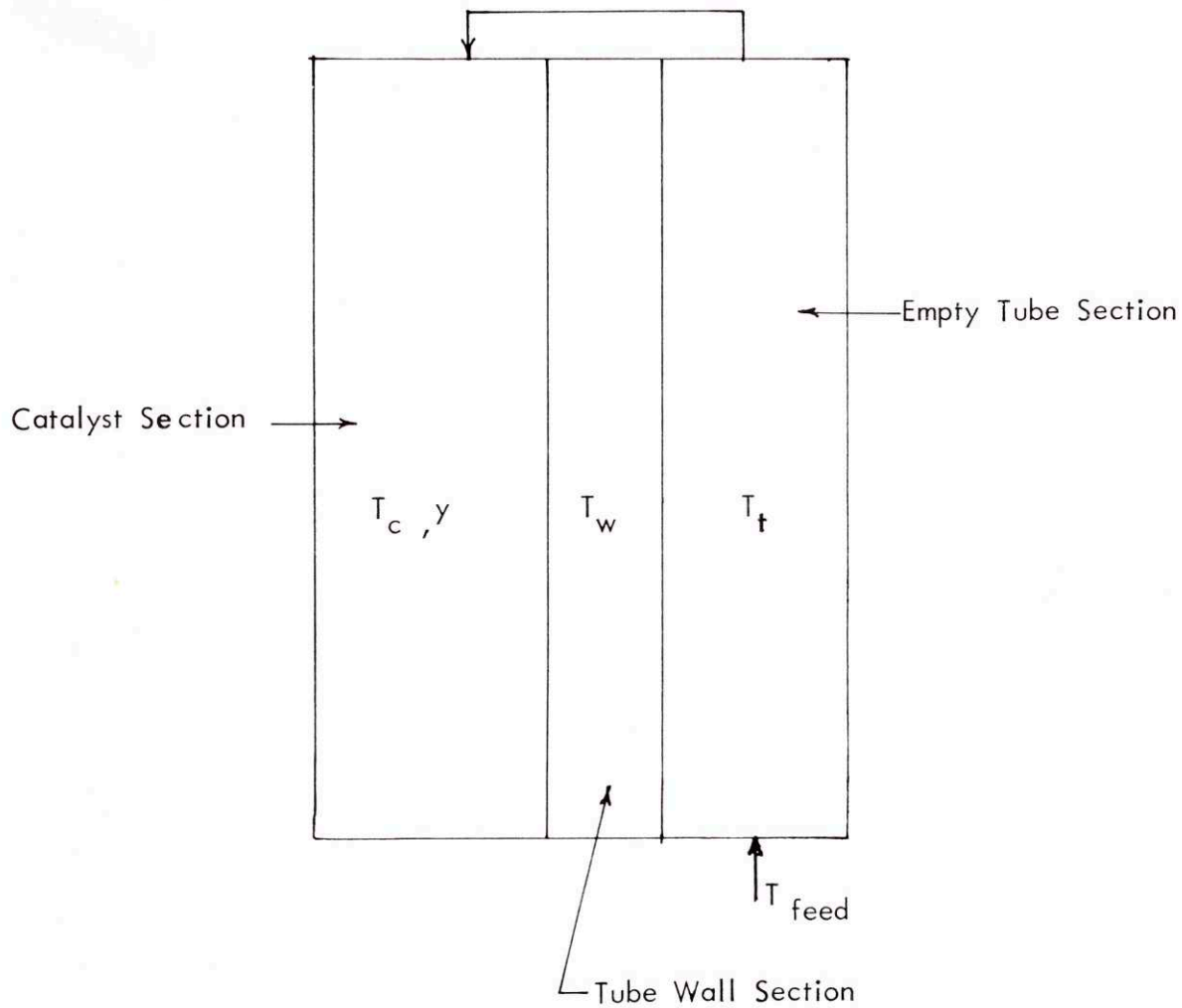


Fig. 4-1 Lumped Model of the Reacting Section of the T.V.A. Reactor

equivalent to say that at each instant the gas fed to the "reacting section" has the temperature and the composition of the gas leaving the empty tube section.

In order to reduce the number of variables the catalyst basket has been neglected in this study. This is equivalent to say that the exchange of heat between the catalyst and its surrounding basket is negligible.

The geometry of the reactor considered, affects the model through the total mass of catalyst, through the total weight of metal in the tube wall section, through the amount of surface area available for heat transfer on each side of the wall and through the coefficients of heat transfer on both sides of the wall, since they are functions of the linear velocity of the gases. The source of perturbation which can affect the reactor are classified into:

flow perturbation corresponding to the changes in feed flow rate and operating pressure.

composition perturbations corresponding to changes of the feed composition.

thermal perturbations corresponding to the changes of the feed temperature.

With each of these sources of perturbation can be associated a time constant which characterizes how fast the system will respond to such a perturbation.

If the reactor is at steady state and if the inlet flow to the reactor suddenly changes, a pressure wave will propagate through the reactor at roughly the speed of sound and the gas velocity at each point in the reactor will start to vary as a function of time and distance. As a result of this change in gas velocity changes in temperature profile will occur until a new steady state distribution of temperature and concentration is achieved in the case of a stable operation or until the reactor "blows out" in the case of an unstable operation. The thermal transient which establishes this new steady state is much slower than the phenomena involved in establishing a new flow pattern. This study only considers the transient behavior resulting from thermal perturbations. It is assumed that changes in flow rate, pressure

and composition propagate instantaneously throughout the reactor and reach at once the steady state value associated with the thermal condition prevailing in the reactor at the considered instant. The results of this study are reported for constant flow rate, pressure and feed composition and present transients due to changes made in the feed temperature.

With the assumptions already presented, a material balance written in the catalyst section and an enthalpy balance written within each of the three sections completely describe the transient behavior of the reactor. In deriving a material balance equation around an infinitesimal volume of reactor the proposed model neglects the

- accumulation of mass within this volume,
- longitudinal diffusion of the reactants,
- effect of pressure drop along the reactor on the rate of reaction.

It is further assumed that the rate of reaction is expressed as a function of temperature, reactant concentration and total pressure only. The same form of overall rate of reaction is considered valid throughout the entire reactor.

In deriving an enthalpy balance around an infinitesimal volume of the empty tube section the proposed model neglects the

- accumulation of enthalpy in the gas phase,
- transfer of enthalpy by conduction within the gas phase,
- transfer of enthalpy resulting from radiation from the tube wall.

The only two fluxes of enthalpy considered in this section are:

- the bulk flow enthalpy flux which represents the enthalpy carried across the surface of the control volume by the mass flow of gas and
- the convected enthalpy flux between the gas and the tube wall.

In deriving an enthalpy balance on the tube wall the proposed model neglects:

- the longitudinal conduction along the metal of the wall
- the energy radiated to the empty tube section and from the catalyst

The only mode of enthalpy transfer considered in this section is the convection of enthalpy from the catalyst section and towards the empty tube section.

Provision is made in this model to store enthalpy within the metal of the wall.

In deriving an enthalpy balance in the catalyst section, the proposed model neglects.

the temperature difference between the catalyst and the gas in this section

enthalpy accumulation in the gas phase present in this section.

The enthalpy modes of transport retained in this section are:

bulk flow enthalpy transfer as defined previously

convection of enthalpy between the catalyst and the tube wall

enthalpy production by chemical reaction

enthalpy diffusion which represents apparent conduction within the gas phase, solid-solid conduction, and radiant energy transmission.

Enthalpy is stored inside the catalyst particles. It will be seen in Chapter V that the introduction of the diffused heat is required to allow for the solution of the simulation. In computing the enthalpy of the flowing gases it has been assumed that, over the range of temperatures prevailing in the converter, molal specific heats remain constant and independent of pressure.

In conclusion, the proposed model is a one-dimensional model which allows for enthalpy storage only inside the catalyst and the metal of the tube wall. The mass balance equation in the catalyst section and the enthalpy balance in the same section are coupled through the temperature and composition dependence of the rate of reaction. The distributed feed back effect due to the coupling between the reacting section and the empty tube section is accounted for through the convected heat term across the tube wall.

In spite of the numerous assumptions built into this model, it is expected to provide the specific dynamic properties of an autothermic process.

Chapter IV, Section C analyses the major assumptions to estimate how close such a model will describe the dynamic behavior of an ammonia reactor as the Tennessee Valley Authority reactor.

B. DERIVATION OF THE MATHEMATICAL MODEL DESCRIBING THE T.V.A. REACTOR

1. Material Balance in the Catalyst Section

The mathematical model under investigation neglects both accumulation of mass in the gas phase, and longitudinal dispersion. Consequently for a given feed composition, the knowledge at a position in the reactor of the mole fraction of one of the four components of the gas mixture (hydrogen, nitrogen, ammonia and inert) is sufficient to determine completely the composition of the gas mixture and the total number of moles flowing per unit of time past that position.

In this investigation the mole fraction y of ammonia is used to express the mole fraction of the three other components. If the feed composition expressed in mole fraction is

$$y_{H_2}^*, y_{N_2}^*, y_{NH_3}^*, y_i^*$$

at a point down the reactor where the mole fraction of ammonia is y the mole fraction of hydrogen, nitrogen and inert obtained by material balance on each of these elements are respectively

$$y_{H_2} = \frac{(y_{H_2}^* + 1.5 y_{NH_3}^*) - (1.5 - y_{H_2}^*) y}{1 + y_{NH_3}^*}$$

$$y_{N_2} = \frac{(y_{N_2}^* + 0.5 y_{NH_3}^*) - (0.5 - y_{N_2}^*) y}{1 + y_{NH_3}^*}$$

$$y_i = \frac{y_i^* (1+y)}{1+y_{\text{NH}_3}^*}$$

As the ammonia synthesis proceeds with a decrease in the number of moles present, the number of moles flowing past a position in the bed is a function of the feed rate (F lb mol/hr) and of the degree of conversion at this position. In term of y , the number of moles flowing past a position in the catalyst bed is expressed by the following expression:

$$F_{(z)} = \frac{F (1+y_{\text{NH}_3}^*)}{(1+y)}$$

A material balance on ammonia around an element of volume $dV = A dz$ of the catalyst bed results in the following terms:

$$\frac{F (1+y_{\text{NH}_3}^*)}{(1+y)} y \quad \text{moles of ammonia entering the section}$$

$$\frac{F (1+y_{\text{NH}_3}^*)}{(1+y)} y + \frac{d}{dz} \left[\frac{F (1+y_{\text{NH}_3}^*)}{1+y} y \right] dz \quad \text{moles of ammonia leaving the section}$$

$$r A dz \quad \text{moles of ammonia produced by chemical reaction}$$

with:

r : number of moles of ammonia produced per unit of time and per unit volume of bulk catalyst (for the conditions of temperature, pressure and reactants concentration,

present at that time, and position). $\frac{\text{lb mole}}{\text{hr ft}^3}$

A : cross-sectional area of the catalyst bed ft^2

z : distance along the catalyst bed (measured from the entrance of the gases into the catalyst section). ft

As mass accumulation is neglected the material balance equation reduces to Eq. 4.1 where A has been replaced by the ratio of the catalyst volume V to the total depth of catalyst l .

$$\frac{dy}{dz} = \frac{V}{F l} \frac{(1+y)^2}{(1+y_{NH_3}^*)} r \quad (4.1)$$

The boundary condition associated with this first order ordinary differential equation is:

$$y = y_{NH_3}^* \quad \text{at} \quad z = 0$$

The rate expression used in this investigation is of the form

$$r = K_1' P_{N_2} \frac{P_{H_2}^{3/2}}{P_{NH_3}} - K_2' \frac{P_{NH_3}^{3/2}}{P_{H_2}}$$

where:

K_1' and K_2'

are two specific rate constants

P_{N_2} , P_{H_2} and P_{NH_3}

are the partial pressures of nitrogen, hydrogen and ammonia.

This expression where fugacities replace partial pressures has been proposed by Mills²⁴ in his study of the kinetics of ammonia synthesis under high pressure. Logeais²² has used the same expression with partial pressure to correlate experimental results obtained by Sidorov²⁸ and to successfully simulate the steady state behavior of the T.V.A. reactor.

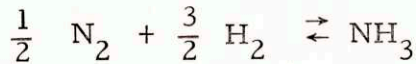
The following expression of the rate of reaction proposed by Logeais has been used in this research:

$$r = K_2' P^{-0.5} \left[K_p^2 P^2 \frac{y_{H_2}^{1.5} y_{N_2}}{y_{NH_3}} - \frac{y_{NH_3}}{y_{H_2}^{1.5}} \right]$$

where:

K_p

is the equilibrium constant of the reaction



P is the total pressure of the system in atmospheres.

The specific rate constant K'_2 is expressed in terms of temperature by the following equation proposed by Logeais.²²

$$K'_2 = \frac{1.75}{T_c} 10^{16} \exp\left(-\frac{20,300}{T_c}\right) \frac{\text{lb mole (Atm)}^{1/2}}{\text{hr ft}^3 \text{ of catalyst}}$$

The rate expression can be expressed as a function of the mole fraction of ammonia alone by Eq. 4.2

$$r = \frac{1.75}{T_c} P^{-0.5} 10^{16} \exp\left(-\frac{20,300}{T_c}\right) \left\{ K_p^2 P^2 \frac{A(B-y)^{1.5}(e-y)}{y} - \frac{Dy}{(B-y)^{1.5}} \right\} \quad (4.2)$$

The dimensionless groups A, B, C and D are function of the feed composition alone through the relations:

$$A = \frac{(1.5 - y_{\text{H}_2}^*)^{1.5} (0.5 - y_{\text{N}_2}^*)}{(1 + y_{\text{NH}_3}^*)^{2.5}}$$

$$B = \frac{y_{\text{H}_2}^* + 1.5 y_{\text{NH}_3}^*}{1.5 - y_{\text{H}_2}^*}$$

$$C = \frac{y_{\text{N}_2}^* + 0.5 y_{\text{NH}_3}^*}{0.5 - y_{\text{N}_2}^*}$$

$$D = \left[\frac{1 + y_{\text{NH}_3}^*}{1.5 - y_{\text{H}_2}^*} \right]^{1.5}$$

After replacing the rate expression r by its value in Eq. 4.1 and normalizing for distance, and temperature, the material balance equation is written

$$\frac{dy}{da} = \frac{A}{T_{ref} V_o} \exp \left(- \frac{25.375}{v} \right) \frac{1}{v} \left[L^2 \frac{A (\beta - y)^{1.5} (\epsilon - y)}{y} - \frac{2y}{(\beta - y)^{1.5}} \right] \frac{(1+y)^2}{1+y} \quad (4.3)$$

- with
- a = normalized distance = z/l
 - l = total length of the catalyst section
 - v = T_c/T_{ref} = normalized catalyst temperature
 - A = $1.75 \cdot 10^{16} P^{-0.5} \times 359 = 6.283 \cdot 10^{18} P^{-0.5}$
 - V_o = space velocity = number of cubic feed of gas (under normal conditions) fed per unit time and per unit volume of catalyst
 - V_o = $\frac{F \times 359}{V} \frac{1}{hr}$
 - L = $K_p P$

The effect of catalyst activity on this equation appears in the dimensionless group

$$\frac{A}{T_{ref} V_o}$$

The dependence of the ammonia mole fraction y with feed rate is included inside the same group through the space velocity V_o . As the reaction is reversible and proceeds with a change in the number of moles, the effect of pressure on the rate expression appears inside two groups $\frac{A}{T_{ref} V_o}$ and L . As the reaction is reversible the effect of temperature on the rate expression appears also in two groups

$$\frac{1}{v} \exp \left(- \frac{25.375}{v} \right) \text{ and } L$$

It was shown before that the effect of feed composition appears inside groups

A, β, ϵ and 2 .

2: Energy Balance

a. Energy balance in the empty tube section: An energy balance around an element of gas of volume $a dz$ inside the empty tube section results in the following terms:

$$F \bar{C}_{po} (T_T - T_B) \quad \text{enthalpy convected in}$$

$$F \bar{C}_{po} (T_T - T_B) - \frac{d}{dz} \left[F \bar{C}_{po} (T_T - T_B) \right] dz \quad \text{enthalpy convected out}$$

$$\frac{h_1 S_1}{I} (T_W - T_T) dz \quad \text{enthalpy transferred from the wall}$$

- with
- a = cross sectional area of the tubes
 - T_T = Temperature of the gas inside the tube
 - T_W = Temperature of the tube wall
 - T_B = Base temperature used to express the enthalpy (298°K will be used)
 - \bar{C}_{po} = Average molal heat capacity of the feed gas measured from the base temperature BTU/lb mole °F
 - h_1 = Average heat transfer coefficient between the tube wall and the gas in the empty tube section BTU/hr sq ft °F
 - S_1 = Total surface area available for heat transfer between the tube wall and the gas in the empty tube section ft²

The mathematical model under investigation neglects heat conduction along the gas phase, radiation from the tube wall, accumulation of enthalpy within the gas phase and assumes that \bar{C}_{po} is a constant independent of temperature; with these assumptions the energy balance equation for the empty tube section is written

$$\frac{dT_T}{dz} = \frac{h_1 S_1}{I F \bar{C}_{po}} (T_T - T_W) \quad (4.4)$$

which after normalization for temperature and distance reduces to Eq. 4.5

$$\frac{dw}{da} = \beta (w - m) \quad (4.5)$$

- with
- w : normalized temperature in the empty tube section = $\frac{T_T}{T_{ref}}$
 - m : normalized temperature of the tube wall section = $\frac{T_W}{T_{ref}}$

$\beta = \frac{h_1 S_1}{F \bar{C}_{po}}$ is the number of transfer units which characterizes one heat exchanger.

The boundary condition associated with this first order ordinary differential equation is

$$w = w_{feed} \text{ for } a = 1.0$$

b. Energy balance in the tube wall: With the assumptions presented at the beginning of this chapter an energy balance around an element of length dz of tube wall results in the following terms

$$\frac{h_2 S_2}{1} (T_c - T_w) dz \quad \text{heat transferred from the catalyst}$$

$$\frac{h_1 S_1}{1} (T_w - T_T) dz \quad \text{heat transferred to the empty tube section}$$

$$\frac{M C_{pm}}{1} \frac{dT_w}{dt} dz \quad \text{heat stored inside the metal of the tube}$$

with h_2 average heat transfer coefficient between the wall and the catalyst $\frac{BTU}{hr ft^2 \text{ } ^\circ F}$

$S_2 =$ total surface area available for heat transfer between the catalyst and the tube wall. ft^2

$T_c =$ temperature of the catalyst section $^\circ F$

$M =$ total weight of the metal inside the tube wall lb

$C_{pm} =$ average heat capacity of the metal of the wall $BTU/lb \text{ } ^\circ F$

$t =$ time hr

The energy balance inside the tube wall is

$$M C_{pm} \frac{dT_w}{dt} = h_2 S_2 (T_c - T_w) - h_1 S_1 (T_w - T_T)$$

This equation normalized for temperature and time takes the form of Eq. 4.7

$$g \frac{dm}{d\theta} = v - m - d(m-v) \quad (4.7)$$

with

$v =$ normalized catalyst temperature $\frac{T_c}{T_{ref}}$

$d = \frac{h_1 S_1}{h_2 S_2}$ ratio of the resistance to heat transfer on both side of the wall.

$$g = \frac{M C_{pm}}{W C_{pc}} = \frac{\text{total heat capacity of tube wall}}{\text{total heat capacity of catalyst}}$$

W = total mass of catalyst lb

C_{pc} = average heat capacity of the catalyst BTU/lb °F

The normalized time θ is given by Eq. 4.8

$$\theta = \frac{h_2 S_2}{W C_{pc}} t \quad (4.8)$$

$\frac{W C_{pc}}{h_2 S_2}$ is the time in hours required to lower the temperature of the whole catalyst bed by 1°C when the difference of temperature between the catalyst and the wall is 1°C.

The boundary condition associated with Eq. 4.7 is

$$m(a) = f(a) \text{ at } \theta = 0.$$

which is equivalent to say that the temperature distribution in the wall of the tube is known at time zero.

c. Energy balance in the catalyst: As the reaction proceeds, the total heat capacity of the flowing gas changes. If $F \bar{C}_{po}$ is the heat capacity of the gas fed per unit time, at a position down the reactor where the mole fraction of ammonia is y the heat capacity of the gas flowing per unit time past this position is

$$F \left[\bar{C}_{po} - \Delta C \frac{y - y_{NH_3}^*}{1 + y} \right]$$

where

$$\bar{C}_{po} = y_{N_2}^* C_{p_{H_2}} + y_{N_2}^* C_{p_{N_2}} + y_{NH_3}^* C_{p_{NH_3}} + y_i^* C_{p_i}$$

is the average feed molal heat capacity. ($C_{p_{H_2}}$, $C_{p_{N_2}}$, $C_{p_{NH_3}}$, C_{p_i} are average molal heat capacity of each component measured between the base temperature and an average bed temperature assumed constant).

$\Delta C = 1.5 C_{p_{H_2}} + 0.5 C_{p_{N_2}} - C_{p_{NH_3}}$ is the decrease in molal heat capacity of the mixture resulting from the formation 1 lb mole of ammonia. In the

remaining part of this chapter the ammonia mole fraction in the feed will be represented by y^* only.

The total enthalpy of the gas flowing past a position in the bed is equal to the sum of the sensible heat of the gas and of the enthalpy of the ammonia expressed as function of the standard enthalpy of formation at the base temperature ΔH_o . With the assumptions presented at the beginning of this chapter, this amounts to:

$$F \left[\bar{C}_{po} - \Delta c \frac{y-y^*}{1+y} \right] [T_c - T_B] + F [\Delta H_o] \left[y^* + \frac{y-y^*}{1+y} \right]$$

The energy balance written around an element of volume $A dz$ of catalyst results in the following terms:

enthalpy convected in:

$$F \left[\bar{C}_{po} - \Delta c \frac{y-y^*}{1+y} \right] [T_c - T_B] + F \Delta H_o \left[y^* + \frac{y-y^*}{1+y} \right]$$

enthalpy diffused in:

$$- D' A \frac{\partial T_c}{\partial z}$$

enthalpy convected out

$$F \left[\bar{C}_{po} - \Delta c \frac{y-y^*}{1+y} \right] [T_c - T_B] + F \Delta H_o \left[y_{NH_3}^* + \frac{y-y^*}{1+y} \right] + \frac{\partial}{\partial z} \left\{ F \left[\bar{C}_{po} - \Delta c \frac{y-y^*}{1+y} \right] [T_c - T_B] + F \Delta H_o \left[y^* + \frac{y-y^*}{1+y} \right] \right\} dz.$$

enthalpy diffused out

$$- D' A \frac{\partial T_c}{\partial z} + \frac{\partial}{\partial z} \left[- D' A \frac{\partial T_c}{\partial z} \right] dz$$

Enthalpy transferred to the wall

$$\frac{h_2 S_2}{l} (T_c - T_w) dz$$

Enthalpy accumulated inside the catalyst

$$\frac{WC_{pc}}{1} \times dz \times \frac{\partial T_c}{\partial t}$$

where D' = effective Longitudinal diffusion = $\frac{BTU}{ft \times hr \times ^\circ F}$

The enthalpy balance in this section writes

$$\begin{aligned} \frac{D'V}{1} \frac{\partial^2 T_c}{\partial z^2} - F [C_{po} - \Delta c \frac{y-y^*}{1+y}] \frac{\partial T_c}{\partial z} - \frac{h_2 S_2}{1} (T_c - T_w) \\ - F [\Delta H_o - \Delta c (T_c - T_B)] \frac{1+y^*}{(1+y)^2} \frac{\partial y}{\partial z} = \frac{WC_{pc}}{1} \frac{\partial T_c}{\partial t} \quad (4.9) \end{aligned}$$

The term in $\frac{\partial y}{\partial z}$ can be replaced by its value taken from Eq. 4.1

$$\frac{F(1+y)^*}{(1+y)^2} \frac{\partial y}{\partial z} = \frac{V}{1} \times r$$

The normalized energy equation in the catalyst section writes

$$\begin{aligned} - D \frac{\partial^2 v}{\partial a^2} + s (1 - h \frac{y-y^*}{1+y}) \frac{\partial v}{\partial a} + v - m \\ + \frac{\partial v}{\partial \theta} - [e + h (v - 0.3725)] s \gamma \frac{1}{v} \exp [- \frac{\eta}{v}] \\ \times \left[\frac{L^{12} \mathcal{A} (\mathcal{B} - y)^{1.5} (\mathcal{E} - y)}{y} - \frac{\mathcal{D} y}{(\mathcal{B} - y)^{1.5}} \right] = 0 \quad (4.10) \end{aligned}$$

with

$$D = \frac{D'V}{1^2 h_2 S_2}$$

$$h = \frac{\Delta C}{C_{po}}$$

$$e = \frac{\Delta H_o}{T_{ref} C_{po}}$$

$$s = \frac{F C_{po}}{h_2 S_2}$$

$$\gamma = \frac{A}{T_{ref} V_o}$$

$$\eta = \frac{20,300}{T_{ref}}$$

The dimensionless group D represent the ratio of the effect of diffusion to the effect of heat transfer towards the wall of the reactor.

s is equal to the length of a heat transfer unit for the catalyst section taken as a tubular reactor.

e is a function of the starting composition through \overline{C}_{po} and represent, how many times T_{ref} the temperature of 1 mole of feed increases every time 1 mole of ammonia is produced at the base temperature.

The fact that the reaction proceeds with a change in sensible heat and at various temperatures is taken into account through the two correcting factors.

$$(1 - h \frac{y-y^*}{1+y})$$

and

$$e + h (v-0.3725)$$

d. Boundary conditions associated with the energy equation inside the catalyst section: The boundary condition imposed at the entrance of the catalyst section is obtained by computing the enthalpy flux flowing past the entrance position of the reactor from the left end side and from the right end side of this position.

At the beginning of this section the assumption is made that the gas leaving the tube section enters a "turn-around section" of no heat capacity where, the gases are well mixed. Consequently the temperature of the gas in this Section is uniform and equal at each instant to the temperature of the gas at the exit of the tube section. On the side of the entrance location facing this section no diffusion occurs. The enthalpy flux entering the reactor reduces to the enthalpy transported by bulk flow, which is written

$$F \overline{C}_{po} (T_{T_{a=0}} - T_B) + F \Delta H_o y^*$$

The enthalpy flux flowing past the location inside the catalyst section within an infinitesimal distance of the entrance is composed of the enthalpy trans-

ported by bulk flow and of the enthalpy diffused longitudinally. It is written

$$F \overline{C}_{po} (T_{c_{a=0}} - T_B) + F \Delta H_o y^* - D'A \left(\frac{\partial T_c}{\partial z} \right)_{a=0}$$

D' being the effective heat diffusion in the catalyst section. By equating the two values of the enthalpy flux the relation between $T_{c_{a=0}}$ and $T_{T_{a=0}}$ is obtained

$$T_{c_{a=0}} = T_{T_{a=0}} + \frac{D'A}{F \overline{C}_{po}} \left(\frac{\partial T_c}{\partial z} \right)_{a=0} \quad (4.11)$$

The boundary condition expressed under this form is equivalent to the expression proposed by Danckwerts¹¹ and later discussed by Wilhelm and Wehner.³⁹

In the section dealing with finite approximation of the partial differential equation the entrance boundary condition will be introduced by making a similar enthalpy balance on a slice of finite dimension rather than to approximate directly Eq. 4.11.

The same concept of enthalpy flux applied at the end of the reactor results in the equation

$$\begin{aligned} T_{c_{z=1-\epsilon}} - \frac{D'A}{F \left[\overline{C}_{po} - \Delta c \frac{y_{z=1} - y}{1 + y_{z=1}} \right]^*} \left(\frac{\partial T_c}{\partial z} \right)_{z=1-\epsilon} \\ = T_{c_{z=1+\epsilon}} - \frac{D''A}{F \left[\overline{C}_{po} - \Delta c \frac{y_{z=1} - y}{1 + y_{z=1}} \right]^*} \left(\frac{\partial T_c}{\partial z} \right)_{z=1+\epsilon} \end{aligned}$$

where D'' is the effective conductivity in the section following the catalyst.

Intuitively one cannot imagine a discontinuity at the outlet of the reactor and as ϵ becomes smaller the temperature on both sides of the outlet boundary must tend to the same limit.

$$T_{c_{z=1-\epsilon}} = T_{c_{z=1+\epsilon}} \quad \text{as } \epsilon \rightarrow 0$$

Under these conditions the boundary equation reduces to

$$\left(\frac{\partial T_c}{\partial z} \right)_{z=1-\epsilon} = \frac{D''}{D'} \left(\frac{\partial T_c}{\partial z} \right)_{z=1+\epsilon}$$

When the packed section is followed by a section where no diffusion occurs ($D'' = 0$) the boundary equations reduces to the form proposed by Danckwerts¹¹ that is to say

$$\left(\frac{\partial T_c}{\partial z} \right)_{z=1} = 0 \quad (4.12)$$

In the section dealing with the finite approximation of the partial differential equation the same flux balance will be made on a slice of finite dimension and use will be made of Eq. 4.12 in computing the heat diffused out of the considered volume of catalyst.

C. DISCUSSIONS OF THE ASSUMPTIONS INCLUDED IN THE MATHEMATICAL MODEL

In this section the more critical assumptions introduced into this model are discussed and the steady state results obtained with the present model will be compared with the experimental results presented in Section B of Chapter III obtained by Slack, Allgood and Maune.²⁹

1. Effect of Neglecting Radial Temperature Gradient

In the T.V.A reactor previously investigated by Kjaer²¹ and Logeais²² experimental results provided by Allgood and reproduced in Table 4.1 show a strong dependence in the temperature at various depths in the reactor with the radial location of the thermocouple measuring this temperature. The off center thermocouple indications differ from the center temperature by more than 80°C near the outlet of the reactor. This temperature difference which if representative of what happens in the reactor will invalidate the present

Table 4.1

Experimental Temperature Profile

Location Ft.	Center Thermocouple °C	off Center Thermocouple °C
0	428	421
1	439	432
2	456	446
3	493	475
4	528	500
5	544	514
6	549	518
7	549	516
8	546	509
9	543	500
10	540	493
11	535	481
12	532	468
13	529	463
14	523	455
15	517	444
16	511	438
17	505	424

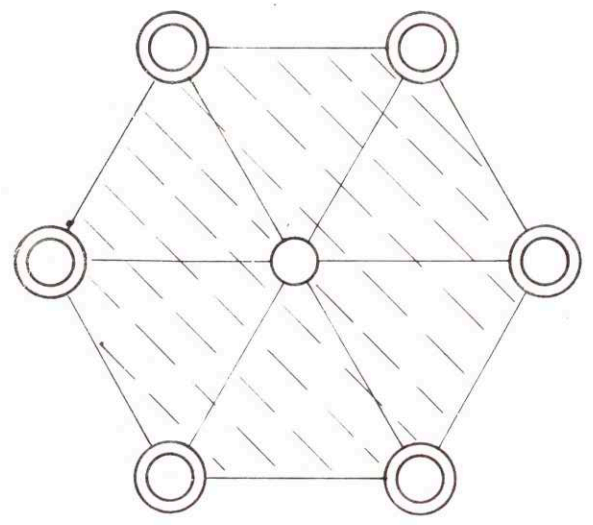
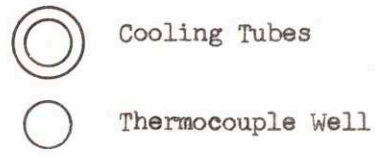
assumption, was explained by both Kjaer and Logeais in terms of the location of the thermocouple well with respect to the cooling tubes. Figure 4.2 shows the thermocouple arrangement for both the center thermocouple and the outer thermocouple. The center thermocouple well replaces a cooling tube while the off center well is located in the middle of the equilateral triangle formed by three cooling tubes.

The hatched area of Fig. 4.2 is cooled by two cooling tubes in the case of the outer thermocouple and by three cooling tubes in the case of the off center thermocouple. This qualitative explanation proposed first by Kjaer was confirmed quantitatively by Logeais who was able to match the indications of the center thermocouple for the same feed conditions by using in his model a heat transfer area equal to $2/3$ the heat transfer area really present. Kjaer, furthermore, computed radial temperature profiles inside the T.V.A. reactor due to the existence of the basket surrounding the catalyst and the cooling tube embedded in the catalyst. He concluded that the radial temperature variations are practically negligible for converters with internal cooling.²¹

Even though complete experimental evidence supporting this assumption is lacking, it is the author's belief that the assumption of uniform radial temperature and composition is justified as a first approach to the description of the dynamic behavior of this class of reactor.

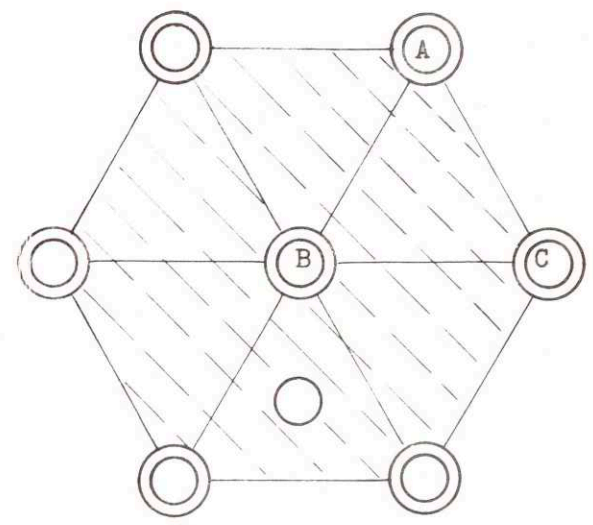
2. Temperature Difference between Catalyst and Gas

The magnitude of the steady state difference in temperature between the catalyst and the gas flowing through it has been investigated experimentally by Jakob²⁰ for the case of hydrogenation of ethylene. He found a temperature difference of the order of 1°C . Wilhelm⁴⁰ reported that experiences in his laboratory indicate this order of magnitude for moderate reactions.



Center Thermocouple

The thermocouple well replaces
a cooling tube



Outer Thermocouple

THERMOCOUPLE ARRANGEMENT

Fig. 4-2

Since the reaction takes place on the catalyst particle, the steady state difference in temperature between the catalyst T_c and the gas flowing through it T_G can be expressed to a first approximation by the equation

$$T_c - T_G = \frac{\Delta H r}{h_v} \quad (4.13)$$

where ΔH is the heat of reaction (BTU/lb mole), r the reaction rate (lb mole/hr ft cube of catalyst), h_v the heat transfer coefficient per unit volume of catalyst. Gamson, Thodos and Hougen¹⁹ have proposed a correlation for the heat transfer coefficient between gas and solids in packed beds which can be used in this section to estimate the steady state temperature difference between the catalyst pellet and the gas flowing through it.

$$h = \frac{h_v}{a_v} = 1.064 G C_p N_{pr}^{-2/3} (N_{re'})^{-0.41} \quad (4.14)$$

for $350 < N_{re'} < 4000$

where a_v is the particle surface area per unit bed volume sq ft/cubic ft.

G mass velocity lb/sq ft, hr

C_p heat capacity of gas BTU/16°F

$N_{re'}$ modified Reynolds number $\frac{D_p G}{\mu}$

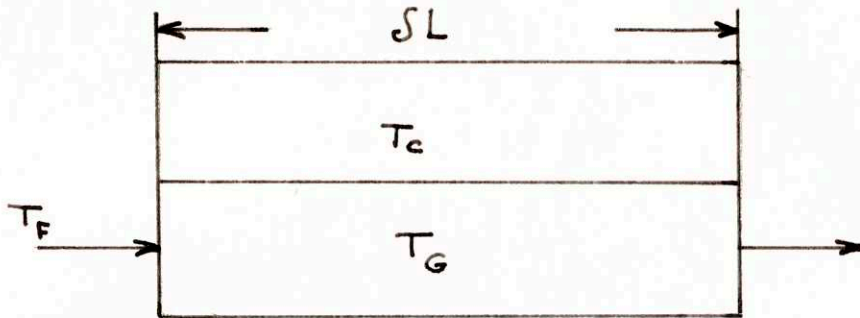
N_{pr} Prandlt number

D_p particle diameter (ft)

Under the conditions existing in the T.V.A. reactor the maximum temperature difference computed exists at the entrance of the reactor where the rate of reaction is maximum and amounts to 2.3°C. This difference in temperature decreases as one proceeds down the reactor to amount to 0.6°C at the middle of the reactor and 0.4°C at the outlet. These results confirm the 2.2°C maximum figure reported by Kjaer.²¹

It appears that neglecting the temperature difference between the catalyst and the gas flowing through it; is justified for steady state computations. In order to prove that this justification can be extended to the

transient case a very simple model is proposed which can show how fast the gases flowing through the bed at a certain location will respond to changes in the catalyst temperature at that location.



The dynamic heat balance equation relating the temperature of the gas in the slice of length δL , considered as a well stirred tank, to the temperature of catalyst is

$$G A C_p (T_G - T_F) + \epsilon A \delta L \rho_g C_{p_g} \frac{dT_G}{dt} = A \delta L h_v (T_C - T_G) \quad (4.15)$$

where A is the cross-sectional area of the reactor (empty), δL is the length element over which the temperature can be considered as constant ρ_g the density of the flowing gases, ϵ the void fraction of the catalyst.

If one considers only changes in the catalyst temperature the transfer function relating the Laplace transform of the changes in gas temperature $\delta \bar{T}_G$ to the Laplace transform of the changes in catalyst temperature $\delta \bar{T}_C$ is written

$$\frac{\delta \bar{T}_G}{\delta \bar{T}_C} = \frac{\frac{h_v}{\epsilon \rho_g C_{p_g}}}{s + \left[\frac{G}{\delta L \epsilon \rho_g} + \frac{h_v}{\epsilon \rho_g C_{p_g}} \right]} \quad (4.16)$$

This equation represents the response of a first order system whose time constant τ is represented by Eq. 4.17

$$\tau = \frac{1}{\frac{G}{\delta L \epsilon \rho_g} + \frac{h_v}{\epsilon \rho_g C_{p_g}}} \quad (4.17)$$

In order to estimate how fast the temperature of the gas changes with changes in the catalyst temperature it is useful to compare the value of τ so defined with the time constants associated with the other transient phenomena.

It should be noted that the present model is only approximate since it breaks the reactor down into a series of well stirred tanks of length δL . At the limit, as δL goes to zero the series of ordinary differential equations becomes a partial differential equation of the form

$$N_T \frac{\partial \bar{T}_G}{\partial L} + (\tau_T s + 1) \bar{T}_G = \bar{T}_C \quad (4.18)$$

where

$$N_T = \frac{G}{\epsilon \rho_g}$$

$$\tau_T = \frac{\epsilon \rho_g C_{p_g}}{h_v}$$

Conclusions are almost impossible to derive from this partial differential equation without solving it since T_C is in this case function of distance .

Nevertheless Eq. 4.17 shows that always

$$\tau < \frac{\epsilon \rho_g C_{p_g}}{h_v}$$

The upper limit of τ encountered in this reactor is of 0.07 seconds. Consequently if the catalyst temperature at any location changes suddenly because of changes in the rate of reaction it would take less than 0.3 sec. (4 time constants) for the gas flowing through it to approach the new steady state value associated with this catalyst temperature. The analysis presented in this section justifies the assumptions made in neglecting the temperature difference between the catalyst and the gases.

3. Relative Magnitude of Enthalpy Storage

The enthalpy is stored in the reactor inside the gas phase in the empty tube section and in the catalyst section, inside the wall metal and inside the catalyst pellets. The enthalpy storage will arise primarily into the system having the higher heat capacity, that is to say, inside the metal of the wall and in the catalyst pellets.

Table 4.2 presents the relative magnitude of the heat-capacity in each section of the reactor. For comparison purposes, the results are presented as the ratio of the heat capacity of each section to the heat capacity of the catalyst.)

Table 4.2

Total heat capacity of catalyst	1.0
Total heat capacity of tube wall	0.30
Total heat capacity of gas in the tube section	0.007
Total heat capacity of gas in the catalyst section	0.025*

* A void fraction of 1/2 was used in this estimate

From the figures reported in Table 4.2 it is clear that the accumulation of energy inside the metal of the wall cannot be neglected in this investigation. Furthermore, the accumulation of enthalpy in the gas phase both in the empty tube section and in the catalyst representing less than 3 percent of the total heat storage capacity can be neglected.

4. Residence Times Compared to Thermal Time Constants

In Section A of Chapter IV it was seen that the proposed model does not take into consideration the flow and pressure variations during a transient and, furthermore, neglects the accumulation of mass in the gas

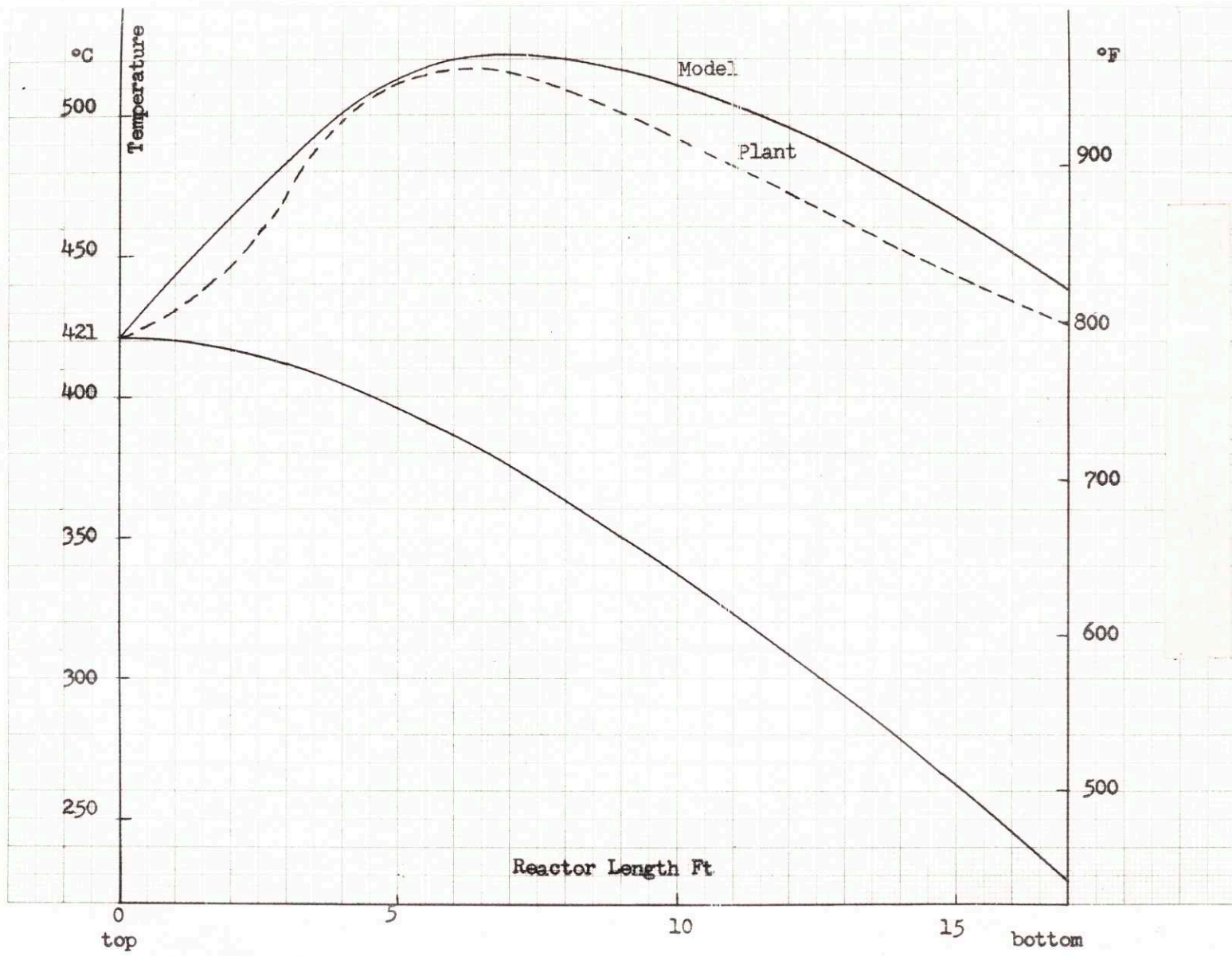
phase. This simplification was proposed in view of the small residence time experienced by the gas in the reactor compared to the time constants associated with the transient of the system.

For the standard conditions investigated the residence time of the gas in the empty tube section amounts to 2 sec. while in the catalyst section it amounts to 15 seconds. On the contrary, if by analogy with a heat exchanger the time required for a perturbation entering the top of the reactor to travel the entire reactor is computed, a value of 375 seconds is found. Always by analogy with a heat exchanger if the ratio of heat capacity of the catalyst per unit volume of reactor to the amount of heat transferred per unit volume of reactor per unit time for a one-degree driving force is used to characterize the rate at which the reactor responds to a thermal perturbation it is found that the value of this time constant is equal to 160 seconds.

From these figures it has been found that the transient associated with the establishment of a flow and pressure pattern are much faster than the transient resulting from the establishment of a thermal profile. Consequently, under the flow conditions at which the reactor is operated, the assumptions uncoupling the pressure and flow transient from the thermal transient and considering the first one as extremely rapid appears justified.

5. Comparison of Computed and Experimental Steady State Results

With the choice of parameters corresponding to the conditions of Table 3.1 the agreement between the experimental results and the computed steady state profiles appears in Fig. 4.3. A relatively good agreement is obtained as far as temperature profile is concerned, however the model production is 12% higher than the reference production. The assumptions of uniform radial temperature and composition, and the use of a rate of reaction obtained for a different catalyst have been offered by Logeais²² as explanation of these



TYPICAL TEMPERATURE PROFILES

Fig. 4-3

discrepancies. The results of this simulation will only approximate quantitatively the dynamic behavior of the T.V.A. reactor from which Allgood, Slack, and Maune results were taken. Nevertheless, it is believed that the transient computed by the proposed mathematical model retain the main features of an industrial ammonia synthesis reactor of this type.

CHAPTER V
COMPUTATION METHOD

There is no analytical solution to the system of nonlinear partial differential equations describing the dynamic behavior of the autothermic reactor which is presented below:

$$\frac{\partial v}{\partial \theta} + s(1-h) \frac{y-y^*}{1+y} \frac{\partial v}{\partial a} + (v-m) - D \frac{\partial^2 v}{\partial a^2} - [e + h(v-0.3725)] sr = 0 \quad (4.10)$$

$$\frac{\partial w}{\partial a} = \beta (w-m) \quad (4.5)$$

$$g \frac{\partial m}{\partial \theta} = v + dw - m(1+d) \quad (4.7)$$

$$\frac{\partial y}{\partial a} = r \frac{(1+y)^2}{1+y^*} \quad (4.3)$$

Consequently, finite difference approximations to these equations were derived and the resulting finite difference equations were solved on a digital computer.

Let j be the subscript used for distance and n the subscript used for time such that the normalized temperature v at a distance $a = j\Delta a$ from the top of the reactor and at an instant $\theta = n\Delta\theta$ from the beginning of a run is $v_{j,n}$.

In the first part of this chapter the finite difference analogs used to represent each equation are presented.

The sequence of computation retained to solve the system is as follows:

1. Solution of the ordinary differential equation representing the energy balance inside the empty tube section (Eq. 4.5) coupled with the equation

representing the energy balance inside the tube wall section (Eq. 4.7). In solving this last equation use is made of the old value of the catalyst temperature; $(v_{j,n})$.

2. Solution of the partial differential equation representing the energy balance inside the catalyst section (Eq. 4.10). In this solution the temperature of the wall is expressed implicitly as a function of the old and new temperatures on both sides of it.

3. Solution of the mass balance equation inside the catalyst section (Eq. 4.3) using the values of the catalyst temperature derived in Step 2. Once this cycle is terminated the time is advanced by $\Delta\Theta$ and the process is resumed. The Fortran program of the computer scheme so derived appears in the Appendix.

In Section B of this chapter, the computer scheme used to approximate Eq. 4.10 is tested for stability and accuracy on a linear partial differential equation obtained by linearization of Eq. 4.10. In Section C of this chapter, the convergence of the proposed scheme is demonstrated for both Δa and $\Delta\Theta$.

In approximating Eq. 4.10 a method directly derived from the Stone-Brian³⁰ method of solving convection problems is used. In Section D of this chapter the results obtained in the present simulation are compared for efficiency with the results obtained with the Courant Isaacson and Rees method¹⁰ of approximation.

A. DERIVATION OF THE COMPUTER ALGORITHM

1. Variable Distance Grid

In preliminary investigations the need for a variable distance grid along the bed appeared. The distance increment must be very small at the entrance of the catalyst section and can be fairly large at the outlet.

In order to achieve these results, the following change in variable is used:

$$a = f(\xi)$$

The new distance variable ξ , so defined, varies from 0 to 1.0 as a varies from 0 to 1.0 and is divided in increments of equal size $\Delta\xi$. The original distance position a_j is represented in terms of the new variable ξ by equation

$$a_j = f(j \times \Delta\xi) \quad (5.1)$$

From Eq. 5.1 it is seen that the increments Δa are variable if $f(\xi)$ is a nonlinear function of ξ and can be varied as desired by a proper choice of the function f . The system of partial differential equation rewritten in terms of ξ reduces to

$$\frac{\partial v}{\partial \theta} + \left[\frac{Df''}{f'3} + \frac{s(1-h) \frac{y-y^*}{1+y}}{f'} \right] \frac{\partial v}{\partial \xi} + v-m - \frac{D}{f12} \frac{\partial^2 v}{\partial \xi^2} - [e+h(v-0.3725)] sr = 0 \quad (5.2)$$

$$\frac{\partial w}{\partial \xi} = \beta f'(w-m) \quad (5.3)$$

$$g \frac{\partial m}{\partial \theta} = v+dw - m(1+d) \quad (5.4)$$

$$\frac{\partial y}{\partial \xi} = rf' \frac{(1+y)^2}{1+y^*} \quad (5.5)$$

The function f used in this study is of the form

$$a = a\xi + (1-a) \xi^2 \quad (5.6)$$

the case $a = 1.0$ corresponding to $a = \xi$.

The first and second derivatives of f are, respectively,

$$f' = a+2(1-a) \xi \quad (5.7)$$

$$f'' = 2(1-a) \quad (5.8)$$

The functions f' and f'' are known at any position and can be entered into the finite difference analogs without difficulty, as will be shown later.

2. Solution of the Energy Equation for the Gas in the Empty Tube Section

The ordinary differential equation

$$\frac{\partial w}{\partial \xi} = \beta f'(w-m) \quad (5.3)$$

is solved by using the implicate finite difference approximation appearing in Eq. 5.9.

$$\frac{w_{j+1,n+1} - w_{j,n+1}}{\Delta \xi} = \beta \left[\frac{f'_{j+1} + f'_j}{2} \right] \left[\frac{w_{j+1,n+1} + w_{j,n+1}}{2} - \frac{m_{j+1,n+1} + m_{j,n+1}}{2} \right] \quad (5.9)$$

In this expression the values of the wall temperature at time n+1 ($m_{j,n+1}$) are unknown. They are given by solving simultaneously the energy equation for the tube wall (Eq. 5.4).

The ordinary differential equation (5.4) is approximated by the following finite difference analog

$$g \frac{m_{j,n+1} - m_{j,n}}{\Delta \Theta} = v_{j,n} + \frac{dw_{j,n+1}}{2} + \frac{dw_{j,n}}{2} - \frac{(1+d)m_{j,n+1}}{2} - \frac{(1+d)m_{j,n}}{2} \quad (5.10)$$

The value of the catalyst temperature at time n+1 being still unknown, v is only expressed in terms of its value at the old time.

Equation 5.10 can be solved for $m_{j,n+1}$

$$m_{j,n+1} = \frac{g - \frac{(1+d)\Delta \Theta}{2}}{g + \frac{(1+d)\Delta \Theta}{2}} m_{j,n} + \frac{\Delta \Theta}{g + \frac{(1+d)\Delta \Theta}{2}} v_{j,n} + \frac{\frac{d\Delta \Theta}{2}}{g + \frac{(1+d)\Delta \Theta}{2}} [w_{j,n+1} + w_{j,n}] \quad (5.11)$$

which is rewritten for simplicity as

$$m_{j,n+1} = a' v_{j,n} + b' (w_{j,n+1} + w_{j,n}) + c' m_{j,n} \quad (5.12)$$

After substituting the value of $m_{j,n+1}$ expressed by Eq. 5.12 into Eq. 5.9 and solving for $w_{j,n+1}$ one obtains

$$\begin{aligned} w_{j,n+1} = & \frac{1 - \frac{\beta \Delta \xi}{4} \times (f'_{j+1} + f'_j) (1-b')}{1 + \frac{\beta \Delta \xi}{4} \times (f'_{j+1} + f'_j) \times (1-b')} \times w_{j+1,n+1} \\ & + \frac{\frac{a' \beta \Delta \xi}{4} \times (f'_{j+1} + f'_j)}{1 + \frac{\beta \Delta \xi}{4} \times (f'_{j+1} + f'_j) \times (1-b')} \times [v_{j+1,n} + v_{j,n}] \\ & + \frac{\frac{c' \beta \Delta \xi}{4} \times (f'_{j+1} + f'_j)}{1 + \frac{\beta \Delta \xi}{4} \times (f'_{j+1} + f'_j) \times (1-b')} \times [m_{j+1,n} + m_{j,n}] \end{aligned} \quad (5.13)$$

The computation process is a marching process originated at

$$j+1 = \text{NSTOP} \quad (\xi=1) \quad \text{with}$$

$$w_{\text{NSTOP}} = w_{\text{feed}}$$

This marching process is stable as long as

$$\beta (f'_{j+1} + f'_j) (1-b')$$

is positive which is always the case in this study. As a result of this investigation the temperature of the gas leaving the empty tube section $w_{1,n+1}$ is known.

3. Solution of the Energy Equation in the Catalyst Section

A finite difference analog derived from the method presented by Stone and Brian³⁰ is used to approximate the partial differential equation representing the energy balance inside the catalyst section (Eq. 5.2). The distance and time derivative are respectively approximated by the following expressions proposed by Stone and Brian.

$$\begin{aligned} \frac{\partial^2 v}{\partial \xi^2} &= \frac{v_{j+1, n+1} - 2v_{j, n+1} + v_{j-1, n+1}}{2\Delta\xi^2} \\ &+ \frac{v_{j+1, n} - 2v_{j, n} + v_{j-1, n}}{2\Delta\xi^2} \end{aligned} \quad (5.14)$$

$$\frac{\partial v}{\partial \xi} = \frac{v_{j+1, n+1} - v_{j-1, n+1}}{4\Delta\xi} + \frac{v_{j+1, n} - v_{j-1, n}}{4\Delta\xi} \quad (5.15)$$

$$\begin{aligned} \frac{\partial v}{\partial \Theta} &= \frac{v_{j+1, n+1} - v_{j+1, n}}{6\Delta\Theta} + \frac{(v_{j, n+1} - v_{j, n}) \times 2}{3\Delta\Theta} \\ &+ \frac{v_{j-1, n+1} - v_{j-1, n}}{6\Delta\Theta} \end{aligned} \quad (5.16)$$

The remaining part of Eq. 5.2 is called a source or sink term according to the position along the reactor.

It is of the form

$$\psi = v^{-m} - [e + h(v - 0.3725)] \text{ sr}$$

Because of the nonlinearity of the rate of reaction term r , it is impossible without iteration to express r in terms of its value at new time represented by $r_{j, n+1}$. Consequently the source or sink term has been weighted in time and distance for the part v^{-m} and only in distance for the remaining part. Equation 5.17 represents the approximation adopted for ψ

$$\begin{aligned}
 \psi = & \frac{v_{j+1, n+1} - m_{j+1, n+1}}{12} + \frac{v_{j, n+1} - m_{j, n+1}}{3} + \frac{v_{j-1, n+1} - m_{j-1, n+1}}{12} \\
 & + \frac{v_{j+1, n} - m_{j+1, n}}{12} + \frac{v_{j, n} - m_{j, n}}{3} + \frac{v_{j-1, n} - m_{j-1, n}}{12} \\
 & - \frac{1}{6} [e + h(v_{j+1, n} - 0.3725)] \text{ sr } (v_{j+1, n}, y_{j+1, n}) \\
 & - \frac{2}{3} [e + h(v_{j, n} - 0.3725)] \text{ sr } (v_{j, n}, y_{j, n}) \\
 & - \frac{1}{6} [e + h(v_{j-1, n} - 0.3725)] \text{ sr } (v_{j-1, n}, y_{j-1, n}) \tag{5.17}
 \end{aligned}$$

In this last equation the value of $m_{j, n+1}$ could be replaced by its value obtained in the previous section (Eq. 5.12). However, it is preferable to rewrite the energy equation on the metal of the tube in order to use both values of v and w at new time. The ordinary differential Eq. 5.6 is now approximated by the following finite difference analog.

$$\begin{aligned}
 g \frac{m_{j, n+1} - m_{j, n}}{\Delta\theta} = & \frac{v_{j, n+1} + v_{j, n}}{2} + \frac{d(w_{j, n+1} + w_{j, n})}{2} \\
 & - \frac{(1+d) \times (m_{j, n+1} + m_{j, n})}{2} \tag{5.18}
 \end{aligned}$$

Equation 5.18 solved for $m_{j, n+1}$ is written:

$$\begin{aligned}
 m_{j, n+1} = & \frac{g - \frac{(1+d)\Delta\theta}{2}}{g + \frac{(1+d)\Delta\theta}{2}} \times m_{j, n} \\
 & + \frac{\frac{\Delta\theta}{2}}{g + \frac{(1+d)\Delta\theta}{2}} \times [v_{j, n+1} + v_{j, n}] \\
 & + \frac{\frac{d\Delta\theta}{2}}{g + \frac{(1+d)\Delta\theta}{2}} \times [w_{j, n+1} + w_{j, n}] \tag{5.19}
 \end{aligned}$$

This finite difference analog is stable since $\frac{g - (1+d)\frac{\Delta\Theta}{2}}{g + \frac{(1+d)\Delta\Theta}{2}}$ is always smaller than 1 as $(1+d) > 0$. For simplicity Eq. 5.19 is written as

$$m_{j,n+1} = a[v_{j,n+1} + v_{j,n}] + b[w_{j,n+1} + w_{j,n}] + c[m_{j,n}] \quad (5.20)$$

After replacing the derivatives by their values in Eq. 5.2 and the source or sink term by Eq. 5.17 the energy balance in the catalyst section takes form of Eq. 5.21

$$\begin{aligned}
 & v_{j+1, n+1} \left\{ \frac{1}{6 \Delta \Theta} - \frac{D}{2 f_j'^2 \Delta \xi^2} + \left[\frac{D f_j''}{f_j'^3} + \frac{s(1-h) \frac{y_{j,n}^{-y}^*}{1+y_{j,n}^*}}{f_j'} \right] \right\} \times \frac{1}{4 \Delta \xi} \\
 & + \frac{1-a}{12} \left. \right\} + v_{j, n+1} \left\{ \frac{2}{3 \Delta \Theta} + \frac{D}{f_j'^2 \Delta \xi^2} + \frac{1-a}{3} \right\} \\
 & + v_{j-1, n+1} \left\{ \frac{1}{6 \Delta \Theta} - \frac{D}{2 f_j'^2 \Delta \xi^2} - \left[\frac{D f_j''}{f_j'^3} + \frac{s(1-h) \frac{y_{j,n}^{-y}^*}{1+y_{j,n}^*}}{f_j'} \right] \right\} \\
 & \times \frac{1}{4 \Delta \xi} + \frac{1-a}{12} \left. \right\} \\
 & = v_{j+1, n} \left\{ \frac{1}{6 \Delta \Theta} + \frac{D}{2 f_j'^2 \Delta \xi^2} - \left[\frac{D f_j''}{f_j'^3} + \frac{s(1-h) \frac{y_{j,n}^{-y}^*}{1+y_{j,n}^*}}{f_j'} \right] \right\} \times \frac{1}{4 \Delta \xi} \\
 & - \frac{1-a}{12} \left. \right\} + v_{j, n} \left\{ \frac{2}{3 \Delta \Theta} - \frac{D}{f_j'^2 \Delta \xi^2} - \frac{1-a}{3} \right\} \\
 & + v_{j-1, n} \left\{ \frac{1}{6 \Delta \Theta} + \frac{D}{2 f_j'^2 \Delta \xi^2} + \left[\frac{D f_j''}{f_j'^3} + \frac{s(1-h) \frac{y_{j,n}^{-y}^*}{1+y_{j,n}^*}}{f_j'} \right] \right\} \times \frac{1}{4 \Delta \xi} \\
 & - \frac{1-a}{12} \left. \right\} + (w_{j+1, n+1} + w_{j+1, n} + w_{j-1, n+1} \\
 & + w_{j-1, n}) \times \frac{b}{12} + (w_{j, n+1} + w_{j, n}) \times \frac{b}{3} + m_{j, n} \times \frac{c+1}{3} \\
 & + (m_{j+1, n} + m_{j-1, n}) \times \frac{c+1}{12} +
 \end{aligned}$$

$$\begin{aligned} & \frac{1}{6} [e + h (v_{j-1, n} - 0.3725)] \text{sr} (v_{j-1, n}, y_{j-1, n}) \\ & + \frac{2}{3} [e + h (v_{j, n} - 0.3725)] \text{sr} (v_{j, n}, y_{j, n}) \\ & + \frac{1}{6} [e + h (v_{j+1, n} - 0.3725)] \text{sr} (v_{j+1, n}, y_{j+1, n}) \end{aligned} \quad (5.21)$$

which can be arranged in the form of Eq. 5.22

$$a_j v_{j-1, n+1} + b_j v_{j, n+1} + c_j v_{n+1, n+1} = d_j \quad (5.22)$$

The stability of such a finite analog is impossible to analyze rigorously because of the nonlinearity present. In Section B of this chapter a stability analysis will be carried out on the equation obtained by linearizing Eq. 5.2, that is to say, on an equation of the form

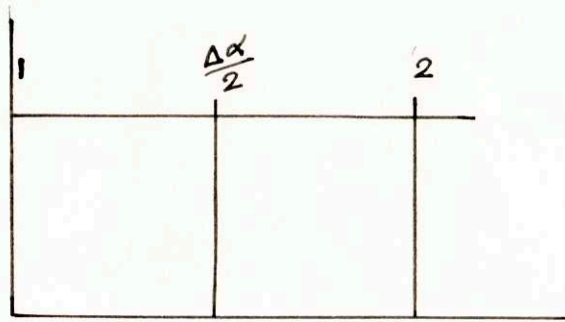
$$D \frac{\partial^2 v}{\partial \xi^2} - V \frac{\partial v}{\partial \xi} - \frac{\partial v}{\partial \theta} - R v = 0 \quad (5.23)$$

As each equation 5.22 contains three unknowns, the solution of the finite difference analog consists of solving a system of linear equations whose matrix of coefficient is a tridiagonal matrix.

In order to truncate this matrix, use is made of the boundary conditions at the entrance and at the exit of the reactor as expressed in Chapter IV. In this Chapter the boundary condition associated with the partial differential Eq. 4.10 has been presented as

$$v_{a=0} = w_{a=0} + \frac{D}{s} \left(\frac{\partial v}{\partial a} \right)_{a=0} \quad (5.24)$$

Rather than approximate the derivative $(\frac{\partial v}{\partial a})$ in terms of finite differences, the concept of enthalpy flux presented in Chapter IV to derive Eq. 5.24 is used here to make an energy balance around a slice of finite dimension.



Using the same notation as in Chapter III an energy balance written around the volume of catalyst enclosed within the planes located at $a = 0$ and $a = \frac{\Delta a}{2}$ from the entrance of the catalyst section results in the following terms:

enthalpy convected in: $F \bar{C}_{po} [T_{T a=0} - T_B] + F \Delta H_o y^*$

enthalpy convected out: $F \left[\bar{C}_{po} - \Delta C \frac{y \frac{\Delta a}{2} - y^*}{1 + y \frac{\Delta a}{2}} \right] [T_{C \frac{\Delta a}{2}} - T_B] +$
 $F \Delta H_o \left[y^* + \frac{y \frac{\Delta a}{2} - y^*}{1 + y \frac{\Delta a}{2}} \right]$

enthalpy diffused out $- D'A \left(\frac{\partial T}{\partial z} \right) \frac{\Delta a}{2}$

enthalpy transferred to the wall

$$\frac{h_2 s_2}{1} \frac{\Delta z}{2} (T_c - T_w)$$

enthalpy accumulated

$$\frac{WC_{Pc}}{1} \frac{\Delta z}{2} \frac{\partial \bar{T}_c}{\partial t}$$

where the subscript $\frac{\Delta a}{2}$ refers to the position located at $\frac{\Delta a}{2}$ from position 1. The energy transferred to the wall and the enthalpy accumulated inside the catalyst are expressed as functions of an average temperature within the

slice $0 + \frac{\Delta a}{2}$ (represented by a bar). After rearrangement and normalization the enthalpy balance around the slice $0 \frac{\Delta a}{2}$ is written:

$$\frac{2s w_1}{\Delta a_i} - \frac{2s}{\Delta a_i} \left(1 - h \frac{y \frac{\Delta a}{2} - y^*}{1 + y \frac{\Delta a}{2}}\right) v \frac{\Delta a}{2} + \frac{2D'}{\Delta a} \left(\frac{\partial v}{\partial a}\right) \frac{\Delta a}{2} - (\bar{v} - m) + (e - 0.3725 h) s \bar{r} = \frac{\partial \bar{v}}{\partial \Theta} \quad (5.25)$$

In deriving a finite difference analog to this equation, the weighting coefficients proposed by Stone and Brian are used. Wherever possible the variables are expressed both at new time and at old time. The value of the variables at the position $\frac{\Delta a}{2}$ is taken as the arithmetic average of the value of the variables at position 1 and 2.

$$\frac{v \Delta a}{2} = \frac{v_1 + v_2}{2} \quad (5.26)$$

The finite difference analog of Eq. 5.15 is written

$$\frac{s x w_{1,n+1}}{\Delta a_i} + \frac{s x w_{1,n}}{\Delta a_i} - \frac{s}{\Delta a_i} \left(1 - h \frac{\frac{y_{1,n} + y_{2,n}}{2} - y^*}{1 + \frac{y_{1,n} + y_{2,n}}{2}}\right) x \frac{v_{1,n+1} + v_{1,n} + v_{2,n+1} + v_{2,n}}{2} + s (e - 0.3725 h) x \left[\frac{2}{3} r(v_{1,n}, y_{1,n}) + \frac{1}{3} \left(\frac{r(v_{1,n}, y_{1,n}) + r(v_{2,n}, y_{2,n})}{2}\right)\right] + \frac{D}{\Delta \xi^2} [v_{2,n+1} - v_{1,n+1} + v_{2,n} - v_{1,n}] + \frac{1}{3} [m_{1,n+1} + m_{1,n}] + \frac{1}{6} \left[\frac{m_{1,n+1} + m_{2,n+1}}{2} + \frac{m_{1,n} + m_{2,n}}{2}\right] - \frac{1}{3} [v_{1,n+1} + v_{1,n}]$$

$$\begin{aligned}
 & - \frac{1}{6} \left[\frac{v_{1,n+1} + v_{2,n+1}}{2} + \frac{v_{1,n} + v_{2,n}}{2} \right] = \\
 & \frac{2}{3} \frac{v_{1,n+1} - v_{1,n}}{\Delta\Theta} + \frac{1}{3} \left[\frac{v_{1,n+1} + v_{2,n+1}}{2} - \frac{v_{1,n} + v_{2,n}}{2} \right] \quad (5.27)
 \end{aligned}$$

This expression can be rearranged in the required form to truncate the tri-diagonal matrix, that is to say

$$b_1 v_{1,n+1} + c_1 v_{2,n+1} = d_1 \quad (5.28)$$

The same concept of rewriting the energy equation for half a slice is used in deriving the end boundary equation. The enthalpy flux leaving the reactor is equal to

$$F \left[\bar{C}_{p_o} - \Delta C \frac{y_{N-y}^*}{1+y_N} \right] [T_{cN} - T_B] + F \Delta H_o \left[y^* + \frac{y_{N-y}^*}{1+y_N} \right]$$

An enthalpy balance around the column of catalyst enclosed within the planes located at $-\frac{\Delta a}{2}$ and 0 from position NSTOP results in the following terms:

Enthalpy convected in:

$$F \left[\bar{C}_{p_o} - \Delta C \frac{y_{N-\frac{\Delta a}{2}-y}^*}{1+y_{N-\frac{\Delta a}{2}}} \right] [T_{c_{N-\frac{\Delta a}{2}}} - T_B] + F \Delta H_o \left[y^* - \frac{y_{N-\frac{\Delta a}{2}-y}^*}{1+y_{N-\frac{\Delta a}{2}}} \right]$$

enthalpy diffused in:

$$-D'A \left(\frac{\partial T_c}{\partial z} \right)_{N-\frac{\Delta a}{2}}$$

enthalpy transferred to the wall:

$$\frac{h_2 s_2}{1} \frac{\Delta z}{2} (\bar{T}_c - \bar{T}_w)$$

enthalpy accumulated inside the catalyst

$$\frac{WC_{p_c}}{1} \frac{\Delta z}{2} \frac{\partial \bar{T}_c}{\partial t}$$

In these expressions the subscript $N - \Delta a/2$ refers to the position distant by $\frac{\Delta a}{2}$ from the outlet of the reactor. After rearrangement and normalization the enthalpy balance is:

$$\begin{aligned} & \frac{2s}{\Delta a_o} \left(1 - h \frac{y_{N-\frac{\Delta a}{2}} - y^*}{1 + y_{N-\frac{\Delta a}{2}}} \right) v_{N-\frac{\Delta a}{2}} - \frac{2s}{\Delta a_o} \left(1 - h \frac{y_N - y^*}{1 - y_N} \right) v_N \\ & - \frac{2D'}{\Delta a} \left(\frac{\partial v}{\partial a} \right)_{N-\frac{\Delta a}{2}} + (e - 0.3725 h) s \bar{r} - (\bar{v} - m) = \frac{\partial \bar{v}}{\partial \theta} \end{aligned} \quad (5.28)$$

With the same method of approximation, the finite difference analog to this equation is:

$$\begin{aligned} & \frac{s}{\Delta a_o} \left(1 - h \frac{\frac{y_{N-1,n} + y_{N,n}}{2} - y^*}{1 + \frac{y_{N-1,n} + y_{N,n}}{2}} \right) \left[\frac{v_{N-1,n+1} + v_{N,n+1}}{2} + \frac{v_{N-1,n} + v_{N,n}}{2} \right] \\ & - \frac{s}{\Delta a_o} \left(1 - h \frac{y_{N,n} - y^*}{1 + y_{N,n}} \right) [v_{N,n+1} + v_{N,n}] - \frac{D}{\Delta a_o} [v_{N,n+1} - v_{N-1,n+1}] \\ & - \frac{D}{\Delta a_o} (v_{N,n} - v_{N-1,n}) + s (e - 0.3725 h) \left[\frac{2}{3} r (v_{N,n}, y_{N,n}) \right. \\ & \left. + \frac{1}{3} \frac{r(v_{N,n}, y_{N,n}) + r(v_{N-1,n}, y_{N-1,n})}{2} + \frac{1}{3} m_{N,n+1} + \frac{1}{3} m_{N,n} \right. \\ & \left. + \frac{1}{6} \left[\frac{m_{N,n+1} + m_{N-1,n+1}}{2} + \frac{m_{N,n} + m_{N-1,n}}{2} \right] \right. \\ & \left. - \frac{1}{3} [v_{N,n+1} + v_{N,n}] - \frac{1}{6} \left[\frac{v_{N,n+1} + v_{N-1,n+1}}{2} \right. \right. \\ & \left. \left. + \frac{v_{N,n} + v_{N-1,n}}{2} \right] = \frac{2}{3} \frac{v_{N,n+1} - v_{N,n}}{\Delta \theta} \right. \\ & \left. + \frac{1}{3} \frac{v_{N,n+1} + v_{N-1,n+1}}{2} - \frac{v_{N,n} + v_{N-1,n}}{2} \right] \frac{1}{\Delta \theta} \end{aligned} \quad (5.29)$$

This expression can be rearranged in the form

$$a_N v_{N-1, n+1} + b_N v_{N, n+1} = d_N$$

In matrix form the system to be solved is written

$$\begin{bmatrix} b_1 & c_1 & 0 & & & & & 0 \\ a_2 & b_2 & c_2 & 0 & & & & \\ & 0 & a_i & b_i & c_i & & & \\ & & & 0 & a_{N-1} & b_{N-1} & c_{N-1} & \\ 0 & & & & 0 & a_N & b_N & \end{bmatrix} \times \begin{bmatrix} v_{1, n+1} \\ v_{2, n+1} \\ v_{i, n+1} \\ v_{N-1, n+1} \\ v_{N, n+1} \end{bmatrix} = \begin{bmatrix} d_1 \\ d_2 \\ d_i \\ d_{N-1} \\ d_N \end{bmatrix} \quad (5.30)$$

A method of solution applicable to such a system of linear equations having a tridiagonal matrix of coefficients is well known^{8, 41} and is used in this thesis.

The computing process consists in transforming the matrix Eq. 5.30 into Eq. 5.31

$$\begin{bmatrix} \beta_1 & c_1 & 0 & & & & & \\ 0 & \beta_2 & c_2 & 0 & & & & \\ & & & 0 & \beta_i & c_i & 0 & \\ & & & & 0 & \beta_{N-1} & c_{N-1} & \\ & & & & & 0 & \beta_n & \end{bmatrix} \times \begin{bmatrix} v_{1, n+1} \\ v_{2, n+1} \\ v_{i, n+1} \\ v_{N-1, n+1} \\ v_{N, n+1} \end{bmatrix} = \begin{bmatrix} \gamma_1 \\ \gamma_2 \\ \gamma_i \\ \gamma_{N-1} \\ \gamma_n \end{bmatrix} \quad (5.31)$$

The coefficients β_i and γ_i are related to a_i, b_i, c_i, d_i by the following relations

$$\beta_i = b_i - \frac{a_i c_{i-1}}{\beta_{i-1}} \quad (5.32)$$

$$\gamma_i = d_i - \frac{a_i \gamma_{i-1}}{\beta_{i-1}} \quad (5.33)$$

The computing process is started with

$$\beta_1 = b_1$$

$$\gamma_1 = d_1$$

and proceeds for i varying from 2 to N .

From Eq. 5.31 it is seen that the v can be computed by a marching process starting with

$$v_{N, n+1} = \frac{\gamma_N}{\beta_N} \quad (5.34)$$

and for which the general equation is:

$$v_{j, n+1} = \frac{\gamma_j - c_j v_{j+1, n+1}}{\beta_j} \quad (5.35)$$

Once the values of $v_{j, n+1}$ are known the temperature of the tube wall is computed by using Eq. 5.20

$$m_{j, n+1} = + a [v_{j, n+1} + v_{j, n}] + b [w_{j, n+1} + w_{j, n}] + c m_{j, n} \quad (5.20)$$

4. Solution of the material balance equation

In order to solve the nonlinear ordinary differential equation representing the mass balance inside the catalyst section (Eq. 5.5) Heun's first method of approximation⁴¹ has been used. This method consists of computing a first approximation to $y_{j+1, n+1}$ by using the simple Euler equation. This first estimate of $y_{j+1, n+1}$ is then used in the "trapezoidal" equation to obtain a better estimate of $y_{j+1, n+1}$. The integrating scheme is written

$$\bar{y}_{j+1, n+1} = y_{j, n+1} + \Delta \xi \frac{f'_j + f'_{j+1}}{2} \frac{[1 + y_{j, n+1}]^2}{1 + y} r(v_{j, n+1}, y_{j, n+1}) \quad (5.36)$$

$$y_{j+1, n+1} = y_{j, n+1} + \frac{\Delta \xi \times [f'_j + f'_{j+1}]}{4} \left\{ \frac{(1 + y_{j, n+1})^2}{1 + y^*} r(v_{j, n+1}, y_{j, n+1}) \right. \\ \left. + \frac{(1 + \bar{y}_{j+1, n+1})^2}{1 + y^*} r(v_{j+1, n+1}, \bar{y}_{j+1, n+1}) \right\} \quad (5.37)$$

This marching process is started with the boundary condition

$$y_{1, n+1} = y_{\text{feed}} = y^* \quad (5.38)$$

T, i. e., data at small β where diffusion is unimportant. This method depends on the fact that the $\ln f$ vs. τ curves are relatively straight, even for large values of β so that an effective first-order rate constant may be assigned to each β . Note that as the $\ln f$. vs. τ curves are not exactly straight, the value of the effective rate constant will depend somewhat upon how these curves are approximated by straight lines. The procedure adopted is for the curve for each value of β to draw a straight line through the points $f = 1, \tau = 0$ and $f = 0.1, \tau = \tau_{0.1}$, where $\tau_{0.1}$ is the value of τ for $f = 0.1$. The effective rate constants obtained from the slopes of the straight lines will best represent the time required to reach a value of $f = 0.1$. If accurate correlations are required at other values of f the correlation procedure must be repeated drawing the straight lines through this new value of f rather than through $f = 0.1$.

Now $\ln\left(\frac{1}{f}\right) = k p_o t = \tau$ at $\beta = 0$ and for the straight line approximations for $\beta > 0$

$$\ln\left(\frac{1}{f}\right) = (ek) p_o t = e\tau_\beta = \tau \quad (3.4)$$

where e is the slope of the straight line at the given value of β and τ_β is the normalized time required to regenerate to f at the given value of β . The effective rate constant is then ek where $e = 1$ at $\beta = 0$ and $e < 1$ for $\beta > 0$. From the model solutions a table of values of e and β can be obtained. Further, for the limiting case of very large values of β the solution of Weisz and Prater, Eq. 3.3 applies.

Hence

$$\frac{\tau_\beta}{\beta} = \frac{\ln(1/f)}{e\beta} = \frac{1}{2} (1 - f^{2/3}) - \frac{1}{3} (1 - f)$$

and for a given f and large β , $e\beta$ is a constant. For $f = 0.1$ $\frac{1}{2} (1 - f^{2/3}) - \frac{1}{3} (1 - f) = 0.0923$ and $\ln(1/f) = 2.303$. Then $e\beta = 2.303/0.0923 = 24.95$.

$$\frac{\partial \delta v}{\partial \Theta} = \frac{D'}{f'^2} \frac{\partial^2 \delta v}{\partial \xi^2} - \left[\frac{D' f''}{f'} + \frac{s (1-h \frac{y-y^*}{1+y^*})}{f'} \right] \frac{\partial \delta v}{\partial \xi} - \delta v \left\{ 1 - \frac{\partial}{\partial v} [(e+h(v^* - 0.3725) sr (v^*))] \right\} \quad (5.41)$$

Equation 5.41 is a linear partial differential equation of the form of Eq. 5.42

$$D \frac{\partial^2 y}{\partial x^2} - V \frac{\partial y}{\partial x} - \frac{\partial y}{\partial t} - R y = 0 \quad (5.42)$$

In Eq. 5.42 the dependent variable is now y , and x and t are the independent variables. The coefficient D, V, R are obtained by identification of Eq. 5.42 with Eq. 5.41. Because of the geometrical configuration of the reactor and the temperature dependence of the rate of reaction, the values of R varies with distance. Near the entrance and the outlet of the reactor R is found negative and Eq. 5.42 contains a source term. On the contrary, in the center section of the reactor, R is positive and Eq. 5.42 contains a sink term. In this section it will be assumed that the coefficient D, V, R are constant, both cases of a sink and a source being considered.

Since Eq. 5.42 is linear, it is possible to solve it analytically for certain boundary conditions and to compare this solution for accuracy with the numerical solutions obtained with the finite difference analogs.

The investigation reported in this section is an extension of the work reported by Stone and Brian³⁰ who studied the accuracy of various finite difference analogs to the following partial differential equation

$$D \frac{\partial^2 y}{\partial x^2} - V \frac{\partial y}{\partial x} - \frac{\partial y}{\partial t} = 0 \quad (5.43)$$

The scope of this investigation is to justify the choice of the finite difference approximations used in this research and to point out the problems of instability associated with the resolution of this type of equation.

1. Analysis of Stone-Brian's Results

Stone and Brian³⁰ have studied the accuracy of various finite difference approximations to the linear partial differential equation represented by Eq. 5.43.

They have written a general difference equation which contains arbitrary weighting of all the possible approximations to $\frac{\partial y}{\partial x}$ and $\frac{\partial y}{\partial t}$ involving three distance positions at two time levels. The final difference analog they investigated was

$$\begin{aligned}
 -D \left[\frac{y_{j+1, n+1} - 2y_{j, n+1} + y_{j-1, n+1}}{2\Delta x^2} \right. \\
 \left. + \frac{y_{j+1, n} - 2y_{j, n} + y_{j-1, n}}{2\Delta x^2} \right] + \frac{V}{\Delta x} [a(y_{j+1, n} - y_{j, n}) \\
 + \frac{\epsilon}{2}(y_{j, n} - y_{j-1, n}) + c(y_{j+1, n+1} - y_{j, n+1}) + d(y_{j, n+1} - y_{j-1, n+1})] \\
 + \frac{1}{\Delta t} [g(y_{j, n+1} - y_{j, n}) + \frac{\Theta}{2}(y_{j-1, n+1} - y_{j-1, n}) \\
 + m(y_{j+1, n+1} - y_{j+1, n})] = 0 \tag{5.44}
 \end{aligned}$$

The weighting coefficients $a, \frac{\epsilon}{2}, c, d, g, \frac{\Theta}{2}, m$ are subject to the restrictions:

$$a + \frac{\epsilon}{2} + c + d = 1$$

$$g + \frac{\Theta}{2} + m = 1$$

Stone and Brian tested the choice of the coefficients by comparing the solution of the resulting difference equation with the analytical solution of Eq. 5.43 for a special boundary condition. The initial condition used is a sine wave of frequency proportional to ω . The reason for studying the behavior of a sine wave initial condition is that any other type of starting condition can be broken down into a Fourier series. Since Eq. 5.43 is linear, the solution can be obtained by a superposition of the solutions for the various harmonics. The analytical solution to this problem is

$$y(x, t) = \text{cst } x \exp[-\omega^2 \pi^2 D t] \times \sin \omega \pi (x - Vt) \quad (5.45)$$

In absence of diffusion the phenomena described by Eq. 5.45 is the propagation of a sine wave down the bed at a velocity V independent of the frequency of the initial sine wave.

In presence of diffusion the wave is still propagated at the same velocity V but is decayed at a rate equal to $e^{-\omega^2 \pi^2 D t}$. In the case of a complex initial condition the higher frequency harmonics are decayed at a much faster rate than the fundamental, such that after a while the lower frequency harmonics only need to be considered in the superposition process.

The solution of the finite difference equation, 5.44, for the same boundary condition can be expressed in the form

$$y_{j, n} = \text{cst } \rho^n \sin \omega \pi (j \Delta x - V \phi n \Delta t) \quad (5.46)$$

where ρ and ϕ are expressed as functions of the new parameters

$\alpha = \frac{2D\Delta t}{\Delta x^2}$ and $\beta = \frac{V\Delta t}{\Delta x}$ by the following relations derived by Stone and Brian

$$\rho^2 = \frac{\left\{ g + \beta(a - \frac{\epsilon}{2}) + \left[\left(\frac{\Theta}{2} + m \right) - \beta(a - \frac{\epsilon}{2}) \right] \cos \omega \pi \Delta x - a \sin^2 \frac{\omega \pi \Delta x}{2} \right\}^2 + \left\{ \left[\beta(a + \frac{\epsilon}{2}) + \left(\frac{\Theta}{2} - m \right) \right] \sin \omega \pi \Delta x \right\}^2}{\left\{ g + \beta(d - c) + \left[\left(\frac{\Theta}{2} + m \right) - \beta(d - c) \right] \cos \omega \pi \Delta x + a \sin^2 \frac{\omega \pi \Delta x}{2} \right\}^2 + \left\{ \left[\beta(c + d) - \left(\frac{\Theta}{2} - m \right) \right] \sin \omega \pi \Delta x \right\}^2} \quad (5.47)$$

$$\phi = \left\{ \frac{1}{\beta \omega \pi \Delta x} \right\} \left\{ \text{artang} \left[\frac{\left[\beta(a + \frac{\epsilon}{2}) + \left(\frac{\Theta}{2} - m \right) \right] \sin \omega \pi \Delta x}{g + \beta(a - \frac{\epsilon}{2}) + \left[\left(\frac{\Theta}{2} + m \right) - \beta(a - \frac{\epsilon}{2}) \right] \cos \omega \pi \Delta x - a \sin^2 \frac{\omega \pi \Delta x}{2}} \right] + \text{artang} \left[\frac{\left[\beta(c + d) - \left(\frac{\Theta}{2} - m \right) \right] \sin \omega \pi \Delta x}{g + \beta(d - c) + \left[\left(\frac{\Theta}{2} + m \right) - \beta(d - c) \right] \cos \omega \pi \Delta x + a \sin^2 \frac{\omega \pi \Delta x}{2}} \right] \right\} \quad (5.48)$$

Physically, Eq. 5.46 describes the propagation of a sine wave at a speed equal to $V \phi$ and the decay of a sine wave at a rate proportional to ρ . Stone and Brian satisfied the condition that ρ should be equal to 1.0 in absence of diffusion for every value of β and every frequency by setting $c = \frac{\epsilon}{2}$, $a = d$ and $m = \frac{\Theta}{2}$. With this new restriction the expression for ϕ reduces to

$$\phi = \frac{2}{\beta \omega \pi \Delta x} \text{artang} \frac{\beta/2 \sin \omega \pi \Delta x}{1 + \left[\beta \left(\frac{1}{2} - \epsilon \right) - \Theta \right] [1 - \cos \omega \pi \Delta x]} \quad (5.49)$$

Equation 5.49 shows that the velocity of travel of the sine wave, $V \phi$, is a function of the frequency of the sine wave. For example, for $\omega \pi \Delta x = 0$ ϕ is equal to 1.0 but for $\omega \pi \Delta x = \pi$, $\phi = 0$, which means that such a frequency does not travel at all. Furthermore, there is no choice of ϵ or Θ which would make ϕ independent of $\omega \pi \Delta x$ for all the values of β .

Stone and Brian have proposed to use $\epsilon = \frac{1}{2}$ and $\Theta = \frac{1}{3}$ as the optimum choice of weighting coefficient. This choice of weighting coefficient makes ϕ remain close to unity over a wider range of frequency of the initial sine wave. This choice of coefficients insures a travel of the lower frequency at a rate very close to V . However, Stone and Brian concluded that there was no scheme which would cause the highest frequency to travel at a correct rate. (for $\omega \pi \Delta x = \pi$, ϕ will always be equal to zero).

In absence of diffusion, this phenomena will result in oscillation in distance of the solution, the high frequency shifting out of phase with the fundamental. In presence of diffusion, the high frequencies are decayed much faster than the fundamental, and the fact that they do not travel at the right rate becomes less important.

As a conclusion of this study, Stone and Brian recommended the introduction of an amount of diffusion which would prevent the largest frequencies from getting out of phase with a magnitude still noticeable.

2. Extension of Stone-Brian's Results to the Case with a Sink or Source Term

At the beginning of this section it was seen that the sink or source term obtained by linearization of Eq. 5.2 can be expressed as

$$R = 1 - \frac{\partial}{\partial v} [e + h(v - 0.3725)] s r(v)$$

Since r is nonlinear, it has been shown in Section A of this chapter that the rate of reaction is always expressed at old time. In order to take this into account in this analysis, the source or sink term has been expressed in two parts. Returning to the present notation where y is the independent variable, the source or sink terms has been written as

$$Ry = y - \Gamma y \tag{5.50}$$

In deriving the finite difference analog of Eq. 5.51

$$D \frac{\partial^2 y}{\partial x^2} - V \frac{\partial y}{\partial x} - \frac{\partial y}{\partial t} - \Gamma y = 0 \quad (5.51)$$

the weighting coefficients defined by Stone and Brian are used for the approximation of the derivatives. Furthermore, the most general way to approximate source or sink term using values at three locations and two time levels (when possible) is presented in Eq. 5.52.

$$\begin{aligned} y - \Gamma y = & a_1 y_{j+1, n} + a_2 y_{j, n} + a_3 y_{j-1, n} + a_4 y_{j+1, n+1} \\ & + a_5 y_{j, n+1} + a_6 y_{j-1, n+1} - 2 a_1 \Gamma y_{j+1, n} \\ & - 2 a_2 \Gamma y_{j, n} - 2 a_3 \Gamma y_{j-1, n} \end{aligned} \quad (5.52)$$

The restriction attached to the new weighting coefficients is

$$a_1 + a_2 + a_3 + a_4 + a_5 + a_6 = 1.0 \quad (5.53)$$

When the same initial condition is used in this analysis, as in Stone and Brian analysis, the analytical solution to Eq. 5.51 is

$$y = \text{cst} \exp [-(D \omega^2 \pi^2 + 1 - \Gamma) t] \sin \omega \pi (x - Vt) \quad (5.54)$$

Equation 5.54 describes a sine wave which is travelling at a velocity V independent of the frequency of the initial condition and which is decayed at a rate equal to $e^{-[\omega^2 \pi^2 D + 1 - \Gamma] t}$ the frequency of the starting condition affects the rate of decay only through the term $D \omega^2 \pi^2$. If $\Gamma > 1 + D \omega^2 \pi^2$ the coefficient of the exponential is > 0 and the analytical solution tends toward $+\infty$ as t tends towards ∞ . If $\Gamma < 1 + D \omega^2 \pi^2$, the analytical solution decays and approaches zero as time approaches infinity.

The solution of the finite difference equation obtained by adding Eq. 5.52 to Eq. 5.44 is

$$y_{j,n} = \text{cst } \rho'^n \sin \omega \pi [j \Delta x - V \phi' n \Delta t] \quad (5.55)$$

with ρ' and ϕ' expressed in function of a , β , Δt and $\Gamma \Delta t$ through the relations 5.56 and 5.57.

$$\rho'^2 = \frac{\left\{ g + \beta(a - \frac{\epsilon}{2}) - a_2(1 - 2\Gamma) \Delta t + \left[\left(\frac{\Theta}{2} + m \right) - \beta(a - \frac{\epsilon}{2}) - (a_1 + a_3)(1 - 2\Gamma) \Delta t \right] \cos \omega \pi \Delta x - a \sin^2 \frac{\omega \pi \Delta x}{2} \right\}^2 + \left\{ \left[\beta(a + \frac{\epsilon}{2}) + \left(\frac{\Theta}{2} - m \right) + (a_1 - a_3)(1 - 2\Gamma) \Delta t \right] \sin \omega \pi \Delta x \right\}^2}{\left\{ g + \beta(d - c) + a_5 \Delta t + \left[\left(\frac{\Theta}{2} + m \right) - \beta(d - c) + (a_4 + a_5) \Delta t \right] \cos \omega \pi \Delta x + a \sin^2 \frac{\omega \pi \Delta x}{2} \right\}^2 + \left\{ \left[\beta(c + d) - \left(\frac{\Theta}{2} - m \right) + (a_4 - a_6) \Delta t \right] \sin \omega \pi \Delta x \right\}^2} \quad (5.56)$$

$$\phi' = \frac{1}{\beta \omega \pi \Delta x} \left\{ \text{artang} \frac{\left[\beta(a + \frac{\epsilon}{2}) + \left(\frac{\Theta}{2} - m \right) + (a_1 - a_3)(1 - 2\Gamma) \Delta t \right] \sin \omega \pi \Delta x}{\left[g + \beta(a - \frac{\epsilon}{2}) - a_2(1 - 2\Gamma) \Delta t + \left[\left(\frac{\Theta}{2} + m \right) - \beta(a - \frac{\epsilon}{2}) - (a_1 + a_3)(1 - 2\Gamma) \Delta t \right] \cos \omega \pi \Delta x - a \sin^2 \frac{\omega \pi \Delta x}{2} \right]} \right. \\ \left. + \text{artang} \frac{\left[\beta(c + d) - \left(\frac{\Theta}{2} - m \right) + (a_4 - a_6) \Delta t \right] \sin \omega \pi \Delta x}{\left[g + \beta(d - c) + a_5 \Delta t + \left[\left(\frac{\Theta}{2} + m \right) - \beta(d - c) + (a_4 + a_6) \Delta t \right] \cos \omega \pi \Delta x + a \sin^2 \frac{\omega \pi \Delta x}{2} \right]} \right\} \quad (5.57)$$

Equations 5.56 and 5.57 reduce to Eqs. 5.47 and 5.48 in absence of a source or sink term. Furthermore, in Eq. 5.55, ρ' and ϕ' have the same physical significance as ρ and ϕ of Eq. 5.46.

If the weighting coefficients proposed by Stone and Brian for the approximation of the derivatives are used ($a=c=d=\frac{\epsilon}{2}=\frac{1}{4}$, $g=\frac{2}{3}$, $m=\frac{\Theta}{2}=\frac{1}{6}$) Eqs. 5.56 and 5.57 reduce to:

$$\rho^2 = \frac{\left\{ \frac{2}{3} + a_2(2\Gamma-1)\Delta t + \left[\frac{1}{3} + (a_1+a_3)(2\Gamma-1)\Delta t \right] \cos \omega \pi \Delta x - a \sin^2 \frac{\omega \pi \Delta x}{2} \right\}^2 + \left\{ \left[\frac{\beta}{2} + (a_1-a_3)(1-2\Gamma)\Delta t \right] \sin \omega \pi \Delta x \right\}^2}{\left\{ \frac{2}{3} + a_5\Delta t + \left[\frac{1}{3} + (a_4+a_6)\Delta t \right] \cos \omega \pi \Delta x + a \sin^2 \frac{\omega \pi \Delta x}{2} \right\}^2 + \left\{ \left[\frac{\beta}{2} + (a_4-a_6)\Delta t \right] \sin \omega \pi \Delta x \right\}^2} \quad (5.58)$$

$$\phi' = \frac{1}{\beta \omega \pi \Delta x} \left\{ \text{artang} \frac{\left[\frac{\beta}{2} + (a_1-a_3)(1-2\Gamma)\Delta t \right] \sin \omega \pi \Delta x}{\frac{2}{3} + a_2(2\Gamma-1)\Delta t + \left[\frac{1}{3} + (a_1+a_3)(2\Gamma-1)\Delta t \right] \cos \omega \pi \Delta x - a \sin^2 \frac{\omega \pi \Delta x}{2}} + \text{artang} \frac{\left[\frac{\beta}{2} + (a_4-a_6)\Delta t \right] \sin \omega \pi \Delta x}{\frac{2}{3} + a_5\Delta t + \left[\frac{1}{3} + (a_4+a_6)\Delta t \right] \cos \omega \pi \Delta x + a \sin^2 \frac{\omega \pi \Delta x}{2}} \right\} \quad (5.59)$$

The major difference between the present case and the case studied by Stone and Brian is that the value of ϕ' corresponding to the zero frequency is not equal to unity. The value of ϕ' for a zero frequency is expressed by Eq. 5.60

$$\phi' = \frac{1}{\beta} \left\{ \frac{\beta/2 + (a_3 - a_1)(2\Gamma - 1)\Delta t}{1 + (2\Gamma - 1)\Delta t(a_1 + a_2 + a_3)} + \frac{\beta/2 + (a_4 - a_6)\Delta t}{1 + \Delta t(a_4 + a_5 + a_6)} \right\} \quad (5.60)$$

Equation 5.60 shows that there is no choice of the weighting coefficients a_i which would make ϕ' equal to unity for any value of β and $\Gamma\Delta t$. Consequently, the finite difference analogs will always introduce an error in the rate of travel of a perturbation. Six choices of the weighting coefficients a_i have been investigated and the values of ρ' and ϕ' corresponding to the zero frequency are presented in Table 5.1.

In cases Nos. 1, 2 and 3 the linear part of the source or sink term is expressed at early and late time. This scheme can be considered as implicit. On the contrary, in cases Nos. 4, 5 and 6 the source or sink term is only expressed at early time. Cases Nos. 1, 3, 5 and 6 allow for weighting the values of the sink or source term at three locations. Cases Nos. 2 and 4 consider only the value of the sink or source term at one location. Table 5.1 also presents the values of ρ' and ϕ' corresponding to the exact solution (Eq. 5.54) for the present values of Γ and Δt . Table 5.1 shows that the accuracy for both ρ' and ϕ' is greater for the implicit schemes.

In the remaining of this section, the weighting coefficients a_i corresponding to case No. 1 are retained to investigate the accuracy of the finite difference analog for different values of the parameters β , and Δt . Even though such a choice of weighting coefficients is used in this research, it has not been demonstrated optimum.

Table 5.1

Effect of Various choices of weighting coefficients a_i
on the values of ρ' and ϕ' for the zero frequency

Case Number	Choice of a_i	ρ'	ϕ'
Fixed parameters	$\beta = 0.80$ $\tau = 2.5$ $\Delta t = 0.01$		
1	$a_1 = a_3 = a_4 = a_6 = \frac{1}{12}$ $a_2 = a_5 = \frac{1}{3}$	1.0149	0.3877
2	$a_1 = a_3 = a_4 = a_6 = 0$ $a_2 = a_5 = 1/2$	1.0149	0.988
3	$a_1 = a_2 = a_3 = a_4 = a_5 = a_6$ $= 1/6$	1.0153	0.9870
4	$a_1 = a_3 = a_4 = a_5 = a_6 = 0$ $a_2 = 1.0$	1.04	0.9807
5	$a_1 = a_3 = \frac{1}{6}$ $a_2 = 2/3$ $a_4 = a_5 = a_6 = 0$	1.04	0.9807
6	$a_1 = a_2 = a_3 = \frac{1}{3}$ $a_4 = a_5 = a_6 = 0$	1.040	0.2807
Exact solution		1.0151	1.0

With the choice of values of a_i corresponding to case No. 1

$$a_1 = a_3 = a_4 = a_6 = \frac{1}{12}$$

$$a_2 = a_5 = 1/3$$

the expressions for ϕ' and ρ' reduce to:

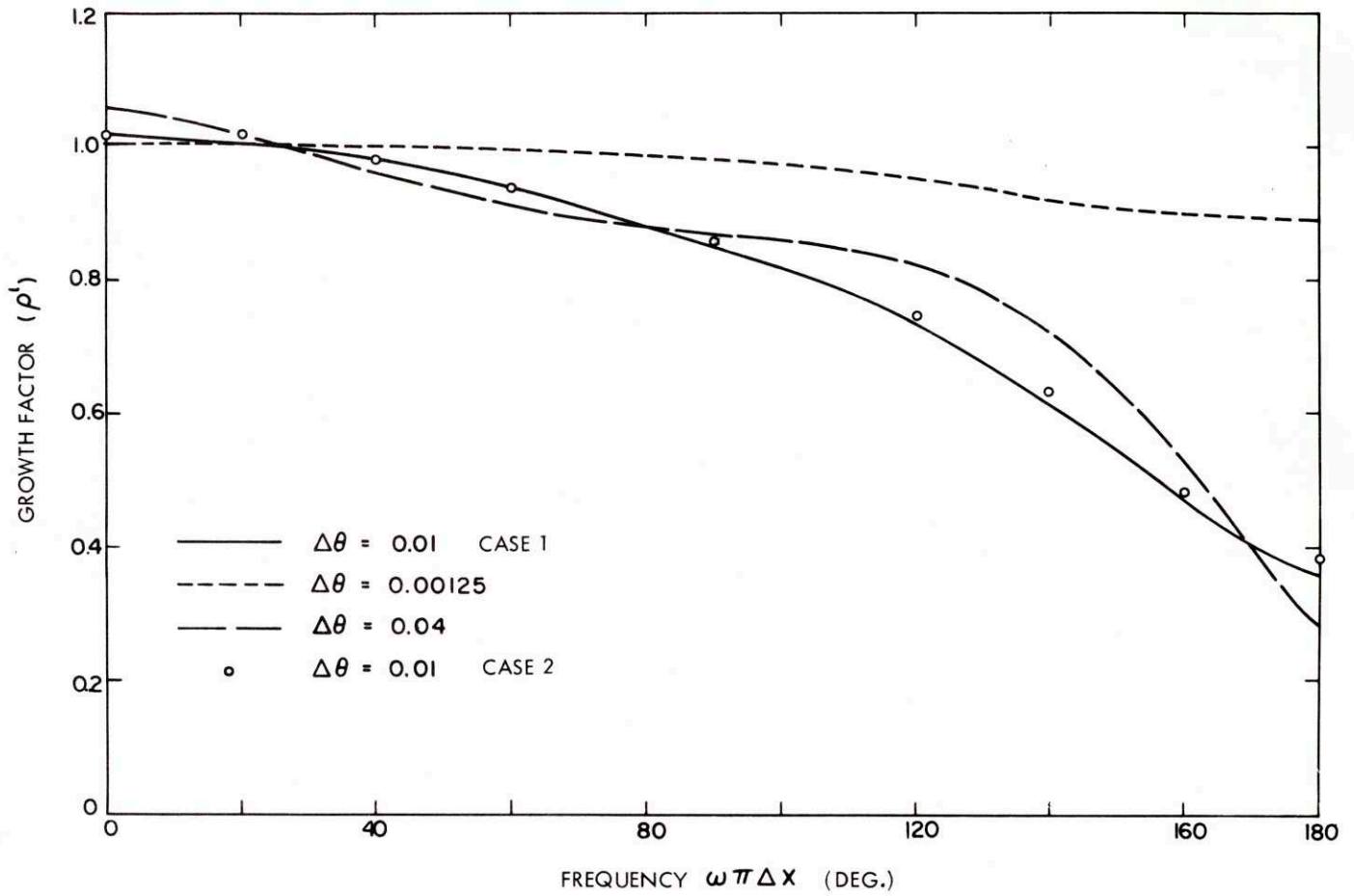
$$\rho'^2 = \frac{\left\{ \frac{2}{3} - \frac{(1-2\Gamma)\Delta t}{3} + \left[\frac{1}{3} - \frac{1-2\Gamma}{6} \Delta t \right] \cos \omega \pi \Delta x - a \sin^2 \frac{\omega \pi \Delta x}{2} \right\}^2 + \left\{ \frac{\beta}{2} \sin \omega \pi \Delta x \right\}^2}{\left\{ \frac{2}{3} + \frac{\Delta t}{3} + \left[\frac{1}{3} + \frac{\Delta t}{6} \right] \cos \omega \pi \Delta x + a \sin^2 \frac{\omega \pi \Delta x}{2} \right\}^2 + \left\{ \frac{\beta}{2} \sin \omega \pi \Delta x \right\}^2} \quad (5.61)$$

$$\phi' = \frac{1}{\beta \omega \pi \Delta x} \left\{ \text{artang} \frac{\frac{\beta}{2} \sin \omega \pi \Delta x}{\frac{2}{3} - \frac{(1-2\Gamma)\Delta t}{3} + \left[\frac{1}{3} - \frac{(1-2\Gamma)\Delta t}{6} \right] \cos \omega \pi \Delta x - a \sin^2 \frac{\omega \pi \Delta x}{2}} + \text{artang} \frac{\frac{\beta}{2} \sin \omega \pi \Delta x}{\frac{2}{3} + \frac{\Delta t}{3} + \left[\frac{1}{3} + \frac{\Delta t}{6} \right] \cos \omega \pi \Delta x + a \sin^2 \frac{\omega \pi \Delta x}{2}} \right\} \quad (5.62)$$

The values of the paramters a and β corresponding to the various choices of Δt investigated appears in Table 5.2

Figure 5.1 shows the dependence of the growth factor ρ' with the frequency of the starting sine wave for the three sets of parameter presented in Table 5.2. The growth factor ρ' corresponding to the zero frequency is larger than unity as it is expected in the case of a source term. In presence of diffusion, as the frequency increases the growth factor decreases and becomes smaller than unity. This observation is in agreement with the analytical solution presented in Eq. 5.54. In presence of diffusion the highest frequency will consequently be decayed and will not affect the stability of the computer scheme. On the contrary it can be shown in Eq. 5.61 that in absence of diffusion the

Fig. 5.1 Dependence with Frequency of the Growth Factor ρ'



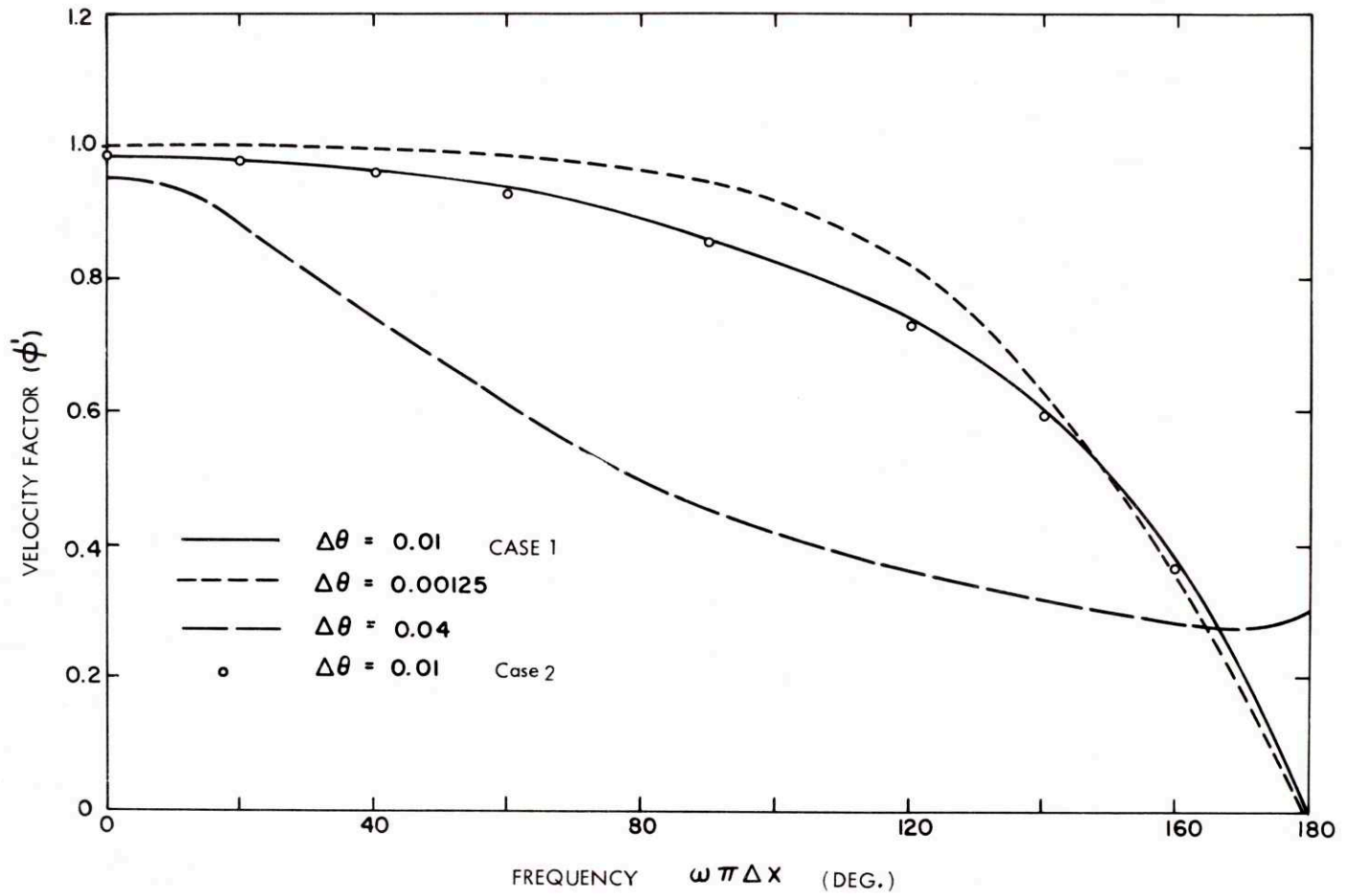


Fig. 5.2 Dependence with Frequency of the Velocity Factor ϕ'

Table 5.2

Parameters hold constant	$D = 2.10^{-4}$
	$r = 2.5$
	$\Delta x = 0.005$
	$V = 0.4$

Parameters changed during investigation

<u>Time increment Δt</u>	<u>Parameter β</u>	<u>Parameter α</u>
0.00125	0.10	0.020
0.010	0.80	0.160
0.040	3.20	0.64

growth factor for the highest frequency is equal to the growth factor for the fundamental, that is to say, is greater than unity. Figure 5.2 illustrates the dependence of the velocity factor with the frequency of the starting sine wave for the same set of parameters α , β and Δt .

The departure from unity of the value ϕ' corresponding to the zero frequency increases as β increases. Furthermore, as β increases the departure of the entire curves from the horizontal axis $\phi' = 1.0$ increases and becomes important for smaller and smaller frequencies. This is equivalent to say, the number of higher harmonics being shifted out of phase with the fundamental, increases as β increases. The use of time and distance increments corresponding to a value of $\beta = 3.2$ are expected to show oscillations in distance since the curve ϕ' corresponding to those conditions departs from the horizontal even for very low frequencies. These oscillations were observed on the computer solutions using the corresponding value of $\Delta\Theta = 0.04$.

From Fig. 5.2 it appears that the conclusions drawn by Stone and Brian apply in this case: since the highest frequencies are not travelled at the same rate as the lower frequencies, they have to be decayed.

In absence of a diffusion term the highest frequencies cannot be decayed since it has been seen previously that their growth factor is greater than unity. It has been found, in fact, that the computation results obtained with

a zero value of the diffusivity D experience oscillations even with very small time and distance increments.

In Figs. 5.1 and 5.2 the values of ρ' and ϕ' corresponding to a different choice of the weighting coefficients α_i are presented for a given set of parameter. (The choice of α_i corresponds to case No. 2 of Table 5.1.) Under these conditions, the values of β' and ϕ' never differ by more than one half percent. It should be pointed out that this comparison has not been carried to the point where the choice of weighting coefficients α_i , used in this research, can be called optimum.

The conclusions reached in this section, for a source term, apply also to the case of a sink. With the choice of parameters α , β and Δt investigated, the growth factor corresponding to a sink is always smaller than unity. Under these conditions any error introduced in the computation is expected to decay.

The results presented in this section show the influence of the time increment on the rate of travel and decay of a sine wave present in the bed at the beginning of a computation. It has been seen that the presence of diffusion is required to eliminate the highest frequencies which are shifted out of phase, and this even more so in the case of a source term.

Since the equations solved on the computer are nonlinear, the results obtained in this section can only be qualitative and must be confirmed by a convergence study of the proposed algorithm. The results of this study are presented in the next section.

C. CONVERGENCE STUDY OF THE PROPOSED SCHEME

To test the convergence of the proposed computer scheme a 5°C step change in the input temperature is imposed on the reactor which was operated at a steady state. The effect of the distance and time increment on the variation of the temperature in the catalyst section are studied for several positions in the bed. The conditions of the runs performed during this investigation are presented in Table 5.3.

Table 5.3

Run n ^o	$\Delta\Theta$	number distance slices	max Δa	min Δa
F-II-1	0.01	200	0.00898	0.00102
F-II-2	0.01	100	0.01792	0.00208
F-III-3	0.01	50	0.03568	0.00432
F-I-1	0.005	100	0.01792	0.00208
F-I-2	0.010	100	0.01792	0.00208
F-I-3	0.020	100	0.01792	0.00208
F-I-4	0.040	100	0.01792	0.00208

Since the computer program uses a variable space grid, the number of slices is complemented by the maximum and the minimum value of Δa used in the run.

Figures 5.3, 5.4, 5.5, and 5.6 present the results obtained with a 200-, 100-, and 50- mesh space-grid at four locations in the reactor. The results obtained with a 200- and 100-mesh space-grid never differed by an amount larger than 0.04°C and did not present any oscillation. The results obtained with a 50-mesh grid presents oscillations when the temperature at the position considered changes rapidly. The oscillations decay but the error introduced travels down the reactor. Figures 5.7 and 5.8 represent the temperature variation for two locations inside the catalyst bed when $\Delta\Theta$ takes the values 0.005, 0.01, 0.020, and 0.04. The results obtained with $\Delta\Theta = 0.005$ and 0.01 show a perfect agreement and do not present oscillations. The results obtained with larger values of $\Delta\Theta$ present oscillations as the temperature starts to change rapidly. The presence of these oscillations can be explained through the results of the stability analysis of Section B of this chapter. When used with large values of β the finite difference equations do not allow even the low frequency to travel at the proper rate.

Fig. 5.3 Effect of Distance Grid Size on Convergence of the Solution at $\alpha = 0$

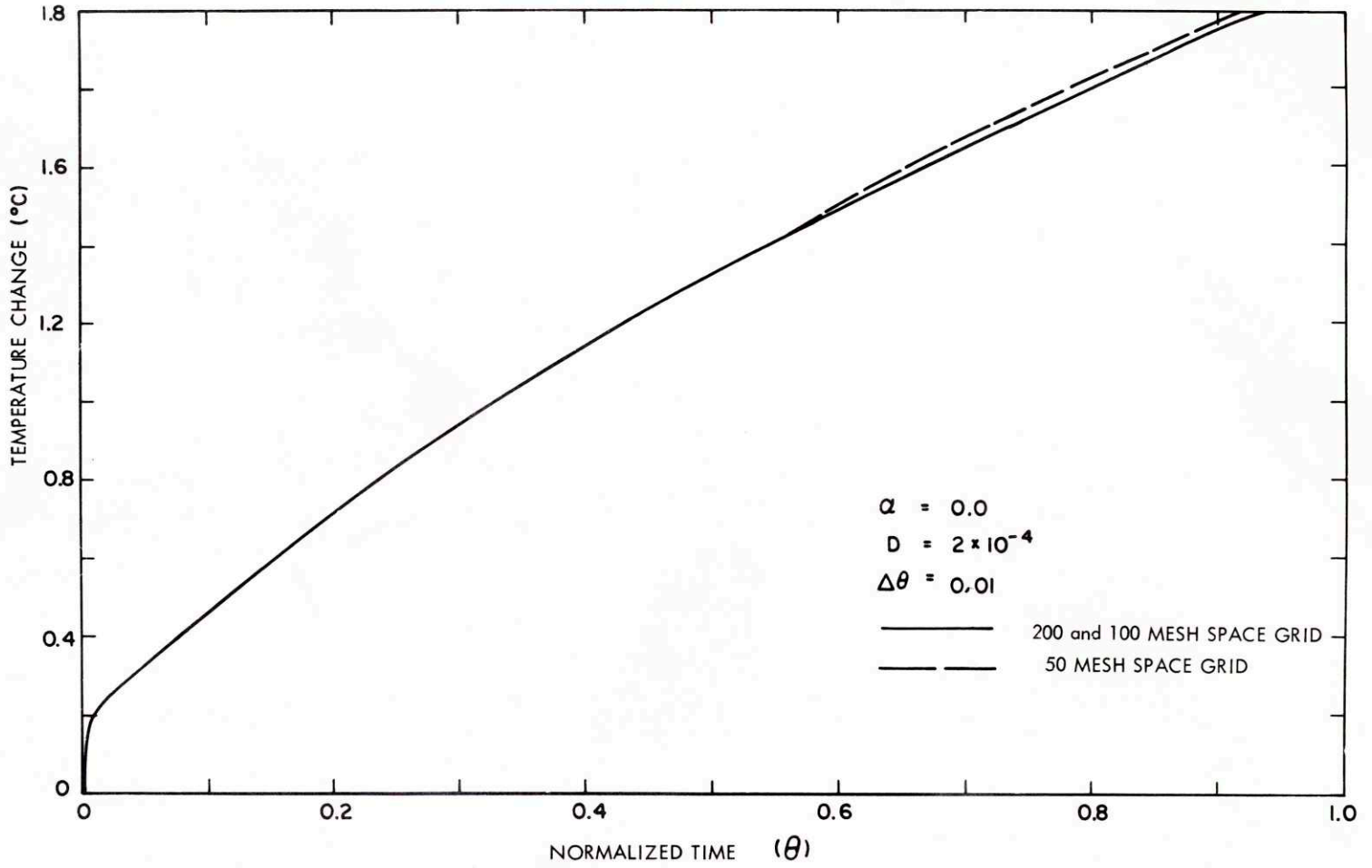
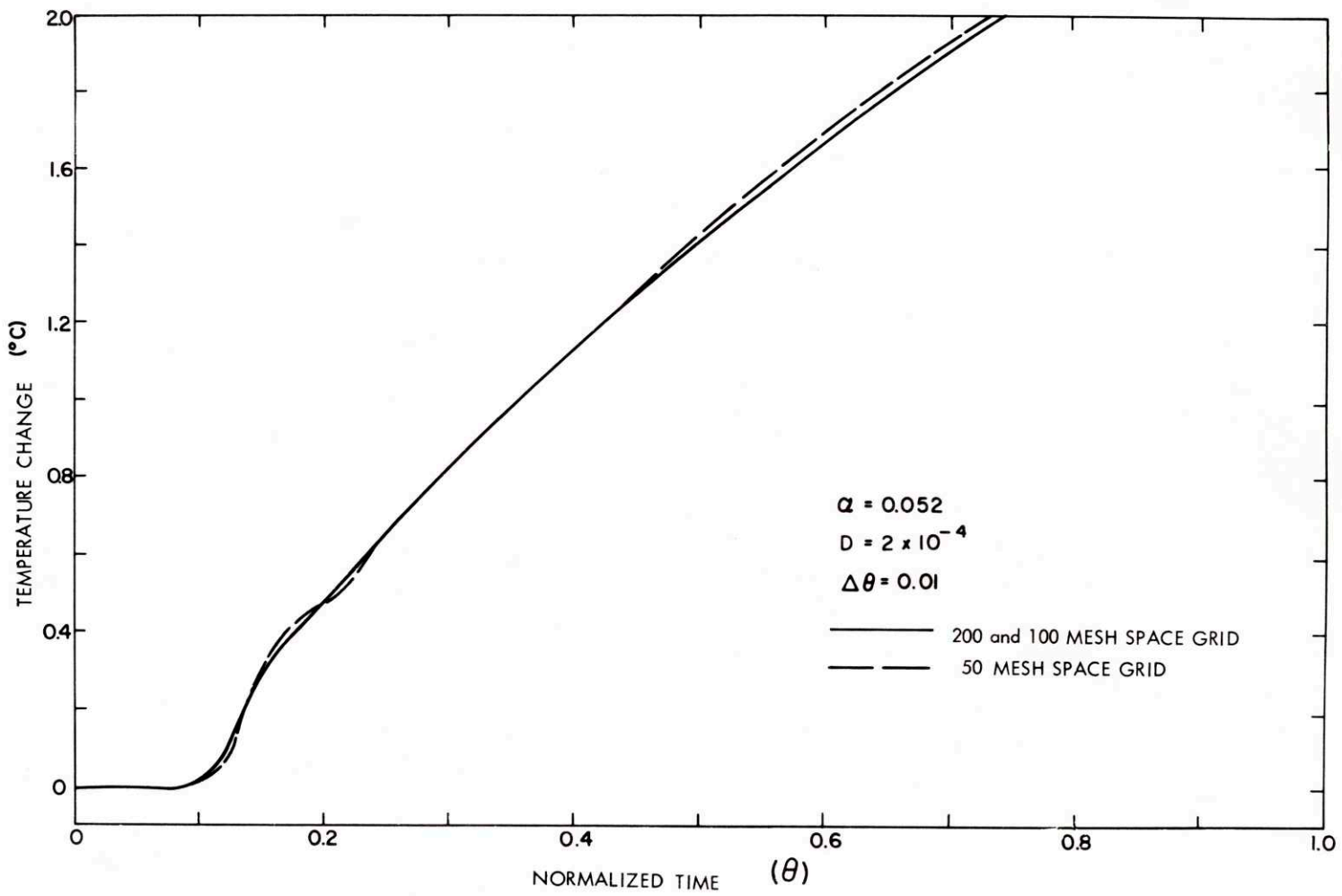


Fig. 5.4 Effect of Distance Grid Size on Convergence of the Solution at $\alpha = 0.052$



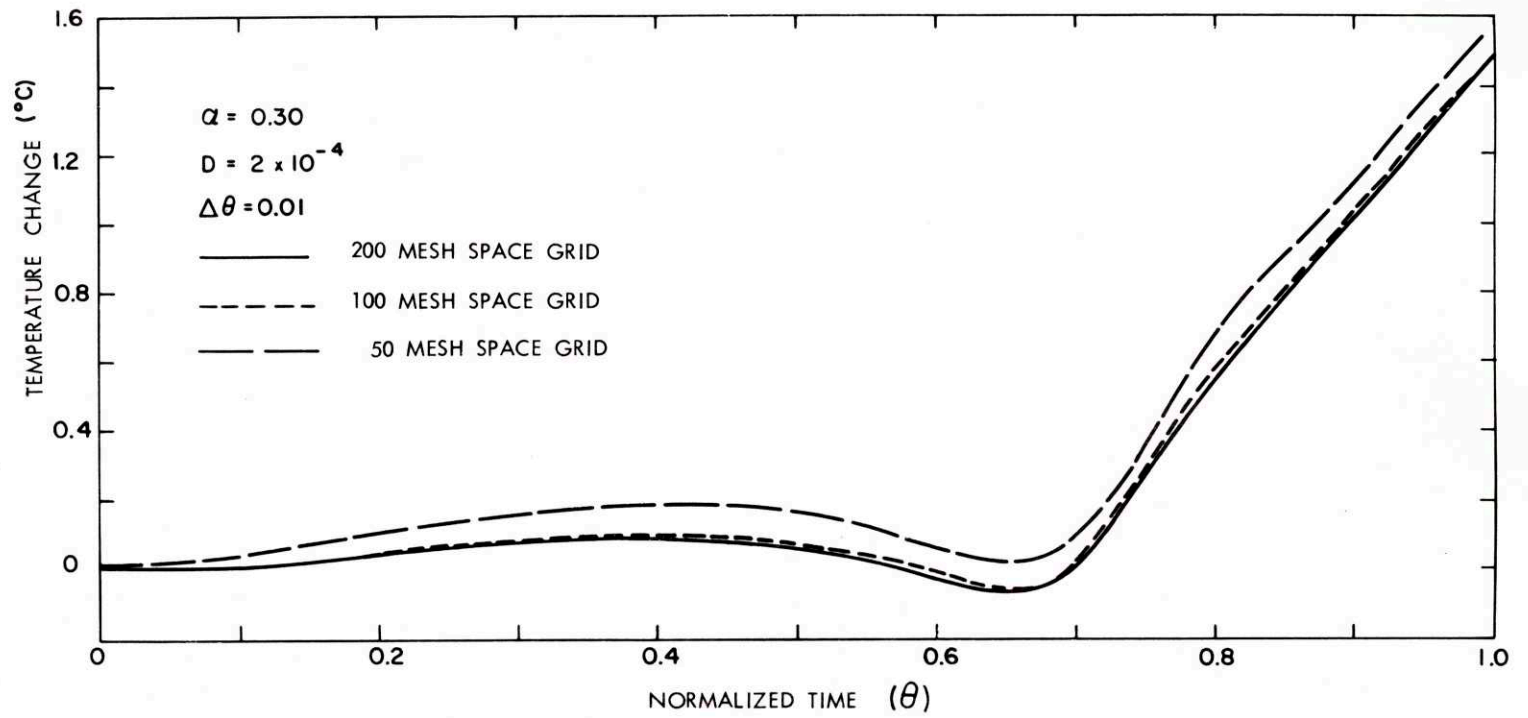


Fig. 5.5 Effect of Distance Grid Size on Convergence of the Solution at $\alpha = 0.30$

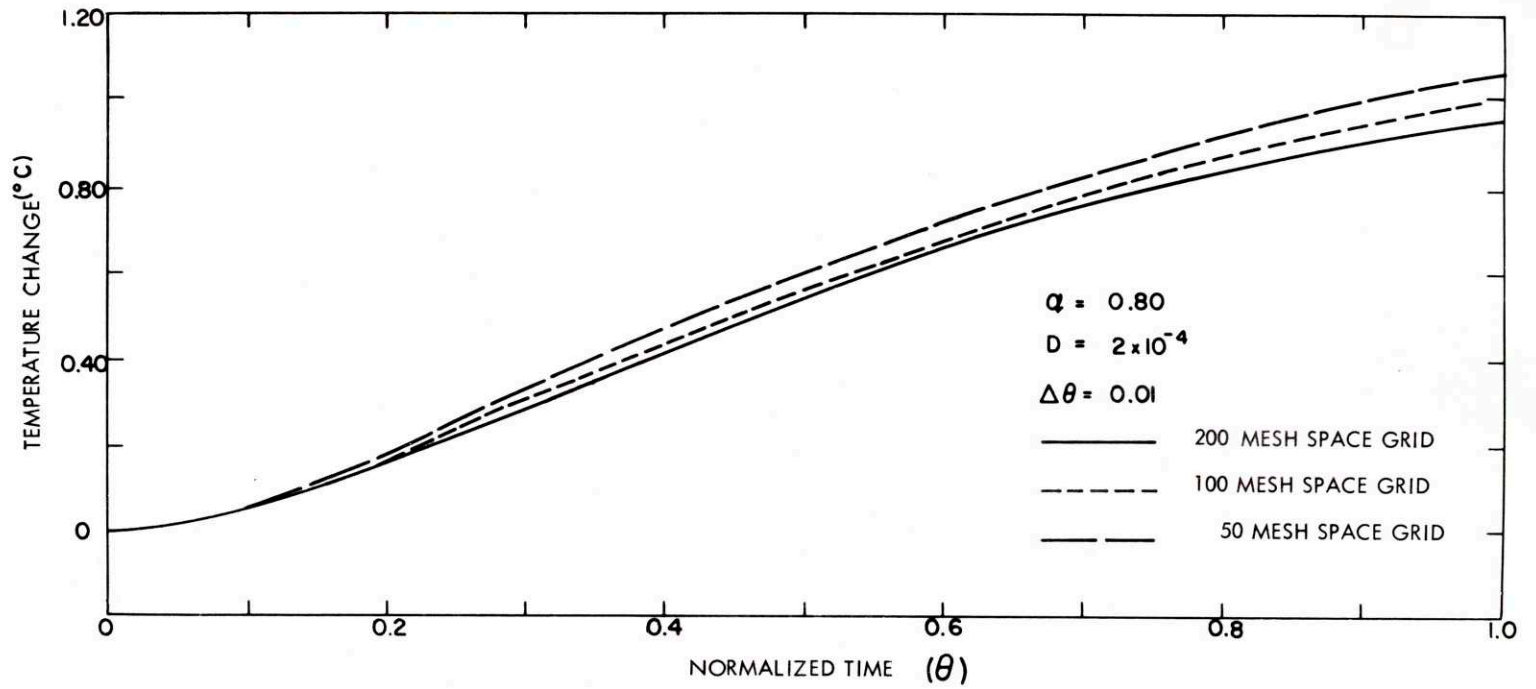


Fig. 5.6 Effect of Distance Grid Size on Convergence of the Solution at $\alpha = 0.80$

Fig. 5.7 Effect of Time Increment on Convergence of the Solution at $\alpha = 0.052$

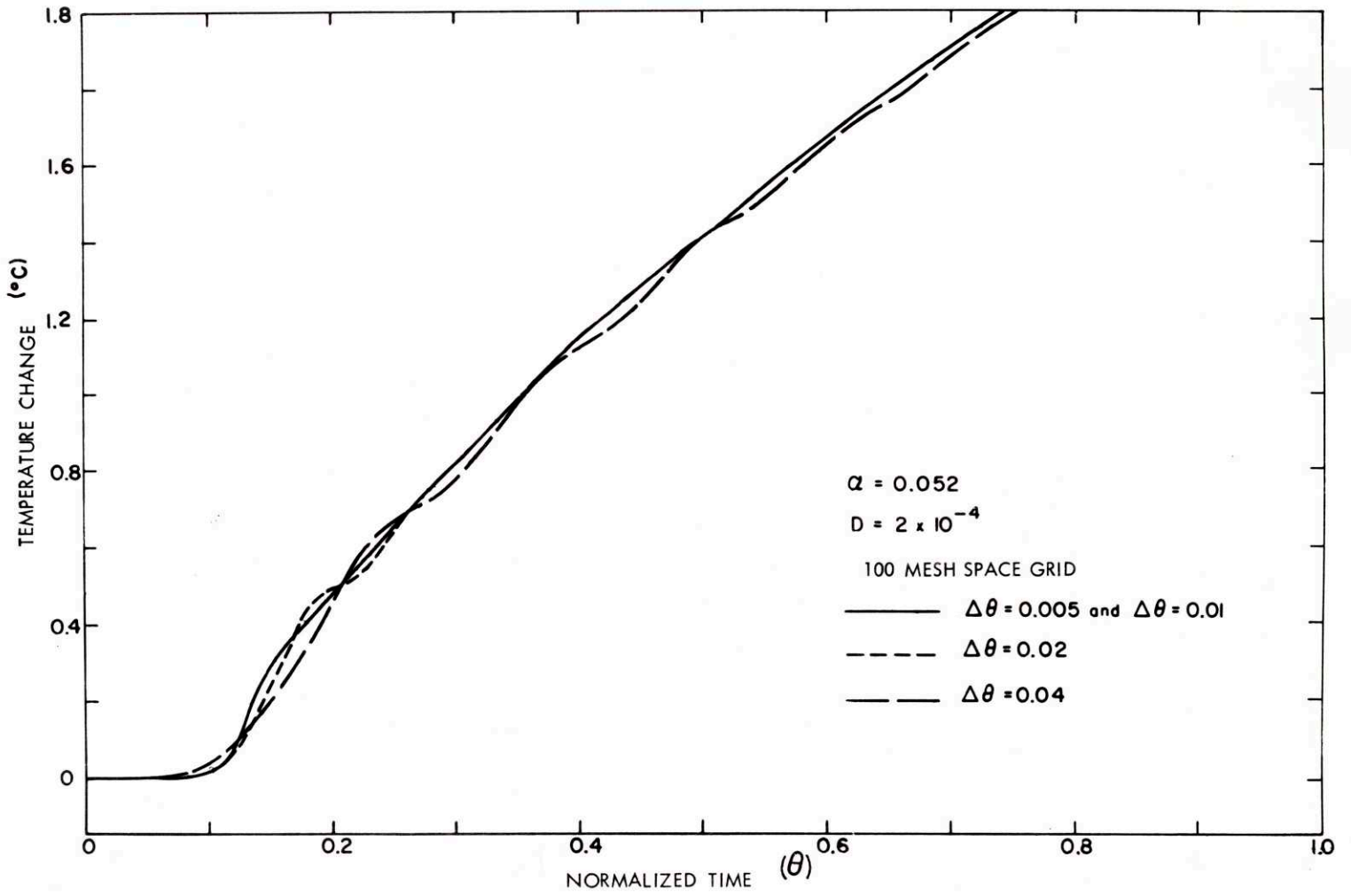
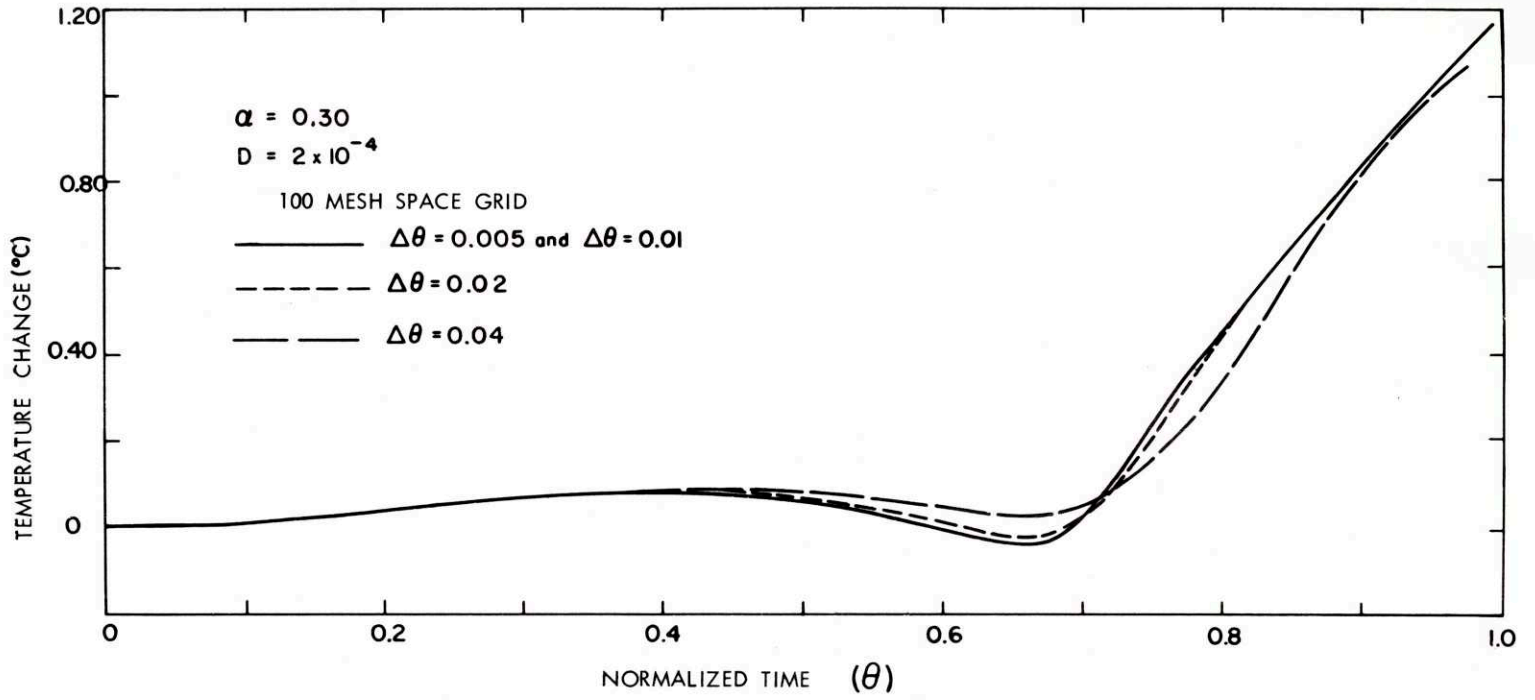


Fig. 5.8 Effect of Time Increment on Convergence of the Solution at $\alpha = 0.30$



The oscillations so generated, however, die rapidly and do not affect the change in temperature at points further down the reactor. Furthermore, the results obtained with large values of $\Delta\Theta$ agrees with the results obtained with the smallest values of $\Delta\Theta$ at every position before the temperature starts to change rapidly. Good agreement also exists when the change has occurred for some length of time. For this reason a small time increment is only needed as long as rapid changes in temperatures occur inside the bed. In Chapter VI it will be seen that the changes in temperature inside the catalyst section can be described as a temperature wave travelling through the bed followed by a slower approach to a new steady state. Small values of the time increment are required as long as the temperature wave remains inside the bed. Since the time required for this wave to travel through the bed can be estimated, it is possible to determine at what time the time increment can be modified.

The following time and distance increment have been used to describe the transient resulting from step changes in the feed temperature.

number of distance slices	100
max Δa	0.01792
min Δa	0.00208
Time increment as long as the wave travel inside the bed	$\Delta\Theta = 0.01$
Time increment after	$\Delta\Theta = 0.04$

During the runs simulating the converter under automatic control the value of $\Delta\Theta = 0.01$ was kept throughout the computation since the feed temperature of the reactor keeps changing with time.

D. COMPARISON WITH THE C.I.R. SCHEME

Stone and Brian have reported that their method of approximating distance and time first derivatives is the most effective for the solution of linear problems. In order to check this result in the nonlinear case under investigation, the Courant-Isaacson and Rees¹⁰ method of solution abbreviated C.I.R. method was used to solve the energy equation inside the catalyst

$$\frac{\partial v}{\partial \theta} + \left[\frac{s}{f'} (1 - h \frac{y-y^*}{1+y}) \right] \frac{\partial v}{\partial \xi} + v - m - [e + h(v - 0.3725)] s r = 0 \quad (5.2)$$

The approximation used for the time and distance derivatives are as follows

$$\frac{\partial v}{\partial \theta} = \frac{v_{j,n+1} - v_{j,n}}{\Delta \theta}$$

$$\frac{\partial v}{\partial \xi} = \frac{v_{j,n} - v_{j-1,n}}{\Delta \xi}$$

The source or sink term present in Eq. 5.2 is always expressed at position j and at early time n . The finite difference approximation of Eq. 5.2 expressed in terms of $v_{j,n+1}$ is written

$$v_{j,n+1} = v_{j,n} \left\{ 1 - \frac{s}{f'_j} (1 - h \frac{y_{j,n} - y^*}{1 + y_{j,n}}) \frac{\Delta \theta}{\Delta \xi} - \Delta \theta \right\} + v_{j-1,n} \left[\frac{s}{f'_j} (1 - h \frac{y_{j,n} - y^*}{1 + y_{j,n}}) \frac{\Delta \theta}{\Delta \xi} \right] + m_{j,n} \Delta \theta + [e + h(v_{j,n} - 0.3725)] s r (v_{j,n}, y_{j,n}) \Delta \theta \quad (5.63)$$

The computing process in this case is a simple marching process since each equation is explicit in $v_{j, n+1}$. The entrance boundary condition retained in this case is:

$$v_{1, n+1} = w_{1, n+1} \quad (5.64)$$

Figures 5.9 and 5.10 present the time variations of the temperature at the location $\alpha = 0.028$ and $\alpha = 0.0528$ in the early instants of a transient resulting from a $+ 5^{\circ}\text{C}$ step change in the feed temperature.

On each of the figures is plotted the results obtained with 50-, 100- and 200-mesh distance grid and a time increment $\Delta\theta = 0.00125$. The results show that under these conditions the convergence of the numerical solution is not obtained.

In Fig. 5.9 it appears that the effect of increasing the distance mesh size is equivalent to a smearing effect on the wave front traveling down the reactor. This effect could be predicted from the results reported by Stone and Brian³⁰ for the linear Eq. 5.65

$$V \frac{\partial y}{\partial x} + \frac{\partial y}{\partial t} = 0 \quad (5.65)$$

The approximations of the C.I.R. method result in the introduction of a dispersion term of the form

$$\frac{V\Delta x}{2} \frac{\partial^2 y}{\partial x^2}$$

since the approximations are only first-order correct in distance. To be able to reduce the diffusion effect introduced by the C.I.R. method to the same order of magnitude as the physical diffusion existing in this reactor, the size of the distance grid must be reduced to 10^{-3} , that is to say, one must use a distance grid of 1000 meshes. Furthermore the results of the Stone and Brian analysis have proven that the C.I.R. method is unstable unless the following restriction is observed

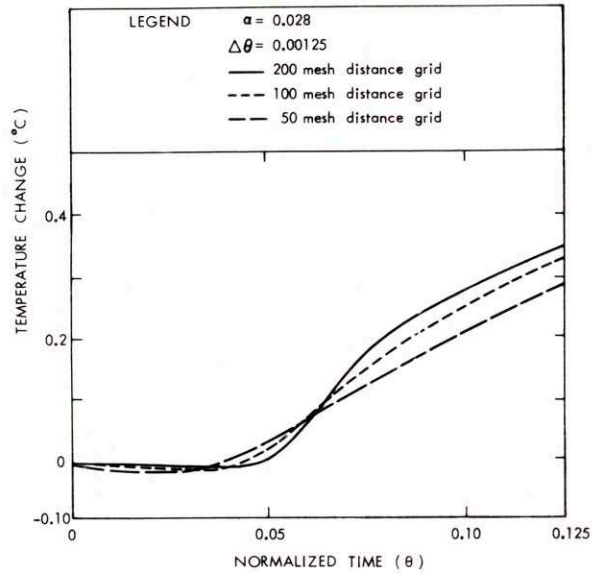


Fig. 5.9 Effect of Distance Grid Size on the Convergence of the C.I.R. Solution at $\alpha = 0.028$

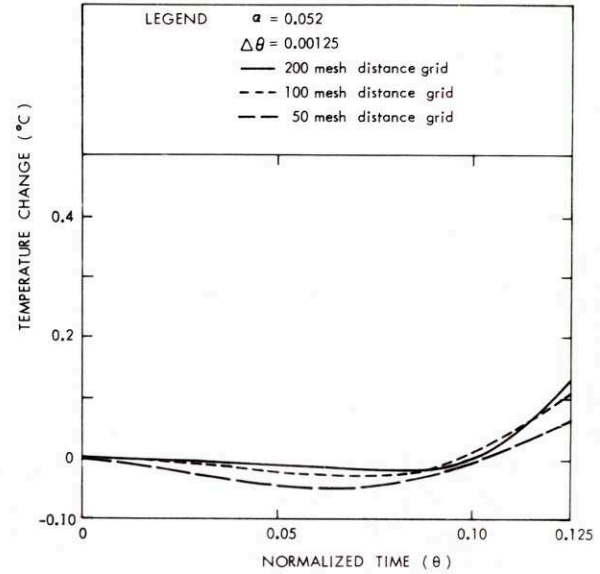


Fig. 5. Effect of Distance Grid Size on the Convergence of the C.I.R. Solution at $\alpha = 0.052$

$$\beta = \frac{V \Delta t}{\Delta x} < 0.5$$

For a value $\Delta x = 10^{-3}$ the corresponding value of time increment is then 10^{-3} . The only advantage of the C.I.R. method, which is that it is explicit, is offset by the extremely small values of the time and distance increments required to obtain convergence of the solution. In the present problem more of the computer time was taken by the estimate at each time and distance step of the rate of reaction. Under these conditions the excess time required to solve the linear system of equations resulting from the Stone Brian method is negligible. Under these conditions the Stone Brian method, in computation time, can be compared directly to the C.I.R. method on the basis of the time and distance increments acceptable for convergence. The present study of the C.I.R. scheme was not carried to the point where convergence of the solution was obtained. But, already with a 200-mesh space-grid, representing an added diffusion five times larger than the physical diffusion, the computer time was greatly in favor of the Stone Brian method of solution.

CHAPTER VI

RESULTS AND DISCUSSION

A. STEADY STATE OF THE REACTOR

In order to characterize the conditions of the T.V.A. reactor at the beginning of a transient the steady state equations describing it, are solved first.

Equations 4.3 and 4.5 apply unchanged to the steady state case since the variable time does not appear explicitly in them. In Eqs. 4.7 and 4.10 the time derivatives $\frac{\partial v}{\partial \Theta}$ and $\frac{\partial m}{\partial \Theta}$ must be removed in order to use these equations for the steady state case.

Logeais²² method of solution of this system of ordinary differential equations provides the steady state profiles in the case where longitudinal diffusion of heat is neglected, that is to say, for the case where Eq. 4.10 is a first-order differential equation.

The presence of the diffusion term forces us to use the method of solution of the transient case, presented in Chapter V, to generate steady state profiles: the transient is computed until the temperature in the reactor stops changing with time. This last method consumes much more computer time in order to generate one steady state profile corresponding to a given feed temperature; furthermore, it was observed that this method of computation allows us to reach only the stable steady state.

It is known⁴² that in industrial reactors of this type the importance of the longitudinal diffusion on the temperature and concentration profiles existing at steady state in the reactor is very small. Nevertheless the longitudinal diffusion has been retained in describing the transient behavior of the reactor in order to obtain stable numerical solutions for the finite difference approximations of Eq. 4.10 as was shown in Chapter V.

The effect of longitudinal diffusion on the steady state behavior of the T.V.A. reactor has been investigated in computing the concentration and temperature profiles corresponding to a feed temperature of 227.6°C

1. for the case where longitudinal diffusion of enthalpy is neglected (the method of solution is the method proposed by Logeais).
2. for the case where longitudinal diffusion of enthalpy, (as it can be estimated for packed bed similar to the reacting section of the T.V.A. reactor) is taken into consideration and the transient method of solution presented in Chapter V is applied in this case.

The results of this investigation are presented in Table 6.1 where the temperature inside the catalyst section, inside the tube wall, inside the empty tube section and the ammonia mole fraction are presented for both cases at different positions in the reactor. The largest temperature differences are encountered in the catalyst section as can be expected. The maximum temperature difference is of the order of 0.6°C and correspond to a location close to the entrance of the reactor.

The temperature profile obtained in the case where longitudinal diffusion is considered is above the temperature profile obtained in absence of the diffusion during the first part of the reactor. This can be explained by the fact that the catalyst temperature at the entrance of the reactor is larger in the case with diffusion. This difference in temperature at $a = 0$ results from the entrance boundary condition associated with each problem. In absence of diffusion the temperature of the catalyst at $a = 0$ is set equal to the temperature of the gas leaving the empty tube section. In presence of diffusion, as shown by Danckwerts,¹¹ the temperature experiences a discontinuity at the entrance of the bed. The existence and the magnitude of the discontinuity was presented in Chapter IV. Since the reacting gas seen by the catalyst located immediately downstream is at a higher

Table 6.1

Effect of longitudinal diffusion on the reactor steady state profile

Normalized Distance for Top of the Reactor	$T_{C_{D=0}}$	$T_{C_{D=physical}}^{\text{diffusion}}$	$T_{T_{D=0}}$	$T_{T_{D=physical}}^{\text{diffusion}}$	$T_{W_{D=0}}$	$T_{W_{D=physical}}^{\text{diffusion}}$	$Y_{D=0}$	$Y_{D=physical}^{\text{diffusion}}$
0.0	427.25	427.61	427.25	427.39	427.25	427.38	0.0500	0.0500
0.100	471.64	472.12	424.04	424.13	443.43	443.68	0.08227	0.08036
0.208	510.18	510.63	413.42	413.45	452.83	453.03	0.11266	0.11286
0.30	528.66	528.91	399.22	399.21	451.94	452.04	0.13510	0.13525
0.408	531.92	531.97	378.40	378.37	440.93	440.94	0.15238	0.15246
0.506	524.97	524.94	357.07	357.04	425.46	425.43	0.16322	0.16328
0.600	514.19	514.14	334.97	334.94	407.97	407.93	0.17213	0.17217
0.719	499.73	499.66	309.50	309.47	386.98	386.93	0.18112	0.18116
0.812	481.29	481.21	280.45	280.42	362.26	362.21	0.19016	0.19019
0.912	461.69	461.61	252.62	252.61	337.78	337.74	0.19756	0.19756
1.0	442.20	442.21	227.58	227.58	314.88	314.88	0.20310	0.20313

temperature, the catalyst temperature at this position will have the tendency to be higher. The original temperature difference, which is of 0.36°C , will be amplified and then attenuated as the gases proceed down the reactor according to the sign and the magnitude of the temperature and concentration dependence of the heat generation by chemical reaction. This amplification and attenuation concept will be discussed in detail in the next section.

Since the effect of the diffusion present in the T.V.A. reactor on the steady state profile was so small, it was neglected and Logeais¹² method of computation was retained in generating steady state profiles for the determination of the "blow out" temperature associated with the present conditions of operation.

The dependence of the temperature at the outlet of the empty tube section with the feed temperature is presented in Fig. 6.1. Under the flow rate and feed conditions investigated, the "blow out" temperature is equal to 220°C . If the feed temperature is larger than 220°C two different temperature profiles would satisfy the steady state equations for the given boundary condition, but the steady state corresponding to the higher conversion only is stable as the considerations of Chapter III show. If the feed temperature to the reactor is lower than 220°C the reactor will "blow out".

Figure 6.2 presents the dependence of the feed temperature on the outlet ammonia mole fraction. The maximum ammonia production corresponds to a feed temperature of 225°C . Since a steady state corresponding to a feed temperature of 227.6°C generated by the transient method of solution was available, the transient behavior of the T.V.A. reactor has been investigated around this temperature which is considered for practical purposes as the optimum temperature of operation.

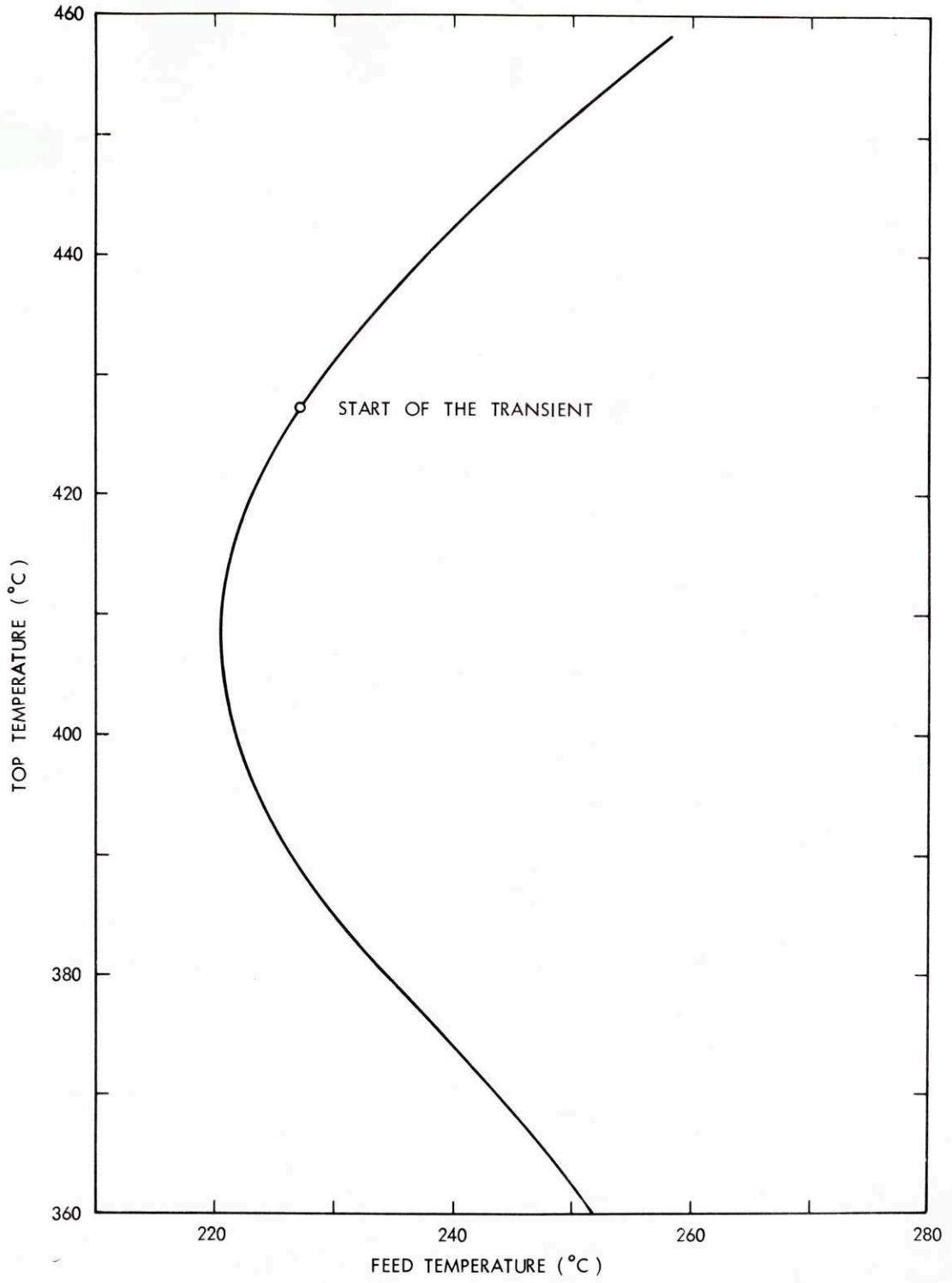


Fig. 6.1 Steady State Relation between Top and Feed Temperature

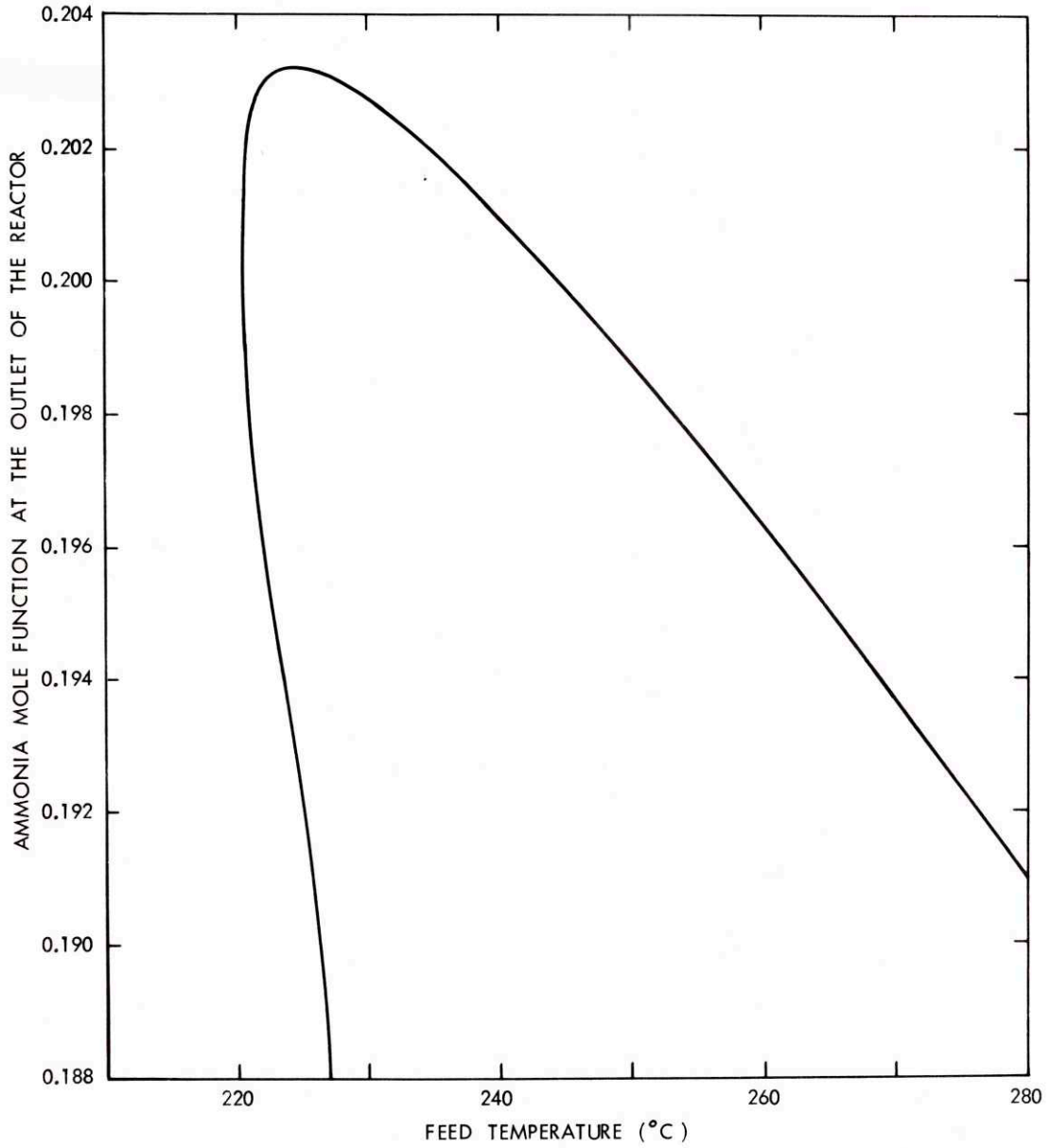


Fig. 6.2 Steady State Relation between Outlet Ammonia Mole Fraction and Feed Temperature

In investigating the transient behavior of the reactor around this temperature, step changes in the feed temperature were performed and the effect of these changes on the temperature and concentration profiles was analysed.

The different values of the feed temperature investigated are presented in Table 6.2.

Table 6.2

Conditions of Transients Performed in this Investigation

<u>Run No.</u>	<u>Starting condition</u>	<u>New Feed temperature</u>	<u>Size of the step</u>
1	steady state corresponding to a feed temperature $T_W = 227.6^\circ\text{C}$	212.6	-15°C
2	" "	217.6	-10°C
3	" "	222.6	-5°C
4	" "	232.6	$+5^\circ\text{C}$
5	" "	237.6	$+10^\circ\text{C}$

The steady state considerations reported before show that the feed temperature used in runs 3, 4 and 5 are above the "blow out" temperature for the flow rate and feed compositions investigated. It is expected that as a result of such a step in the feed temperature the reactor will approach a new stable steady state.

In the same way, since the feed temperature used in runs 1 and 2 are below the "blow out" temperature, the reactor is expected to "blow off" that is to say--to experience a decrease in temperature and conversion which would force the operator after a certain time to use the heater to restore the reactor in its optimum conditions of operation.

In this chapter, Section B describes qualitatively and discusses the changes in temperature and concentration generated during run 4.

Section C describes the same changes when the reactor blows off (run 1). Since the magnitude of the step change in feed temperature affects

so strongly the final steady state approached, the present reactor is tested for dynamic linearity in Section D. A linear range of operation is defined and the transient results obtained within this range are used, in Section E to generate frequency response curves and derive the form of simplified transfer function relating the changes in temperature at various locations in the catalyst section to changes in the feed temperature.

In order to introduce the concept of control, the effect of "blow out" perturbations of finite duration are investigated in Section F. In Section G a closed loop ideal controller is tested on the simulation for changes in the amount of ammonia recycled in the feed.

B. DYNAMIC OPERATION OF THE REACTOR UNDER STABLE CONDITION

1. Description of the Results

At the beginning of the transient the temperature and concentration profiles in the reactor correspond to the steady state profiles computed with a feed temperature of 227.6°C. At time zero the feed temperature is stepped by 5°C to 232.6°C. As it is expected the reactor approaches the stable steady state corresponding to the new value of the feed temperature.

Figure 6.3 describes the variations with time of the changes in the catalyst temperature ΔT_c at different locations in the reactor. The temperature change ΔT_c is defined in Eq. 6.1 as the difference between the temperature at any instant and the steady state value of the temperature at the same location at the beginning of the transient.

$$\Delta T = T_c - T_c^* \quad (6.1)$$

Figure 6.4 is an enlargement of the part of Fig. 6.3 corresponding to the early instants of the transient. On both figures and in the remaining figures of this chapter the time is expressed in a dimensionless unit Θ' , defined by Eq. 6.2

$$\Theta' = \frac{F \bar{C}_{p0}}{W C_{pc}} t \quad (6.2)$$

It will be seen later that this unit of time corresponds in the present model to the time required for a thermal perturbation introduced at the entrance of the catalyst section to travel the entire catalyst bed when no reaction takes place. For the conditions under investigation in the T.V.A. reactor, one time unit corresponds approximately to six minutes and 15 seconds. The temperature at the entrance of the catalyst section ($\alpha = 0$) as shown in Fig. 6.3 and 6.4 experiences a rapid change in temperature in the

Fig. 6.3 Changes in Temperature during a $+5^{\circ}\text{C}$ Step Transient

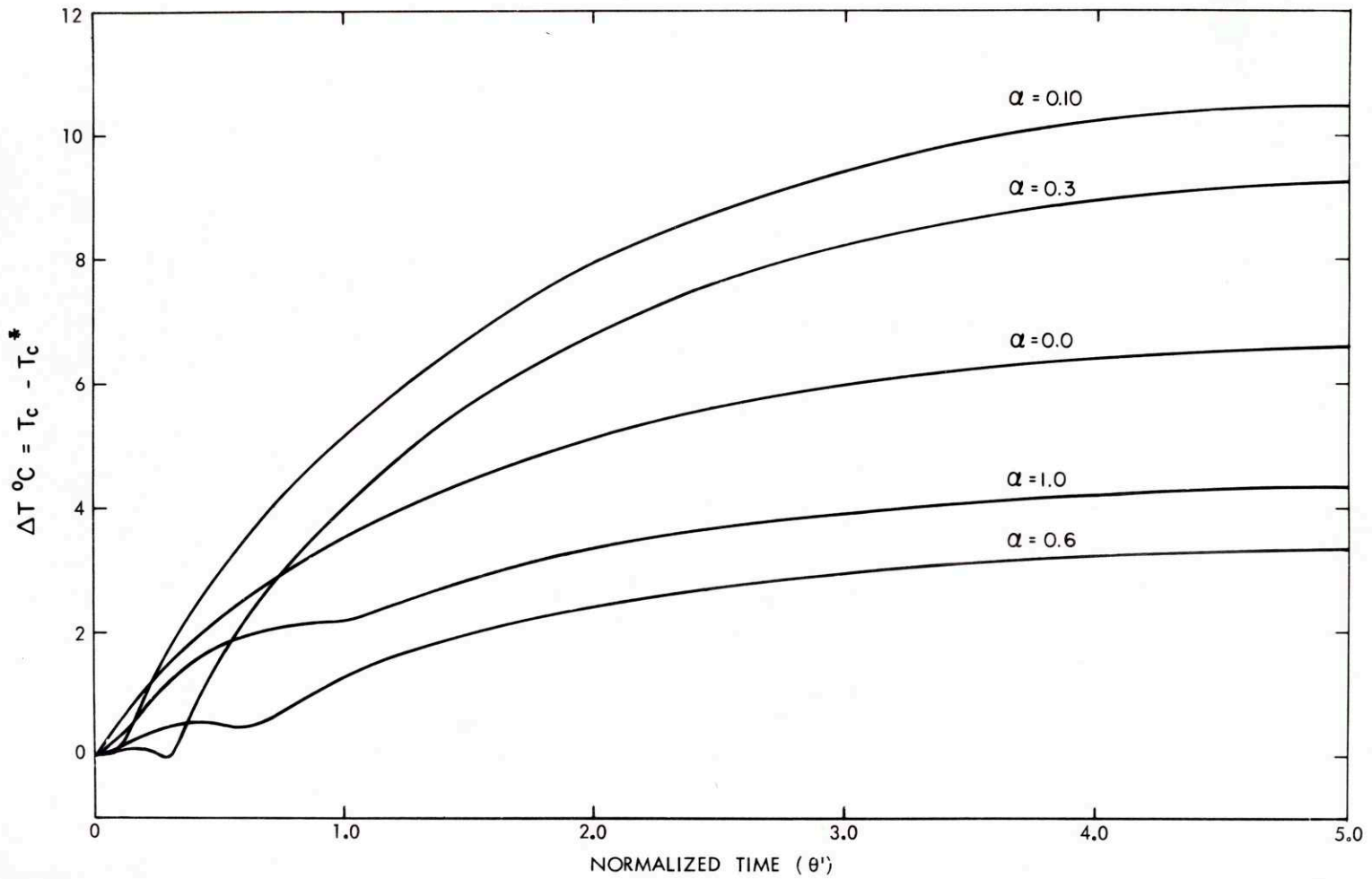
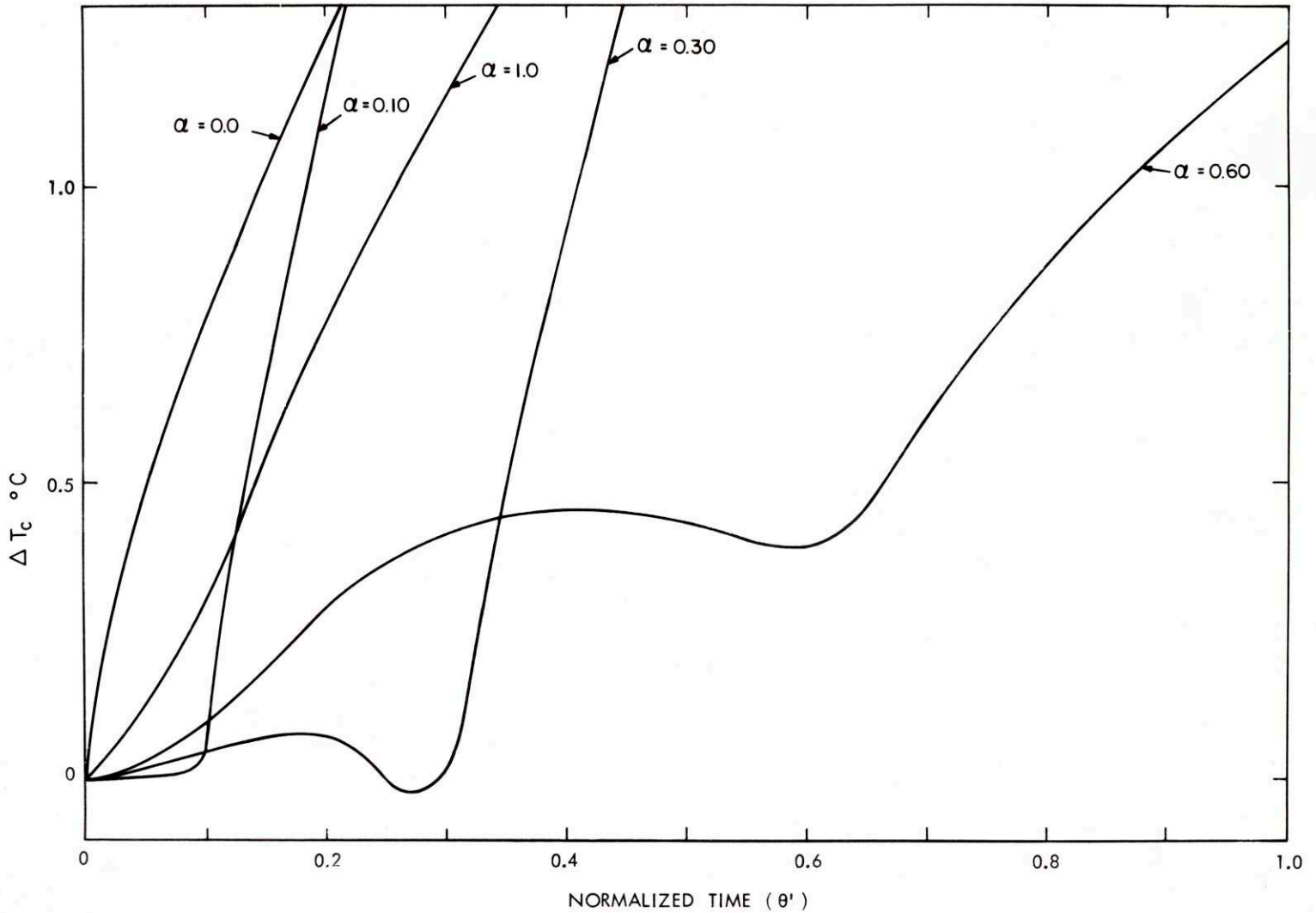


Fig. 6.4 Changes in Temperature during the First Period of a 50C Step Transient



early instant of the transient, followed by a slower approach to the new steady state value. The temperature at a position $\alpha = 0.10$ experiences little change in temperature as long as Θ' is smaller than approximately 0.10 and then an increase in temperature until the new steady state value is approached. The same phenomena is observed for the variations in temperature at a position corresponding to $\alpha = 0.30$. The temperature at that position increases slowly during the first instant of the transient, then slightly dips down before recovery and again initiates an increase until the steady state value is obtained. This last increase in temperature happens at approximately $\Theta' = 0.30$.

The existence of this delay before any appreciable variation in temperature occurs, is characteristic of a perturbation generated in the feed to the catalyst section which travels down the reactor at a finite speed.

The increase in temperature observed at the beginning of the transient experienced by the position $\alpha = 0.30$, becomes more and more pronounced as the value of α increases. The curves of Fig. 6.4 for $\alpha = 0.6$ and $\alpha = 1.0$ show a larger increase in temperature during the first instants of the transient. This phenomena results from changes in the wall temperature of the tubes.

The temperature variations during the first instants of a transient resulting from a step change in the feed temperature can be qualitatively represented as the sum of the perturbations due to the changes in the feed temperature to the catalyst section and of the perturbations due to the variations of the boundary conditions of the catalyst section: the wall temperature. The results of the first type of perturbation can be represented during the first part of

the transient as a "thermal wave" travelling down the reactor at a finite speed, being amplified or attenuated according to the location in the reactor.

The term "thermal wave" is used in this research to describe at a given location rapid changes in temperature occurring at a finite amount of time after the introduction of the feed perturbation; the time delay experienced in the temperature response is a function of the location. In absence of diffusion a thermal wave is characterized by no change in temperature before the arrival of the wave front, then by an instantaneous temperature change as the front passes the location. In this research the presence of diffusion smears the front of the wave and changes in temperature occur before and after the passage of what is still considered the front of the wave.

Figure 6.5 presents the same results but in a different way. The "gain" of the reacting section defined as the ratio of the temperature variations at a certain position to the magnitude of the step change in the feed temperature $\frac{\Delta T_c}{\Delta T_{\text{feed}}}$ is plotted versus the position a in the reactor at different times θ' .

For $\theta' = 0.11$ Fig. 6.5 shows that rapid changes in temperature occur around the location $a = 0.11$. For all the locations corresponding to values of a smaller than 0.11 changes in temperature have already been experienced; on the contrary, at the locations corresponding to values of a between 0.13 and 0.5, the steady state conditions prevailing at the beginning of the transient are still observed. Already at that time the second half of the reactor has experienced temperature changes felt everywhere at the same time but whose magnitudes are functions of the location. For this reason these changes are not describable by a thermal wave.

At time $\theta' = 0.37$ the zone of rapid changes in temperature has penetrated inside the bed as far as location $a = 0.37$. At the same time the magnitudes of the changes experienced in the second half of the reactor have increased

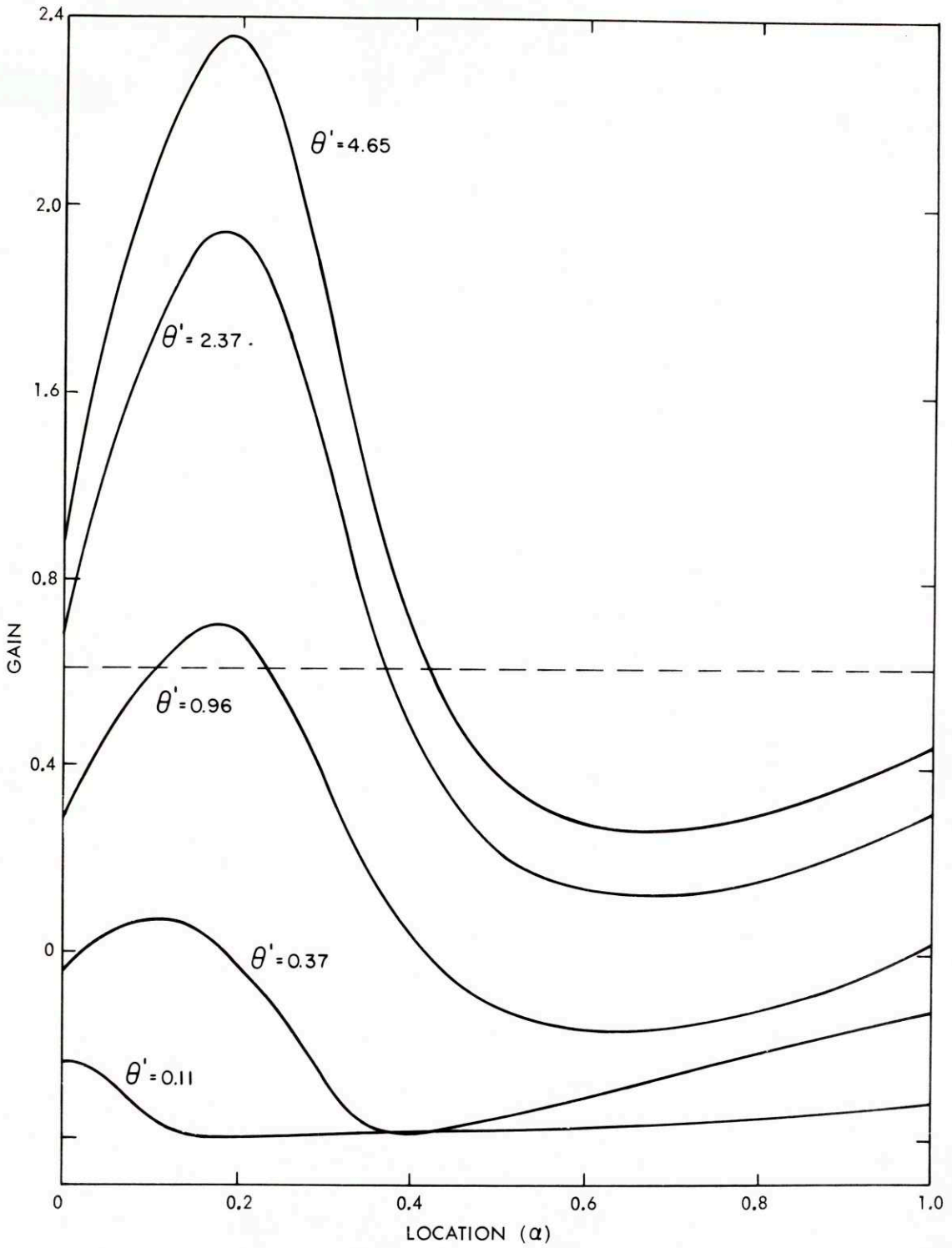


Fig. 6.5 Dynamic "Gains" of the Reactor

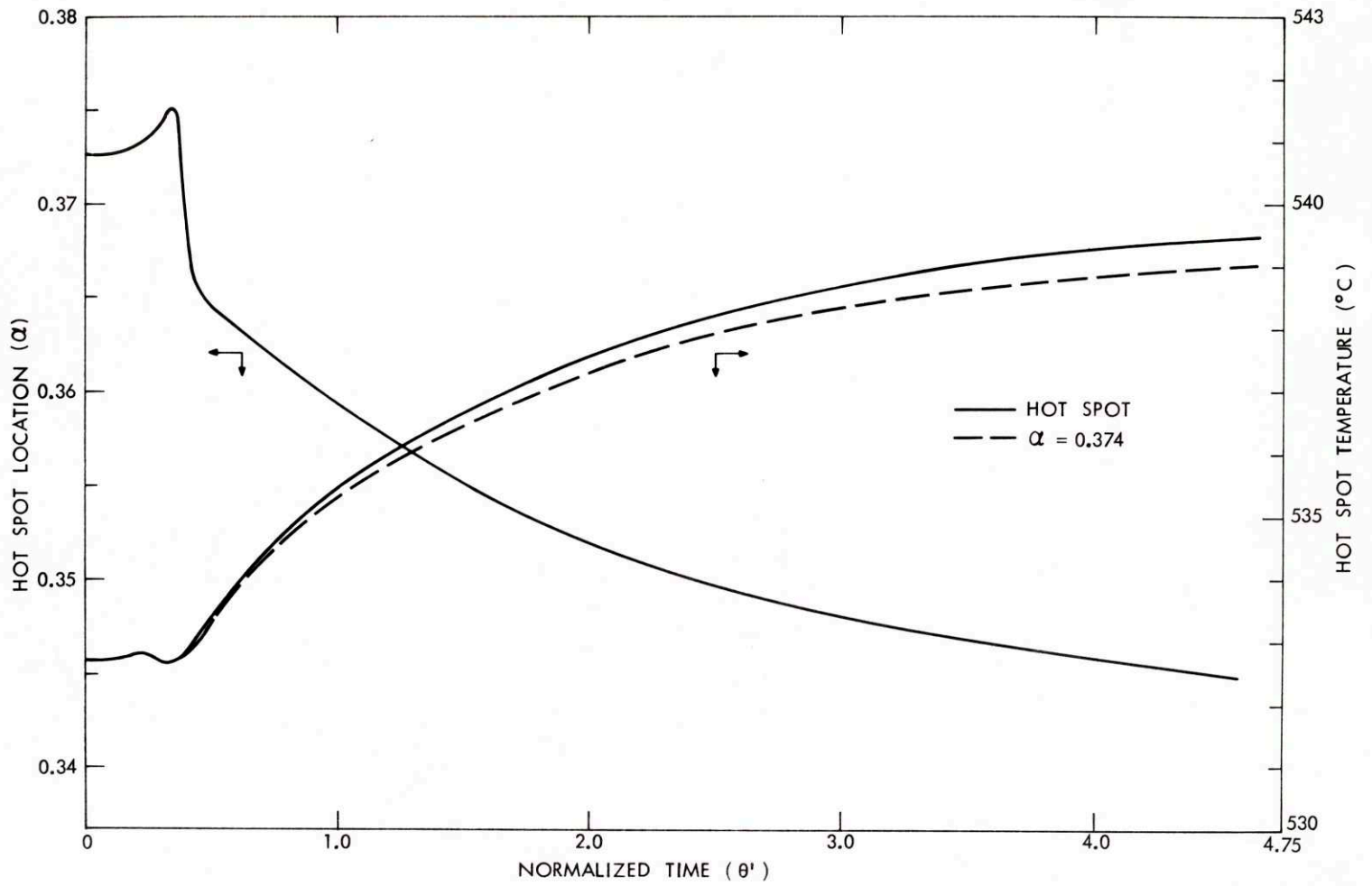
and only a small section of the reactor near $u = 0.4$ is still under the temperature conditions existing at the beginning of the transient. At $\theta' = 0.964$ the two effects presented before are now blended together. There is no location in the reactor where the temperature has been left unchanged.

It further appears from the curves corresponding to $\theta' = 2.37$ and 4.65 that the catalyst temperature continues to change even after the original perturbation has traveled down the entire bed. This results from the fact that the boundary conditions associated with the catalyst section (feed temperature and wall temperature profile) continue to change with time. For this reason the time required for the T.V.A. reactor to reach a steady state corresponding to a new value of the feed temperature is expected to be much larger than the time required for an identical packed bed whose feed does not exchange heat with the catalyst section before entering it. This result is in agreement with Boyle's⁴³ observations of regenerative processes.

From the shape of the curves presented in Fig. 6.5 it appears that the temperature "gain" is a strong function of the location in the reactor even when the new steady state is reached as is almost the case for, $\theta' = 4.65$. A temperature perturbation introduced at the entrance of the catalyst section is amplified during the first $4/10$ of the reactor and then attenuated during the remaining part of the reactor.

The strong dependence of the "gain" of the process with the location in the reactor results in the travel of the maximum temperature in the reactor during the transient. Figure 6.6 presents the variations with time of the location and of the magnitude of this hot spot temperature. The delay phenomena described before appears also in this figure. During the transient resulting from a five-degree step increase in the feed temperature, the peak temperature has moved by 0.5 foot or 3 percent of the total reactor length. The magnitude of the peak temperature has changed by 7°C . In the

Fig. 6.6 Location and Magnitude of the Hot Spot during a +50C Step Transient



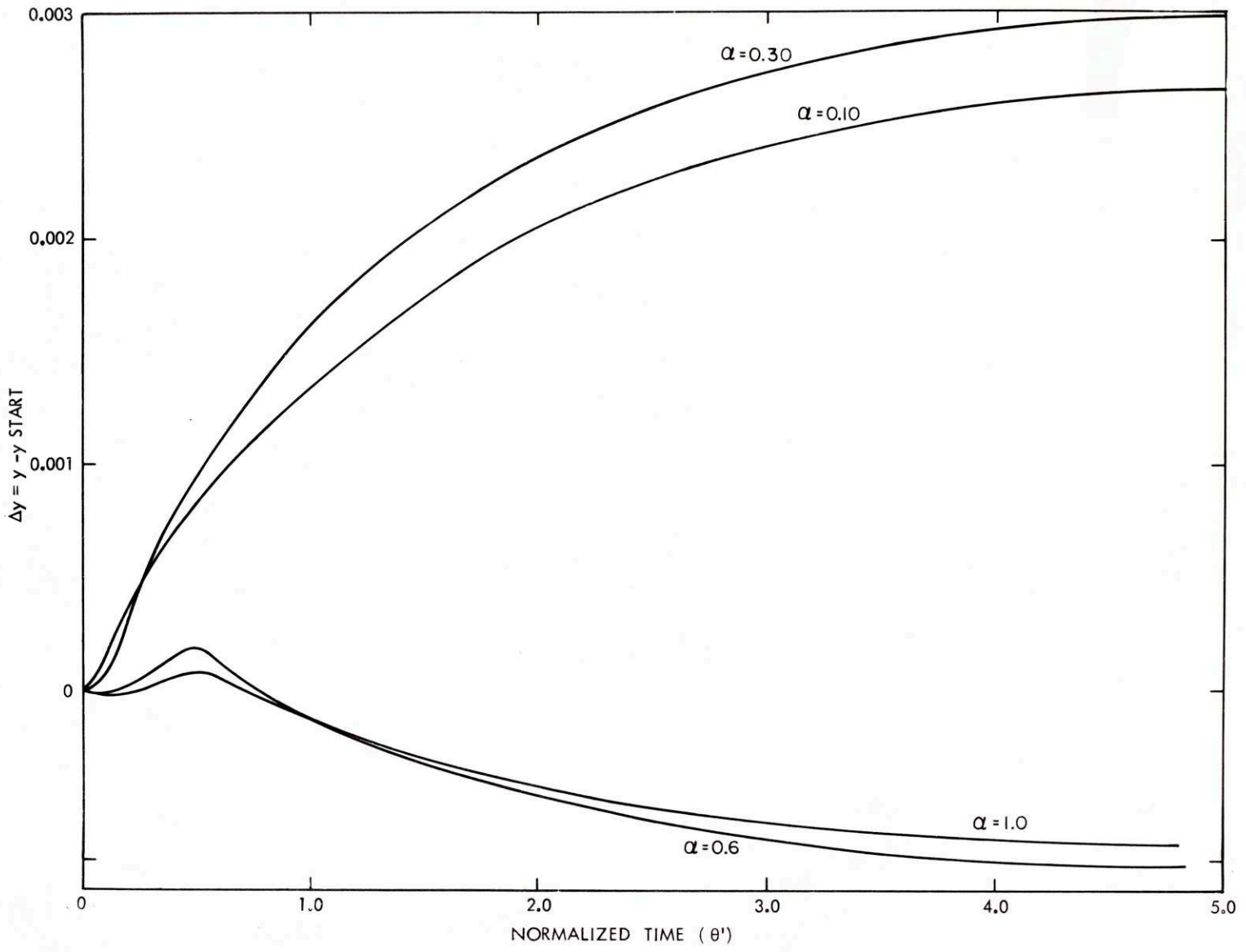
same figure is plotted the variation with time of the temperature at position $\alpha = 0.374$ where the peak temperature was located at the beginning of the transient. As long as θ' is smaller than 0.374, that is to say, before the thermal wave reaches the considered location, the two temperatures are similar. As the transient proceeds the difference between the peak temperature and the temperature at $\alpha = 0.374$ increases to reach the maximum value of 0.5°C at steady state.

Figure 6.7 presents the variation with time of the changes in ammonia mole fraction Δy at the locations reported in Fig. 6.3. At each location the change in ammonia mole fraction, Δy , is defined as the difference between the ammonia mole fraction at any instant and the steady state value existing at the beginning of the transient.

Figure 6.7 shows that the changes of the ammonia concentration during the transient do not experience delays as the temperature did. This results from the fact that the mathematical model under investigation neglects the accumulation of mass in the gas phase. A change in temperature at the entrance of the reactor affects the reaction rate at this point which in turn affects, instantaneously, the reactant concentration and the rate of reaction at each location downstream of it. For the position $\alpha = 0.1$ and $\alpha = 0.30$ Fig. 6.7 shows that the step change of 5°C in the feed temperature results in a monotonic increase of the ammonia mole fraction. For the positions $\alpha = 0.6$ and $\alpha = 1.0$ a slow initial decrease in the ammonia concentration is followed by a recovery and then a further decrease until a new steady state value is reached. From the steady state considerations discussed in Section A of this chapter it has been established that a step change in the feed temperature of $+5^{\circ}\text{C}$ would result ultimately in a decrease in the ammonia mole fraction at the outlet ($\alpha = 1.0$) of the reactor.

The next section will discuss the fact that the phenomena described in this section can be explained through the temperature and concentration dependence of the rate of reaction.

Fig. 6.7 Changes in Ammonia Mole Fraction during a +50°C Step Transient



2. Discussion of the Results

In order to discuss qualitatively the temperature changes during the transient, each term of the energy equation written in the catalyst section is considered as a function of the location in the reactor.

If diffusion is neglected, for simplicity of presentation, the energy equation in the catalyst at steady state reduces to Eq. 6.3

$$-s \left(1-h \frac{y-y^*}{1+y}\right) \frac{\partial v}{\partial a} + (m-v) + [e+h(v-0.3725)]^2 sr(v, y) = 0 \quad (6.3)$$

$q_1 = s \left(1-h \frac{y-y^*}{1+y}\right) \frac{\partial v}{\partial a}$ represents the amount of energy carried in by bulk flow

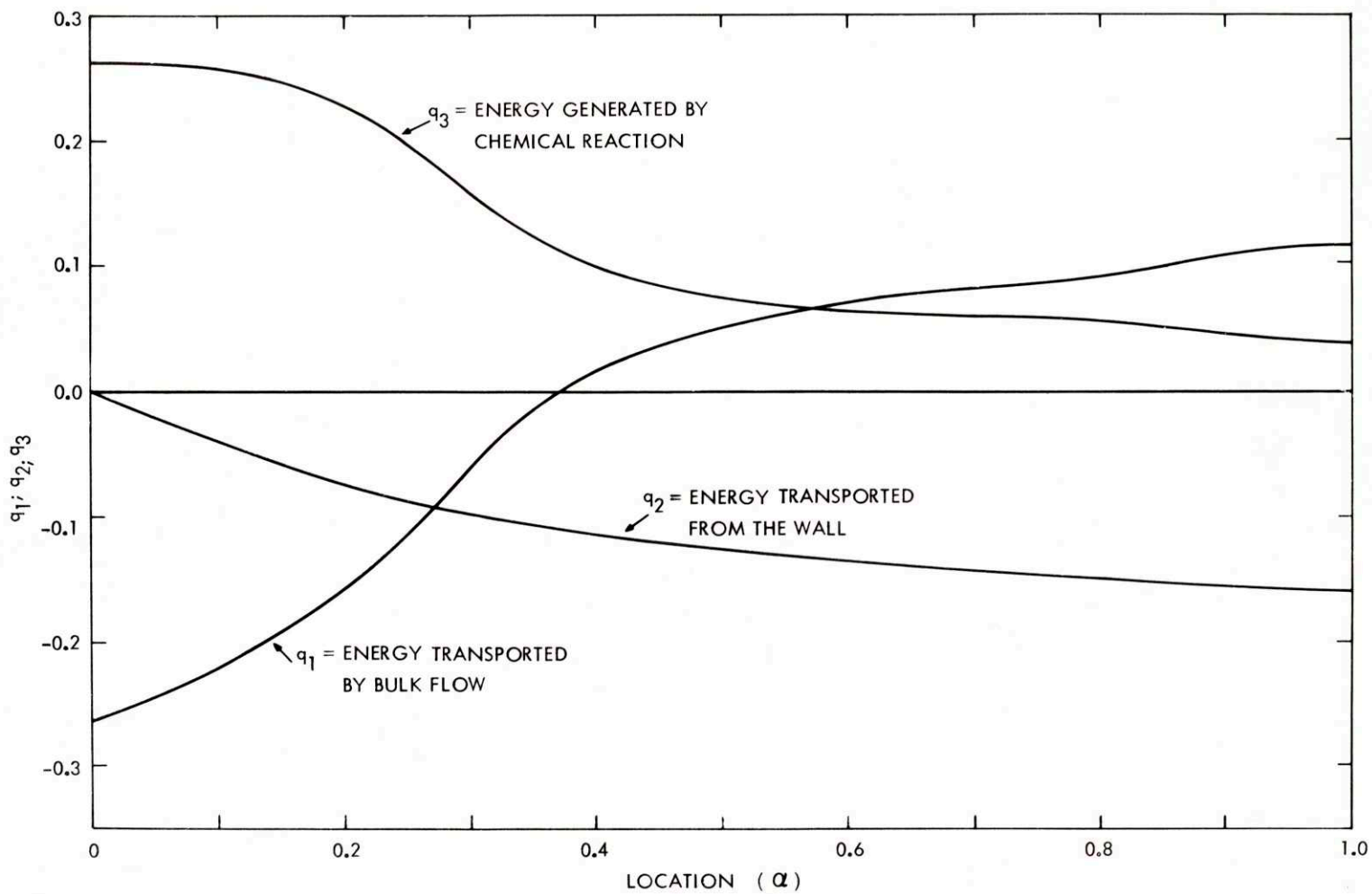
$q_2 = (m-v)$ represents the amount of energy convected from the wall

$q_3 = [e+h(v-0.3725)]^2 sr(v, y)$ represents the amount of energy produced by the chemical reaction.

The magnitude of these three terms are presented as a function of the position in the reactor in Fig. 6.8 for the steady state conditions existing at the beginning of the transient. Near the entrance of the reactor the only source of enthalpy is by chemical reaction. The elimination of enthalpy by transfer to the wall is much less important than the elimination by bulk flow. On the contrary, near the outlet of the reactor the heat released by chemical reaction is much smaller than the heat convected to the wall and enthalpy transported by bulk flow makes up for the difference. The dependence on position in the reactor of the relative magnitude of heat generated by reaction and heat removed by transfer to the wall will be used later to explain the phenomena described in the previous section.

It is advantageous to know the effect of a change in temperature or reactant concentration on the heat generation by chemical reaction at each position in the reactor since this is represented in Eq. 6.3 by a highly nonlinear term.

Fig. 6.8 Dependence with Location of the Enthalpy Transport and Generation Processes



Figures 6.9 and 6.10 present the values of the derivatives $\frac{\partial q_3}{\partial v}$ and $\frac{\partial q_3}{\partial y}$ as a function of the location in the reactor. The ordinates of these figures are proportional to the amount of additional BTU released per hour per cubic foot of catalyst when the temperature at the considered location increases by 1° or when the ammonia mole fraction at that position changes by one unit. Figure 6.9 shows that an increase in temperature at any position corresponding to $\alpha < 0.275$, results in an increase in the amount of heat generated by the chemical reaction. The same phenomena occurs at the location corresponding to $\alpha > 0.845$. On the other hand, for all the positions located between $\alpha = 0.275$ and $\alpha = 0.845$, an increase in temperature results in a decrease in the amount of heat generated. This behavior is characteristic of a reversible exothermic reaction. Figure 6.10, on the other hand, shows that an increase in ammonia mole fraction, that is to say, a decrease in reactant concentration, always results in a decrease in the amount of heat generated by the chemical reaction.

With the assumptions built into the mathematical model of the reactor, the temperature in the empty tube section is given by Eq. 6.4 obtained by integration of Eq. 4.3

$$w = w_{\text{feed}} e^{-\beta(1-\alpha)} + \beta e^{\beta\alpha} \left[\int_{\alpha}^1 m(\xi) e^{-\beta\xi} d\xi \right] \quad (6.4)$$

A step change in the feed temperature affects instantaneously the temperature $w(\alpha)$ through the term

$$w_{\text{feed}} e^{-\beta(1-\alpha)}$$

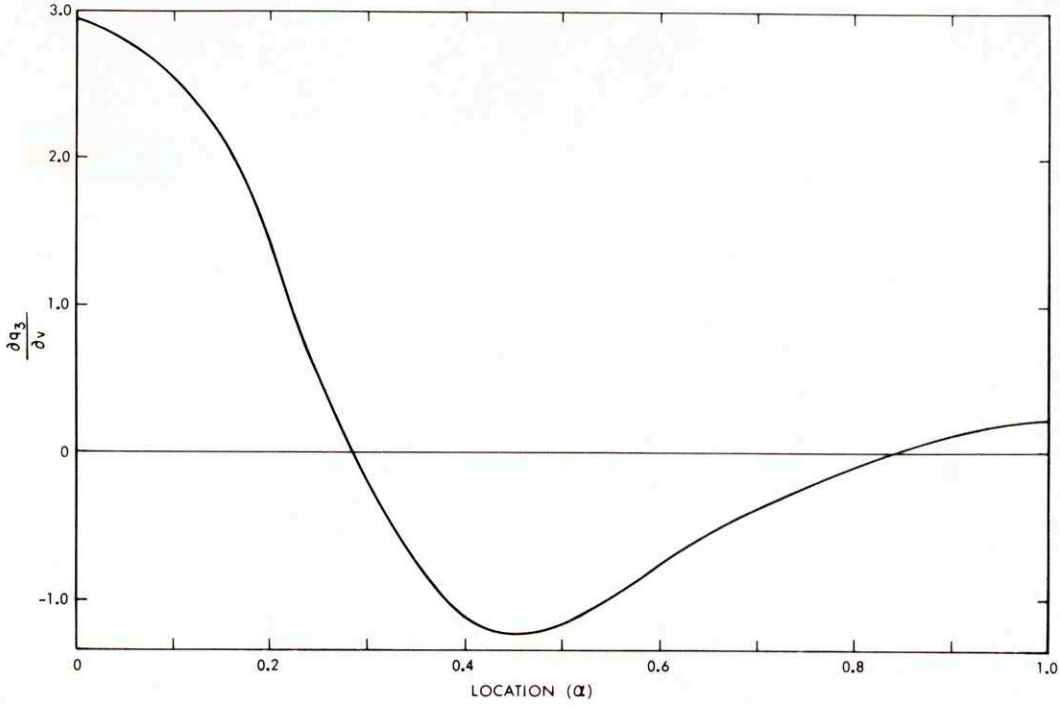


Fig. 6.9 Effect of Temperature Change on the Heat Generation by Chemical Reaction

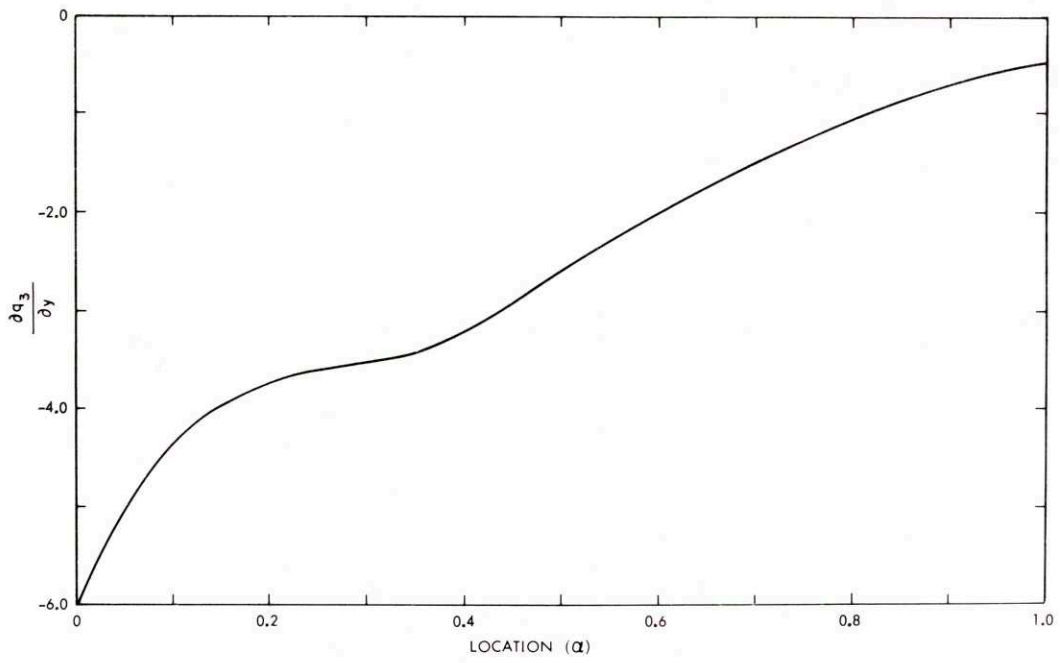


Fig. 6.10 Effect of Ammonia Mole Fraction Change on the Heat Generation by Chemical Reaction

then as a function of time through the value of the finite integral which involves the wall temperature profile. Since the outlet temperature of the empty tube section constitutes the feed to the reacting section, the catalyst section experiences an initial step change in its feed temperature whose magnitude is equal to $e^{-\beta} \Delta w_{\text{feed}}$. It should be noted that the magnitude of this initial step depends on the number of heat transfer units in the empty tube section.

The rate of travel of the thermal wave generated at the entrance of the bed is a function of the heat capacity of the flowing gases, of the heat capacity of the solid particles and of the extent of the chemical reaction. To prove these points the two extreme cases which can happen in a packed bed reactor are considered:

1. when non-reacting gases flow through the packing.
2. when the gases flowing through the bed are so reacting that equilibrium exists at any location along the bed.

The last case corresponds to an excellent catalyst which is so active that equilibrium is instantaneously reached.

In the case of non-reacting gases Aris⁴⁴ reported that a perturbation moves through the bed at a constant velocity u_p related to the gas flow velocity u_G by the equation

$$u_p = u_G \times \frac{\text{Total heat capacity of the gases in the reactor}}{\text{Total heat capacity of the gases and of the catalyst}} \quad (6.5)$$

Aris considered the effect of longitudinal diffusion and reported that the thermal pulse introduced at the entrance of the bed becomes "smeared" as it proceeds down the bed. The spreading effect on the pulse was reported to be a function

of the particles shape as well as the other system parameters, but the average flow velocity of the heat wave was reported independent of the particle shape and given by Eq. 6.5.

To investigate the effect of the chemical reaction on the rate of travel of the thermal wave let us return to Eq. 4.9 which represents an enthalpy balance around an infinitesimal slice of catalyst section

$$\begin{aligned}
 & -F \left[\bar{C}_{p_o} - \Delta C \frac{y-y^*}{1+y} \right] \frac{\partial T_c}{\partial z} - \frac{h_2 s_2}{l} (T_c - T_w) \\
 & - [\Delta H_o - \Delta C (T_c - T_b)] F \frac{1+y^*}{(1+y)^2} \frac{\partial y}{\partial z} \\
 & = \frac{W C_{p_c}}{l} \frac{\partial T_c}{\partial t} \qquad (4.9)
 \end{aligned}$$

In the case where equilibrium exists everywhere, y , the ammonia mole fraction, becomes dependent of temperature through an algebraic relation of the form

$$y = f(T_c)$$

obtained by writting the equilibrium condition

$$\frac{P_{NH_3}}{P_{N_2}^{0.5} P_{H_2}^{1.5}} = K_p(T_c)$$

This relation does not involve time, distance or boundary conditions and consequently the value y can be eliminated from Eq. 4.9 by replacing its partial derivative with respect to distance by the following expression:

$$\frac{\partial y}{\partial z} = \frac{\partial T_c}{\partial z} \left(\frac{dy}{dT} \right)_{\text{equilibrium}}$$

Under these conditions Eq. 4.9 reduces to Eq. 6.6

$$\begin{aligned}
 -F \bar{C}_{p_o} \left\{ 1 - \frac{\Delta C}{\bar{C}_{p_o}} \left(\frac{y-y^*}{1+y} \right) + \left[\frac{\Delta H_o}{\bar{C}_{p_o}} - \frac{\Delta C}{\bar{C}_{p_o}} (T_c - T_b) \right] \times \right. \\
 \left. \frac{1+y^*}{(1+y)^2} \left(\frac{dy}{dT_c} \right)_{\text{eq1.}} \right\} \frac{\partial T_c}{\partial z} - \frac{h_2 s_2}{l} (T_c - T_w) \\
 = \frac{WC_{pc}}{l} \frac{\partial T_c}{\partial t} \tag{6.6}
 \end{aligned}$$

In computing the velocity of travel of the thermal wave the heat capacity of the flowing gases $\bar{C}_{p_o} \left(1 - \frac{\Delta C}{\bar{C}_{p_o}} \left(\frac{y-y^*}{1+y} \right) \right)$ must now be replaced by the effective heat capacity \bar{C}_{p_e}

$$\begin{aligned}
 \bar{C}_{p_e} = \bar{C}_{p_o} \left\{ 1 - \frac{\Delta C}{\bar{C}_{p_o}} \left(\frac{y-y^*}{1+y} \right) + \left[\frac{\Delta H_o}{\bar{C}_{p_o}} - \frac{\Delta C}{\bar{C}_{p_o}} (T_c - T_b) \right] \right. \\
 \left. \times \frac{1+y^*}{(1+y)^2} \left(\frac{dy}{dT_c} \right)_{\text{eq1.}} \right\}
 \end{aligned}$$

which is no longer a constant but a function of the extent of the reaction, that is to say, of the composition of ammonia at equilibrium. The value of the correcting factor $\left[\frac{\Delta H_o}{\bar{C}_{p_o}} - \frac{\Delta C}{\bar{C}_{p_o}} (T_c - T_b) \right] \frac{1+y^*}{(1+y)^2} \left(\frac{dy}{dT_c} \right)_{\text{equilibrium}}$ has been computed for various values of the ammonia mole fraction y in the case where there is no inert present and when hydrogen and nitrogen are in the ratio of 3 to 1. This case was chosen for reasons of simplicity. Figure 6.11 presents the variation of the correcting factor with the ammonia mole fraction at equilibrium. The correcting factor is maximum for an ammonia mole fraction of 0.42 and is equal to 1.55. Under these conditions the effective heat capacity of the flowing gases is two and a half times larger than their sensible heat capacity. Consequently the speed of travel of the thermal perturbation (represented by Eq. 6.7)

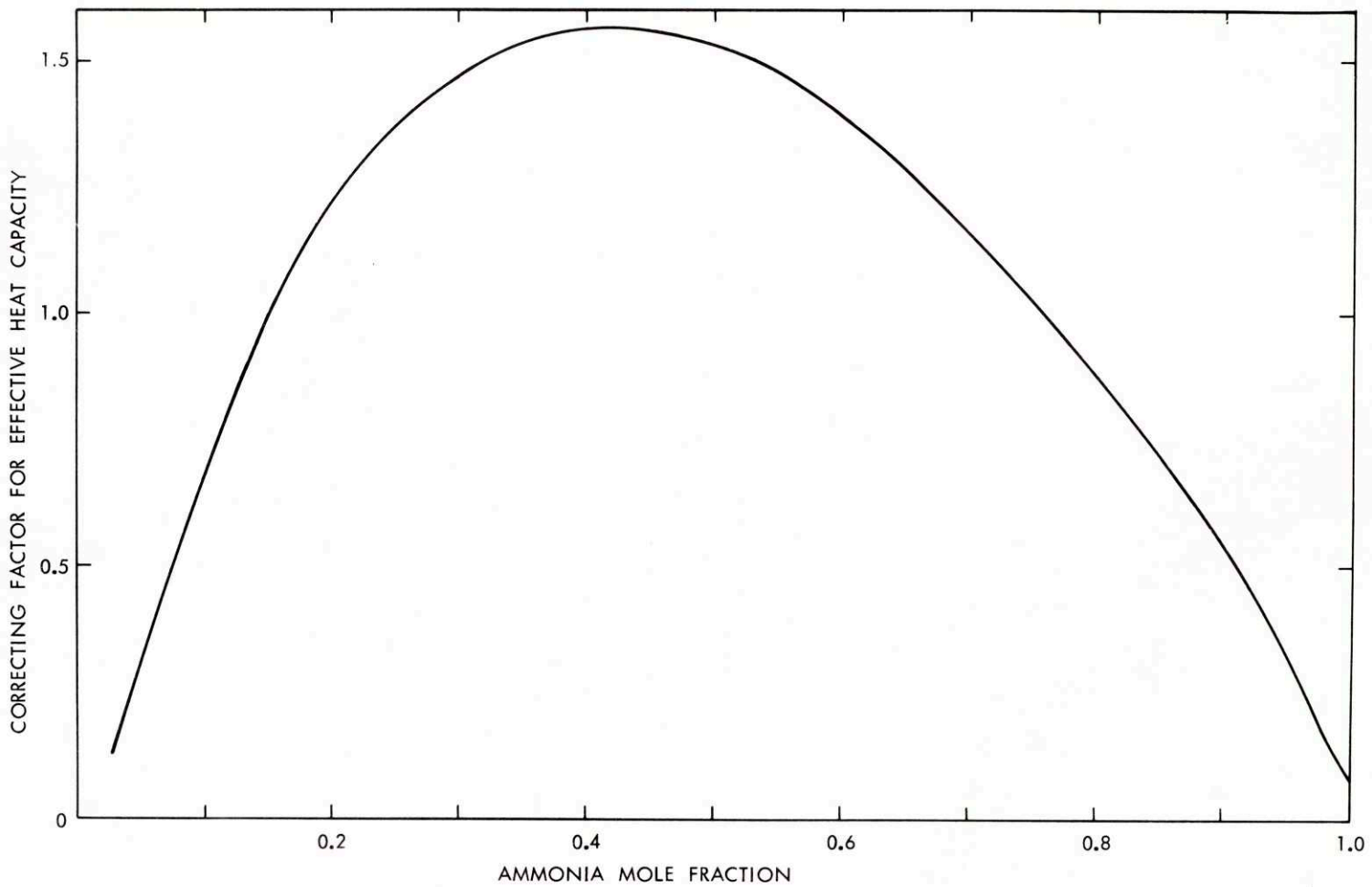


Fig. 6.11 Correction for the Heat Capacity of the Gas under Equilibrium Conditions

$$u_p = \frac{1}{\frac{WC_{pc}}{F\bar{C}_{p_0}}} = \frac{1 F \bar{C}_{p_0}}{WC_{pc}} \quad (6.7)$$

is two and a half larger than the speed of travel of the perturbation in absence of chemical reaction.

If the ammonia mole fraction is equal to five percent, the magnitude of the correcting factor is only 0.3 and the rate of travel of the thermal wave is 1.3 times faster in presence of chemical reaction.

In the present case where equilibrium is not obtained, the relation between y and T_c is no longer an algebraic relation but a differential equation involving time, distance and the associated boundary conditions. Mathematically the substitution of $\frac{\partial y}{\partial z}$ by $\frac{\partial T}{\partial z} \times \left(\frac{dy}{dT}\right)$ has no meaning and the only method left is to solve simultaneously the two equations as was done in this research. The results of the simulation shows that the rate of travel of the thermal wave is almost unaffected by the chemical reaction. Figure 6.4, presented before, shows that the thermal wave reaches the location 0.10, 0.3 and 0.6 at times very close to the time evaluated if the gases were non-reacting gases ($\Theta' = 0.1$, $\Theta' = 0.3$ and $\Theta' = 0.6$). The explanation given of this result lies in the very poor reactivity of the catalyst present in the reactor. In order to check this explanation a run was done in which the activity of the catalyst was increased by a factor of 5. This result was achieved by increasing the frequency factor associated with the Arrhenius expression of the rate of reaction by a factor of five. A new steady state profile was obtained and starting from these conditions a 5°C step in the feed temperature was performed.

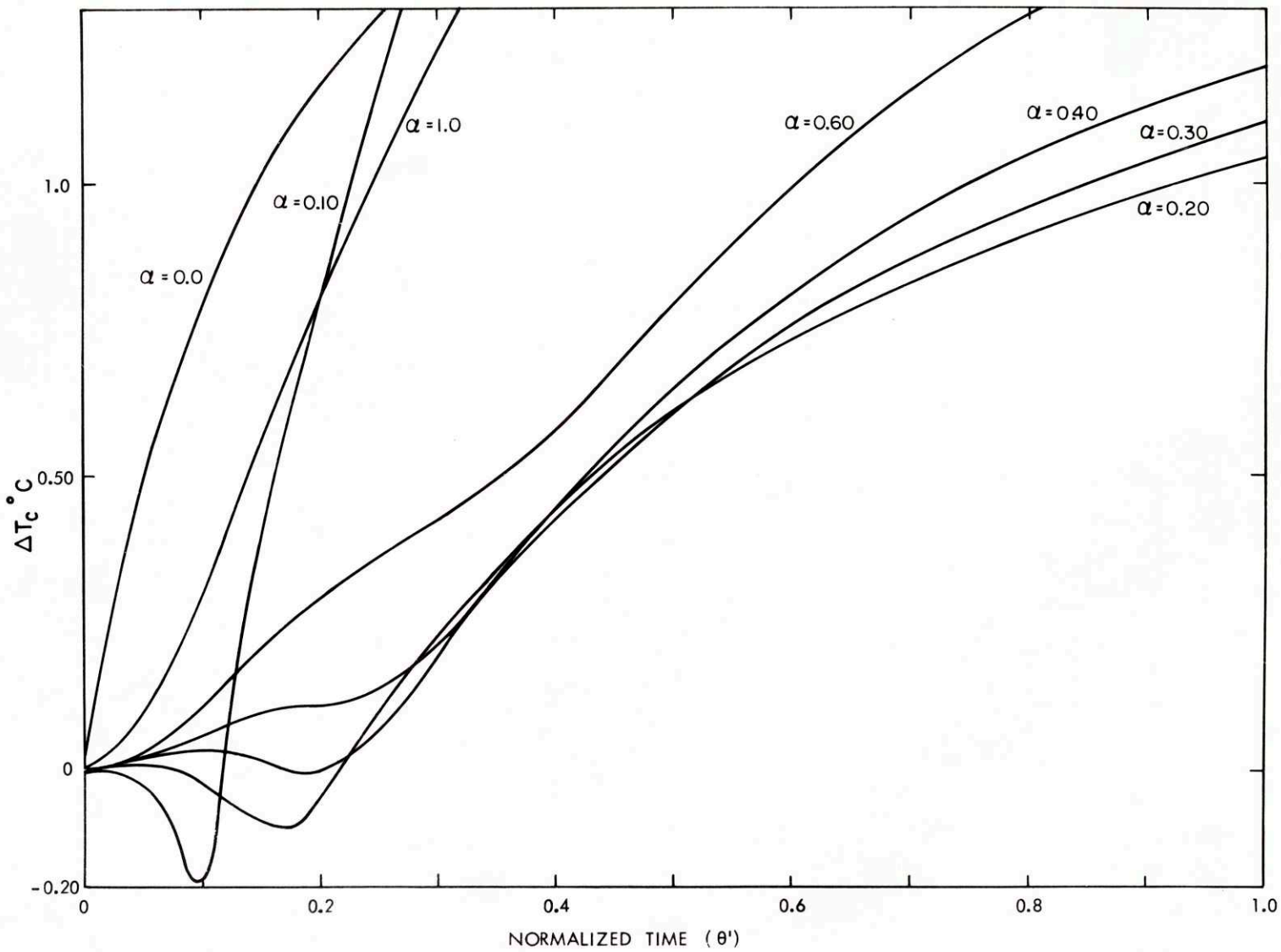
Figure 6.12 presents the changes in temperatures during the first instants of this transient. The response at location $\alpha = 0.1$ shows little effect of the catalyst activity on the rate of travel of the heat wave. But for locations 0.2, 0.3, 0.4, 0.6 it is seen that the thermal wave reaches these locations at an earlier time than it would be if estimated for the case of non-reacting gases.

The fact that the time at which location $\alpha = 0.20$ and $\alpha = 0.30$ are reached by the thermal wave is more affected by the catalyst activity results from the fact that at these locations the reacting gases are closer to the equilibrium condition.

The previous results show that the perturbation originated in the feed temperature to this reactor propagates down the reactor at a rate almost unaffected by the extent of the chemical reaction because of the poor reactivity of the catalyst present in the T.V.A. reactor.

To this inlet perturbation are in fact added all the perturbations generated within the reactor by changes in the wall temperature or in the reactant concentration and which travel also down the reactor at approximately unit speed. Figure 6.4 shows that at a position $\alpha = 0.10$ before the arrival of the thermal wave the temperature has a tendency to increase since the wall temperature at that position has increased. On the contrary the increase in ammonia concentration apparent in Fig. 6.7 has the tendency to decrease the temperature since it decreases the amount of enthalpy generated by the chemical reaction. The magnitudes of these two effects are expected to be very small and apparently almost cancel each other during the first instants of the transient. When the thermal wave reaches the location $\alpha = 0.10$ the increase in temperature felt by the catalyst becomes

Fig. 6.12 Changes in Temperature during a +50°C Step
Transient for an Active Catalyst



predominant over the negative effect of the conversion increase.

Furthermore the magnitude of the thermal wave reaching that location is further amplified since the rate of heat generation by chemical reaction increases as the temperature increases. It has been seen before that the relative magnitude of the energy transferred to the wall over the energy released by chemical reaction increases as one proceeds down the reactor. At position $\alpha = 0.3$, during the first instants of the transient the increase in wall temperature forces the temperature to increase. Since Fig. 6.9 and 6.10 show that an increase in temperature and in ammonia mole fraction decrease the amount of energy generated by the reaction ($\frac{\partial q_3}{\partial v}$ and $\frac{\partial q_3}{\partial y}$ are both negative) the temperature at $\alpha=0.3$ will soon stop increasing and, once the wall temperature has stopped to change rapidly will dip down before the arrival of the thermal wave. When the thermal front passes that position the temperature will increase since the gas reacting at that position arrives hotter, and this despite the two negative effects on the heat generation by reaction. The two negative effects of temperature and conversion increase nevertheless appear in the fact that the "gain" obtained at the location $\alpha = 0.30$ is smaller than the "gain" obtained at position $\alpha = 0.2$.

The same sequence of phenomena is described in Fig. 6.3 and 6.4 for the position $\alpha = 0.6$. By now the energy transferred to the wall is predominant and as a result of the increase in the wall temperature the temperature at that position increases during the first instants of the transient despite the two negative effects of temperature and conversion changes on the heat generation by reaction.

No dip down in the catalyst temperature is experienced at $\alpha = 1.0$. The increase in the wall temperature stops only at the time when the ammonia mole fraction at the outlet of the reactor starts to decrease as it appears on

Fig. 6.7. Consequently both reactants concentration and temperature changes occurring at the end of the reactor increase the amount of energy produced by the chemical reaction, further increasing the temperature at that location.

The effect of temperature and ammonia concentration variations on the rate of reaction can be represented by similar curves as Fig. 6.9 and 6.10. At the entrance or near the outlet of the reactor, an increase in temperature results in an increase in ammonia production; on the contrary, in the center part of the reactor an increase in the temperature results in a decrease in the rate of reaction.

Figure 6.7 shows that during the first instants of the transient the increase in temperature at the entrance of the reactor results in an increase in ammonia mole fraction leaving this section. Despite the decrease in ammonia production (due to a decrease in reactants concentration) downstream of the first half of the reactor, this initial increase generates an increase in the ammonia mole fraction observed. The magnitude of this variation decreases as one proceeds down the reactor to ultimately correspond to a decrease in the ammonia mole fraction observed in the second half of the reactor. It should be pointed out that the decrease in ammonia mole fraction is less pronounced at the outlet of the reactor than at location $a = 0.6$ since the temperature variations reported for the outlet of the reactor on Fig. 6.4 result in an increase in the ammonia production.

As the ammonia mole fraction leaving the first half of the reactor further increases the decreasing trend of the ammonia mole fraction for the locations in the second half of the reactor is reversed. This increase lasts as long as the "thermal wave" does not reach the region where a decrease in

production corresponds to an increase in temperature. At location $\alpha = 0.5$ Fig. 6.9 shows that an increase in temperature decreases the amount of reaction. The ammonia mole fraction leaving this section after the passage of the thermal wave will be smaller than before since less ammonia will be produced. As a consequence, the mole fraction observed at locations further down the reactor will also decrease. The simplified attempt presented in this section to interpret qualitatively the temperature and ammonia concentration variations during a transient has shown the complexity of the phenomena encountered in the T.V.A. reactor. To obtain any quantitative information one must consider simultaneously all the elementary processes analyzed before and the solution of the simulation as presented in Chapter V is the only method available for this purpose.

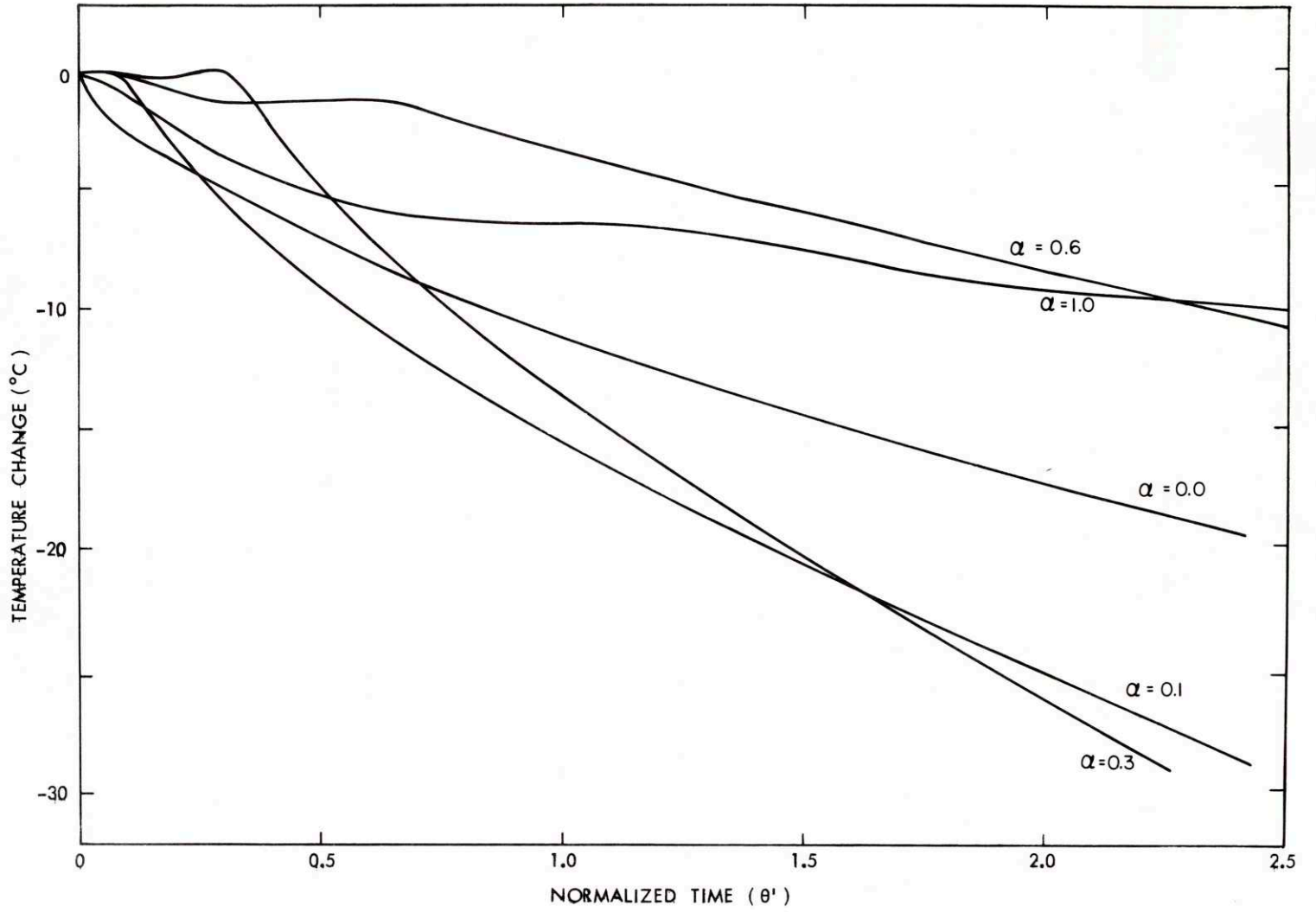
C. "BLOW OUT" OF THE REACTOR

At the beginning of the transient the reactor operates under the steady state conditions corresponding to a feed temperature of 227.6°C . A step of -15°C in the feed temperature brings it to 212.6°C which is below the "blow out temperature" of 220°C reported in Section A. It has been shown in Chapter III that there is a stable steady state corresponding to a feed temperature below the "blow out" temperature, but that it corresponds to almost no production of ammonia since the temperature inside the catalyst is uniformly equal to the feed temperature. The negligible conversion obtained under these conditions makes that condition of operation unacceptable. The instability encountered in the reactor, when the feed temperature falls below the "blow out" temperature, corresponds to an approach to a new steady state under which no reaction takes place.

Since large temperature changes occur before the new steady state is reached (the average bed temperature has to cool from 475°C to 212°C) the time required for the present transient is expected to be very large. The results reported in this section were obtained during the first 15 minutes of the "blow off". Fifteen minutes after the change in feed temperature the temperature drop experienced at any location in the reactor never exceeds 35°C .

The variations with time of the changes in temperatures experienced at the locations $a = 0$, $a = 0.1$, $a = 0.3$, $a = 0.6$ and $a = 1.0$ are presented in Fig. 6.13. The variations with time of the changes in ammonia mole fraction at the same positions are presented in Fig. 6.14. These results show that the nature of these changes encountered during the first part of the blow off are similar (in absolute value) to those presented in Section B, Chapter VI for a $+5^{\circ}\text{C}$ step in the feed temperature.

Fig. 6.13 Changes in Temperature during a "Blow Off"



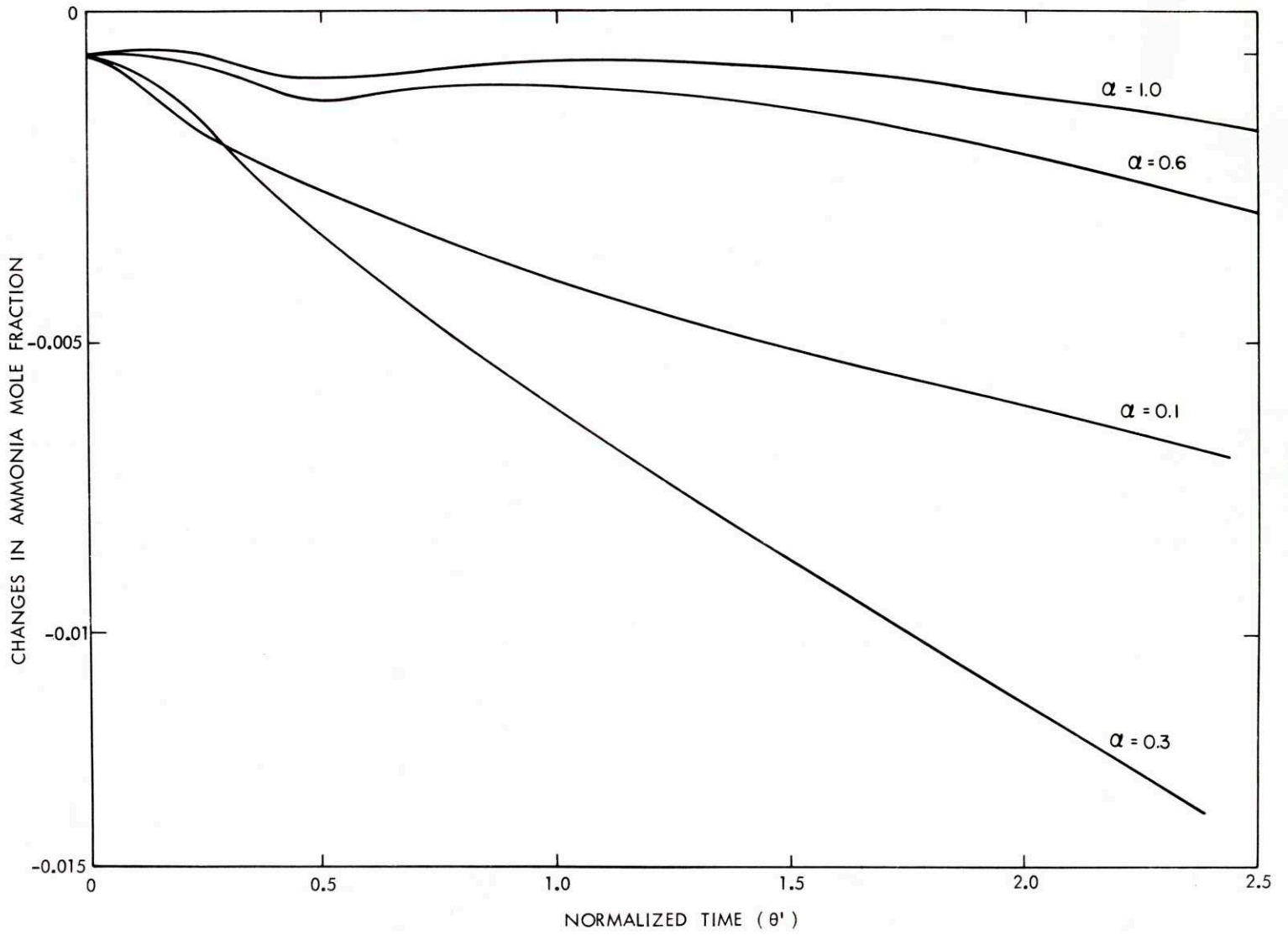


Fig. 6.14 Changes in Ammonia Mole Fraction during a "Blow Off"

Figure 6.13 shows that the temperature at the entrance of the catalyst section responds instantaneously by a decrease to the step change in the feed temperature. The temperature at the entrance of the bed keeps decreasing monotonically during the whole transient. The temperatures at locations $\alpha = 0.10$ and 0.3 experience very little change until the thermal wave reaches these locations, respectively, at time $\theta' = 0.1$ and $\theta' = 0.3$. After the passage of the thermal wave the temperature at these locations decreases monotonically. Figure 6.13 shows that at location $\alpha = 0.6$ and $\alpha = 1.0$ the temperature of the catalyst decreases as soon as the feed temperature is changed and follows the temperature changes generated in the tube wall. The passage of the thermal wave originated at the entrance of the catalyst section further decreases the temperature at these locations.

The results presented in Fig. 6.14 show that for $\alpha = 0.1$ and 0.3 the ammonia mole fraction experiences an immediate decrease. As it was explained in Section B this results from the instantaneous propagation of concentration in the present model. The passage of the thermal wave through the section of the reactor where a decrease in temperature is accompanied by an increase in production results in Fig. 6.14 in a temporary increase in the ammonia mole fraction observed at location 0.6 and 1.0 .

Figure 6.15 shows the gain of the reactor (defined as the ratio of the change in temperature at any location to the change in feed temperature) plotted versus location at different times. The gains reported in Fig. 6.5 appear also in Fig. 6.15. For small values of time the gains obtained in both cases are very close to each other. As time grows the curves depart from each other as it is expected since the steady profile obtained at the end of the "blow off" corresponds to a flat profile quite different from the steady state profile associated to a feed temperature of 227.6°C .

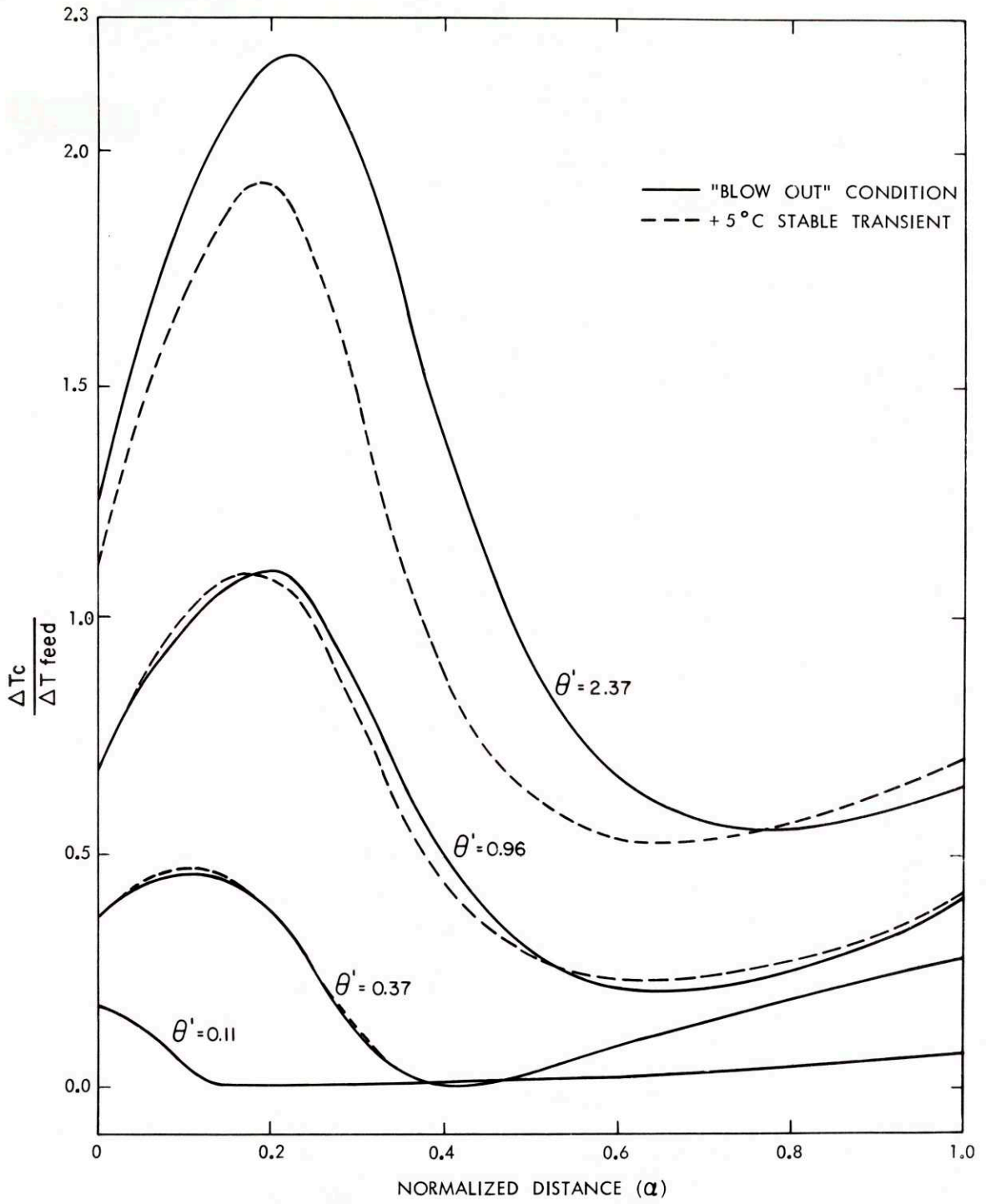


Fig. 6.15 Dynamic "Gain" of the Process During a "Blow Off"

The kind of instability which results from a decrease in the feed temperature below the blow out temperature is of the so-called "snow ball" type of instability since no oscillation in temperature and composition has been observed during the transient of the uncontrolled reactor.

In this section it has been seen that the phenomena describing the first instants of the "blow out" of the reactor are of the same nature as the phenomena presented in Section B, Chapter VI. In the next section the effect of the initial step in feed temperature on temperature changes occurring in the first instants of the transient will be investigated quantitatively.

D. NONLINEARITY OF THE SYSTEM

Since the mathematical system describing the transient behavior of the reactor includes two nonlinear differential equations, the response of the simulation to large changes in the feed temperature is expected to be a function of both the location in the reactor and the magnitude of the step changes from a given steady state.

Figure 6.16 presents at time $\theta' = 0.964$ the variations of the "gain" defined as $\frac{\Delta T_c}{\Delta T_{\text{feed}}}$ with position in the reactor for the conditions reported in Table 6.2. Even though step changes of -10° and -15°C result in "blow off" of the reactor the "gains" for these transients appear on the same figure. During the first instants of the transient, the nonlinearity of the process affects very little the response of the reactor. At time $\theta' = 0.964$ when the thermal wave has almost traveled down the entire length of the reactor, the results obtained for a $+5^\circ\text{C}$ or a $+10^\circ\text{C}$ step never differ by more than 10 percent. The discrepancies between the results corresponding to a $+5$ and -5°C steps are much larger, particularly in the second half of the reactor.

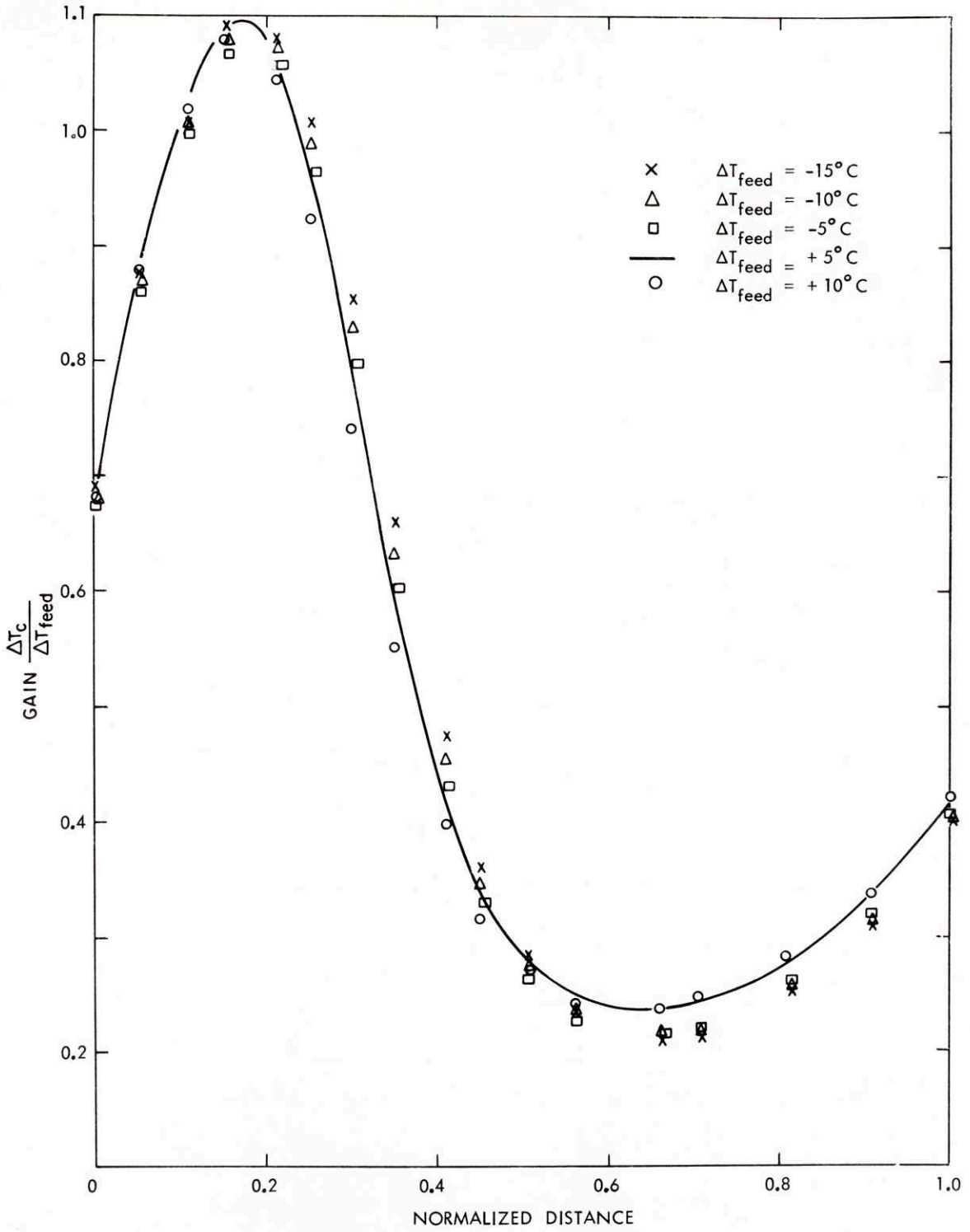


Fig. 6.16 Effect of the Magnitude of the Step Change on the Dynamic Gain at $\theta' = 0.964$

The results corresponding to the "blow-off" cases depart already at $\theta' = 0.964$ from the results obtained with a $+5^{\circ}\text{C}$ change. Figure 6.17 presents the gain at $\theta' = 2.10$ for step changes of -15 , -5 and $+5^{\circ}\text{C}$. The difference between the $+5$ and -5°C step results has further increased. The position at which the two "gain profiles" intersect has moved towards the outlet of the reactor. If the transient had been followed until steady state was reached the gain profile corresponding to a -5°C step would have been above the gain profile corresponding to a $+5^{\circ}\text{C}$ step since the steady state gain for the outlet temperature is larger in the case of a -5°C step than in the case of a $+5^{\circ}\text{C}$ step.

Figure 6.18 presents the variation with time of the "gain" for position $\alpha = 0.374$ where the hot spot was located at the beginning of the transient, for different values of the step change in feed temperature. At $\theta' = 1.0$ the results obtained for the stable runs do not differ by more than 10 percent. In the case of "blow off" the difference is already more than 20 percent at that time, and will continue to increase. For the stable runs as the new steady state is approached the values of the gain will be expected to depart further from one another since the "steady state gains" are respectively 2.61, 1.24 and 1.09 for step changes in the feed temperature of -5 , $+5$ and $+10^{\circ}\text{C}$. Figure 6.19 presents the variation with time of the temperature "gain" at the outlet of the reactor. During the first part of the transient resulting from changes in the wall temperature, the results are very linear and the gain is independent of the size of the step. As soon as θ' is larger than unity, that is to say, as soon as the thermal wave has traveled the entire length of the reactor the nonlinearity starts to appear in the transient. The steady state gain approached in the stable runs are respectively 1.08, 0.840 and 0.830 for step changes of -5 , $+5$ and $+10^{\circ}\text{C}$.

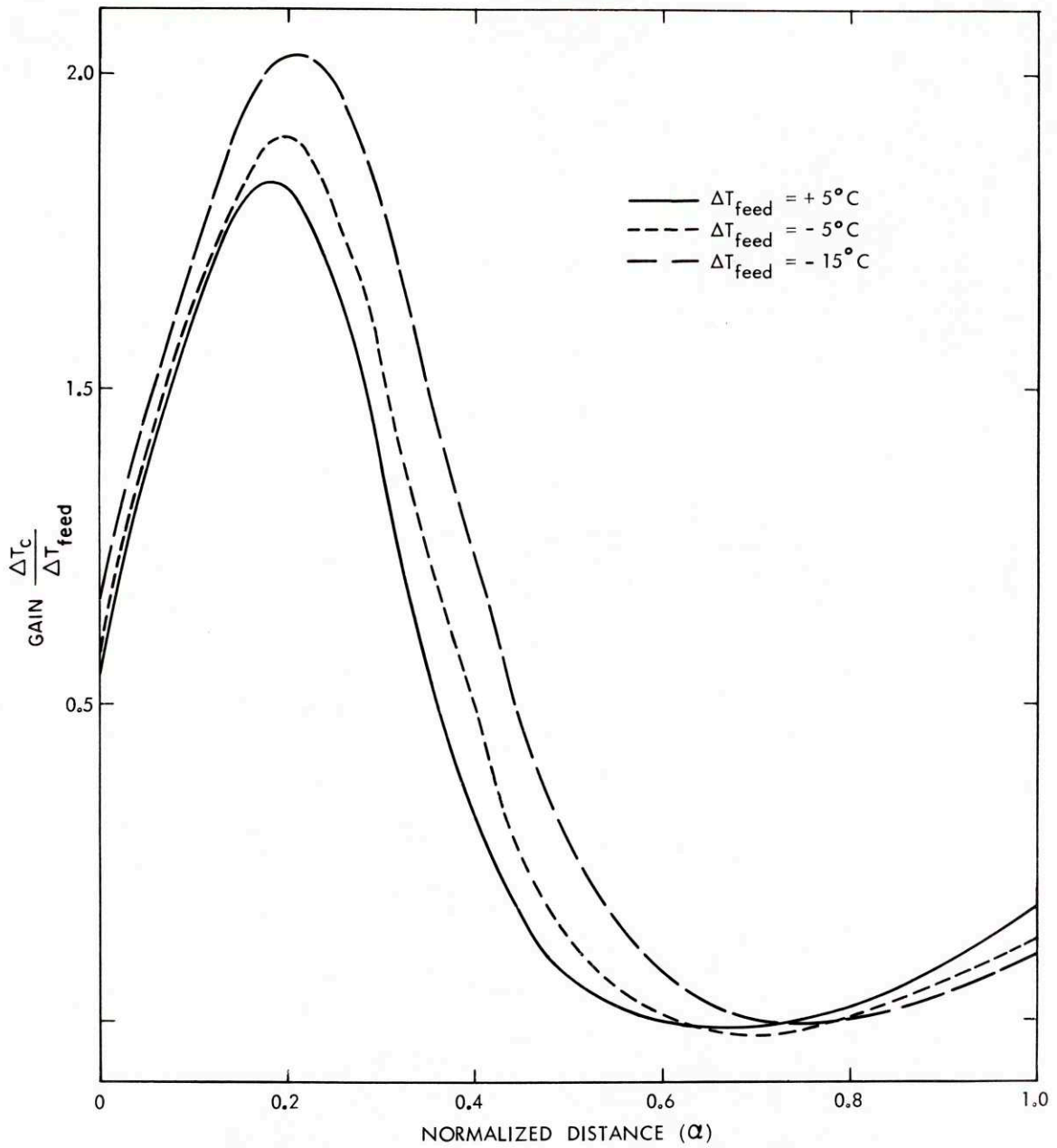


Fig. 6.17 Effect of the Magnitude of the Step Change on the Dynamic Gain at $\theta' = 2.10$

Fig. 6.18 Effect of the Magnitude of the Step Change on the Dynamic Gain for Location $\alpha = 0.374$

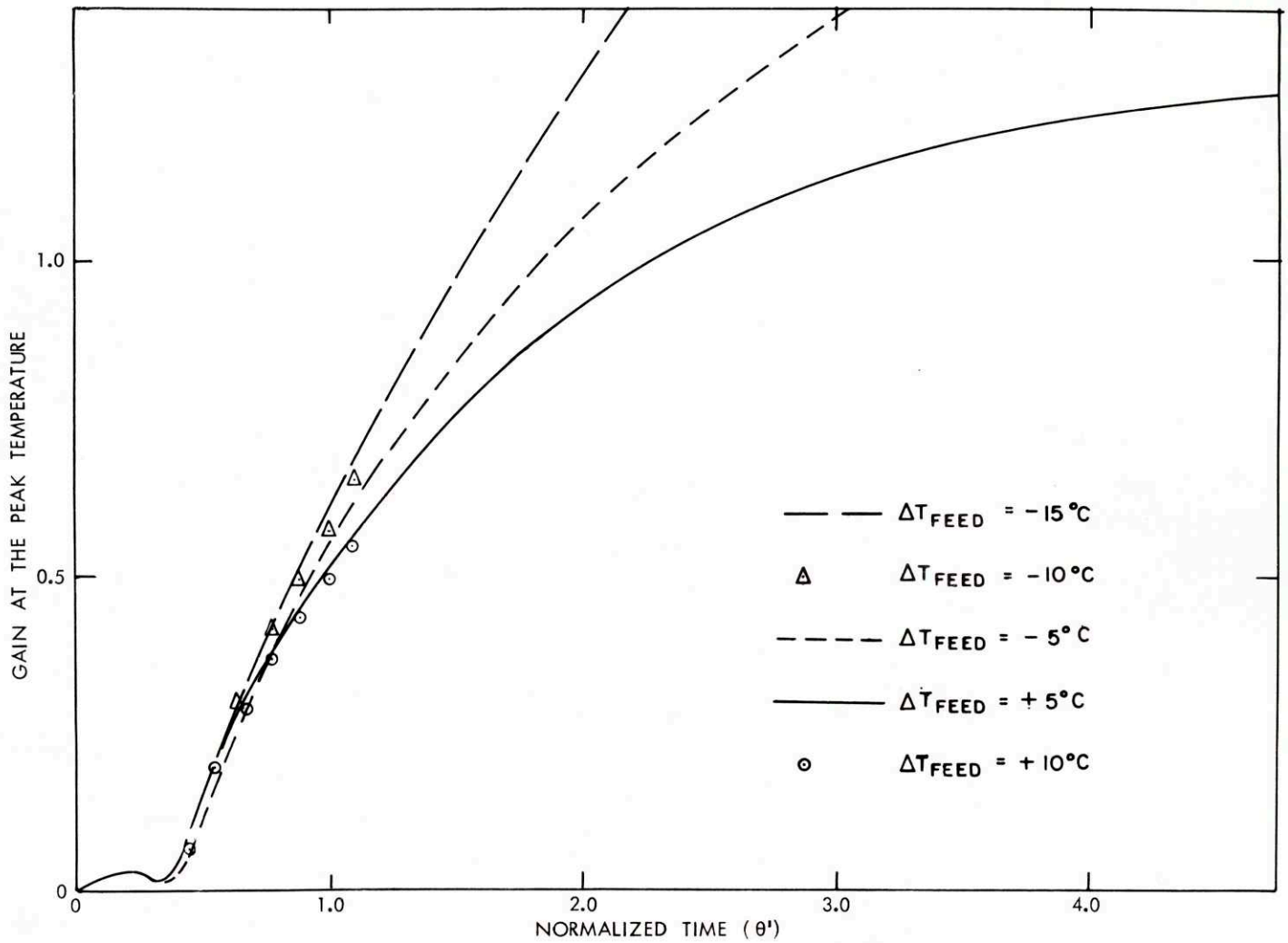
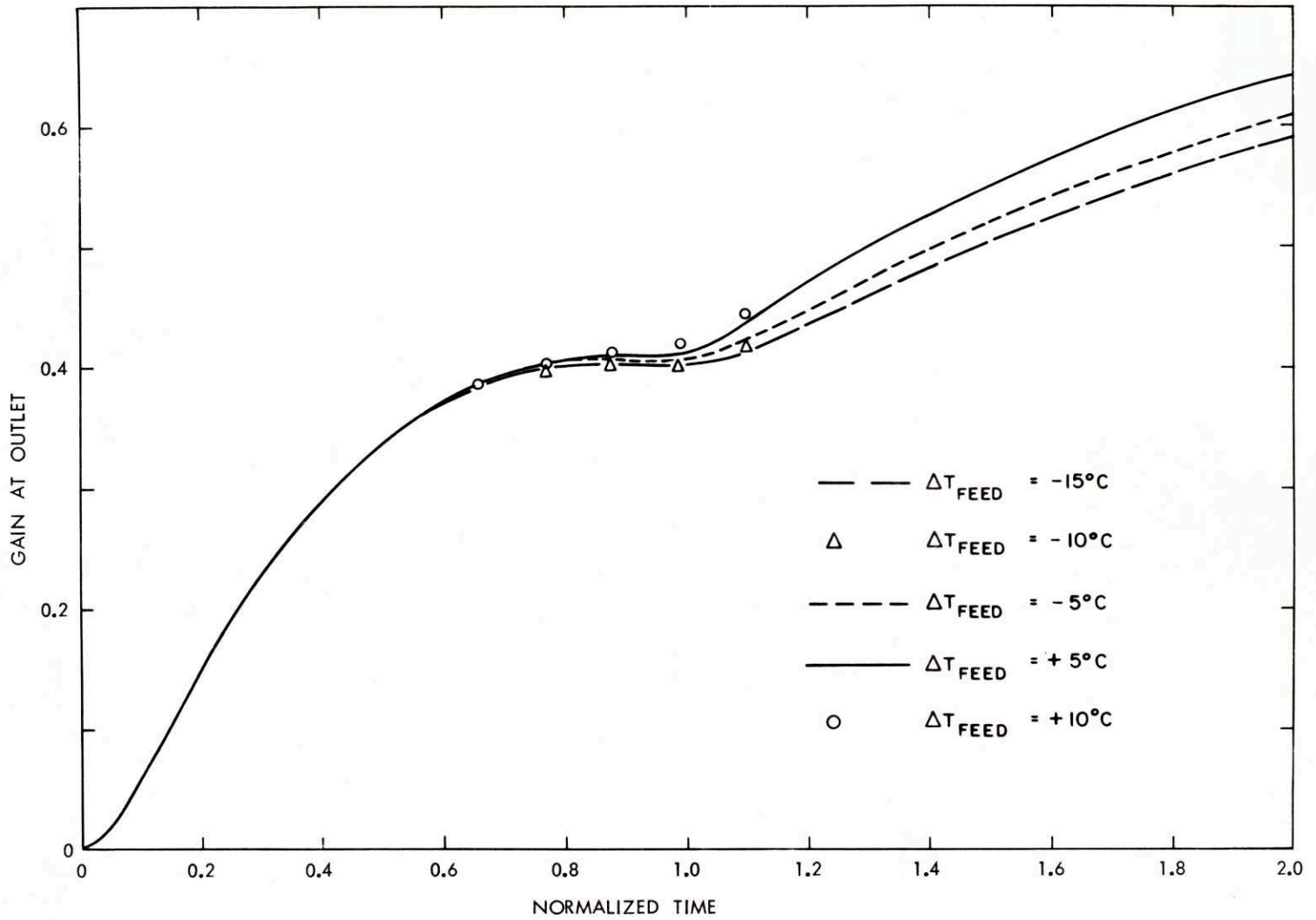


Fig. 6.19 Effect of the Magnitude of the Step Change on the Dynamic "Gain" for Location $\alpha = 1.0$



From the results of Section A of this chapter the steady state gains corresponding to an infinitesimal change in feed temperature can be obtained for the location $\alpha = 0.0$ as the slope of the tangent to the curve of Fig. 6, 1 at the point of operation.

In Table 6.3 the differential gain for positions $\alpha = 0$, $\alpha = 0.374$, and $\alpha = 1.0$ are compared with the steady state gains corresponding to step changes of -5 , $+5$ and $+10^{\circ}\text{C}$.

Table 6.3
Steady State Gains

<u>Position</u>	<u>Differential Gain</u>	<u>Step -5°C</u>	<u>Step $+5^{\circ}\text{C}$</u>	<u>Step $+10^{\circ}\text{C}$</u>
$\alpha = 0$	1.43	2.0	1.30	1.22
$\alpha = 0.374$	1.57	2.61	1.24	1.09
$\alpha = 1.0$	0.85	1.08	0.84	0.83

The steady state gains of Table 6.3 and the dynamic results presented in the first part of this section confirm the strong nonlinearity of the described process. From these considerations it appears that two different approaches can be used to describe the transient of the T.V.A. reactor.

1) For small changes in the feed temperature resulting in stable operation of the reactor its dynamic behavior can be considered as approximately linear and describable mathematically by transfer functions relating the changes in desirable variable to changes in the feed temperature. The transfer functions so defined will be valid only for small perturbations around the steady state conditions of operation considered. If the reactor is to be operated under different flow and feed composition conditions these transfer functions will have to be reestimated.

2) For large changes in feed temperature and for changes resulting in "blow off" of the reactor the simulation presented in Chapter V is the only

way to describe the dynamics of the reactor. Under these conditions the concept of transfer function loses its meaning. The results presented in this section show that a 5°C change in the feed temperature around the optimum conditions of operation is the maximum tolerable change in considering the system as linear. Even though the steady state "gain" for the outlet temperature differs only by 1 percent from the differential steady state gain, at the location $\alpha = 0.374$ the difference between the two gains is already of the order of 70 percent. From the shape of the steady state relations presented in Section A of this chapter it is expected that the reactor will respond more linearly if it is operated in the stable region further away from its optimum conditions of operation.

In the next chapter, the results obtained with a $+5^{\circ}\text{C}$ step change in the feed temperature will be used to derive approximate transfer functions relating changes in temperature at various locations in the reactor to changes in the feed temperature. These approximate transfer functions will be checked in both time and frequency domain with the results of the simulation.

E. DESCRIPTION OF THE REACTOR IN ITS LINEAR RANGE OF OPERATION

When the T.V.A. reactor operates in its linear range as is the case for feed temperature perturbations smaller than 5°C around 227.6°C , its dynamic behavior can be described mathematically in terms of a "transfer function". The transfer function of a process $G(s)$ (where s is a complex variable called the Laplace variable) is defined as the ratio of the Laplace transform of an output variable of the process to the Laplace transform of an input variable called forcing variable. In the present situation the forcing variable investigated is the change in feed temperature ΔT_F which is defined as the difference between the feed temperature at any time t and the feed temperature at the beginning of the transient. The output variable corresponding to a given location in the catalyst section of the reactor, consists of the change in temperature ΔT_c defined as the difference between the temperature observed at any time t and the steady state value of the temperature existing at the beginning of the transient.

The transfer function or system function relating the variables just defined is written as

$$G(s) = \frac{\overline{\Delta T_c}(s)}{\overline{\Delta T_F}(s)} \quad (6.8)$$

the bar above ΔT_c and ΔT_F means the Laplace transform of these quantities has been taken. It should be noted that one can determine a system function for each location in the reactor one wishes to investigate. The results presented in this section concern three locations only: the entrance of the catalyst section, ($a=0$), the location $a = 0.374$ where the hot spot is located at the beginning of the transient and the outlet of the reactor ($a = 1.0$).

A physical interpretation of a transfer function is obtained in considering the results of sinusoidal input to a process. It is well known that if a sinusoidal input variable of amplitude unity and frequency ω is imposed on a linear process, sinusoidal oscillations in the output variable are observed. The magnitude and phase lag angle of the sinusoidal oscillations in the output variable are given by the magnitude and the angle of the complex number obtained by replacing the Laplace variable s by the imaginary number $j\omega$ in the transfer function.

In cases where the equations describing the dynamic behavior of a process are ordinary differential equations it is possible to derive directly from them closed form expression for $G(s)$. The linearization of the system of partial differential equations describing the dynamics of the T.V.A. reactor does not simplify them to the point where closed form transfer functions can be obtained. This results from the distributed effect present in reactors of this type.

The well known method⁴⁵ of determination of the transfer function in the frequency domain from transient results in the time domain has been used in this research. This method is briefly presented in Appendix D. The numerical solution obtained for a 5°C step change in the feed temperature has been used to determine the exact form of the system function. These results have suggested simplified closed form transfer function which are presented in the following part of this section.

The simplified transfer functions have been tested in both the frequency and the time domain against the results obtained directly from the simulation. The variations with frequency of the magnitude and the angle of the system function corresponding to the 3 locations investigated are presented in Fig. 6.20, 6.21, 6.22.

The magnitude is expressed as

$$10 \log_{10} \left[\frac{\text{magnitude of } G(j\omega)}{\text{magnitude of } G(\omega=0)} \right]$$

The magnitude of the system function for a frequency equal to zero is equivalent to the steady state gain of the process. The values of $G(\omega=0)$ corresponding to the three locations investigated are respectively 1.326, 1.292 and 0.860. The angle of the system function are expressed in degree.

In Fig. 6.20 corresponding to the entrance of the reactor it appears that the angle never becomes smaller than -90° throughout the range of frequencies investigated.

This observation suggests that the dynamics of the reactor for that location be approximated by a first order system whose transfer function appears on Eq. 6.9

$$G(s) = \frac{k_1}{\tau_1 s + 1} \quad (6.9)$$

In Fig. 6.20 the magnitude and the angle corresponding to this simplified transfer function are presented for a value of the time constant $\tau_1 = 1.25$ normalized time unit. The agreement between the frequency response of the simplified transfer function and the frequency response obtained from the simulation results is excellent for the low frequencies. At high frequencies the agreement is not as good but the simplified model retains the fact that the angle approaches -90° .

In Fig. 6.21 corresponding to the location $a = 0.374$ it appears that the angle decreases without bound as the frequency increases. This observation characterizes a series of distributed resistances and capacitances. Similar variations of the angle are obtained with systems involving a pure delay represented by e^{-Ts} .

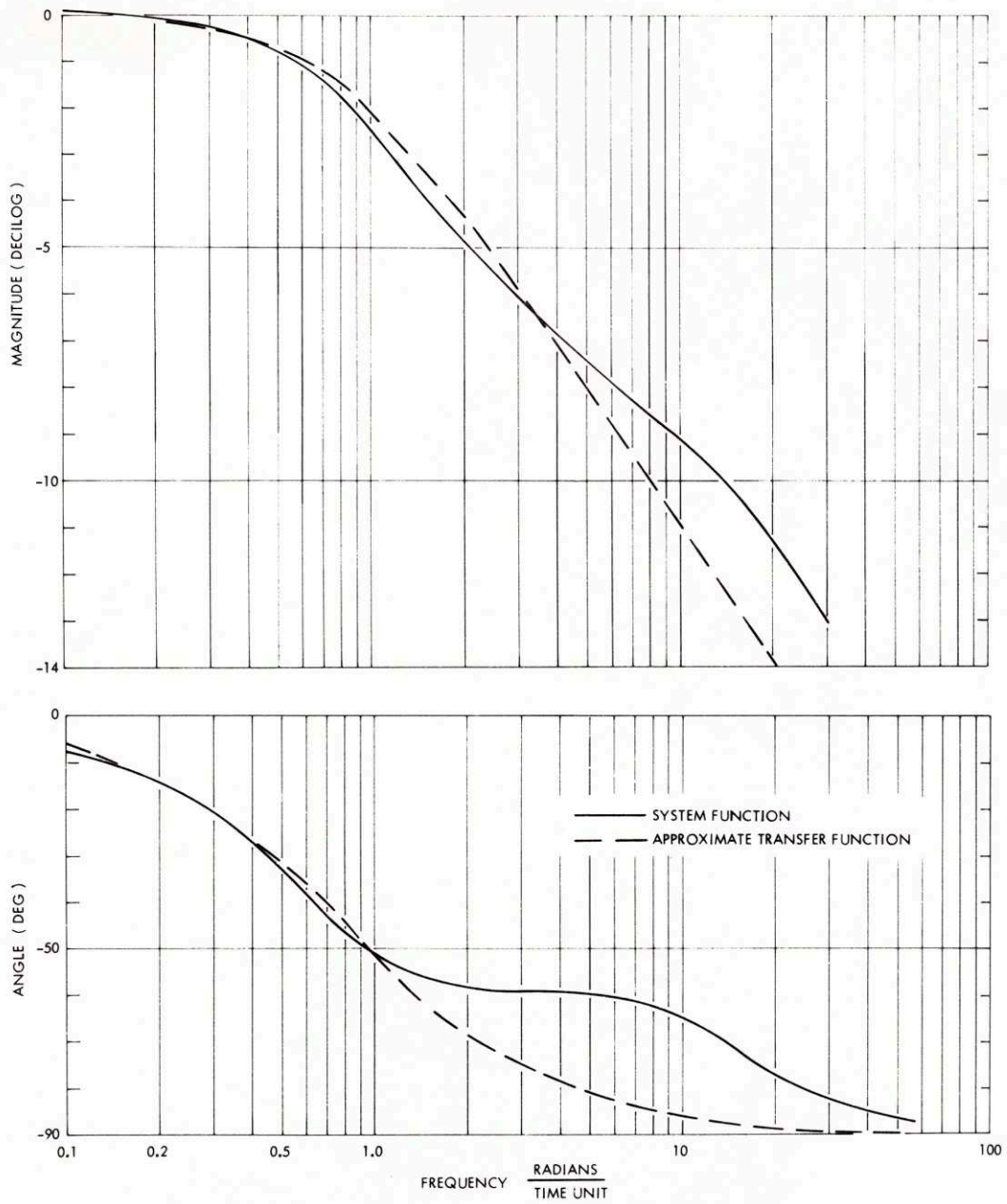


Fig. 6.20 Frequency Response Curves for Location $\alpha = 0$

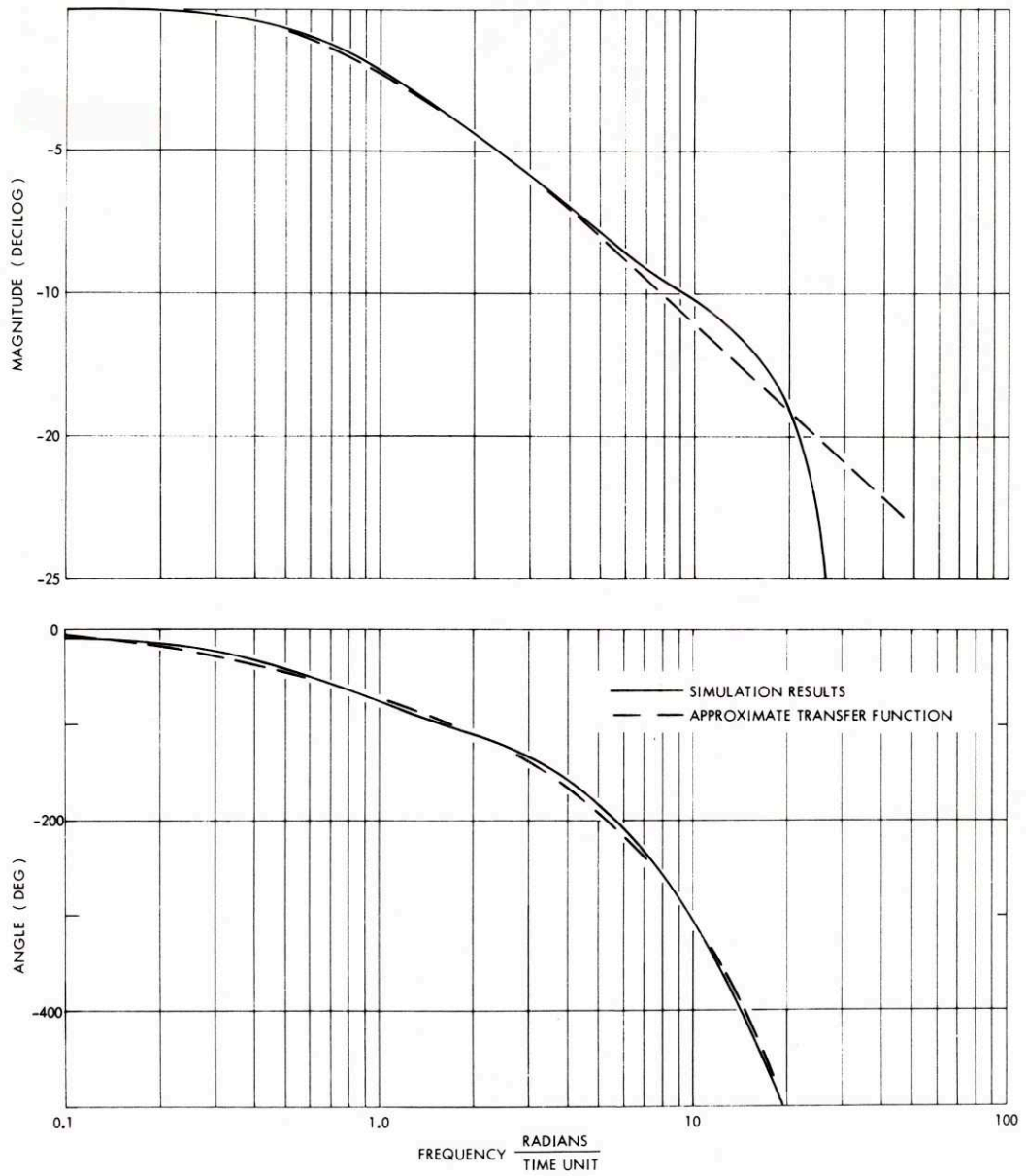


Fig. 6.21 Frequency Response Curves for Location $\alpha = 0.374$

The form of the simplified transfer function proposed for this location is

$$G(s) = \frac{k_1 e^{-\tau_2 s}}{\tau_1 s + 1} \quad (6.10)$$

It represents a first order system coupled with a pure delay time.

In Fig. 6.21 the magnitude and the angle corresponding to the simplified transfer function are presented for the following values of the time constants expressed in normalized time unit

$$\tau_1 = 1.25$$

$$\tau_2 = 0.374$$

The agreement reported for the angle is surprisingly good and justifies the choice of the parameter τ_2 . τ_2 was chosen equal to the normalized location a investigated. It already appeared in Section B Chapter VI that it corresponds to the time at which the thermal wave reaches the location under investigation.

In Fig. 6.22 corresponding to the location $a = 1.0$ it appears that the angle never becomes smaller than -135° and as frequency increases tends to oscillate around a value close to 100° . The amplitude curve presents similarly a series of maxima and minima. The order of magnitude of the difference in frequency corresponding to two consecutive maxima is of 6 radians per normalized time unit.

The approximate transfer functions proposed for this location consists of the sum of two transfer functions and appears in Eq. 6.11

$$G(s) = \frac{k_1}{\tau_1 s + 1} + \frac{k_2 e^{-\tau_3 s}}{\tau_2 s + 1} \quad (6.11)$$

The first part of $G(s)$ characterizes a first order system with a time constant τ_1 . The second part corresponds to a first order system and a pure delay. For larger values of the frequency the proposed transfer

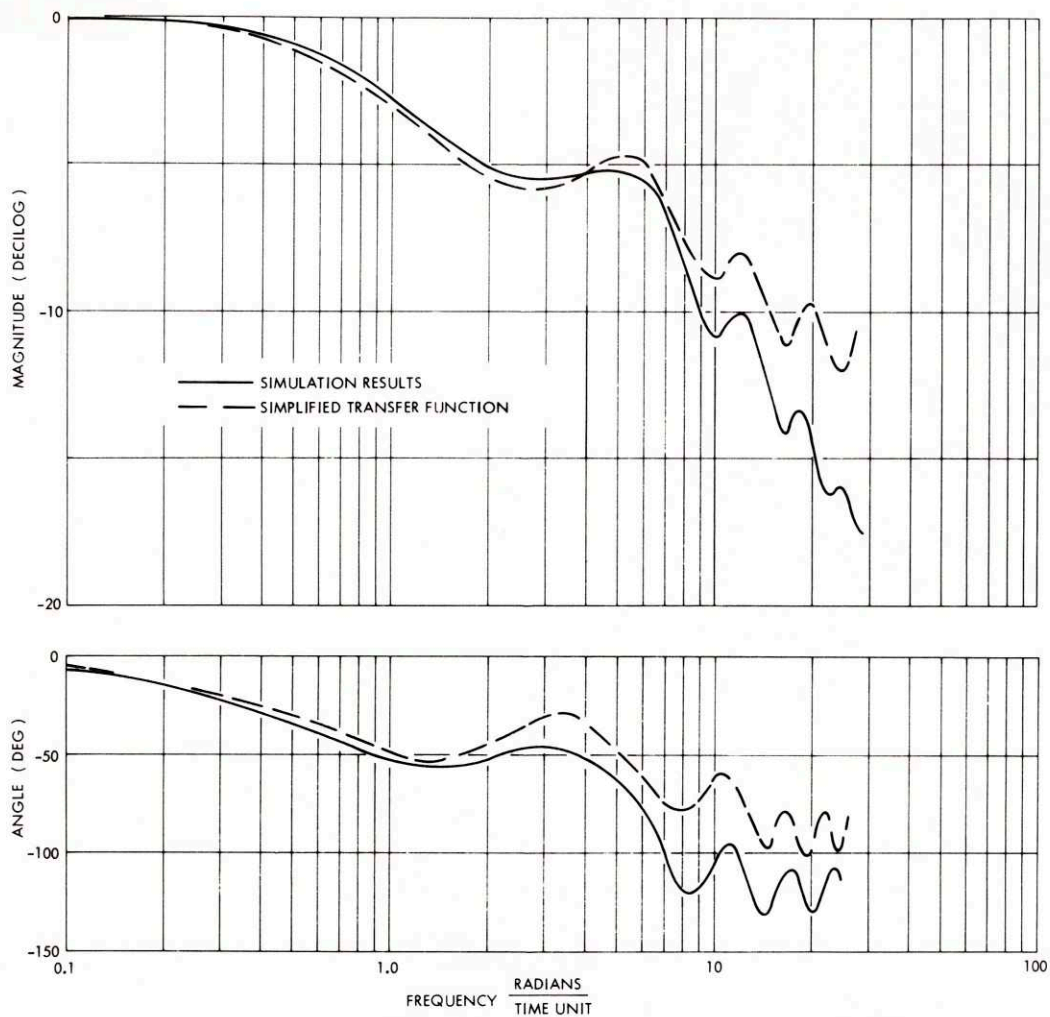


Fig. 6.22 Frequency Response Curves for Location $\alpha = 1.0$

function simplifies to

$$G(s) = \frac{k_1\tau_2 + k_2\tau_1 e^{-\tau_3 s}}{\tau_1\tau_2 s} \quad \text{as } s \rightarrow \infty$$

It can be seen that if $k_1\tau_2$ is greater than $k_2\tau_1$ the angle of the system function increases indefinitely on the contrary if $k_1\tau_2$ is smaller than $k_2\tau_1$ the angle will oscillate around -90° , or -450° or -810° and so on.

In approximating the frequency response curve obtained for the outlet of the reactor by the simplified transfer function of Eq. 6.11 the following choice of the coefficient is proposed

$$\begin{aligned} k_1 &= 0.44 & k_2 &= 0.42 \\ \tau_1 &= 0.30 & \tau_2 &= 1.4 & \tau_3 &= 1.0 \end{aligned}$$

Under these conditions the angle of the approximate transfer function oscillates around -90° . In Fig. 6.22 the angle and the magnitude curve for the approximate transfer function presents also a series of maxima and minima. It can be proven that the values of the frequency corresponding to two consecutive maxima is only a function of τ_3 and is equal to 6.30 radians/unit of time. The accordance of this observation with the results presented before supports the choice of 1.0 made for the value of τ_3 .

In order to interpret physically the signification in the time domain of the proposed simplified transfer functions, the next paragraph analyses the response to a step change in the feed temperature predicted by these transfer functions.

Equation 6.9 predicts that a unit step change in feed temperature is followed immediately by a monotonic increase in the temperature at the inlet of the reactor represented by Eq. 6.12

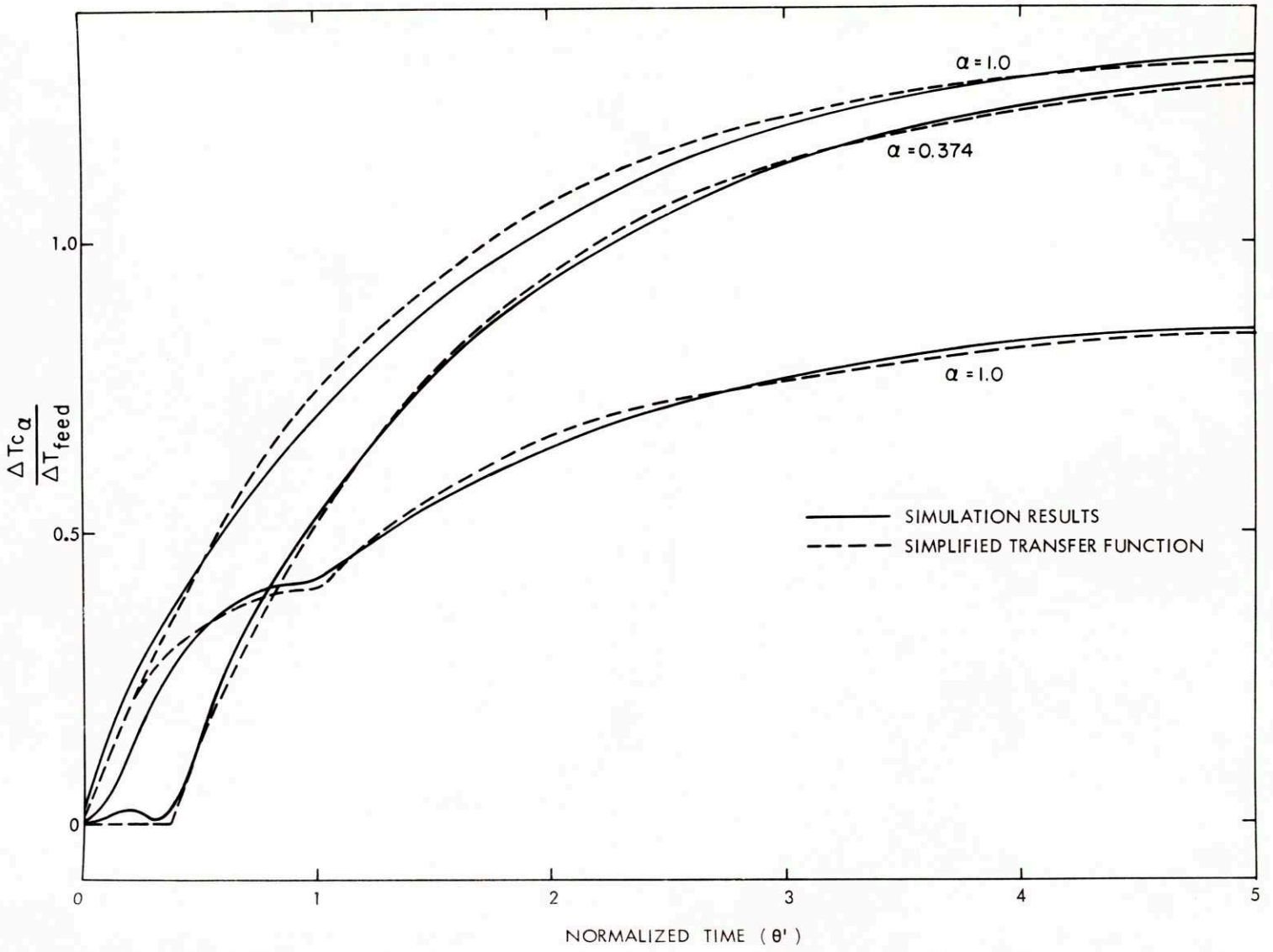
$$\Delta T_c(\Theta) = k_1(1 - e^{-\Theta/\tau_1}) \quad (6.12)$$

In Fig. 6.23 the variations with time of $\frac{\Delta T_c}{\Delta T_F}$ predicted by the simplified transfer function and obtained during the simulation are presented. The agreement between the two curves is good. The transfer function represented in Eq. 6.10 predicts that no change in temperature is experienced as long as Θ' is smaller than 0.374. After $\Theta' = 0.374$ the temperature changes are described by the same equation as Eq. 6.12 where Θ' is replaced now by $(\Theta' - 0.374)$. The poor agreement between the approximation and the results of the simulation during the first part of the transient is apparent in Fig. 6.23. It was shown in Section B, Chapter VI that small changes in temperature resulting from changes in the wall temperature and in the reactants concentration occur before the passage of the thermal wave. Nevertheless, the magnitude of these changes are so small that they have been neglected in the derivation of an approximate transfer function. The use of a second order system to represent the early instant of the transient could be proposed but will defeat the objective of this approach which is to provide simplified transfer function retaining the major characteristics of the transient.

The first part of Eq. 6.11 means that the temperature at the outlet of the reactor changes as it was described in Eq. 6.12 as long as Θ' is smaller than τ_3 ; when Θ' is greater than τ_3 , to this response is added a second first order response delayed by a time equal to τ_3 . Equation 6.13 describes mathematically the transient resulting from a unity step change in the feed temperature

$$\begin{aligned} \Theta' < \tau_3 & \quad \Delta T_c = k_1 (1 - e^{-\Theta'/\tau_1}) \\ \Theta' > \tau_3 & \quad \Delta T_c = k_1 (1 - e^{-\Theta'/\tau_1}) + k_2 (1 - e^{-(\Theta' - \tau_3)/\tau_2}) \end{aligned} \quad (6.13)$$

Fig. 6.23 Time Domain Comparison of Approximate Transfer Functions and Simulation Results



In Fig. 6.23 it appears that Eq. 6.13 does not represent exactly the early instant of the computed transient. The improvement proposed for the location $\alpha = 0.374$ could also apply in this case.

In this section the frequency response curves corresponding to three locations in the reactor have been presented. In order to interpret physically the signification of these system functions a simplified transfer function of the form presented in Eq. 6.11 has been proposed. The relative magnitude of the two parts of this transfer function depends on the location in the reactor. At the entrance of the catalyst section the magnitude of the first part of the transfer function is so small that it can be neglected and Eq. 6.11 reduces to Eq. 6.9 and 6.10.

The numerical value of the constants appearing in this expression depends on the conditions around which the transient is performed as the nonlinearity of the T.V.A. reactor described in Section D, Chapter VI showed it.

F. EFFECT OF "BLOW OUT" PERTURBATION IMPOSED DURING A FINITE AMOUNT OF TIME

In this section the dynamic behavior of the T.V.A. reactor is investigated when a perturbation in the feed temperature which, if sustained, would "blow off" the reactor, is imposed for a finite length of time. At the beginning of the run the reactor operates under the steady state conditions corresponding to a feed temperature of 227.6°C , a step change of -15°C in the feed temperature is imposed at $\Theta' = 0$. The feed temperature is then restored to its initial value of 227.6°C at $\Theta' = 1.139$. Under these conditions the results presented in this section show that the reactor can be restored to its starting conditions. Figure 6.24 presents the variations with time of the temperature at the locations corresponding to $\alpha = 0, 1$ and $\alpha = 0.3$,

Fig. 6.24 Temperature Variations during a Perturbation of Finite Duration

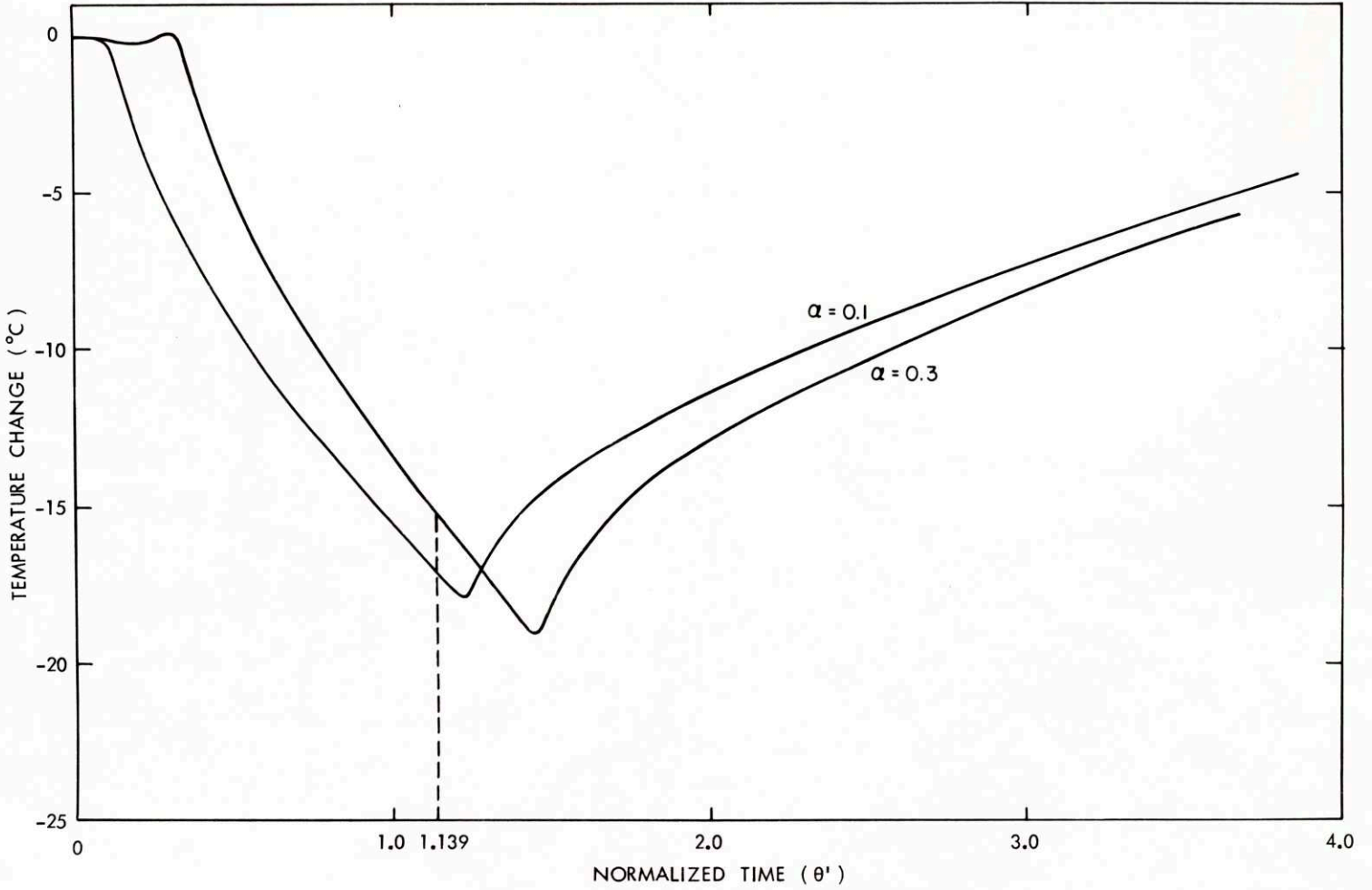


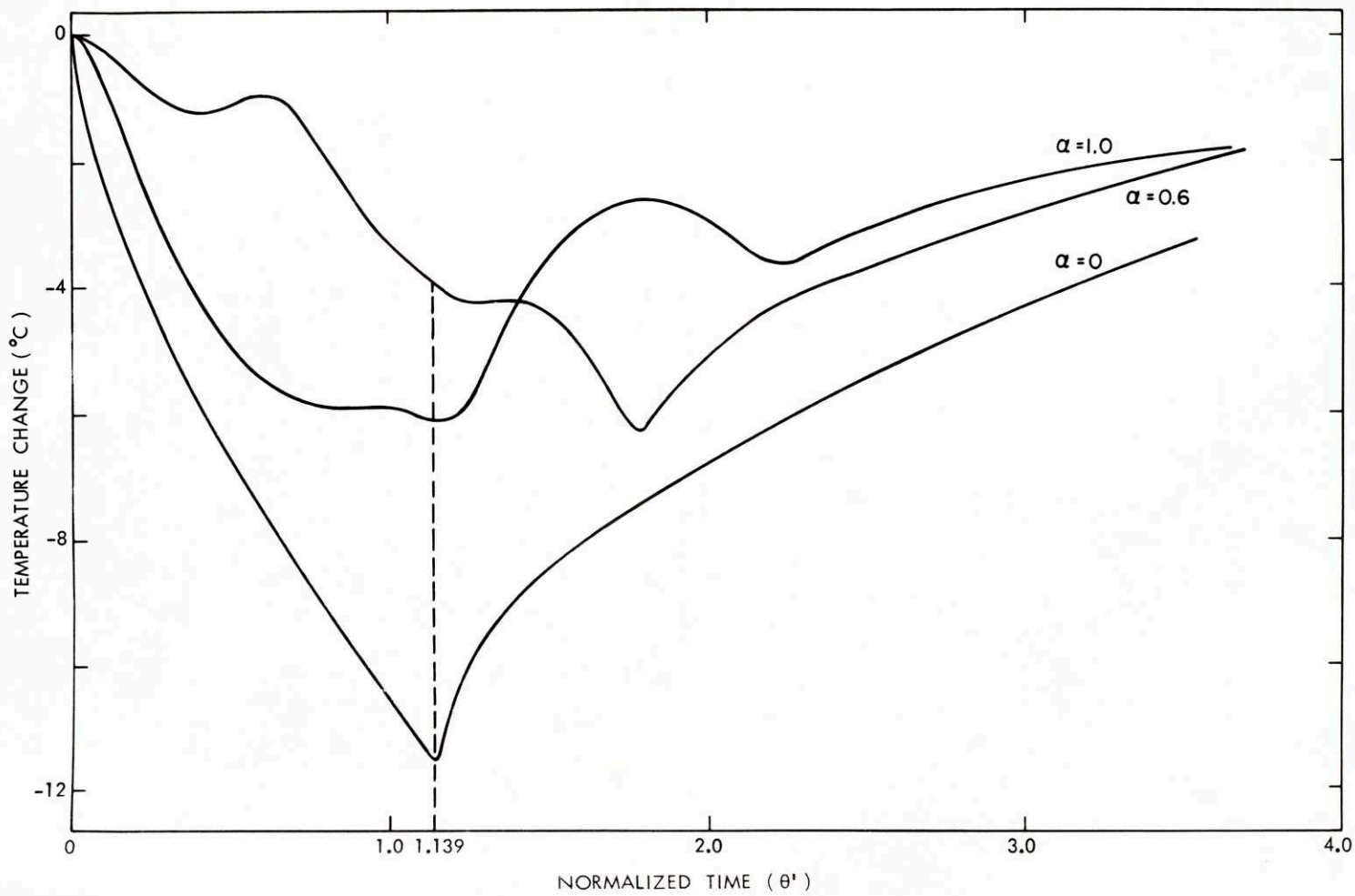
Figure 6.25 presents the same variations at the locations corresponding to $\alpha = 0$, $\alpha = 0.6$ and $\alpha = 1.0$.

At location $\alpha = 0$, the $+15^{\circ}\text{C}$ step change in the feed temperature occurring at time $\Theta' = 1.139$ is immediately felt. Restoration of the feed temperature to its original value affects the temperature at location $\alpha = 0.10$ only after a delay time $\Delta\Theta' = 0.1$. From $\Theta' = 1.140$ to $\Theta' = 1.24$ Fig. 6.25 shows that the temperature of the reactor continues to decrease as if no correcting action had taken place. After $\Theta' = 1.24$ the temperature at $\alpha = 0.1$ returns to its original value in a similar fashion as described in Section B, Chapter VI. The existence of the initial delay appears also at location $\alpha = 0.3$. For all the locations presented so far the effect of changes in the wall temperature and ammonia concentrations are almost negligible and the transient response at these locations can be completely described in term of the travel of two thermal waves down the reactor. The first one resulting from the original step of -15°C , the second one from the restoration of the feed temperature to 227.6°C .

At location $\alpha = 0.6$ the effect of the return of the feed temperature to its original value is felt almost immediately. It was already seen that the wall responds very fast to temperature changes on the empty tube section side and consequently forces the temperature of the catalyst to change more rapidly at the locations where energy transferred to the wall becomes the predominant term of the energy balance.

During the first instant of the return process, rapid changes in the wall temperature slow down the temperature decrease originated by the -15°C step change. When the wall temperature stops changing rapidly, the initial decrease in temperature is resumed until the second thermal wave reaches location $\alpha = 0.6$; the remaining part of the transient for that location being equivalent to the one described in Section B, Chapter VI.

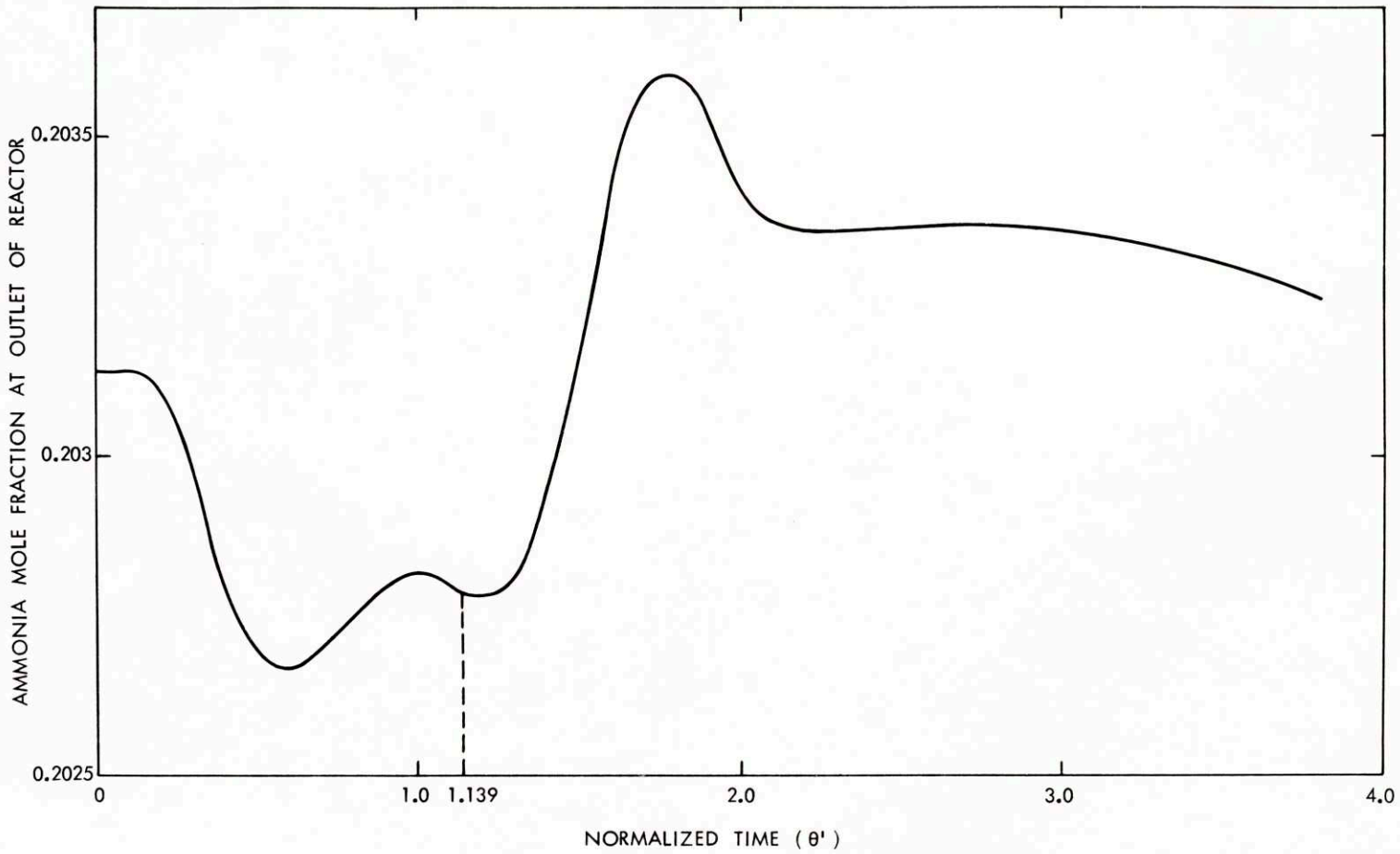
Fig. 6.25 Temperature Variations during a Perturbation of Finite Duration



The initial temperature recovery due to the change in the wall temperature is more pronounced at the outlet of the reactor and results in an increase followed by a decrease of the temperature at that location as it appears in Fig. 6.25. Figure 6.26 presents the variations of the ammonia mole fraction at the outlet of the reactor during the same transient. An overshoot in the production of ammonia is observed at time $\Theta' = 1.80$. The explanation of this observation lies in the fact that at $\Theta' = 1.80$ the temperature is minimum in the center part of the reactor as it appears in the curve for $\alpha = 0.6$ of Fig. 6.25. At these locations the rate of production of ammonia is larger than at the beginning of the transient. Since at the same time the temperature near the entrance and at the outlet of the reactor has already started to recover the reactor is under conditions more favorable for the production of ammonia than the conditions existing at steady state at the beginning of the transient. As it appears in Fig. 6.26 these conditions do not persist and the ammonia mole fraction at the outlet returns to its initial value as the feed is brought back to 227.6°C . The results presented in this section show that after a -15°C offset in the feed temperature lasting for $\Theta = 1.139$ (approximately 7 minutes) it was possible to restore the reactor to its original temperature by using the same feed temperature at which it was operated before.

If the -15°C offset had been sustained during a very large period of time, such that the average bed temperature of the bed had fallen below the ignition temperature (defined in Chapter III) associated with a feed temperature of 227.6°C it would have been impossible to restore the reactor to its original conditions of operation by bringing the feed temperature back to

Fig. 6.26 Outlet Ammonia Mole Fraction during a Perturbation of Finite Duration



227.6°C. The reactor would have continued to "blow off" and would have ended up operating under the low conversion steady state conditions associated with this feed temperature.

No proof of this statement is given in this research since the computer time required to carry out such a run appeared too large. Nevertheless a run was done starting from an arbitrary temperature profile in the reactor below the ignition temperature associated with a feed temperature of 227.6°C. Bringing the temperature to 227.6°C resulted in a "blow off" of the reactor, that is to say, to a further decrease in the bed temperature and in the ammonia production. In the next section the modification of the feed temperature is done by automatic control using the temperature at the entrance of the reactor as the controlled variable.

G. AUTOMATIC CONTROL OF THE T.V.A. REACTOR

In Chapter III it was seen that the only variable at the disposition of the operator to compensate for perturbations in the feed conditions is the setting of the by-pass valve of the heat exchanger.

The first method of control suggested to avoid the "blow off" of the reactor consists in using the measured temperature at a given location in the reactor to operate on the by-pass valve setting. Changes in the by-pass flow will in turn affect the temperature of the gases leaving the heat exchanger section and the temperature of the gases fed to the reacting section under investigation (See Fig. 3.1). The responses of changes in feed temperature to changes in the controller output depends in practice on the dynamics of the heat exchanger. In order to avoid the coupling of the two sections of the T.V.A. reactor the following control scheme is proposed.

The by-pass setting of the heat exchanger section is fixed by a second controller using the feed temperature to the reacting section as measured variable. The temperature inside the reactor is used in a cascade type of control to fix the set point of the second controller just described. Figure 6.27 represents a schematic diagram of the process with the control connections presented by dotted lines.

In this research since the dynamic behavior of the reacting section only has been investigated it will be assumed that the second control loop representing the heat exchanger and the by-pass valve is ideal, that is to say, the temperature T_{feed} at the entrance of the reacting section is at each instant equal to the value required by the controller 1. This is equivalent to saying that the heat exchanger, controller 2, and the control valve behave as a servomechanism of gain unity and zero angle (independent of frequency) which forces the feed temperature to follow exactly the changes of its reference value. The process block diagram corresponding to this simplified case appears in Fig. 6.28. G_p is the transfer function which relates the temperature where the thermocouple is located to the feed temperature. G_c is the controller system function which relates the error in measured temperature $\epsilon = T_{\text{measured}} - T_{\text{reference}}$ to the correcting effect on the feed temperature.

From linear control theory it is known that the stability of the closed loop system is determined by the zeros of the function

$$1 + G_p G_c$$

In the following part of this section the case of a pure proportional controller, for which the system function G_c reduces to a constant K_c , will be considered.

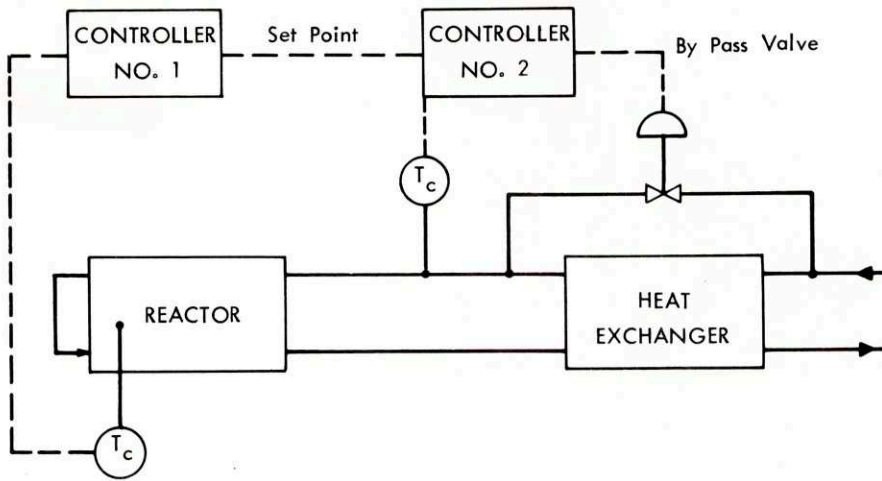


Fig. 6.27 Schematic Diagram of the Control Scheme

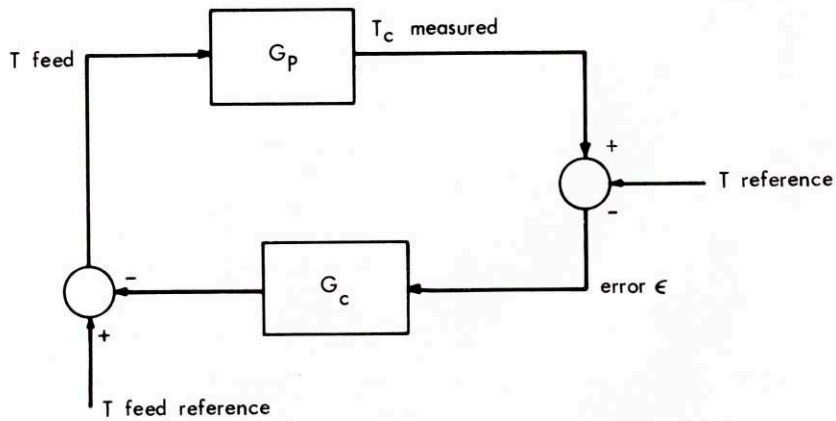


Fig. 6.28 Block Diagram of the Close Control Loop

The linear results obtained in Section E, Chapter VI have been used in defining the limitations imposed on the value of K_c for stability according to the location of the thermocouple in the reactor. Since $K_c G_p$ has the same angle as the process transfer function G_p the largest gain K_c that one can tolerate for stability is the value for which the magnitude of $K_c G_p$ is equal to unity when its angle is -180° .

Table 6.4 presents for different locations in the reactor the values of the frequency at which the angle of $K_c G_p$ becomes -180° and the values of the proportional gain K_c which would make the magnitude of the quantity $K_c G_p$ equal to unity.

Table 6.4

<u>Location</u>	<u>$\omega -180^\circ$</u>	<u>K_{max}</u>
0	no limitation	no limitation
0.374	4.8	4.51
0.6	3.5	14.5
1.0	no limitation	no limitation

Since the angles of the transfer function defined in Section F, Chapter VI for the locations $a = 0$ and $a = 1.0$ never become smaller than -180° in theory the value of the proportional gain associated with these locations is not limited by the stability of the feed back loop. In order to determine the location of the thermocouple in the reactor, the steady state results of Logeais²² have been analyzed. It was found that for all the perturbations investigated by Logeais it is possible from a steady state point of view to avoid the "blow out" of the reactor by keeping the top temperature of the reactor constant. It should be noted that keeping the top temperature constant

avoids the reactor "blow off" but does not maximize the production after the introduction of the perturbation. Consequently the control scheme presented in this section does not constitute the ultimate control for this installation.

In the simulation of the reactor under close loop conditions the thermocouple has been located near the inlet of the reactor in order to allow the use of large controller gains. The results of a typical controlled run are presented in Fig. 6.29 and 6.30. At the beginning of the transient the reactor operates at steady state. A step change in the ammonia mole fraction in the feed from 5% to 6% occurs at time zero. From the steady state results of Logeais such a disturbance will blow the uncontrolled reactor out. The proportional gain used in this study is equal to 10. In Fig. 6.29 the changes with time of the measured temperature are presented. After a time equal to 10 minutes the reactor has recovered from this perturbation and the offset present at the inlet of the reactor is equal to 1.87°C. It was observed that the low value of the proportional gain used in this study assures a very damped response of the temperature everywhere in the reactor and an over shoot of the temperature is only experienced near the outlet of the reactor, as it appears in Fig. 6.30. On this example the possibility of avoiding the blow off of the reactor by using a proportional controller is demonstrated when an increase in the ammonia recycled occurs.

The use of larger values of the proportional gain will result in a faster recovery of the T.V.A. reactor but also in a less damped response. In order to avoid the existence of the offset in the controlled variable at the end of the transient the use of a pure integral controller was simulated. The transfer function retained was of the form $\frac{k_I}{s}$ and the value of the gain tested was 50.

Fig. 6.29 Changes in Temperature at $\alpha = 0$ under Automatic Control of the Reactor

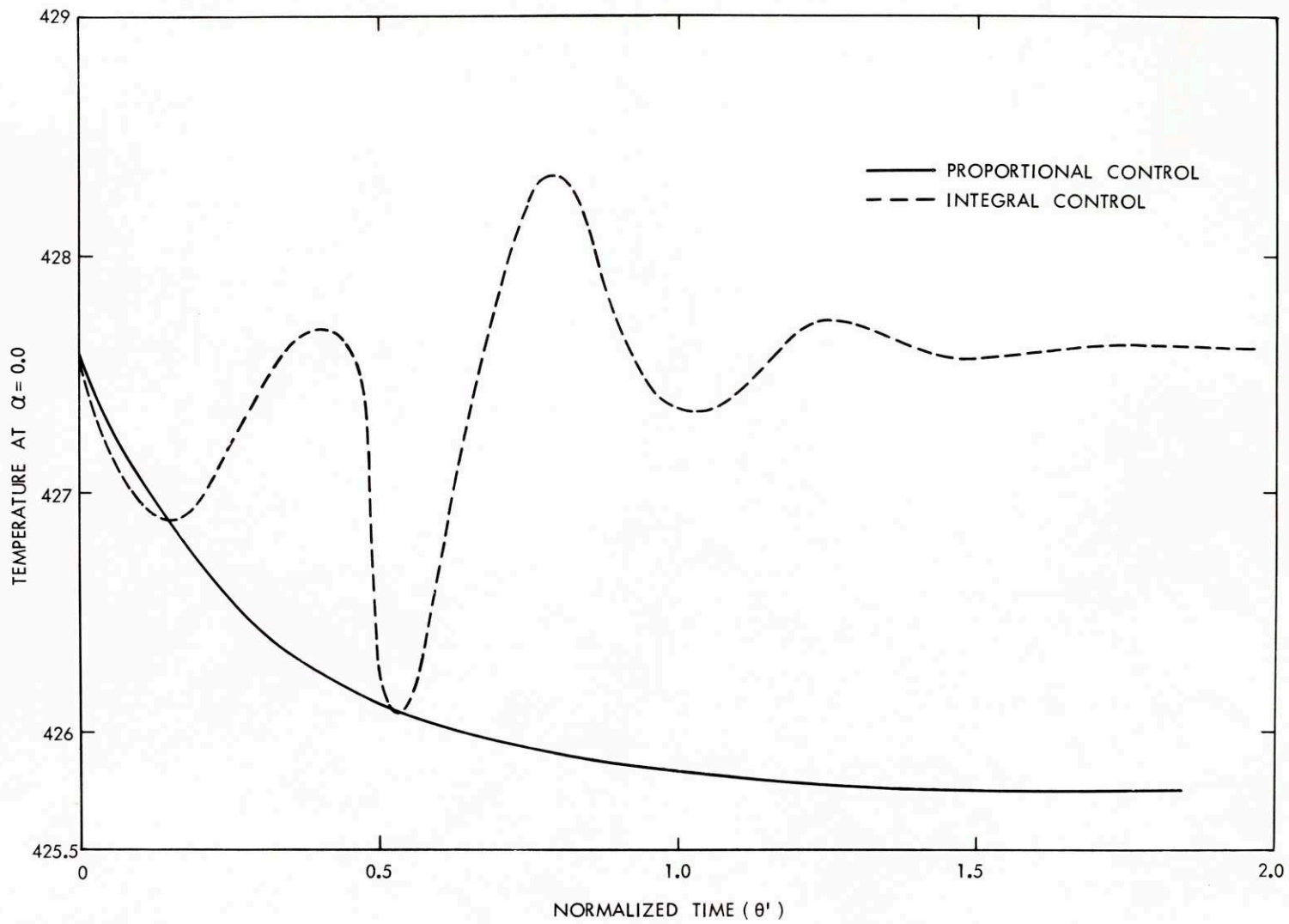
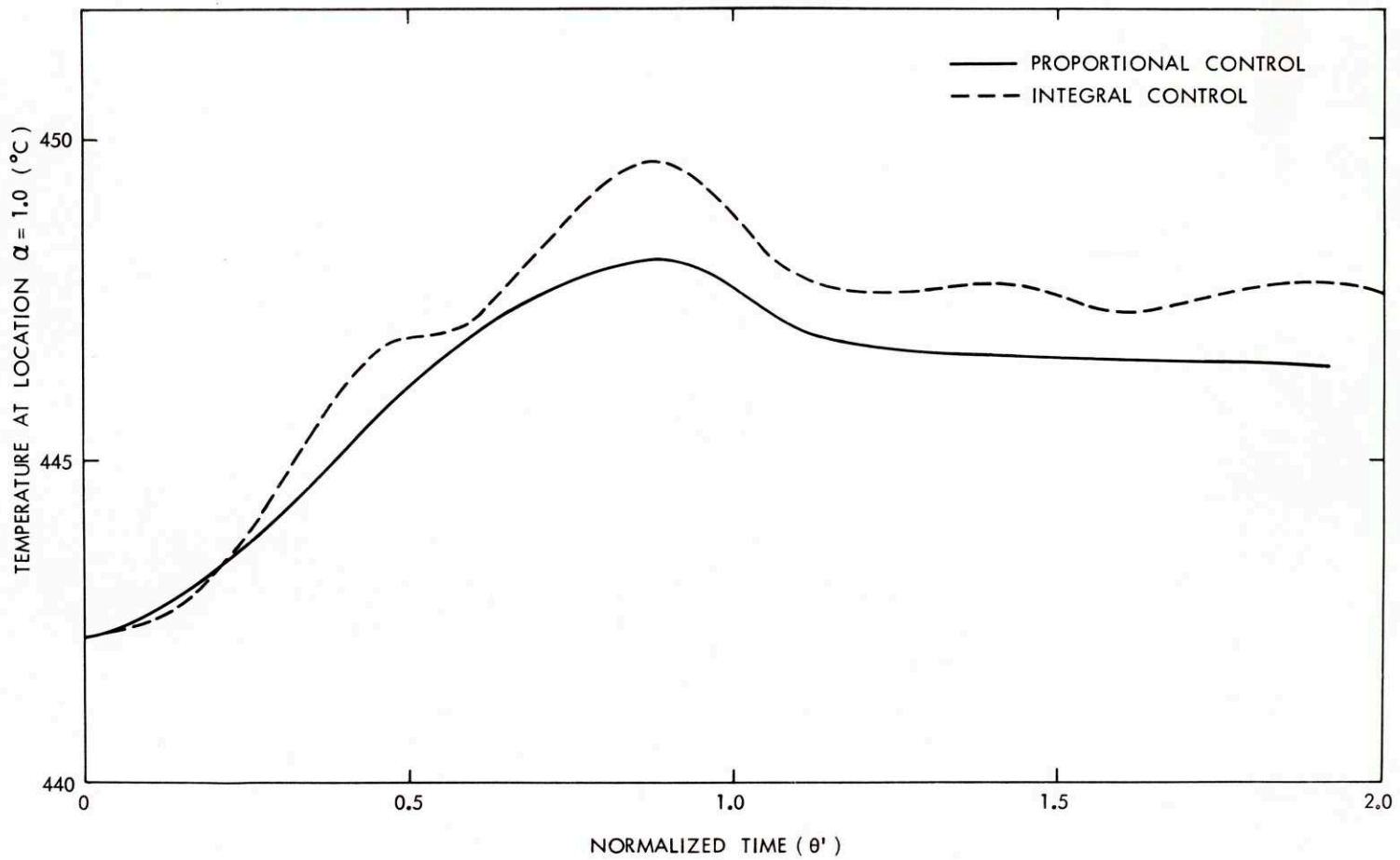


Fig. 6.30 Changes in Temperature at $\alpha = 1.0$ under Automatic Control of the Reactor



Under these conditions the recovery of the temperature inside the reactor experienced oscillations as Fig. 6.29 and 6.30 show it. The oscillations were still present in the reactor after 15 minutes but had the tendency to die out. It is expected that the use of a smaller gain will reduce these oscillations.

The scope of this section was to test the simulation under closed loop control conditions. Runs made with the control thermocouple located near the hot spot temperature (that is to say at location $\alpha = 0.374$) with gain values that were too large resulted in instability and oscillations which blew the reactor out. With the present assumption concerning the response of the feed temperature to controller output, it is demonstrated that the stabilization of the reactor presents very few problems when the measuring element is located near the top of the reactor.

The type of control considered so far did not take into consideration the problem of hot spot temperature nor of optimum production. Since the location and the magnitude of the hot spot vary during a transient, the entire temperature distribution in the reactor needs to be sampled in order to locate and measure the hot spot accurately during a transient. This problem falls outside the range of standard control theory and beyond the scope of this research.

The optimum control of the reactor affected by random changes in the feed conditions is also a very difficult problem which is not considered in this research. Nevertheless, the simulation presented here constitutes a tool to test economical criteria of optimization on this installation.

CHAPTER VII

CONCLUSION AND RECOMMENDATION

During this research a mathematical model describing the dynamic behavior of an ammonia synthesis reactor was derived. This mathematical model provides (at the end of a transient) steady-state profiles which are in fair agreement with experimental results obtained for a specific T.V.A. reactor. Despite the absence of experimental results to support the transient results obtained in this research the mathematical model is expected to describe adequately the reactor since:

The equations derived take into account the major transport phenomena of enthalpy and matter known to occur in such a reactor.

The assumptions made can be justified on the grounds of experimental evidences obtained by previous investigations on similar reactors.

The values of the parameters used in this research come from previous investigations which were able to predict experimental steady state temperature and composition profiles.

The transient results obtained from this simulation have been justified and interpreted by considering the changes occurring during a transient on each enthalpy transport and generation process. The predicted effects of changes in model parameters have been confirmed by the simulation results. The mathematical system of partial differential equations describing the dynamics of the reactor has been solved by a series of finite difference approximations. The finite difference analog of the enthalpy equation in the catalyst used the Stone-Brian method of approximation. This method, which was demonstrated by its authors to represent more accurately the solution of linear partial

differential equation, was applied successfully to the solution of a nonlinear partial differential equation. Even though a complete comparison of the present method with other schemes was not carried through it is believed that the Stone-Brian method represents a definite improvement for the solution of parabolic equations.

The transient behavior of the T.V.A. reactor resulting from step changes in the feed temperature was characterized by two major effects.

1. The effect of changes in temperature originated at the entrance of the catalyst section and travelling down the reactor.
2. The effect of changes in temperature resulting from the coupling between the catalyst section and the empty tube section through the metal of the tube wall.

At the beginning of the transient the only effect felt near the top of the reactor was the first effect, resulting in a "thermal wave" which propagated down the reactor at a speed which was only a function of the ratio of heat capacity of the gases to that of the catalyst. The fact that the travel of this thermal wave was weakly affected by the extent of the chemical reaction was explained by the poor reactivity of the catalyst. Near the end of the reactor the first instants of the transient could be completely described in terms of changes in the wall temperature of this section. To this initial change in temperature is then added after a delay function of the position in the reactor, the thermal wave resulting from the perturbation at the entrance of the catalyst bed.

Because of the coupling between the empty tube section and the catalyst section, the time required for the reactor to recover from a change in the feed temperature is much longer than in the uncoupled case.

As a result of a drop in the feed temperature below the "blow off" limit, the reactor was demonstrated to cool down uniformly; the type of instability encountered in this case being of the "snow-ball type". The effect of the size of the feed temperature perturbations on the response of the reactor was

investigated to test the linearity of this process. It was demonstrated that the dynamic behavior of the reactor was highly non-linear. For small changes (less than 5°C) in the feed temperature around the optimum conditions of operation the behavior of the reactor could, nevertheless, be treated as linear without introducing errors that are too large. Under these conditions the transient behavior of the reactor was represented by frequency response curves and, for a few positions, by simplified transfer functions. If the conditions of operation change, so do the frequency response and the values of the constants introduced in the simplified transfer function. For large changes in the feed temperature resulting in "blow off" of the reactor the results previously obtained do not apply, and changes in temperature and composition can only be obtained through the solution of the simulation.

The impossibility to generalize quantitatively the results of this investigation to other types of operating conditions has appeared. The form of the proposed simplified transfer function nevertheless remains unchanged and the quantitative determination of the frequency response and of the constants involved in the transfer function can be obtained through the use of the proposed simulation under different operating conditions.

The results obtained for the T.V.A. reactor around its optimum condition of operation were used to design an ideal controller acting on the feed temperature of the reactor.

Both a proportional and a pure integral controller were demonstrated as adequate to avoid the "blow off" of the reactor resulting from an increase in the amount of ammonia recycled in the feed. The sensing element was located at the entrance of the reactor in order to allow for large gain values. No attempt was made to optimize the proposed control scheme.

The recommendations for further work concern two areas:

1. The description of the uncontrolled reactor during a transient in its linear range.
2. The description of the reactor under close loop control conditions and the derivation of an automatic controller optimizing the production of this reactor.

In investigating further the dynamic behavior of the uncontrolled reactor, the proposed simulation should be used to derive the values of the time constants of the simplified transfer function under different operating conditions. The sensitivity of these time constants to the steady state around which the transient is performed, should be investigated. An attempt should be made to correlate these time constants with the dimensionless groups appearing in the mathematical model. A particular attention should be paid to the effect of the design variables and the catalyst activity on the values of the time constants.

In investigating the ammonia reactor under close loop control conditions the coupling between the reacting section investigated in this thesis and the heat exchanger section preceding it should be investigated. As a first approach to this problem the simplified transfer functions derived in this thesis should be used with transfer functions reported in the literature for countercurrent tubular heat exchanger.

As a second step, the present simulation should be used for the design of an automatic controller fulfilling the three requirements.

1. Avoid the "blow off" of the reactor.
2. Avoid the peak temperature to be greater than the value at which the catalyst is deteriorated.
3. Optimize the production during a transient.

APPENDIX A

The design characteristics of the T.V.A. reactor under investigation have been reported by Logeais.²² In this section the pertinent numerical values required for the estimation of the model parameters are presented with the values of the parameters retained for the simulation.

1. DESIGN CHARACTERISTICS

a) Catalyst

Total volume	144 cu. ft.
Depth in reactor	17 ft.
Bulk density	169 lb/cu. ft.
Total charge of catalyst	24,340 lb
Particle size: equivalent diameter	0.2"

b) Cooling Tubes

Number	84
Total inside area	$S_1 = 540 \text{ ft.}^2$
Total outside area	$S_2 = 750 \text{ ft.}^2$
Total flow cross section	$A = 0.572 \text{ ft.}^2$
Total mass of metal in tube wall	$M = 7810 \text{ lb}$

2. OPERATING VARIABLES

The operating variables corresponding to the standard conditions under investigation are presented below.

Space velocity	$V_o = 13800 \text{ l/hr}$
Molal flow rate	$F = 5540 \text{ lb mole/hr}$
Mass flow rate inside tubes	$G_T = 106,300 \text{ lb/hr sq. ft.}$
Mass flow rate in catalyst	$G' = 7,260 \text{ lb/hr sq. ft.}$
Pressure	300 atm
Feed mole fraction	
Hydrogen	0.653
Nitrogen	0.217
Ammonia	0.05
Inert	0.08

3. THERMODYNAMICS DATA

The following molal heat capacities are taken from Kelley⁴⁶ at a temperature equal to 427°C

Hydrogen	$C_{P_{H_2}} = 7.19$	Btu/lb mole °F
Nitrogen	$C_{P_{N_2}} = 7.20$	Btu/lb mole °F
Ammonia	$C_{P_{NH_3}} = 11.12$	Btu/lb mole °F
Inert	$C_{P_i} = 6.67$	Btu/lb mole °F
	$\bar{C}_{P_o} = 7.35$	Btu/lb mole °F
	$\Delta C_p = 3.26$	Btu/lb mole °F
	$C_{P_c} = C_{P_m} = 0.172$	Btu/lb mole °F

The enthalpy of formation of ammonia at 298 °K is taken from Rossini and al⁴⁷

$$\Delta H_{238}^{\circ} = -19,870 \text{ Btu/lb mole}$$

4. HEAT TRANSFER DATA

The heat transfer data used in this simulation are obtained from the results reported by Logeais.²² An overall heat transfer coefficient $US = 55,000$ was retained since this value was found by Logeais to provide the best fit between the steady state experimental temperature profiles of Slack, Allgood and Maune²⁹ and his computed profiles. The distribution of the estimated resistances to heat transfer between the catalyst side and the cold gas side are presented below

<u>Nature of resistance</u>	<u>% of total resistance</u>
film resistance in the catalyst side $\frac{1}{h_2}$	48 %
film resistance in the cool gas side $\frac{S_2}{S_1 h_1}$	33 %

<u>Nature of resistance</u>	<u>% of total resistance</u>
resistance to conduction in the metal of the wall	6 %
resistance due to fouling	$\frac{13 \%}{100 \%}$

In the present model the total resistance to heat transfer is broken down into two terms only.

$$\frac{1}{U} = \frac{1}{h_2} + \frac{S_2}{S_1 h_1}$$

Under this assumption the fouling factor and the resistance due to conduction across the metal of the wall are lumped with each film resistance; the heat transfer coefficient corresponding to the standard conditions of operation are, respectively

$$h_1 = 250 \quad \text{Btu/hr sq. ft } ^\circ\text{F}$$

$$h_2 = 124 \quad \text{Btu/hr sq. ft } ^\circ\text{F}$$

The value of the longitudinal Taylor diffusion D' has been computed from the modified longitudinal Peclet number Pe_z reported for gas flow through packed bed by McHenry and Wilhelm.²⁸

The expression proposed for D' is:

$$D' = \frac{D_p G C_p}{Pe_z}$$

where

c_p is the heat capacity of the gas	$\frac{\text{BTU}}{\text{lb } ^\circ\text{F}}$
G the mass flow rate	$\frac{\text{lb}}{\text{ft}^2 \text{ hr}}$
D_p the particle diameter	ft
D' the Taylor heat diffusivity	$\frac{\text{BTU}}{\text{hr ft } ^\circ\text{F}}$

With a Peclet number of 2.0 as it has been reported the Taylor heat diffusivity corresponding to the operating conditions of the T.V.A. reactor is equal to 40 Btu/hr ft. °F.

5. PARAMETERS USED IN THE SIMULATION

The reference temperature used in the simulation is $T_{ref} = 800^{\circ}\text{K}$. The values of the groups defined in Chapter IV corresponding to the standard conditions of operation appear in Table A.1.

Table A.1

Numerical Values of the Groups used in the Simulation

<u>Group</u>	<u>Numerical Value</u>
<i>A</i>	0.1952
<i>B</i>	0.8584
<i>C</i>	0.8584
<i>D</i>	.3550
D	0.0002
d	1.4550
e	1.8783
g	0.3209
h	0.4444
s	0.4382
β	3.320
γ	3.2855 10^{11}
η	25.375

APPENDIX B

RESOLUTION OF THE STEADY STATE EQUATIONS

The system of ordinary differential equations representing the steady state behavior of the reactor where longitudinal diffusion is neglected, can be obtained from Eqs. 5.2, 5.3 and 5.5 by eliminating the time derivatives, the second derivative with respect to distance and replacing everywhere it appears the normalized wall temperature m by its value obtained in Eq. 5.4

$$m = \frac{1}{1+d} v + \frac{d}{1+d} w$$

For simplicity of presentation the distance derivatives have been rewritten in terms of the function F , G , and H as it appears in Eqs. B.1, B.2 and B.3

$$\frac{dy}{d\xi} = F(y, v) \quad (\text{B.1})$$

$$\frac{dv}{d\xi} = G(v, w, y) \quad (\text{B.2})$$

$$\frac{dw}{d\xi} = H(w, v) \quad (\text{B.3})$$

The signification of the functions so defined appears in Eqs. B.4, B.5 and B.6

$$F(y, v) = \frac{(1+y)^2}{1+y} f' r(y, v) \quad (\text{B.4})$$

$$G(v, w, y) = \frac{[e + h(v - 0.375)] sr(v, y) + \frac{d}{1+d}(w - v)}{\frac{s}{f'} (1 - h \frac{y - y_0}{1 + y})} \quad (\text{B.5})$$

$$H(w, v) = \frac{\beta f'}{1+d} (w-v) \quad (B.6)$$

As proposed by Logeais,²² the Runge-Kutta formulas⁴¹ have been used to approximate and solve these differential equations simultaneously. Because of the boundary conditions associated with this problem, the starting conditions of the computation are presented in Eq. B.7

$$\begin{aligned} \xi &= 0 \\ y &= y^* \\ v = w &= v_{\text{top}} \end{aligned} \quad (B.7)$$

The approximating equations used to derive the values of the increments Δy , Δv and Δw corresponding to the increment $\Delta \xi$ of the distance variable are presented in Table B.1.

The computation process is a marching process, which has been demonstrated stable and convergent when a 100 mesh distance grid is used.

The next pages present the Fortran program corresponding to this algorithm. In Table C.1 the variable names used in the Fortran program are defined in terms of the symbols presented in this research.

Table B.2 presents the dependence of reactor temperatures and outlet ammonia mole fraction with the feed temperature

Table B.1
Runge Kutta Formulas

$$y = y^*$$

$$v = v_{\text{Top}}$$

$$w = v_{\text{Top}}$$

$$k_1 = F(y, v) \Delta \xi$$

$$l_1 = G(v, w, y) \Delta \xi$$

$$m_1 = H(v, w) \Delta \xi$$

$$k_2 = F\left(y + \frac{k_1}{2}, v + \frac{l_1}{2}\right) \Delta \xi$$

$$l_2 = G\left(v + \frac{l_1}{2}, w + \frac{m_1}{2}, y + \frac{k_1}{2}\right) \Delta \xi$$

$$m_2 = H\left(v + \frac{l_1}{2}, w + \frac{m_1}{2}\right) \Delta \xi$$

$$k_3 = F\left(y + \frac{k_2}{2}, v + \frac{l_2}{2}\right) \Delta \xi$$

$$l_3 = G\left(v + \frac{l_2}{2}, w + \frac{m_2}{2}, y + \frac{k_2}{2}\right) \Delta \xi$$

$$m_3 = H\left(v + \frac{l_2}{2}, w + \frac{m_2}{2}\right) \Delta \xi$$

$$k_4 = F(y + k_3, v + l_3) \Delta \xi$$

$$l_4 = G(v + l_3, w + m_3, y + k_3) \Delta \xi$$

$$m_4 = H(v + l_3, w + m_3) \Delta \xi$$

$$\Delta y = \frac{1}{6} (k_1 + 2k_2 + 2k_3 + k_4)$$

$$\Delta v = \frac{1}{6} (l_1 + 2l_2 + 2l_3 + l_4)$$

$$\Delta w = \frac{1}{6} (m_1 + 2m_2 + 2m_3 + m_4)$$

$$y = y^* + \Delta y$$

$$v = v_{\text{Top}} + \Delta v$$

$$w = v_{\text{Top}} + \Delta w$$

FORTRAN PROGRAM FOR THE RESOLUTION OF THE STEADY
STATE EQUATIONS (RUNGE-KUTTA METHOD)

FORMAT STATMENTS

```
DIMENSION CATEM(300),GASTEM(300),ETEM(300),CONCT(300),PARTAL(300),  
1 COFK(4),COFL(4),COFM(4),ALPHA(300)  
2 FORMAT(4E18.8)  
3 FORMAT(4I18)  
4 FORMAT(5H DATA)  
5 FORMAT(I8,4E18.8)  
6 FORMAT(8H RESULTS)  
7 FORMAT(5E16.8)  
8 FORMAT(11X5HALPHA,11X5HCATEM,10X6HGASTEM,12X4HETEM,11X5HCONCT)
```

PROBLEM DOCUMENTATION

```
9 PRINT 3  
10 READ 2,NSTOP  
11 PRINT 2,NSTOP  
12 READ 1,AGROUP,BGROUP,CGROUP,DGROUP,PRESS,SPACE,BETAR,DOUBLE,SHC,ST  
13 ICON,SETA,DORIS  
14 PRINT 1,AGROUP,BGROUP,CGROUP,DGROUP,PRESS,SPACE,BETAR,DOUBLE,SHC,S  
15 1TCON,SETA,DORIS  
16 READ 1,DELDIS,VOL  
17 PRINT 1,DELDIS,VOL  
18 READ 1,CAFED  
19 PRINT 1,CAFED  
20 IF(CAFED-0.1000)700,18,18  
21 NTOP=NSTOP-1
```

VARIABLE DISTANCE GRID

```
22 SECOND=2.0*(1.0-VOL)  
23 DO 23 J=1,NSTOP  
24 PARTAL(J)=VOL+SECOND*DELDIS*FLOATF(J-1)  
25 ALPHA(J)=VOL*DELDIS*FLOATF(J-1)+(1.0-VOL)*((FLOATF(J-1)*DELDIS)**2  
26 1)  
27 CONTINUE  
28 PRINT 25  
29 FORMAT(23X1HJ,10X5HALPHA,18X6HPARTAL)  
30 FORMAT(I24,2E24.8)  
31 PRINT 26,(J,ALPHA(J),PARTAL(J),J=1,NSTOP)
```

RUNGE-KUTTA METHOD

```
32 CATEM(1)=CAFED  
33 GASTEM(1)=CAFED  
34 CONCT(1)=STCON
```

```
33  GAMMA=BETAR/(1.0+DORIS)
50  DO 500 J=1,NTOP
70  PART=CATEM(J)
75  CORT=CONCT(J)
80  GART=GASTEM(J)
85  TEMCA=PART
86  CETCON=CORT
87  CALL RATSER(TEMCA,CETCON,PRESS,AGROUP,BGROUP,CGROUP,DGROUP,STCON,S
1PACE,RATE)
90  COFK(1)=(((1.0+CORT)**2.0)/(1.0+STCON))*RATE*DELDIS*(PARTAL(J)+PAR
1TAL(J+1))/2.0
95  COFL(1)=DELDIS*(GAMMA*(GART-PART)+(DOUBLE+SHC*(PART-0.3725))*RATE)
1*(PARTAL(J)+PARTAL(J+1))/2.0/(1.0-SHC*(CORT-STCON)/(1.0+CORT))
100 COFM(1)=GAMMA*DELDIS*(GART-PART)*(PARTAL(J)+PARTAL(J+1))/2.0
110 CORT=CONCT(J)+COFK(1)/2.0
115 GART=GASTEM(J)+COFM(1)/2.0
120 PART=CATEM(J)+COFL(1)/2.0
122 TEMCA=PART
123 CETCON=CORT
124 CALL RATSER(TEMCA,CETCON,PRESS,AGROUP,BGROUP,CGROUP,DGROUP,STCON,S
1PACE,RATE)
125 COFK(2)=(((1.0+CORT)**2.0)/(1.0+STCON))*RATE*DELDIS*(PARTAL(J)+PAR
1TAL(J+1))/2.0
126 COFL(2)=DELDIS*(GAMMA*(GART-PART)+(DOUBLE+SHC*(PART-0.3725))*RATE)
1*(PARTAL(J)+PARTAL(J+1))/2.0/(1.0-SHC*(CORT-STCON)/(1.0+CORT))
127 COFM(2)=GAMMA*DELDIS*(GART-PART)*(PARTAL(J)+PARTAL(J+1))/2.0
128 CORT=CONCT(J)+COFK(2)/2.0
129 GART=GASTEM(J)+COFM(2)/2.0
130 PART=CATEM(J)+COFL(2)/2.0
131 TEMCA=PART
132 CETCON=CORT
133 CALL RATSER(TEMCA,CETCON,PRESS,AGROUP,BGROUP,CGROUP,DGROUP,STCON,S
1PACE,RATE)
135 COFK(3)=(((1.0+CORT)**2.0)/(1.0+STCON))*RATE*DELDIS*(PARTAL(J)+PAR
1TAL(J+1))/2.0
136 COFL(3)=DELDIS*(GAMMA*(GART-PART)+(DOUBLE+SHC*(PART-0.3725))*RATE)
1*(PARTAL(J)+PARTAL(J+1))/2.0/(1.0-SHC*(CORT-STCON)/(1.0+CORT))
137 COFM(3)=GAMMA*DELDIS*(GART-PART)*(PARTAL(J)+PARTAL(J+1))/2.0
200 CORT=CONCT(J)+COFK(3)
201 GART=GASTEM(J)+COFM(3)
202 PART=CATEM(J)+COFL(3)
203 TEMCA=PART
204 CETCON=CORT
205 CALL RATSER(TEMCA,CETCON,PRESS,AGROUP,BGROUP,CGROUP,DGROUP,STCON,S
1PACE,RATE)
210 COFK(4)=(((1.0+CORT)**2.0)/(1.0+STCON))*RATE*DELDIS*(PARTAL(J)+PAR
1TAL(J+1))/2.0
215 COFL(4)=DELDIS*(GAMMA*(GART-PART)+(DOUBLE+SHC*(PART-0.3725))*RATE)
1*(PARTAL(J)+PARTAL(J+1))/2.0/(1.0-SHC*(CORT-STCON)/(1.0+CORT))
220 COFM(4)=GAMMA*DELDIS*(GART-PART)*(PARTAL(J)+PARTAL(J+1))/2.0
250 DELCON=(COFK(1)+2.0*COFK(2)+2.0*COFK(3)+COFK(4))/6.0
260 DELCAT=(COFL(1)+2.0*COFL(2)+2.0*COFL(3)+COFL(4))/6.0
270 DELGAS=(COFM(1)+2.0*COFM(2)+2.0*COFM(3)+COFM(4))/6.0
300 CONCT(J+1)=CONCT(J)+DELCON
```



```
310 CATEM(J+1)=CATEM(J)+DELCA  
320 GASTEM(J+1)=GASTEM(J)+DELGAS  
500 CONTINUE  
510 DO 520 J=1,NSTOP  
515 ETEM(J)=(CATEM(J)+DORIS*GASTEM(J))/(1.0+DORIS)  
520 CONTINUE
```

PRESENTATION OF THE RESULTS

```
550 PRINT 5  
560 PRINT 7  
600 PRINT 6,(ALPHA(J),CATEM(J),GASTEM(J),ETEM(J),CONCT(J),J=1,NSTOP)  
610 PUNCH 4,(J,CATEM(J),GASTEM(J),ETEM(J),CONCT(J),J=1,NSTOP)  
650 GO TO 15  
700 CALL EXIT  
END
```

RATE OF REACTION

```
SUBROUTINE RATSER(TEMCA,CETCON,PRESS,AGROUP,BGROUP,CGROUP,DGROUP,S  
ITCON,SPACE,RATE)  
X=-11.590978+5.97023725/TEMCA-2.4943*LOGF(TEMCA)-0.23130496*TEMCA+  
10.2734408*(TEMCA**2)  
CONTEQ=(EXPF(X)*PRESS)**2  
ODP=(BGROUP-CETCON)*SQRTF(BGROUP-CETCON)  
FIRST=CONTEQ*AGROUP*ODP*(CGROUP-CETCON)/CETCON  
SECP=DGROUP*CETCON/ODP  
RATE=SPACE*(EXPF(-25.375/TEMCA))*(FIRST-SECP)/TEMCA  
RETURN  
END
```

144

TOTAL 144*

Table B.2
Steady State Relations

$T_{c_{\alpha=0}}$ °C	T_{feed} °C	$T_{c_{\alpha=0.374}}$ °C	$T_{c_{\text{out}}}$ °C	$T_{c_{\text{maximum}}}$ °C	α_{maximum}	$y_{\alpha=1.0}$
360	251.9	408.0	393.5	418.80	0.614	0.1475
370	243.4	427.2	405.6	438.7	0.600	0.1628
380	234.4	447.3	416.0	458.8	0.572	0.1775
385	230.26	457.6	420.2	468.6	0.559	0.1840
397.3	222.6	483	427.8	491.0	0.527	0.1959
402.3	221.03	493	430.1	499.3	0.492	0.1990
407.3	220.5	502.6	432.3	507.0	0.471	0.2011
412.3	220.9	511.5	434.4	514.1	0.439	0.2024
417.3	222.2	519.5	436.7	520.70	0.418	0.20311
422.3	224.4	526.5	439.3	526.8	0.399	0.2033
427.3	227.4	532.6	442.20	532.6	0.374	0.2031
432.3	231.0	537.6	445.4	536.2	0.408	0.2026
442.3	240.0	545.6	452.7	547.7	0.316	0.2009
447.3	245.2	548.9	456.8	552.5	0.299	0.1998
457.2	256.8	554.6	465.8	560.7	0.266	0.1971
462.2	263.1	557.2	470.1	564.7	0.250	0.1955
467.2	269.8	559.8	474.8	568.5	0.234	0.1937
472.2	276.7	562.4	479.6	572.2	0.219	0.1918

APPENDIX C

FORTRAN PROGRAM FOR THE COMPUTING ALGORITHM PRESENTED IN CHAPTER V AND NUMERICAL RESULTS

The computer program corresponding to the algorithm derived in Chapter V is written in Fortran language and presented on the following pages.

Table C.1 gives the correspondance between the names of the variables used in the program and the nomenclature already defined. The variables appearing in this program but not defined in this table correspond to parts of an equation computed separately so as to decrease the time of computation.

Table C.1

A. Non-subscript Variables

1. Fixed point Variables

<u>Fortran Name</u>	<u>Nomenclature</u>	<u>Signification or equation where the variable is defined</u>
I	n	time subscript
ICHANT		number of changes of the time increment
IFL		Total number of prints output requested
IPE		Subscript used for DELA (IPE) and ICHAN (IPE)
IPU		Subscript used for IPUNCH (IPU)
IPUT		Total number of punch output
J	j	Distance subscript
JPE		Subscript used for IPRINT (JPE)
NSTOP	N	Total number of points in the distance grid

2. Floating Point Variables

<u>Fortran Name</u>	<u>Nomenclature</u>	<u>Signification or equation where the variable is defined</u>
A GROUP	\mathcal{A}	4.2
ART	a_j	5.22
BERT	b_j	5.22
BETAR	β	4.5
B GROUP	\mathcal{B}	4.2
C GROUP	\mathcal{C}	4.2
DELDIS	$\Delta\xi$	Distance increment
DELT	d_j	5.22
D GROUP	\mathcal{D}	4.2
DIF	D	4.10
DORIS	d	4.7
DOUBLE	e	4.10
GAP	g	4.7
GASFED	w_{feed}	Normalized feed temperature
PRESS	p	Pressure
SECOND	f'_j	5.8
SEMA	a'	5.12
SEMB	b'	5.12
SEMC	c'	5.12
SETA	s	4.10
SHC	h	4.10
SMALA	a	5.20
SMALB	b	5.20
SMALC	c	5.20
SPACE	$\frac{A}{T_{\text{ref}} V_o}$	4.10
STCON	y^*	ammonia mole fraction in the feed
VOL	a	5.6

B. SUBSCRIPT VARIABLES

1. Fixed Point Variables

<u>Fortran Name</u>	<u>Nomenclature</u>	<u>Signification or equation where the variable is defined</u>
ICHAN (IPE)		Value of the time subscript at which the time increment is changed
I PRINT (JPE)		Value of the time subscript at which a printed output is represented
IPUNCH (IPU)		Value of the time subscript at which a punch output is requested

2. Floating Point Variables

<u>Fortran Name</u>	<u>Nomenclature</u>	<u>Signification or equation where the variable is defined</u>
ALPHA (J)	a_j	5.6
BETA (J)	β_i	5.32
CATEM (J)	$v_{j,n+1}$	5.14
CERT (J)	c_j	5.22
CONCT (J)	$y_{j,n+1}$	5.36
DELA (IPE)	$\Delta \theta$	time increment
ETEM (J)	$m_{j,n+1}$ and $m_{j,n}$	5.9
GAMMA (J)	γ_j	5.33
GASTEM (J)	$w_{j,n+1}$	5.9
OCATEM (J)	$v_{j,n}$	5.14
OGASTE (J)	$w_{j,n}$	5.9
PARTAL (J)	f'_j	5.7
RATEP(J)	$r_{j,n}$	5.17

FORTRAN PROGRAM FOR THE RESOLUTION OF THE TRANSIENT BEHAVIOR
OF AN AMMONIA REACTOR

```
DIMENSION CATEM(300),GASTEM(300),ETEM(300),CONCT(300),RATEP(300),A  
1ALPHA(300),PARTAL(300),CERT(300),BETA(300),GAMMA(300),IPRINT(200),D  
2ELA(50),ICHAN(50),IPUNCH(200),OGASTE(300),OCATEM(300),CONTEQ(300),  
3BRATO(300),OCONCT(300),COFRE(300)
```

FORMAT STATEMENTS

```
1 FORMAT(4E18.8)  
2 FORMAT(4I18)  
3 FORMAT(I8,4E18.8)  
4 FORMAT(5H DATA)  
5 FORMAT(5E16.8)  
6 FORMAT(11X5HALPHA,11X5HCATEM,10X6HGASTEM,12X4HETEM,11X5HCONCT)  
7 FORMAT(I24,2E24.8)  
8 FORMAT(2E30.8)  
9 FORMAT(I8,3E18.8)
```

PROBLEM DOCUMENTATION

```
10 READ 2,IFL,ICHANT,NSTOP,IPUT  
11 READ 2,((IPRINT(I),I=1,IFL)  
12 READ 2,((ICHAN(I),I=1,ICHANT)  
13 READ 1,(DELA(I),I=1,ICHANT)  
14 READ 1,DELDIS,VOL  
15 READ 1,AGROUP,BGROUP,CGROUP,DGROUP,PRESS,SPACE,BETAR,SETA,DOUBLE,G  
16 AP,DORIS,STCON,GASFED,DIF,SHC  
17 READ 3,(J,CATEM(J),GASTEM(J),ETEM(J),CONCT(J),J=1,NSTOP)  
18 READ 2,((IPUNCH(I),I=1,IPUT)  
19 PRINT 4  
20 PRINT 2,IFL,ICHANT,NSTOP,IPUT  
21 PRINT 2,((IPRINT(I),I=1,IFL)  
22 PRINT 2,((ICHAN(I),I=1,ICHANT)  
23 PRINT 1,(DELA(I),I=1,ICHANT)  
24 PRINT 1,DELDIS,VOL  
25 PRINT 1,AGROUP,BGROUP,CGROUP,DGROUP,PRESS,SPACE,BETAR,SETA,DOUBLE,  
26 1GAP,DORIS,STCON,GASFED,DIF,SHC  
27 PRINT 3,(J,CATEM(J),GASTEM(J),ETEM(J),CONCT(J),J=1,NSTOP)  
28 PRINT 2,((IPUNCH(I),I=1,IPUT)
```

VARIABLE DISTANCE GRID

```
35 SECOND=2.0*(1.0-VOL)  
40 DO 50 J=1,NSTOP  
45 PARTAL(J)=VOL+SECOND*DELDIS*FLOATF(J-1)  
46 ALPHA(J)=VOL*DELDIS*FLOATF(J-1)+(1.0-VOL)*((FLOATF(J-1)*DELDIS)**2  
47 1)  
50 CONTINUE
```

```

51 PRINT 52
52 FORMAT(23X1HJ,19X5HALPHA,18X6HPARTAL)
53 PRINT 7,(J,ALPHA(J),PARTAL(J),J=1,NSTOP)

```

STARTING CONDITIONS

```

55 IPU=1
56 I=1
57 IPE=1
58 JPE=1
59 NTOP=NSTOP-1
60 NOP=NSTOP-2
61 DO 75 J=1,NSTOP
62 X=-11.590978+5.97023725/CATEM(J)-2.4943*LOGF(CATEM(J))-0.23130496*
1CATEM(J)+0.2734408*(CATEM(J)**2)
63 CONTEQ(J)=(EXPF(X)*PRESS)**2
65 ODP=(BGROUP-CONCT(J))*SQRTF(BGROUP-CONCT(J))
68 RATEP(J)=SPACE*(EXPF(-25.375/CATEM(J)))*((CONTEQ(J)*AGROUP*ODP*(CG
1ROUP-CONCT(J))/CONCT(J))-DGROUP*CONCT(J)/ODP)/CATEM(J)
75 CONTINUE
80 DELTIM=DELA(IPE)
86 SMALA=DELTIM/(2.0*(GAP+0.5*DELTIM*(1.0+DORIS)))
87 SMALB=DORIS*SMALA
88 SMALC=1.0-2.0*(SMALA+SMALB)
89 SIDEV=(1.0-SMALA)/12.0
90 CENTV=(1.0-SMALA)/3.0
91 SIDW=SMALB/12.0
92 SIDET=(1.0+SMALC)/12.0
93 CENTET=(1.0+SMALC)/3.0
94 SIDTIM=1.0/(6.0*DELTIM)
95 CENTIM=2.0/(3.0*DELTIM)
96 CENTW=SMALB/3.0

```

RESOLUTION OF THE ENTHALPY EQUATION IN THE EMPTY TUBE SECTION

```

97 GASTEM(NSTOP)=GASFED
98 SEMA=DELTIM/(GAP+0.5*DELTIM*(1.0+DORIS))
99 SEMB=0.5*SEMA*DORIS
100 SEMC=1.0-SEMA-2.0*SEMB
101 DO 106 J=1,NSTOP
102 OCATEM(J)=CATEM(J)
103 OGASTE(J)=GASTEM(J)
106 CONTINUE
107 GASTEM(NSTOP)=GASFED
109 DO 115 K=1,NTOP
110 J=NSTOP+1-K
111 COF=BETAR*DELDIS*(PARTAL(J)+PARTAL(J-1))/4.0
112 GASTEM(J-1)=(GASTEM(J)*(1.0-COF*(1.0-SEMB)))+(OCATEM(J)+OCATEM(J-1)
1)*SEMA*COF+(ELEM(J)+ELEM(J-1))*COF*SEMC+(OGASTE(J)+OGASTE(J-1))*CO
2F*SEMB)/(1.0+COF*(1.0-SEMB))
115 CONTINUE

```

RESOLUTION OF THE ENTHALPY EQUATION IN THE CATALYST SECTION

```

120  J=1
121  CORECT=SETA*(1.0-SHC*(CONCT(2)-STCON)/(2.0+CONCT(2)+STCON))/(2.0*ALPHA(2))
122  DIFCO=DIF/(ALPHA(2)**2)
123  BERT=5.0/(6.0*DELTIM)+CORECT+DIFCO+5.0*(1.0-SMALA)/12.0
124  CERT(1)=1.0/(6.0*DELTIM)+CORECT-DIFCO+(1.0-SMALA)/12.0
125  BETA(1)=BERT
135  DERT=OCATEM(1)*(5.0/(6.0*DELTIM)-CORECT-DIFCO-5.0*(1.0-SMALA)/12.0
1    1)+OCATEM(2)*(1.0/(6.0*DELTIM)-CORECT+DIFCO-(1.0-SMALA)/12.0)+(GAST
2    2EM(1)+OGASTE(1))*(SETA/ALPHA(2)+5.0*SMALB/12.0)+(GASTEM(2)+OGASTE(
3    32))*SMALB/12.0+(5.0*ETEM(1)+ETEM(2))*(SMALC+1.0)/12.0+(DOUBLE-0.37
4    425*SHC)*SETA*(5.0*RATEP(1)+RATEP(2))/6.0
136  GAMMA(1)=DERT
140  DO 200 J=2,NTOP
141  CORECT=(DIF*SECOND/((PARTAL(J)**2)*PARTAL(J))+SETA*(1.0-SHC*(CONCT
1    1(J)-STCON)/(1.0+CONCT(J)))/PARTAL(J))/(4.0*DELDIS)
142  DIFCO=DIF/(2.0*((PARTAL(J)*DELDIS)**2.0))
143  ART=-DIFCO-CORECT+SIDTIM+SIDEV
144  BERT=2.0*DIFCO+CENTIM+CENTV
145  CERT(J)=-DIFCO+CORECT+SIDTIM+SIDEV
150  DERT=CATEM(J+1)*(DIFCO-CORECT+SIDTIM-SIDEV)+CATEM(J)*(CENTIM-2.0*D
1    1IFCO-CENTV)+CATEM(J-1)*(DIFCO+CORECT+SIDTIM-SIDEV)+(GASTEM(J+1)+GA
2    2STEM(J-1)+OGASTE(J+1)+OGASTE(J-1))*SIDW+(GASTEM(J)+OGASTE(J))*CENT
3    3W+(ETEM(J-1)+ETEM(J+1))*SIDET+ETEM(J)*CENTET+(DOUBLE+SHC*(CATEM(J-
4    41)-0.3725))*SETA*RATEP(J-1)/6.0+(DOUBLE+SHC*(CATEM(J)-0.3725))*SET
5    5A*RATEP(J)*2.0/3.0+(DOUBLE+SHC*(CATEM(J+1)-0.3725))*SETA*RATEP(J+1
6    6)/6.0
160  BETA(J)=BERT-(ART*CERT(J-1))/BETA(J-1)
165  GAMMA(J)=DERT-(ART*GAMMA(J-1))/BETA(J-1)
200  CONTINUE
201  J=NSTOP
205  DIFCO=DIF/((1.0-ALPHA(NTOP))**2)
206  CORECT=SETA*(1.0-SHC*(CONCT(NTOP)+CONCT(NSTOP)-2.0*STCON)/(2.0+CON
1    1CT(NTOP)+CONCT(NSTOP)))/(2.0*(1.0-ALPHA(NTOP)))
207  ART=1.0/(6.0*DELTIM)-CORECT-DIFCO+(1.0-SMALA)/12.0
208  BERT=5.0/(6.0*DELTIM)-CORECT+DIFCO+5.0*(1.0-SMALA)/12.0+SETA*(1.0-
1    1SHC*(CONCT(NSTOP)-STCON)/(1.0+CONCT(NSTOP)))/(1.0-ALPHA(NTOP))
210  DERT=OCATEM(NTOP)*(1.0/(6.0*DELTIM)+CORECT+DIFCO-(1.0-SMALA)/12.0)
1    1+OCATEM(NSTOP)*(5.0/(6.0*DELTIM)+CORECT-DIFCO-5.0*(1.0-SMALA)/12.0
2    2-SETA*(1.0-SHC*(CONCT(NSTOP)-STCON)/(1.0+CONCT(NSTOP)))/(1.0-ALPHA
3    3(NTOP)))+(GASTEM(NTOP)+OGASTE(NTOP))*SMALB/12.0+(GASTEM(NSTOP)+OGA
4    4STE(NSTOP))*5.0*SMALB/12.0+(5.0*ETEM(NSTOP)+ETEM(NTOP))*(SMALC+1.0
5    5)/12.0+(DOUBLE-0.3725*SHC)*SETA*(5.0*RATEP(NSTOP)+RATEP(NTOP))/6.0
220  BETA(NSTOP)=BERT-ART*CERT(NSTOP-1)/BETA(NSTOP-1)
225  GAMMA(NSTOP)=DERT-ART*GAMMA(NSTOP-1)/BETA(NSTOP-1)
230  CATEM(NSTOP)=GAMMA(NSTOP)/BETA(NSTOP)
240  DO 250 L=1,NTOP :
241  J=NSTOP-L
245  CATEM(J)=(GAMMA(J)-CERT(J)*CATEM(J+1))/BETA(J)

```


250 CONTINUE

RESOLUTION OF THE ENTHALPY EQUATION IN THE TUBE WALL SECTION

```
260 DO 270 J=1,NSTOP
265 ETEM(J)=ETEM(J)*SMALC+(CATEM(J)+OCATEM(J))*SMALA+(GASTEM(J)+OGASTE
1(J))*SMALB
270 CONTINUE
```

RESOLUTION OF THE MASS BALANCE EQUATION IN THE CATALYST

```
280 DO 300 J=1,NSTOP
281 X=-11.590978+5.97023725/CATEM(J)-2.4943*LOGF(CATEM(J))-0.23130496*
1CATEM(J)+0.2734408*(CATEM(J)**2)
285 CONTEQ(J)=(EXPF(X)*PRESS)**2
290 COFRE(J)=SPACE*(EXPF(-25.375/CATEM(J)))/CATEM(J)
300 CONTINUE
310 CONCT(1)=STCON
350 DO 470 J=1,NTOP
370 ODP=(BGROUP-CONCT(J))*SQRTF(BGROUP-CONCT(J))
380 RATEP(J)=COFRE(J)*((CONTEQ(J)*AGROUP*ODP*(CGROUP-CONCT(J))/CONCT(J
1))-DGROUP*CONCT(J)/ODP)
385 ROI=0.5*DELDIS*(PARTAL(J)+PARTAL(J+1))*RATEP(J)*((1.0+CONCT(J))**2
1)/(1.0+STCON)
390 OCONCT(J)=CONCT(J)+ROI
395 ODP=(BGROUP-OCONCT(J))*SQRTF(BGROUP-OCONCT(J))
400 RATO(J)=COFRE(J+1)*((CONTEQ(J+1)*AGROUP*ODP*(CGROUP-OCONCT(J))/OCO
1NCT(J))-DGROUP*OCONCT(J)/ODP)
410 ROB=0.5*DELDIS*(PARTAL(J)+PARTAL(J+1))*RATO(J)*((1.0+OCONCT(J))**2
1.0)/(1.0+STCON)
415 CONCT(J+1)=CONCT(J)+0.5*(ROI+ROB)
470 CONTINUE
475 ODP=(BGROUP-CONCT(NSTOP))*SQRTF(BGROUP-CONCT(NSTOP))
480 RATEP(NSTOP)=COFRE(NSTOP)*((CONTEQ(NSTOP)*AGROUP*ODP*(CGROUP-CONCT
1(NSTOP))/CONCT(NSTOP))-DGROUP*CONCT(NSTOP)/ODP)
```

CHANGE OF TIME INCREMENT

```
900 IF(I-ICHAN(IPE))1001,905,1001
905 IPE=IPE+1
910 DELTIM=DELA(IPE)
911 SMALA=DELTIM/(2.0*(GAP+0.5*DELTIM*(1.0+DORIS)))
912 SMALB=DORIS*SMALA
913 SMALC=1.0-2.0*(SMALA+SMALB)
920 SIDEV=(1.0-SMALA)/12.0
922 CENTV=(1.0-SMALA)/3.0
925 SIDW=SMALB/12.0
```

```
930 SIDET=(1.0+SMALC)/12.0
935 CENTET=(1.0+SMALC)/3.0
940 SIDTIM=1.0/(6.0*DELTIM)
945 CENTIM=2.0/(3.0*DELTIM)
950 CENTW=SMALB/3.0
955 SEMA=DELTIM/(GAP+0.5*DELTIM*(1.0+DORIS))
960 SEMB=0.5*SEMA*DORIS
965 SEMC=1.0-SEMA-2.0*SEMB
966 COF1=DELTIM/(2.0*DER)
967 COF2=DELTIM/(2.0*TIMC)
968 COF3=(1.0-COF1)/(1.0+COF1)
969 COF4=GAIN*(1.0+COF2)/(1.0+COF1)
970 COF5=GAIN*(1.0-COF2)/(1.0+COF1)
```

PRESENTATION OF THE RESULTS

```
1001 IF(I-IPRINT(JPE))1010,1100,1010
1010 I=I+1
1011 GO TO 101
1100 PRINT 1101
1101 FORMAT(8H RESULTS)
1102 PRINT 2,I
1103 PRINT 6
1104 PRINT 5,(ALPHA(J),CATEM(J),GASTEM(J),ETEM(J),CONCT(J),J=1,NSTOP)
1126 IF(I-IPUNCH(IPU))1129,1127,1129
1127 PUNCH 3,(J,CATEM(J),GASTEM(J),ETEM(J),CONCT(J),J=1,NSTOP)
1128 IPU=IPU+1
1129 JPE=JPE+1
1130 IF(JPE-IFL)1010,1010,1200
1200 CALL EXIT
      END
```

250

TOTAL 250*

The results of the computations are filed in a separate data book kept in Professor R. F. Baddour office.

In the following pages the numerical results corresponding to the figures appearing in the text have been tabulated.

Table C.2

Temperature Changes During a
+5°C Step Transient

Time θ	Time θ'	$\Delta T_{c_{\alpha=0}}^{\circ C}$	$\Delta T_{c_{\alpha=0.1}}^{\circ C}$	$\Delta T_{c_{\alpha=0.3}}^{\circ C}$	$\Delta T_{c_{\alpha=0.6}}^{\circ C}$	$\Delta T_{c_{\alpha=1.0}}^{\circ C}$
0.10	0.044	0.45	0.01	0.02	0.03	0.11
0.20	0.088	0.70	0.02	0.05	0.09	0.26
0.30	0.132	0.93	0.52	0.07	0.17	0.45
0.45	0.197	1.23	1.12	0.08	0.28	0.74
0.65	0.285	1.47	1.80	-0.04	0.40	1.09
0.75	0.329	1.72	2.09	0.25	0.44	1.24
1.0	0.438	2.09	2.76	1.23	0.45	1.57
1.10	0.482	2.20	2.97	1.51	0.44	1.65
1.30	0.570	2.46	3.40	2.07	0.39	1.82
1.45	0.635	2.64	3.71	2.43	0.44	1.91
1.75	0.767	2.97	4.29	3.06	0.79	2.02
2.0	0.876	3.23	4.73	3.53	1.02	2.07
2.20	0.964	3.43	5.06	3.87	1.18	2.19
2.60	1.140	3.78	5.66	4.51	1.45	2.27
3.0	1.315	4.11	6.22	5.05	1.70	2.53
4.0	1.753	4.79	7.39	6.20	2.16	3.02
5.0	2.191	5.30	8.27	7.06	2.52	3.37
6.0	2.629	5.69	8.94	7.70	2.79	3.64
7.0	3.067	5.97	9.43	8.18	2.98	3.74
8.0	3.506	6.18	9.79	8.53	3.13	3.99
9.0	3.944	6.34	10.07	8.78	3.24	4.10
10.0	4.382	6.45	10.27	8.97	3.32	4.19
10.6	4.645	6.51	10.36	9.06	3.36	4.23

Table C.3

Ammonia Mole Fraction Changes
During a +5°C Step Transient

Time θ	Time θ'	$10^3 \times \Delta y_{\alpha=0.1}$	$10^3 \times \Delta y_{\alpha=0.3}$	$10^3 \times \Delta y_{\alpha=0.6}$	$10^3 \times \Delta y_{\alpha=1.0}$
0.10	0.044	0.04	0.01	-0.004	-0.006
0.20	0.088	0.13	0.05	-0.007	-0.009
0.30	0.132	0.24	0.11	-0.005	-0.012
0.45	0.197	0.38	0.25	0.015	-0.006
0.65	0.285	0.53	0.49	0.08	0.022
0.75	0.329	0.60	0.60	0.12	0.042
1.0	0.438	0.76	0.83	0.18	0.078
1.10	0.482	0.81	0.90	0.18	0.080
1.30	0.570	0.91	1.05	0.14	0.065
1.45	0.635	0.99	1.15	0.09	0.041
1.75	0.767	1.13	1.32	0.002	-0.024
2.0	0.876	1.24	1.46	-0.058	-0.081
2.20	0.964	1.32	1.56	-0.110	-0.121
2.60	1.140	1.47	1.73	-0.180	-0.187
3.0	1.315	1.61	1.89	-0.249	-0.243
4.0	1.753	1.90	2.21	-0.393	-0.358
5.0	2.191	2.12	2.44	-0.506	-0.453
6.0	2.629	2.28	2.61	-0.606	-0.526
7.0	3.067	2.40	2.73	-0.678	-0.582
8.0	3.506	2.50	2.81	-0.732	-0.625
9.0	3.944	2.56	2.88	-0.773	-0.656
10.0	4.382	2.61	2.92	-0.803	-0.680
10.6	4.645	2.64	2.94	-0.818	-0.692

Table C.4

Location and Magnitude of Peak Temperature

Time θ	Time θ'	Location α	Magnitude	$T_{c_{\alpha=0.374}}$
0	0	0.373	532.67	532.67
0.10	0.044	0.373	532.69	532.69
0.20	0.088	0.373	532.72	532.72
0.30	0.132	0.373	532.76	532.76
0.45	0.197	0.373	532.79	532.80
0.65	0.285	0.374	532.75	532.76
0.75	0.329	0.375	532.69	532.69
1.0	0.438	0.365	533.11	533.07
1.10	0.482	0.365	533.35	533.31
1.30	0.570	0.364	533.85	533.79
1.45	0.635	0.363	534.16	534.09
1.75	0.767	0.362	534.68	534.59
2.0	0.876	0.360	535.05	534.95
2.20	0.964	0.360	535.34	535.21
2.60	1.140	0.358	535.84	535.69
3.0	1.315	0.357	536.26	536.10
4.0	1.753	0.353	537.19	536.93
5.0	2.191	0.351	537.88	537.57
6.0	2.629	0.349	538.39	538.03
7.0	3.067	0.348	538.77	538.37
8.0	3.506	0.347	539.04	538.63
9.0	3.944	0.346	539.31	538.81
10.0	4.382	0.345	539.47	538.95
10.6	4.645	0.345	539.52	539.01

Table C.5

Transient Dynamic "Gain" of the Reactor During
A +5°C Step Transient

Location a	0	0.106	0.208	0.30	0.408	0.506	0.60	0.702	0.812	0.912	1.0
Time	0	0.106	0.208	0.30	0.408	0.506	0.60	0.702	0.812	0.912	1.0
$\theta' = 0.110$	0.164	0.030	0.006	0.011	0.015	0.020	0.025	0.035	0.044	0.057	0.070
$\theta' = 0.372$	0.373	0.472	0.363	0.130	0.004	0.052	0.090	0.135	0.181	0.230	0.276
$\theta' = 0.964$	0.686	1.025	1.064	0.774	0.418	0.276	0.235	0.245	0.276	0.325	0.418
$\theta' = 2.10$	1.003	1.578	1.722	1.315	0.768	0.536	0.462	0.463	0.499	0.556	0.634
$\theta' = 4.65$	1.302	2.108	2.346	1.811	1.082	0.773	0.671	0.663	0.701	0.763	0.845

Table C.6

Enthalpy Generation and Transport

Location a	q_1	q_2	q_3	$\frac{\partial q_3}{\partial v}$	$\frac{\partial q_3}{\partial y}$
0	-0.2609	-0.0002	0.2611	2.953	-6.066
0.106	-0.2233	-0.0356	0.2589	2.541	-4.278
0.208	-0.1522	-0.0720	0.2242	1.232	-3.690
0.30	-0.0594	-0.0961	0.1555	-0.248	-3.538
0.374	-0.0049	-0.1092	0.1141	-0.948	-3.354
0.408	0.0195	-0.1138	0.0943	-1.177	-3.139
0.506	0.0514	-0.1244	0.0730	-1.141	-2.557
0.6	0.0674	-0.1328	0.0654	-0.737	-1.988
0.702	0.0806	-0.1409	0.0603	-0.410	-1.445
0.812	0.0947	-0.1488	0.0541	-0.058	-0.986
0.912	0.1082	-0.1548	0.0466	+0.156	-0.669
1.0	0.1209	-0.1592	0.0383	+0.247	-0.462

Table C.7

Temperature Changes During a Blow Off Transient

Time θ	Time θ'	$-\Delta T_{c_{a=0}}$	$-\Delta T_{c_{a=0.1}}$	$-\Delta T_{c_{a=0.3}}$	$-\Delta T_{c_{a=0.6}}$	$-\Delta T_{c_{a=1.0}}$
0.10	0.044	1.34	0.0	0.02	0.07	0.22
0.20	0.088	2.10	0.03	0.07	0.25	0.75
0.30	0.131	2.78	1.52	0.13	0.48	1.35
0.45	0.197	3.66	3.28	0.13	0.82	2.23
0.65	0.285	4.67	5.29	-0.27	1.16	3.27
0.75	0.329	5.12	6.15	0.62	1.25	3.72
1.0	0.438	6.16	8.02	3.58	1.26	4.64
1.30	0.570	7.31	9.96	6.46	0.95	5.44
1.50	0.657	8.03	11.16	8.05	1.20	5.77
1.75	0.767	8.89	12.57	9.86	2.04	5.99
2.0	0.876	9.70	13.89	11.55	2.77	6.05
2.20	0.986	10.49	16.15	13.16	3.40	6.00
2.70	1.183	11.84	17.30	15.88	4.41	6.51
3.0	1.315	12.70	18.66	17.61	5.06	7.00
4.0	1.753	15.38	22.85	23.06	7.07	8.26
5.0	2.191	17.83	26.64	28.08	9.07	9.29
5.40	2.36	18.77	28.07	40.00	9.87	9.68

Table C.8

Changes in Ammonia Mole Fraction
During a Blow Off

Time θ	Time θ'	$-10^3 \times \Delta y_{\alpha=0.1}$	$-10^3 \times \Delta y_{\alpha=0.3}$	$-10^3 \times \Delta y_{\alpha=0.6}$	$-10^3 \times \Delta y_{\alpha=1.0}$
0.10	0.044	0.116	0.059	0.004	0.003
0.20	0.088	0.376	0.172	0.000	-0.003
0.30	0.131	0.697	0.355	0.010	-0.003
0.45	0.197	1.098	0.767	0.078	0.028
0.65	0.285	1.474	1.496	0.285	0.145
0.75	0.329	1.737	1.853	0.415	0.224
1.0	0.438	2.167	2.667	0.678	0.398
1.30	0.570	2.624	3.536	0.732	0.47
1.50	0.657	2.905	4.076	0.661	0.447
1.75	0.767	3.236	4.728	0.610	0.387
2.0	0.876	3.547	5.358	0.613	0.334
2.20	0.986	3.843	5.965	0.652	0.315
2.70	1.183	4.345	7.03	0.783	0.365
3.0	1.315	4.663	7.718	0.903	0.421
4.0	1.753	5.631	9.948	1.443	0.725
5.0	2.19	6.49	12.039	2.170	1.156
5.40	2.36	6.82	12.852	2.508	1.364

Table C.9

Dynamic Gain During a "Blow Off"

Location α											
Time	0	0.106	0.208	0.30	0.408	0.506	0.60	0.702	0.812	0.912	1.0
$\theta' = 0.110$	0.163	0.028	0.003	0.007	0.012	0.018	0.024	0.032	0.045	0.060	0.070
$\theta' = 0.372$	0.370	0.463	0.361	0.125	-0.005	0.045	0.086	0.129	1.82	0.234	0.276
$\theta' = 0.964$	0.689	1.007	1.084	0.856	0.475	0.283	0.219	0.213	0.252	0.316	0.401
$\theta' = 2.10$	1.156	1.755	2.029	1.807	1.196	0.778	0.578	0.499	0.504	0.552	0.606
$\theta' = 2.37$	1.251	1.903	2.215	2.00	1.354	0.890	0.658	0.559	0.553	0.595	0.645

Table C.10

Effects of the Magnitude of the Step Change
on the Dynamic Gain at $\theta' = 0.964$

Location a											
Magnitude of step change	0	0.106	0.208	0.30	0.408	0.505	0.60	0.702	0.812	0.912	1.0
-15°C	0.689	1.007	1.084	0.856	0.475	0.283	0.219	0.213	0.252	0.316	0.401
-10°C	0.684	1.006	1.074	0.830	0.454	0.276	0.219	0.217	0.258	0.322	0.403
- 5°C	0.678	1.001	1.057	0.798	0.430	0.266	0.218	0.218	0.263	0.331	0.405
+ 5°C	0.686	1.025	1.064	0.774	0.418	0.276	0.235	0.245	0.276	0.336	0.418
+10°C	0.679	1.019	1.043	0.741	0.400	0.269	0.235	0.246	0.282	0.234	0.420

Table C.11

Effects of the Magnitude of the Step Change
on the Dynamic Gain at $\theta' = 2.10$

Location a											
Magnitude of step change	0	0.106	0.208	0.30	0.408	0.505	0.60	0.702	0.812	0.912	1.0
-15°C	1.156	1.755	2.029	1.807	1.196	0.778	0.578	0.499	0.504	0.552	0.606
- 5°C	1.079	1.675	1.893	1.564	0.950	0.626	0.503	0.470	0.508	0.574	0.626
+ 5°C	1.043	1.648	1.805	1.382	0.810	0.568	0.490	0.490	0.526	0.583	0.658

Table C.12

Effect of the Magnitude of the Step Change
on the "Gain" at $\alpha = 0.374$

Magnitude of Step	-15°C	-10°C	-5°C	+5°C	+10°C
Time θ'					
0.044	0.002	0.002	0.001	0.003	0.003
0.088	0.007	0.007	0.006	0.010	0.009
0.131	0.013	0.013	0.011	0.018	0.016
0.175	0.019	0.018	0.027	0.024	0.022
0.219	0.020	0.019	0.017	0.026	0.024
0.329	-0.001	-0.002	0.008	0.004	0.001
0.438	0.065	0.064	0.061	0.080	0.072
0.548	0.203	0.199	0.192	0.202	0.195
0.657	0.320	0.311	0.299	0.303	0.292
0.767	0.420	0.406	0.388	0.385	0.369
0.876	0.512	0.492	0.468	0.456	0.436
0.986	0.600	0.572	0.542	0.519	0.495
1.095	0.684	0.649	0.612	0.581	0.548
1.315	0.845		0.741	0.686	
1.534	1.001		0.858	0.784	
1.753	1.154		0.968	0.853	
1.972	1.303		1.068	0.925	
2.20	1.448			0.979	
2.37	1.563			1.020	
Steady State	Blow Off	Blow Off	2.61	1.24	1.09

Table C.13

Effect of the Magnitude of the Step Change
on the gain at $\alpha = 1.0$

Step Magnitude					
Time θ'	-15°C	-10°C	-5°C	+5°C	+10°C
0.044	0.0145	0.0135	0.0106	0.022	0.0195
0.088	0.050	0.050	0.049	0.052	0.051
0.131	0.090	0.090	0.090	0.090	0.090
0.175	0.129	0.130	0.130	0.129	0.129
0.219	0.167	0.167	0.167	0.170	0.166
0.329	0.248	0.248	0.248	0.248	0.248
0.438	0.311	0.311	0.310	0.313	0.310
0.548	0.356	0.355	0.354	0.356	0.355
0.657	0.385	0.384	0.383	0.386	0.385
0.767	0.399	0.399	0.398	0.404	0.403
0.876	0.403	0.404	0.404	0.414	0.413
0.986	0.400	0.403	0.405	0.419	0.421
1.095	0.412	0.417	0.421	0.441	0.444
1.315	0.466		0.480	0.506	
1.534	0.512		0.529	0.558	
1.753	0.551		0.570	0.604	
1.972	0.586		0.606	0.638	
2.10	0.606		0.626	0.657	
2.20	0.619			0.674	
2.37	0.645			0.697	
Steady State	Blow Off	Blow Off	1.08	0.86	0.83

Table C.14

Changes in Temperature During Restoration
of the Reactor to its Original Conditions

Time θ	$-\Delta T_{c_{\alpha=0}}$	$-\Delta T_{c_{\alpha=0.1}}$	$-\Delta T_{c_{\alpha=0.3}}$	$-\Delta T_{c_{\alpha=0.6}}$	$-\Delta T_{c_{\alpha=1.0}}$
1.139	11.54	16.83	15.29	4.19	6.34
1.143	10.94	16.88	15.35	4.22	6.35
1.183	10.50	17.29	15.86	4.34	6.26
1.227	10.03	17.71	16.37	4.37	5.92
1.270	9.64	16.70	16.87	4.36	5.49
1.314	9.31	16.00	17.39	4.34	5.05
1.358	9.04	15.35	17.99	4.33	4.64
1.402	8.81	14.81	18.72	4.37	4.26
1.446	8.61	14.35	19.06	4.45	3.92
1.489	8.43	13.97	18.02	4.59	3.62
1.577	8.11	13.34	16.49	5.05	3.16
1.709	7.77	12.58	14.86	6.18	2.79
1.752	7.53	12.35	14.47	6.48	2.75
1.796	7.40	12.12	14.12	6.26	2.75
2.015	6.76	11.08	12.72	5.05	3.21
2.059	6.64	10.88	12.47	4.83	3.39
2.103	6.52	10.69	12.23	4.76	3.59
2.147	6.40	10.50	11.99	4.64	3.79
2.235	6.16	10.13	11.54	4.43	3.82
2.454	5.58	9.21	10.48	3.98	3.26
2.673	5.05	8.34	9.46	3.59	2.89
2.892	4.55	7.53	8.51	3.24	2.61
3.111	4.10	6.79	7.64	2.91	2.37
3.330	3.69	6.11	6.86	2.61	2.15
3.461	3.45	5.73	6.42	2.44	2.02

Table C.15

Ammonia Mole Fraction During Restoration
of the Reactor to its Original Condition

Time θ'	$y_a=0.1$	$y_a=0.3$	$y_a=0.6$	$y_a=1.0$
0.0	0.08035	0.13525	0.17217	0.20313
1.139	0.076118	0.128452	0.171427	0.202783
1.143	0.076113	0.128431	0.171425	0.202782
1.183	0.076119	0.128276	0.171405	0.202778
1.227	0.076255	0.128173	0.171392	0.202784
1.270	0.076445	0.128146	0.1714008	0.202802
1.314	0.076597	0.128201	0.171439	0.202837
1.358	0.076726	0.128342	0.171513	0.202892
1.402	0.076835	0.128563	0.171624	0.202969
1.446	0.076927	0.128839	0.171768	0.203066
1.489	0.077006	0.129095	0.171931	0.203175
1.577	0.077142	0.129501	0.172237	0.203387
1.709	0.077316	0.129938	0.172448	0.203572
1.752	0.077370	0.130059	0.172443	0.203590
1.796	0.077423	0.130172	0.172426	0.203592
2.015	0.077670	0.130679	0.172389	0.203491
2.059	0.077717	0.130771	0.172392	0.203471
2.103	0.077762	0.130862	0.172396	0.203458
2.147	0.77808	0.130980	0.172400	0.203450
2.235	0.077898	0.131122	0.172410	
2.454	0.0781206	0.131535	0.172435	0.203455
2.673	0.078331	0.131923	0.172457	0.203460
2.782	0.078430	0.132104	0.172463	0.203458
3.001	0.078616	0.132440	0.172466	0.203448
3.220	0.078787	0.132762	0.172462	0.203432
3.330	0.078857	0.132882	0.172458	0.203423
3.461	0.078959	0.133040	0.177451	0.203412

Table C.16

Changes in Temperature for an Active Catalyst

θ	θ	$\Delta T_{\alpha=0}^{\circ\text{C}}$	$\Delta T_{\alpha=0.106}$	$\Delta T_{\alpha=0.208}^{\circ\text{C}}$	$\Delta T_{\alpha=0.30}^{\circ\text{C}}$	$\Delta T_{\alpha=0.408}^{\circ\text{C}}$	$\Delta T_{\alpha=0.6}^{\circ\text{C}}$	$\Delta T_{\alpha=1.0}^{\circ\text{C}}$
0.10	0.044	0.44	-0.016	0.005	0.010	0.014	0.025	0.081
0.20	0.088	0.70	-0.20	-0.008	0.028	0.049	0.086	0.256
0.30	0.131	0.93	0.22	-0.085	0.023	0.086	0.164	0.464
0.90	0.175	1.135	0.59	-0.108	-0.008	0.106	0.244	0.678
0.50	0.220	1.32	0.95	0.005	0.010	0.116	0.315	0.887
0.60	0.263	1.48	1.28	0.125	0.100	0.151	0.375	1.085
0.70	0.307	1.63	1.57	0.23	0.215	0.227	0.431	1.28
0.85	0.372	1.82	1.93	0.38	0.322	0.330	0.53	1.47
1.0	0.438	1.98	2.24	0.50	0.51	0.53	0.66	1.75
1.20	0.526	2.17	2.58	0.63	0.66	0.70	0.85	2.00
1.40	0.613	2.33	2.85	0.74	0.77	0.84	1.02	2.22
1.60	0.701	2.47	3.08	0.83	0.871	0.95	1.16	2.42
1.80	0.789	2.59	3.28	0.90	0.95	1.04	1.28	2.62
2.0	0.876	2.69	3.44	0.97	1.02	1.12	1.38	2.81
2.40	1.051	2.86	3.71	1.07	1.13	1.24	1.53	3.15

APPENDIX D

The method used to obtain the frequency response of a system from transient results in the time domain is well known.⁴⁵ It consists of the determination of the Fourier Transform of the transient response to an input signal. The Fourier transform of the function $\Delta T_c(t)$ is defined as

$$\overline{\Delta T}_c(j\omega) = \int_{-\infty}^{+\infty} e^{-j\omega t} \Delta T(t) dt$$

It is complex number whose real part A and imaginary part B are given by the two equations

$$A = \int_{-\infty}^{+\infty} \Delta T(t) \cos \omega t dt$$

$$B = - \int_{-\infty}^{+\infty} \Delta T(t) \sin \omega t dt$$

The transfer function of the process is obtained as the ratio of the two Fourier transforms of ΔT_c and ΔT_{feed}

$$G(j\omega) = \frac{\overline{\Delta T}_c(j\omega)}{\overline{\Delta T}_F(j\omega)}$$

The advantage of using input perturbations such as unit impulse or unit steps is that their Fourier transforms are respectively 1, and $1/j\omega$ and consequently only the determination of the Fourier transform $\overline{\Delta T}_c(j\omega)$ of the response ΔT_c is required.

The values of ΔT_c resulting from a step change in the feed temperature remains finite at the end of a transient and for this reason the Fourier transform of the quantity $\Delta \bar{T}_c$ is not defined. To avoid this difficulty a step change of magnitude equal to minus the steady state gain or D.C. level of the process is superposed on ΔT_c at each instant, and the Fourier transform $F(j\omega)$ of the function.

$F(t) = \Delta T_c$ - step change at $t = 0$ of magnitude ΔT_{ss} is determined.

Since the Fourier transform of the step change ΔT_{ss} is $\frac{\Delta T_{ss}}{j\omega}$, the Fourier transform of $\Delta \bar{T}_c$ is obtained as

$$\Delta \bar{T}_c(j\omega) = \bar{F}(j\omega) + \frac{\Delta T_{ss}}{j\omega}$$

and the transfer function $G(j\omega)$ defined as

$$G(j\omega) = \frac{\Delta \bar{T}_c(j\omega)}{\frac{1}{j\omega}}$$

equals

$$G(j\omega) = j\omega F(j\omega) + \Delta T_{ss}$$

The real part R and the imaginary part I of $G(j\omega)$ are expressed as functions of the frequency ω by the two relations

$$R = \Delta T_{ss} - \omega \int_{-\infty}^{+\infty} (\Delta T_c(t) - \Delta T_{ss}) \sin \omega t \, dt$$

$$I = \omega \int_{-\infty}^{+\infty} (\Delta T_c(t) - \Delta T_{ss}) \cos \omega t \, dt$$

because of the definition of ΔT_c and ΔT_{ss} the integrant is zero for negative time and becomes practically zero after a finite amount of time T after which the new steady state is obtained. Consequently, the value of the finite integral is only computed between 0 and T.

A subroutine available in the M.I.T. Computation Center library called AA HAN3 has been used to estimate these finite integrals. The computer program written to generate the quantities R and I from the results obtained by the simulation is presented on the following page.

Once these quantities are obtained it is possible to generate the frequency surface curve since

$$\begin{aligned} \text{Magnitude} &= \sqrt{R^2 + I^2} \\ \text{Angle} &= -\text{artang}\left(\frac{I}{R}\right) \end{aligned}$$

The magnitude and the angle of the frequency responses for the locations $\alpha = 0.0$ $\alpha = 3.74$ and $\alpha = 1.0$ are tabulated in the next pages.

Table D-4 presents the numerical values appearing on Fig. 6.24 where the results of the simulation are compared with the response of the simplified transfer functions for a step change in temperature of 5°C .

DERIVATION OF THE FREQUENCY RESPONSES OF THE PROCESS
FROM TRANSIENT DATA

```
DIMENSION D(1000),A(10),R(1000),DATA(1000),Z(1000),REAL(1000),CIM(
11000),CATEM(1000)
1  FORMAT(4I18)
2  FORMAT(4E18.8)
3  FORMAT(5H DATA)
4  FORMAT(8H RESULTS)
5  PRINT 3
10  READ 2,DELFRE,PERIOD,DIFT
11  PRINT 2,DELFRE,PERIOD,DIFT
20  READ 1,N,J,K
21  PRINT 1,N,J,K
22  READ 2,(CATEM(NS),NS=1,N)
23  DO 25 NS=1,N
24  DATA(NS)=(CATEM(NS)-CATEM(1))/DIFT
25  CONTINUE
26  DO 28 NS=1,N
27  D(NS)=DATA(NS)-DATA(N)
28  CONTINUE
29  PRINT 2,(D(NS),NS=1,N)
40  A(1)=DELFRE
50  A(2)=PERIOD
70  CALL HARAN3(N,J,D,R,K,A)
71  PRINT 4
72  FORMAT(5E16.8)
73  FORMAT(7X9HFREQUENCY,8X8HREAL COF,3X13HIMAGINARY COF,7X9HREAL PART
1,2X14HIMAGINARY PART)
74  PRINT 73
76  JK=J+1
80  DO 100 L=1,JK
81  K1=L
82  K2=L+JK
83  K3=L+2*JK
85  REAL(K1)=DATA(N)+R(K1)*R(K3)
86  CIM(K1)=R(K1)*R(K2)
90  PRINT 72,R(K1),R(K2),R(K3),REAL(K1),CIM(K1))
100  CONTINUE
105  FORMAT(21X9HFREQUENCY,21X9HMAGNITUDE)
107  PRINT 105
108  FORMAT(2E30.8)
110  DO 120 L=1,JK
115  Z(L)=SQRTF(REAL(L)**2+CIM(L)**2)
116  PRINT 108,R(L),Z(L)
120  CONTINUE
170  CALL EXIT
200  END
```

Table D.1

Frequency Response for $\alpha = 0.0$

Frequency ω radian/unit time	Transfer Function		Approximate Transfer Function	
	Magnitude	Angle ($^{\circ}$)	Magnitude	Angle ($^{\circ}$)
0	1.326	0	1.326	0
0.1	1.330	-7	1.316	-7 $^{\circ}$ 11'
0.3	1.254	-21	1.241	-20 $^{\circ}$ 34'
0.6	1.045	-39	1.061	-36 $^{\circ}$ 52'
1.0	0.758	-52	0.828	-51 $^{\circ}$ 21'
2.0	0.448	-59	0.491	-68 $^{\circ}$ 13'
3.0	0.328	-59	0.341	-75 $^{\circ}$ 5'
4.0	0.272	-59	0.260	-78 $^{\circ}$ 42'
5.0	0.242	-60	0.209	-80 $^{\circ}$ 55'
6.0	0.217	-61	0.175	-82 $^{\circ}$ 25'
7.0	0.194	-61	0.150	-83 $^{\circ}$ 29'
8.0	0.179	-62	0.131	-84 $^{\circ}$ 18'
9.0	0.171	-63	0.117	-84 $^{\circ}$ 55'
10.0	0.160	-64	0.106	-85 $^{\circ}$ 26'
15.0	0.119	-70	0.070	-86 $^{\circ}$ 57'
20.0	0.095	-77	0.053	-87 $^{\circ}$ 43'
25.0	0.079	-80	0.042	-88 $^{\circ}$ 10'

Table D.2

Frequency Response for $\alpha = 0.374$

Frequency ω radian/unit time	Transfer Function		Approximate Transfer Function	
	Magnitude	Angle ($^{\circ}$)	Magnitude	Angle($^{\circ}$)
0	1.292	0	1.292	0
0.1	1.283	- 9	1.282	- 8 $^{\circ}$ 15'
0.3	1.220	- 26 $^{\circ}$ 30'	1.210	- 27 $^{\circ}$
0.6	0.764	- 50 $^{\circ}$ 30'	1.034	- 49 $^{\circ}$ 40'
1.0	0.704	- 73	0.807	- 72 $^{\circ}$ 50'
2.0	0.455	-109	0.479	-110 $^{\circ}$ 40'
3.0	0.320	-130	0.333	-139 $^{\circ}$ 20'
4.0	0.258	-155	0.253	-164 $^{\circ}$ 12'
5.0	0.215	-180	0.204	-188 $^{\circ}$
6.0	0.176	-206	0.170	-211 $^{\circ}$
7.0	0.155	-233	0.146	-234 $^{\circ}$
8.0	0.139	-257	0.128	-256 $^{\circ}$
9.0	0.126	-283	0.114	-279 $^{\circ}$
10.0	0.124	-310	0.103	-300 $^{\circ}$
15.0	0.086	-420	0.068	-408 $^{\circ}$
20.0	0.049	-512	0.051	-516 $^{\circ}$
25.0	0.017	-603	0.041	-623 $^{\circ}$

Table D.3

Frequency Response for $\alpha = 1.0$

Frequency ω radian/unit time	Transfer Function		Approximate Transfer Function	
	Magnitude	Angle ($^{\circ}$)	Magnitude	Angle ($^{\circ}$)
0	0.860	0	0.860	0
0.1	0.847	- 7	0.830	- 10
0.3	0.797	- 22	0.790	- 20
0.6	0.656	- 41	0.62	- 38
1.0	0.452	- 56	0.46	- 51
2.0	0.262	- 53	0.225	- 49
3.0	0.239	- 45	0.225	- 32
4.0	0.259	- 53	0.306	- 35
5.0	0.267	- 69	0.275	- 45
6.0	0.241	- 75	0.275	- 51
7.0	0.186	-106	0.20	- 75
8.0	0.127	-120	0.15	- 78.5
9.0	0.0815	-117	0.125	- 72.5
10.0	0.0692	- 99	0.108	- 62
11.0	0.0793	- 94	0.132	- 60
12.0	0.0837	-106	0.137	- 69
15.	0.0397	-127	0.078	- 96.5
16.	0.0340	-113	0.106	- 83.5
18.	0.0397	-114	0.078	-101
20	0.0287	-130	0.080	- 98
22	0.0197	-112	0.075	- 81
24	0.0216	-110	0.064	-100
25	0.0206	-114	0.048	- 85

Table D.4
 Comparison of Transient Data with
 Results of Approximate Transfer Functions

Time θ'	$\alpha = 0$		$\alpha = 0.374$		$\alpha = 1.0$	
	ΔT_c simulation	ΔT approx.	ΔT_c simulation	ΔT_c approx.	ΔT_c simulation	ΔT_c approx.
0.044	0.45	0.23	0.02	0.00	0.11	0.26
0.088	0.70	0.45	0.05	0.00	0.26	0.53
0.132	0.93	0.61	0.09	0.00	0.45	0.75
0.197	1.23	0.815	0.13	0.00	0.74	0.99
0.285	1.47	1.35	0.09	0.00	1.09	1.29
0.329	1.72	1.53	0.02	0.00	1.24	1.42
0.438	2.09	1.96	0.44	0.40	1.57	1.61
0.482	2.20	2.12	0.69	0.53	1.65	1.68
0.570	2.46	2.43	1.18	0.94	1.82	1.78
0.635	2.64	2.64	1.49	1.15	1.91	1.84
0.767	2.97	3.05	2.01	1.68	2.02	1.93
0.876	3.23	3.34	2.38	2.14	2.07	1.98
0.964	3.43	3.64	2.66	2.43	2.19	2.01
1.140	3.78	3.86	3.02	2.96	2.27	2.29
1.315	4.11	4.32	3.43	3.42	2.53	2.52
1.753	4.79	5.00	4.26	4.31	3.02	3.01
2.191	5.30	5.48	4.90	4.95	3.37	3.36
2.629	5.69	5.82	5.36	5.40	3.64	3.61
3.067	5.97	6.06	5.70	5.77	3.74	3.80
3.506	6.18	6.23	5.96	5.93	3.99	3.93
3.944	6.34	6.35	6.13	6.09	4.10	4.03
4.382	6.45	6.36	6.28	6.21	4.19	4.10
4.645	6.51	6.37	6.34	6.22	4.23	4.14

APPENDIX E

LITERATURE CITATIONS

1. N.R. Amundson and R. Aris, Chemical Engineering Sciences Vol. 7, pg. 121, (1958).
2. D. Annable, Chem. Eng. Sciences, Vol. 1, pg. 145-154, (1952).
3. C.H. Barkeley, Chem. Eng. Progress Symposium Series, Vol. 37, pg. 25-55, (1959).
4. O. Bilous and N.R. Amundson, A.I.Ch.E. Journal, Vol.1. , pg. 513, (1955).
5. O. Bilous and N.R. Amundson, A.I.Ch.E. Journal, Vol. 2, pg. 117, (1956).
6. O. Bilous, H.D. Block, E.L. Piret, A.I.Ch.E. Journal, Vol. 3, pg. 248, (1957).
7. G.L. Bridger, G.R. Pole, A.W. Beinlich and H.L. Thompson, Chem. Eng. Progress, Vol. 43, pg. 291-302 (1947).
8. Bruce, D.W., Peaceman and M.H. Racheford, Trans. AIME Vol. 79, pg. 198, (1953).
9. P.H. Calderbank, Chem. Eng. Progress, Vol. 49, pg. 585-590, (1953).
10. R. Courant, E. Issacson, M. Rees, Commun, Pure and Applied Math. Vol. 5, pg. 243-255, (1952).
11. P.V. Danckwerts, Chem. Eng. Sciences, Vol. 2, pg. 1 (1953).
12. K.G. Denbigh, K.J. Cannon, Chem. Eng. Sci. Vol. 6, pg. 155, (1957).
13. K.G. Denbigh, M. Hicks and F.M. Page, Trans. Faraday Soc., Vol. 44, pg. 479, (1948).
14. A.S. Foss, Chemical Engineering Progress Symposium Series, Vol. 47, pg. 25-55, (1959).
15. D.A. Frank-Kamenetskii, Diffusion and Heat Exchange in Chemical Kinetics, Princeton University Press, Princeton, N.Y.
16. S.L. Grotch, M.I.T. Chemical Eng. Sc.D. Thesis (1959).

17. L.B. Hein, Chemical Eng. Progress, Vol. 48, pg. 412-418, (1952).
18. J.Z. Hirniak, Z. Physik Chem., Vol. 75, pg. 675-80, (1910).
19. O.A. Hoogen, B.W. Gamson, G. Thodos, Trans. A.I.Ch.E., Vol. 39, pg. 1-35, 583-584, (1943).
20. M. Jakob, Trans. A.I.Ch.E., Vol. 35, pg 563, (1934).
21. J. Kjaer, "Measurement and Calculation of Temperature and Conversion in Fixed Bed Catalytic Reactors," Jull. G. Jellerups Forlag, Copenhagen, (1958).
22. B. Logeais, M.I.T. Chemical Eng., M.S. Thesis (1959).
23. A.J. Lotka, J. Am. Chem. Soci., Vol. 42, pg. 1595, (1920).
24. Mills, Bennet, "Reactions in the Synthesis of Ammonia," Purdue University, paper presented at the 40th national meeting of A.I.Ch.E. (May 1959).
25. I.E. Salinkov, Doklady Akad Navk USSR, Vol. 60, pg. 405, (1948), and Vol. 60, pg. 611 (1948).
26. Shean-Lin Liu and N.R. Amundson, IEC Fundamentals, Vol. 1 No. 3, pg. 200, (1962).
27. Shean-Lin Liu, N.R. Amundson, R. Aris, IEC Fundamentals, Vol. 2, No. 1, pg. 12, (1963).
28. Sidorov and Livshits, J. Phys. Chem. USSR, Vol. 21, pg. 1177, (1947),
29. A.V. Slack, H.Y. Allgood, H.E. Maune, Chem. En g. Prog., Vol. 49, pg. 393-403, (1953).
30. H.L. Stone, P.L.T. Brian, A.I.Ch.E. Journal, Vol. 9, No. 5, pg. 681, (1963).
31. J.W. Tierney, C.W. Homan, D.J. Nemanic, N.R. Amundson, Control Eng., Vol. 4, No. 9, pg. 166-175, (1957).
32. Temkin J. Phys. Chem. (USSR) Vol. 24, pg. 1312, (1950).
33. Temkin and Pyzhev ACTA Phys. Chem., (USSR), Vol. 12, pg. 327, (1946).
34. C. Van Heerden, IEC, Vol. 45, pg. 1242-1247 (1953).
35. E. Wicke Alta Technologia Chimica, Accademia Nazionale dei Lincei, lecture course, Varese Sept. 26, 1960.
36. E. Wicke, Chem. Ing. Tech., Vol. 29, pg. 305, (1957).

37. E. Wicke, Z. Elektro-chem., Vol. 65, pg. 267, (1961).
38. E. Wicke, D. Vortmayer, Z Elektro-chem., Vol. 63, pg. 145, (1959).
39. R.H. Wilhelm, J.F. Wehner, Chem. Eng. Sci., Vol. 6, pg. 89, (1956).
40. R.H. Wilhelm, W.C. Johnson, R. Wynkoop, D.W. Collier, Chem. Eng. Prog., Vol. 44, pg. 105, (1948).
41. L. Lapidus, Digital Computation for Chemical Engineers, McGraw-Hill Book Company, (1962).
42. J.J. Carberry, A.I.Ch.E., New York Meeting, December 1961.
43. T.J. Boyle, S.c.D. Thesis, Chem. Eng., M.I.T., (1963).
44. R. Aris, Chem. Eng. Sci., 7, 8, (1957).
45. J.C. Truxel, Control System Synthesis, McGraw-Hill, pg. 375-390, (1955).
46. Kelley, U.S. Bureau of Mines, Bulletin 371, (1934).
47. Rossini and Al "Selected Values of Chemical Thermo-dynamic Properties" Circular 500, U.S. National Bureau of Standards (1952).
48. McHenry, K.W., and R.H. Wilhelm, A.I.Ch.E. Journal, Vol. 3, pg. 83, (1957).

APPENDIX F
NOMENCLATURE

The subscripts " H_2 ", " N_2 ", " NH_3 ", "inert" used with the mole fraction y and the molal heat capacity C_p denote the specie under consideration. The subscript "feed" used with the temperature denotes the conditions of the gas entering the reactor. The subscript " $a=0.374$ " associated with the temperature changes refer to the location 0.374 in the reactor where this change takes place. The subscript j and n are used with the variables appearing in the finite difference equation to characterize a location and an instant.

The superscript $*$ is used to denote the mole fraction in the feed gas.

The presence of a bar above a variable means that the Laplace transform or the Fourier transform of it has been taken.

LIST OF SYMBOLS

- A - Cross sectional area of the catalyst ft^2
- A - Symbol used to represent the quantity $6.2825 \cdot 10^{18} P^{-0.5}$
- a - Total cross sectional area of the tubes ft^2
- a - Weighting coefficient used in the accuracy analysis of Chapter V
- a - Constant appearing in the definition of function f(Eq. 5.6)
- a - Coefficient of Eq. 5.20
- a' - Coefficient of Eq. 5.12
- a_j - Coefficient of Eq. 5.22
- \mathcal{A} - Dimensionless group characterizing the feed composition
- b - Coefficient of Eq. 5.12
- b' - Coefficient of Eq. 5.20
- b_j - Coefficient of Eq. 5.22
- \mathcal{B} - Dimensionless group characterizing the feed composition
- c - Weighting coefficient used in the accuracy analysis of Chapter V
- \mathcal{C} - Dimensionless group characterizing the feed composition
- C_{p_c} - Heat capacity of the catalyst $\frac{\text{BTU}}{\text{lb}^\circ\text{F}}$
- C_{p_m} - Heat capacity of the metal $\frac{\text{BTU}}{\text{lb}^\circ\text{F}}$
- \bar{C}_{p_o} - Average molal heat capacity $\frac{\text{BTU}}{\text{lb mole}^\circ\text{F}}$
- \bar{C}_{p_x} - Molal heat capacity of specie x $\frac{\text{BTU}}{\text{lb mole}^\circ\text{F}}$
- D - Dimensionless diffusion group $\frac{D'V}{1^2 \text{ h}_2 \text{ S}^2}$
- D' - Taylor longitudinal heat diffusion $\frac{\text{BTU}}{\text{hr ft}^\circ\text{F}}$
- d - Ratio of heat transfer resistance on both sides of the wall $d = \frac{h_1 s_1}{h_2 s_2}$

LIST OF SYMBOLS (Continued)

- d - Weighting coefficient used in the accuracy analysis of Chapter V
- d_j - Coefficient of Eq. 5.22
- \mathcal{D} - Dimensionless group characterizing the feed composition
- e - Dimensionless group characterizing the liberation of enthalpy by reaction $\frac{\Delta H_o}{T_{ref} C_{p_o}}$
- F - Molal feed rate $\frac{\text{lb mole}}{\text{hr}}$
- $f(\xi)$ - Function defining the distance variable ξ
- f' - First derivative of f with respect to ξ
- f'' - Second derivative of f with respect to ξ
- G - Mass flow rate in the catalyst $\frac{\text{lb}}{\text{hr ft}^2}$
- G_c - Controller transfer function
- G_p - Process transfer function
- g - Ratio of the total heat capacity of the wall to the total heat capacity of the catalyst $g = \frac{M C_{p_m}}{W C_{p_c}}$
- g - Weighting coefficient appearing in the accuracy analysis of Chapter V
- h_1 - Heat transfer coefficient between the feed gas and the tube wall $\frac{\text{BTU}}{\text{hr ft}^2 \text{ } ^\circ\text{F}}$
- h_2 - Heat transfer coefficient between the catalyst and the tube wall $\frac{\text{BTU}}{\text{hr ft}^2 \text{ } ^\circ\text{F}}$
- h - Dimensionless group characterizing the change in heat capacity due to reaction $\frac{\Delta C}{C_{p_o}}$
- K_1, K_2 - Gains appearing in simplified transfer function
- K_1' - Specific rate constant (formation of ammonia) $\frac{\text{lb mole}}{\text{hr ft}^3 (\text{atm})^{1.5}}$

LIST OF SYMBOLS (Continued)

K_2'	-	Specific rate constant (dissociation)	$\frac{\text{lb mole (atm)}^{0.5}}{\text{hr ft}^3}$
K_c	-	Proportional gain of the controller	
K_I	-	Integral gain of the controller	
K_{\max}	-	Maximum tolerable gain for stability	
K_p	-	Equilibrium constant for the synthesis of ammonia	$\frac{1}{\text{atm}}$
l	-	Reactor length	ft
L	-	Dimensionless group	$P K_p$
M	-	Total mass of catalyst	lb
m	-	Normalized wall temperature	$\frac{T_w}{T_{\text{ref}}}$
m	-	Weighting coefficient used in the accuracy analysis of Chapter V	
N	-	Total number of position in the distance grid	
P	-	Total pressure	atm
P_x	-	Partial pressure of specie x	atm
q_1	-	Heat introduced by bulk flow (dimensionless form)	
q_2	-	Heat transported from the wall (dimensionless form)	
q_3	-	Heat generated by the chemical reaction (dimensionless form)	
R	-	Coefficient for sink or source term in the accuracy analysis	
r	-	Rate of reaction	$\frac{\text{lb mole}}{\text{hr ft}^3 \text{ catalyst}}$
$r(v, y)$	-	Rate of reaction	dimensionless form
S_1	-	Total inside area of the tube	ft^2
S_2	-	Total outside area of the tubes	ft^2
s	-	Dimensionless group characterizing the heat transfer on the catalyst side of the wall	$s = \frac{F C_{p0}}{h_2 S_2}$
s	-	Laplace variable	

LIST OF SYMBOLS (Continued)

T_B	-	Base temperature for the estimation of the sensible heat	$^{\circ}\text{R}$
T_c	-	Catalyst temperature	$^{\circ}\text{R}$
T_{ref}	-	Reference temperature	$^{\circ}\text{R}$
T_T	-	Gas temperature in the tubes	$^{\circ}\text{R}$
T_w	-	Wall temperature	$^{\circ}\text{R}$
t	-	Time	
u_G	-	Linear velocity of the gas in the catalyst	$\frac{\text{ft}}{\text{hr}}$
u_p	-	Velocity of propagation of a thermal perturbation	$\frac{\text{ft}}{\text{hr}}$
V	-	Volume of catalyst	ft^3
V	-	Velocity term in the accuracy analysis	
V_o	-	Space velocity	$\frac{1}{\text{hr}}$
v	-	Normalized catalyst temperature	$\frac{T_c}{T_{\text{ref}}}$
w	-	Normalized gas temperature in the tubes	$\frac{T_w}{T_{\text{ref}}}$
y	-	Ammonia mole fraction	
y^*	-	Ammonia mole fraction in the feed	
y_x	-	Mole fraction of specie x	
$\bar{y}_{j+1, n+1}$	-	Estimate of $y_{j+1, n+1}$ in the solution of the mass balance equation	
z	-	Distance along the reactor	ft

GREEK SYMBOLS

α	-	Normalized distance in the reactor z/l
α	-	Diffusion parameter in the accuracy analysis of Chapter V
		$\alpha = \frac{2D\Delta t}{\Delta x^2}$
α_j	-	Weighting coefficients, used in the accuracy analysis of Chapter V
β	-	Number of heat transfer units in the empty tube section
		$\frac{h_1 S_1}{F C_{p_0}}$
β	-	Velocity parameter in the accuracy analysis of Chapter V
		$\beta = \frac{V\Delta t}{\Delta x}$
β_i	-	Coefficient of Eq. 5.31
γ	-	Dimensionless group $\frac{A}{T_{ref} V_0}$
γ_i	-	Coefficient of Eq. 5.31
ΔC	-	Change in molal heat capacity of the mixture resulting from the formation of lb mole of ammonia $\frac{BTU}{lb\ mole\ ^\circ F}$
ΔH_0	-	Enthalpy of formation of ammonia $\frac{BTU}{lb\ mole}$
ΔT	-	Temperature change $^\circ F$
Δt	-	Time change hr
Δz	-	Distance increment ft
$\Delta \alpha$	-	Normalized distance increment $\frac{\Delta z}{l}$
$\Delta \theta$	-	Normalized time increment
$\Delta \xi$	-	Size of a distance grid mesh

BIOGRAPHICAL NOTE

The author was born in Darby, Pennsylvania, on March 25, 1936. He did elementary schooling at Friends School, Wilmington, Delaware. In 1954 he entered Cornell University and received the degree of Bachelor of Chemical Engineering in 1959. In September 1959 he entered the M.I.T. Graduate School.